



# Maejo International Journal of Science and Technology

Volume 2, Issue 2 April – July 2008

Coverage by Abstracting Service : This journal is covered by Science Citation Index Expanded (SciSearch), Journal Citation Reports/Science Edition, Zoological Record, SciFinder Scholar, Chemical Abstracts, DDAJ, and AGRIS. Available online at [www.mijst.mju.ac.th](http://www.mijst.mju.ac.th)



- ◆ Potential of wind power for Thailand : An assessment
- ◆ Changes in viscoelastic properties of longan during hot-air drying in relation to its indentation
- ◆ Stopped-flow injection spectrophotometric method for determination of chlorate in soil
- ◆ Water quality of Wenchi Crater Lake in Ethiopia

### **Journal Information**

*Maejo International Journal of Science and Technology* (ISSN 1905-7873 © 2008), the international journal for the rapid publication of all preliminary communication in Science and Technology is the first peer-refereed scientific journal of Maejo University ([www.mju.ac.th](http://www.mju.ac.th)). Intended as a medium for communication, discussion, and rapid dissemination of important issues in Science and Technology, articles are initially published online in an open access format, thereby giving authors the chance to communicate with a wide range of readers in an international community.

### **Publication Information**

MIJST is published twice each year. Articles are available online and can be accessed free of charge at <http://www.mijst.mju.ac.th> Printed and bound copies of each volume are produced and distributed to authors and selected groups or individuals. This journal and the individual contributions contained in it are protected under the copyright by Maejo University.

### **Abstracting/Indexing Information**

MIJST is covered and cited by Science Citation Index Expanded (SciSearch®), Journal Citation Reports/Science Edition, Directory of Open Access Journals (DOAJ), SciFinder Scholar, Chemical Abstract Service (CAS) and AGRIS.

### **Contact Information**

Editorial office: Maejo International Journal of Science and Technology (MIJST), 1st floor, Orchid Building, Maejo University, San Sai, Chiang Mai 50290, Thailand  
Tels: +66-53-87-3880, Fax: +66-53-87-3880  
E-mail: [duang@mju.ac.th](mailto:duang@mju.ac.th)

# MAEJO INTERNATIONAL JOURNAL OF SCIENCE AND TECHNOLOGY

## Editor :

Duang Buddhasukh, *Maejo University, Thailand*

## Editorial Assistants :

James F. Maxwell, *Chiang Mai University, Thailand*  
Asst. Prof. Morakot Sukchotiratana, *Chiang Mai University, Thailand*  
Jirawan Banditpuritat, *Maejo University, Thailand*

## Managing Editor :

Asst. Prof. Jatuphong Varith, *Maejo University, Thailand*

## Board of Consulting Editors :

Prof. Kunimitsu Kaya	Tohoku University, Japan
Prof. Paisarn Sithigorngul	Srinakharinwirot University, Thailand
Prof. Maitree Suttajit	Chiang Mai University, Thailand
Prof. Stephen G. Pyne	University of Wollongong, Australia
Prof. Mary Garson	University of Queensland, Australia
Prof. Dallas E. Alston	University of Puerto Rico, USA
Prof. Richard L. Deming	California State University Fullerton, USA
Prof. Renato G. Reyes	Central Luzon State University, Philippines
Prof. Cynthia C. Divina	Central Luzon State University, Philippines
Emeritus Prof. Bela Ternai	La Trobe University, Australia
Prof. Amarendra N. Misra	Fakir Mohan University, Orissa, India
Assoc. Prof. Siripen Traichaiyaporn	Chiang Mai University, Thailand
Assoc. Prof. Margaret E. Kerr	Worcester State College, USA
Assoc. Prof. Chatchai Tayapiwatana	Chiang Mai University, Thailand
Assoc. Prof. Kriangsak Mengumpan	Maejo University, Thailand
Assoc. Prof. Niwoot Whangchai	Maejo University, Thailand
Assoc. Prof. Duangrat Inthorn	Mahidol University, Thailand
Asst. Prof. Ma. Elizabeth C. Leoveras	Central Luzon State University, Philippines
Asst. Prof. Joselito DG. Dar	Central Luzon State University, Philippines
Asst. Prof. Jatuphong Varith	Maejo University, Thailand
Asst. Prof. Sangtong Pongjareankit	Maejo University, Thailand
Asst. Prof. Pramual Suteecharuwat	Chulalongkorn University, Thailand
Asst. Prof. Mayuso Kuno	Srinakharinwirot University, Thailand
Asst. Prof. Andrzej Komosa	University of Maria-Curie Sklodowska, Poland
Asst. Prof. Narin Tongwittaya	Maejo University, Thailand
Asst. Prof. Ekachai Chukeatirote	Mae Fah Luang University, Thailand
Dr. Ignacy Kitowski	University of Maria-Curie Sklodowska, Poland
Dr. Settha Siripin	Maejo University, Thailand
Dr. Waya Sengpracha	Silpakorn University, Thailand

## Consultants :

Assoc. Prof. Thep Phongparnich, Ed. D., President of Maejo University  
Assoc. Prof. Chalermchai Panyadee, Ph.D., Vice President in Research of Maejo University

MAEJO INTERNATIONAL JOURNAL  
OF SCIENCE AND TECHNOLOGY

*The International Journal for the Rapid Publication of Preliminary  
Communications in Science and Technology*



---

<http://www.mijst.mju.ac.th>  
ISSN 1905-7873 © 2008 by Maejo University

# MAEJO INTERNATIONAL JOURNAL OF SCIENCE AND TECHNOLOGY

Volume 2, Issue 2 (April –July 2008)

## CONTENTS

Articles	Page
Journal impact factors .....	i-vi
Potential of wind power for Thailand: an assessment <i>Stuart Major, Terry Commins, and Annop Noppharatana</i> .....	255-266
Vehicle jack with wedge mechanism <i>Ademola A. Dare and Sunday A. Oke</i> .....	267-273
Determination of abscisic acid hormone (ABA), mineral content, and distribution pattern of 13C photoassimilates in bark-ringed young peach trees <i>A. B. M. Sharif Hossain and Fusao Mizutani</i> .....	274-284
Elementary theory of quantum Hall effect <i>Keshav N. Shrivastava</i> .....	285-297
Characterisation of sewage wastewater and assessment of downstream pollution along Huluka River of Ambo, Ethiopia <i>Padanilly Chidambaram Prabu , Zerihun Teklemariam, Tadele Nigusse, Sevanan Rajeshkumar, Lakew Wondimu, Alemayehu Negassa, Ephrem Debebe, Esayas Aga, Asfaw Andargie, and Asefa Keneni</i> .....	298-307
Theoretical analysis and design of double implanted MOSFET on 6H silicon carbide wafer for low power dissipation and large breakdown voltage <i>Munish Vashishath and Ashoke Kumar Chatterjee</i> .....	308-320
Changes in viscoelastic properties of longan during hot-air drying in relation to its indentation <i>Jatuphong Varith, Chanisara Noochuay, Tipaporn Khamdang and Adisorn Ponpai</i> ....	321-330
A survey on the energy consumption and demand in a tertiary institution <i>Adekunle O. Adelaja, Olatunde Damisa, Sunday A. Oke*, Akinwale B. Ayoola, and Allen O. Ayeyemitan</i> .....	331-344
Abundance, food habits, and breeding season of exotic <i>Tilapia zillii</i> and native <i>Oreochromis niloticus</i> L. fish species in Lake Zwai , Ethiopia <i>Alemayehu Negassa and Padanilly C. Prabu</i> .....	345-360
Water quality of Wenchi Crater Lake in Ethiopia Ecotoxicology Research Center , Ambo University College , P.O.Box.19, Ambo Town , Western Shoa , Ethiopia <i>Malairajan Singanan, Lakew Wondimu, and Mitiku Tesso</i> .....	361-373
Design and fabrication of a micro-volume autotitrator with potentiometric end-point detection for the determination of acidity of some fruit juices <i>Prinya Masawat, Saisunee Liawruangrath, and Suphachock Upalee</i> .....	374-382
Stopped-flow injection spectrophotometric method for determination of chlorate in soil <i>Sarawut Somnam 1 , Kate Grudpan 1,2 , and Jaroon Jakmunee</i> .....	383-390
Effect of heavy metals on the level of vitamin E, total lipid and glycogen reserves in the liver of common carp ( <i>Cyprinus carpio</i> L.) <i>Vinodhini Rajamanickam and Narayanan Muthuswamy</i> .....	391-399

Effects of <i>Terminalia bellerica</i> Roxb. methanolic extract on mouse immune response in vitro <i>Aurasorn Saraphanchotiwitthaya, Pattana Sripalakit, and Kornkanok Ingkaninan</i> .....	<b>400-407</b>
A flow injection system for the spectrophotometric determination of lead after preconcentration by solid phase extraction onto Amberlite XAD-4 <i>Jintana Klamtet, Nungruthai Suphrom, and Chonthicha Wanwat</i> .....	<b>408-417</b>
On-line preconcentration and determination of tetracycline residues in milk using solid-phase extraction in conjunction with flow injection spectrophotometry <i>Prinya Masawat, Sutthinee Mekprayoon, Saisunee Liawruangrath, Suphachock Upalee, and Napaporn Youngvises</i> .....	<b>418-430</b>
Variability in growth, nutrition and phytochemical constituents of <i>Plectranthus amboinicus</i> (Lour) Spreng. as influenced by indigenous arbuscular mycorrhizal fungi <i>Sevanan Rajeshkumar, Mathan C. Nisha, and Thangavel Selvaraj</i> .....	<b>431-439</b>
Preparation of aluminium lakes by electrocoagulation <i>Prapai Pradabkham and Neeranuch Chairungsi</i> .....	<b>440-443</b>

---

<http://www.mijst.mju.ac.th>

ISSN 1905-7873 © 2008 by Maejo University

# MAEJO INTERNATIONAL JOURNAL OF SCIENCE AND TECHNOLOGY

*Volume 2, Issue 2 (April –July 2008)*

<b>Author Index</b>			
<b>Author</b>	<b>Page</b>	<b>Author</b>	<b>Page</b>
Adelaja A. O.	331	Nisha M. C.	431
Aga E.	298	Nigusse T.	298
Andargie A.	298	Noochuay C.	320
Ayoola A. B.	331	Noppharatana A.	255
Ayeyemitan A.O.	331	Oke S. A.	267,331
Chairungsi N.	440	Ponpai A.	320
Chatterjee A. K.	308	Prabu P. C.	298,345
Commins T.	255	Pradabkham P.	440
Damisa O.	331	Rajamanickam V.	391
Dare A. A.	267	Rajeshkumar S.	298,431
Debebe E.	298	Saraphanchotiwitthaya A.	400
Grudpan K.	383	Selvaraj T.	431
Hossain A. B. M. S.	274	Singanam M.	361
Ingkaninan K.	400	Shrivastava K. N.	285
Jakmunee J.	383	Somnam S.	383
Keneni A.	298	Sripalakit P.	400
Khamdang T.	320	Suphrom N.	408
Klamtet J.	408	Teklemariam Z.	298
Liawruangrath S.	374,418	Tesso M.	360
Major S.	255	Upalee S.	374,418
Masawat P.	374,418	Varith J.	320
Mekprayoon S.	418	Vashishath M.	308
Mizutani F.	274	Wanwat C.	408
Molloy R.	i	Wondimu L.	298,361
Muthuswamy N.	391	Youngvises N.	418
Negassa A.	298,345		

## Instructions for Authors

### Manuscript Preparation

Manuscripts should be prepared in English using a word processor. MS Word for Macintosh or Windows, and .doc or .rtf files are preferred. Manuscripts may be prepared with other software, provided that the full document (with figures, schemes and tables inserted into the text) is exported to a MS Word format for submission. Times or Times New Roman font is preferred. The font size should be 12 pt. and the line spacing "at least" 17 pt. The printing area is 17.5cm x 24.7cm (6.9" x 9.73"). For A4 paper, margins must be 1.5 cm on top, 3.5cm at the bottom and 1.75 cm on both left and right sides of the paper. For US letter-sized paper, margins must be 1.5 cm (0.59") on top, 1.74 cm (0.68") at the bottom and 2.05 cm (0.8") on both left and right sides. Although our final output is in .pdf format, authors are asked NOT to send manuscripts in this format as editing them is much more complicated.

Authors' full mailing addresses, homepage addresses, phone and fax numbers, e-mail addresses and homepages can be included in the title page and these will be published in the manuscripts and the Table of Contents. The corresponding author should be clearly identified. It is the corresponding author's responsibility to ensure that all co-authors are aware of and approve of the contents of a submitted manuscript.

A brief (200 word maximum) Abstract should be provided. The use in the Abstract of numbers to identify compounds should be avoided, unless these compounds are also identified by names.

A list of three to five keywords must be given, and placed after the Abstract. Keywords may be single words or very short phrases.

Although variations in accord with a manuscript's contents are permissible, in general all papers should have the following sections: Introduction, Materials and Methods, Results and Discussion, Conclusions, Acknowledgments (if applicable), and References.

Authors are encouraged to prepare figures and schemes in colour. Full colour graphics will be published free of charge.

Tables should be inserted into the main text, and numbers and titles supplied for all tables. All table columns should have an explanatory heading. To facilitate layout of large tables, smaller fonts may be used, but in no case should these be less than 10 pt. in size. Authors should use the Table option of MS Word to create tables, rather than tabs, as tab-delimited columns are often difficult to format in .pdf for final output.

Figures and schemes should also be placed in numerical order in the appropriate place within the main text. Numbers, titles and legends should be provided for all schemes and figures. These should be prepared as a separate paragraph of the main text and placed in the main text before the figure or scheme. Chemical structures and reaction schemes should be drawn using an appropriate software package designed for this purpose. As a guideline, these should be drawn to a scale such that all the details and text are clearly legible when placed in the manuscript (i.e. text should be no smaller than 8-9 pt.).

For bibliographic citations the reference numbers should be placed in square brackets, i.e., [ ], and placed before the punctuation, for example [4] or [1-3], and all the references should be listed separately and as the last section at the end of the manuscript.

(Download template file at [www.mijst.mju.ac.th](http://www.mijst.mju.ac.th))

### Format for References

#### Journals:

1. D. Buddhasukh, J. R. Cannon, B. W. Metcalf, and A. J. Power, "Synthesis of 5-n-alkylresorcinol dimethyl ethers and related compounds *via* substituted thiophens", *Aust. J. Chem.*, **1971**, *24*, 2655-64.

*Texts:*

2. A. I. Vogel, "A Textbook of Practical Organic Chemistry", 3rd Edn., Longmans, London, 1956.

*Chapter in an Edited Text:*

3. P. H Gore, in "Friedel-Crafts and Related Reactions" (Ed. G. A. Olah), Vol. 3, Interscience, London, 1964, Ch. 31.

*Thesis / Dissertation:*

4. W. phutdhawong, "Isolation of glycosides by electrolytic decolourisation and synthesis of pentinomycin", *PhD. Thesis*, 2002, Chiang Mai University, Thailand.

*Patents:*

5. K. Miwa, S. Maeda, and Y. Murata, " Purification of Stevioside by Electrolysis", *Jpn. Kokai Tokkyo Koho* 79 89,066 (1979).

**Referees**

Authors should suggest at least 3 referees with appropriate technical expertise, although the editor may not necessarily approach them. Their addresses, homepage addresses, phone and fax numbers and e-mail addresses should be provided as fully as possible.

**English corrections**

This journal is published in English, so it is essential that for proper refereeing and quick publication all manuscripts be submitted in grammatically correct English and style. For this purpose we ask that non-native English authors ensure that their manuscripts are checked before submitting them for consideration. We suggest that for this purpose your manuscript be revised by an English speaking colleague before submission.

**Submission**

Manuscripts should be submitted by e-mail to [duang@mju.ac.th](mailto:duang@mju.ac.th)

# Maejo International Journal of Science and Technology

ISSN 1905-7873

Available online at [www.mijst.mju.ac.th](http://www.mijst.mju.ac.th)

Invited Article

## Journal impact factors--their use and misuse

Robert Molloy\*

*Dr. Robert Molloy has been a lecturer in Physical Chemistry in the Department of Chemistry, Faculty of Science, Chiang Mai University, since 1978. His area of specialisation is Polymer Chemistry and he is the Coordinator of the Polymer Research Group. He is also International Relations Adviser to the Dean of the Faculty of Science and an Associate Editor of the Chiang Mai Journal of Science.*



\*E-mail: [robert@chiangmai.ac.th](mailto:robert@chiangmai.ac.th)

Received: 26 May 2008 / Published: 13 June 13, 2008

**Abstract:** With increasing importance being attached nowadays to doing research and writing papers for publication, the question of journal selection arises. Apart from the obvious criterion of choosing a journal which corresponds with the subject area of the paper, it has become fashionable to use the *journal impact factor* as a criterion for selection. Indeed, it is almost as though the value of the impact factor is becoming more important than the journal itself. But what exactly is this “impact factor” and how useful is it?

---

Historically, the idea of an impact factor was first mentioned by Eugene Garfield in *Science* magazine in 1955 [1]. That paper is considered to be the primordial reference for the concept of what we know today as the *Science Citation Index*. Some years later, in the early 1960s, Garfield and Irving Sher created the *journal impact factor* to help select journals for

the new Science Citation Index. The impact factor was based on 2 elements: the *numerator*, which is the number of cites in a given year to articles published in the journal in the previous 2 years, and the *denominator*, which is the number of articles published in the journal in the same previous 2 years. Thus, a journal's impact factor for 2007 would be:

$$\text{Impact Factor 2007} = \frac{\text{number of cites in 2007 to articles published in 2005 + 2006}}{\text{number of articles published in 2005 + 2006}}$$

Nowadays, both journals and publishers alike attach great importance to their impact factors. If they are high enough, they use them for promotional purposes. This is a far cry from Garfield's original intention. At the *International Congress on Peer Review and Biomedical Publication* in Chicago, USA, in 2005, Garfield reflected on the past 50 years since his original idea and commented:

*"In 1955, it did not occur to me that "impact" would one day become so controversial. Like nuclear energy, the impact factor is a mixed blessing. I expected it to be used constructively while recognizing that in the wrong hands it might be abused."*

During its lifetime, the impact factor has gradually evolved into being an indicator that now far outweighs its intended purpose. For example, it now influences research assessments, grant applications, and even staff promotions in ways that Garfield could never have imagined. Even in its main role as an index of journal impact, its value is often overstated. I have heard it said, even by respected academics, that journals with impact factors of less than 1 are not worth considering for publication. But the fact is that there are many high quality journals in the fields of science, technology and engineering with impact factors of less than 1. Our Polymer Research Group, for example, has just had a paper published in the journal *International Polymer Processing* which is generally regarded as being one of the leading journals for the polymer industry worldwide, yet it has a 2006 impact factor of 0.563. This is because some journals, especially industry-related journals, tend to publish a proportionately larger number of articles (the denominator) that are general interest rather than research articles and which tend not to be cited (the numerator). Other journals simply publish in specialist areas that are well read by a particular community but are also not well cited. This skewness of citations amongst journals is well known and is one of the main arguments used by critics of the impact factor.

In addition to the impact factor, there are two other indicators created by the Institute of Scientific Information (ISI) which are used to measure how a journal receives citations to its articles over time. These are the so-called *immediacy index* and the *cited half-life*. The immediacy index is a measure of how quickly items in a journal get cited after publication, while the cited half-life is a measure of how long articles in a journal continue to be cited after publication. However, neither the immediacy index nor the cited half-life is as commonly used as the impact factor. Consequently, this article focuses its attention on the impact factor and the extent to which it is used or misused as the case may be.

One of the least appreciated, or simply misunderstood, features about the impact factor is how variable it is with respect to both sociological and statistical factors [2]. Sociological factors include the subject area of the journal, the type of journal (letters, full papers, reviews), and the average number of authors per paper (which is related to subject area). Statistical factors include the size of the journal and the length (years) of the citation measurement window (usually 2 years but sometimes as long as 5 years). Some examples of how these various factors affect a journal's impact factor and the precautions that should be taken in making comparisons are listed below:

- **Subject Area** - Generally, fundamental and pure subject areas have higher average impact factors than specialized or applied ones. Indeed, this variation can be so great that the top journal in one field may have a lower impact factor than the bottom journal in another field. To refer back to the previous example, it is meaningless to compare the 2006 impact factors of *International Polymer Processing* (= 0.563) with, say, the *Journal of Organic Chemistry* (= 3.790) or even the *Journal of Polymer Science, Part A: Polymer Chemistry* (= 3.405). Comparisons of impact factors should only be made for journals in the same subject area.
- **Multiple Authorship** - The average number of authors per paper also varies according to subject area, from the social sciences (about 2) to the fundamental life sciences (about 4). Given the tendency of authors to cite their own work, it is therefore not surprising that journals in subject areas with a higher average number of authors per paper have higher average impact factors.

- **Article and Journal Type** - Even within the same subject area, there are significant variations in impact factor due to article and journal type. For example, review journals invariably have higher impact factors than other types of journals simply because review articles attract more citations and review journals publish relatively fewer articles.
- **Journal Size** - Journal size in terms of the number of articles published per year is a statistical factor that affects the extent to which the journal's impact factor varies from year to year. As would be expected, the smaller the number of articles, the greater the variation. It has been estimated that, year to year, the impact factors of smaller journals (< 35 articles per year) vary on average by more than  $\pm 40\%$ , whereas those of larger journals (> 150 articles per year) vary only by around  $\pm 15\%$  [2]. This does not mean that smaller journals are less consistent in their standards. It simply means that the impact factor of a smaller journal needs to vary more than that of a larger journal to be statistically significant. Thus, small increases in impact factor from one year to the next are often statistically insignificant, despite what journals and publishers may say. As a rule of thumb, it can be considered that journals in the same subject area with impact factors that differ by less than 25% belong together in the same rank.
- **The Numerator/Denominator Problem** - Since the impact factor is a ratio, clear and unambiguous definitions for the top (numerator) and bottom (denominator) terms are essential. But what exactly counts as a paper? Do letters to the editor or editorials or "Viewpoint" articles such as this count? ISI classifies papers into various categories such as research articles, reviews, proceedings papers, editorials, letters to the editor, news items, etc. Whereas only those classified as research articles, reviews and proceedings papers are counted in the denominator, citations to all papers (including editorials, letters to the editor and news items) are counted for the numerator. This can lead to an exaggerated impact factor, but more so for some journals than others. For example, letters to the editor in medical journals (which are not "letter papers" in the sense used in physical science journals) often attract lively debate resulting in significant numbers of citations, thus enhancing the numerator without adding to the denominator. This so-called "numerator/denominator problem" is yet another example of why considerable care needs to be taken when using impact factors.

With these observations in mind, we can now return to the title of this article: ***Journal Impact Factors – Their Use and Misuse***. It is fair to say that, over the years, journal impact factors have been the subject of much debate which has given rise to many conflicting opinions. Hoeffel [3] expressed an opinion shared by many that:

*“Impact Factor is not a perfect tool to measure the quality of articles or journals but there is nothing better and it has the advantage of already being in existence and is, therefore, a good technique for scientific evaluation. Experience has shown that in each specialty the best journals are those in which it is most difficult to have an article accepted, and these are the journals that have a high impact factor. Most of these journals existed long before the impact factor was devised. The use of impact factor as a measure of quality is widespread because it fits well with the opinion that we have in each field of the best journals in our specialty.”*

Personally, I would not disagree with this view. The system is clearly not perfect but it is the best that we have. Some observers, including librarians, have argued that the numerator (number of cites) in the impact factor calculation is much more relevant to a journal’s “impact” than the denominator (number of articles). Therefore, why not weight them differently or just ignore the denominator completely and consider only the number of cites. They claim that this would also bring review journals more into line with research journals since the high impact factors of review journals are artificially enhanced by the relatively low number of articles that they publish. The detailed arguments for and against impact factors are too numerous to mention here. Suffice it to say that it is not so much their “use” as their “misuse” (some would say “abuse”) which is the main cause for criticism.

Returning to the theme of journal selection, it was mentioned at the start of this article that there is a growing trend for aspiring authors to select journals primarily by impact factor rather than journal content. In my opinion, while the impact factor is certainly important, it should not be the prime consideration in journal selection. The prime consideration should be the suitability (in terms of content and style) of the journal itself for the subject matter of the paper. Not only does this enhance the paper’s chances of being accepted, it also ensures that it will be read by fellow workers in the same specialist field. Going for a higher impact factor in a less suitable journal only increases the risk of rejection.

In conclusion, journal impact factors are undoubtedly useful if used constructively. Until someone comes up with a better idea, they are here to stay for the foreseeable future, probably with some fine adjustments along the way. Since the idea of an impact factor was first introduced in 1955, it has undergone an amazing transformation from being an obscure bibliometric indicator to being the chief quantitative measure of the quality of a journal. However, when impact factors start being used to assess the quality of research work, the researchers who wrote the paper, and even the institution in which they work, we are entering dangerous territory. Impact factors are certainly useful as indicators of the influence that a particular journal has within in its own subject area, but they are not direct measures of research quality. With this in mind, we should accept the limits of their usefulness and be extremely careful not to venture into areas where they can be misused.

#### **References (cited in the text)**

1. E. Garfield, "Citation indexes to science: A new dimension in documentation through association of ideas", *Science*, **1955**, 122, 108-111.
2. M. Amin and M. Mabe, "Impact factors: Use and abuse", *Perspectives in Publishing*, No. 1, 1-6 October **2000**.
3. C. Hoeffel, "Journal impact factors" [letter], *Allergy*, **1998**, 53, 1225.

#### **Additional References (not cited in the text)**

4. R. Molloy "Journal impact factors – How useful are they?", *Chiang Mai J. Sci.*, **2007**, 34, 269-271.
5. J. Svasti and R. Asavisanu, "Aspects of quality in academic journals: A consideration of the journals published in Thailand", *Science Asia*, **2007**, 33, 137-143.

*Review Article*

## **Potential of wind power for Thailand: an assessment**

**Stuart Major<sup>1</sup>, Terry Commins<sup>2,\*</sup> and Annop Noppharatana<sup>2</sup>**

<sup>1</sup>Energy Consultant, Melbourne, Australia

<sup>2</sup>Pilot Plant Development & Training Institute, King Mongkut's University of Technology Thonburi, Ratburana, Bangkok 10140, Thailand

\* Author to whom correspondence should be addressed, e-mail: [thefox@loxinfo.co.th](mailto:thefox@loxinfo.co.th)

*Received: 23 January 2008 / Accepted: 22 March 2008 / Published: 31 March 2008*

---

**Abstract:** This paper reviews the potential for wind-power generated electricity in Thailand by means of a wide-ranging literature survey. Proposed application at a university campus is used as a case study to demonstrate that wind power is unlikely to be economically competitive where grid-connected electricity is available. The need for improved low wind speed turbine performance for Thai applications is highlighted by comparing the output of commercially available wind turbines with the characteristics of Thai wind; the challenges of improving low wind speed turbine performance are discussed. It is concluded that for Thailand in the foreseeable future the benefits of economic wind power electricity generation will probably be confined to small remote isolated installations including traditional applications.

---

### **Introduction**

Energy extraction from the wind is philosophically appealing, having a negligible impact on the energy content of the resource itself and minimal, if any, physically destructive side effects. However, the energy intensity of the wind itself is generally low, as well as being quite variable, which means that for significant electrical power generation applications, large installations (i.e. combinations of turbine numbers and sizes) are required at favourable wind locations, which in turn are often remote from electrical load centres and from transmission grid networks.

While the demand on some of the other (non-renewable) resources required, e.g. construction materials, may be small, the additional infrastructure resources required for grid connected systems including backup power generation capacity can be large. Worldwide, there is currently more than

about 48 GW of installed wind power generating capacity (representing about 0.6 % of total world electricity production, with capacity growing at around 20% pa), of which Thailand has less than 0.001%. However, for Thailand the economics of wind power installations may be unattractive and not competitive with other alternative energy sources now, or in the foreseeable future.

This paper was originally prepared as the result of an internal Joint Graduate School of Energy and Environment/ King Mongkut's University of Technology, Thonburi, (JGSEE/KMUTT) study on the potential for wind-power generated electricity for the Bangkhuntien Campus of KMUTT. It developed into a more general review of the wind power potential for Thailand. The paper has now been reviewed to determine whether the original findings should be modified in the light of developments in wind technology knowledge in the intervening 4 years.

A wind map has been produced for Thailand [1], which combines and updates the wind speed data previously available. Thailand experiences generally very low wind speeds with typically average speeds of not above 3 m/s. A Department of Energy Development and Promotion, Thailand (DEDP) report [2] produced around the same time as the wind map identifies in general terms the potential wind resource available for power generation as follows (Table 1):

**Table 1.** Wind energy potential in Thailand [1, 2]

Average wind speed and characteristic	Poor (<6m/s)	Fair (6-7m/s)	Good (7-8m/s)	Very Good (8-9m/s)	Excellent (>9m/s)
Land area (sq. km.)	477,157	37,337	748	13	0
% of Total land area	92.6	7.2	0.2	0	0
MW potential	NA	149,348	2,992	52	0

Note: For large wind turbines only. Potential MW assumes an average wind turbine density of 4MW per square kilometre and no exclusion for parks, urban or inaccessible areas. Wind speeds are for 65m height in the predominant land cover with no obstructions.

Those areas identified as having sufficiently high wind speeds for practical electricity power generation are for the most part inland areas presenting accessibility difficulties (as would be offshore sites) and therefore the potential for economic wind power generated electricity is probably considerably less than that indicated in the table.

The physical requirements for useful energy extraction remain as discussed in the original KMUTT study – the problem of the cubic relation between wind speed and power generating capacity remains. Currently available commercial wind turbines generally have the following characteristics:

- cut-in wind speed of 4 to 5 m/s (large turbines) and 3 to 4m/s (small)
- peak-power generation wind speed of  $\pm 15$  m/s (large) to  $\pm 12$  m/s (small)
- cut-out wind speed of  $\sim 25$  m/s
- capability to safely withstand storm force winds of  $\sim 60$  m/s +

An example of wind speed – power characteristics for the Bonus (Siemens) commercial range of wind turbines (Table 2) is given in Figure 1.

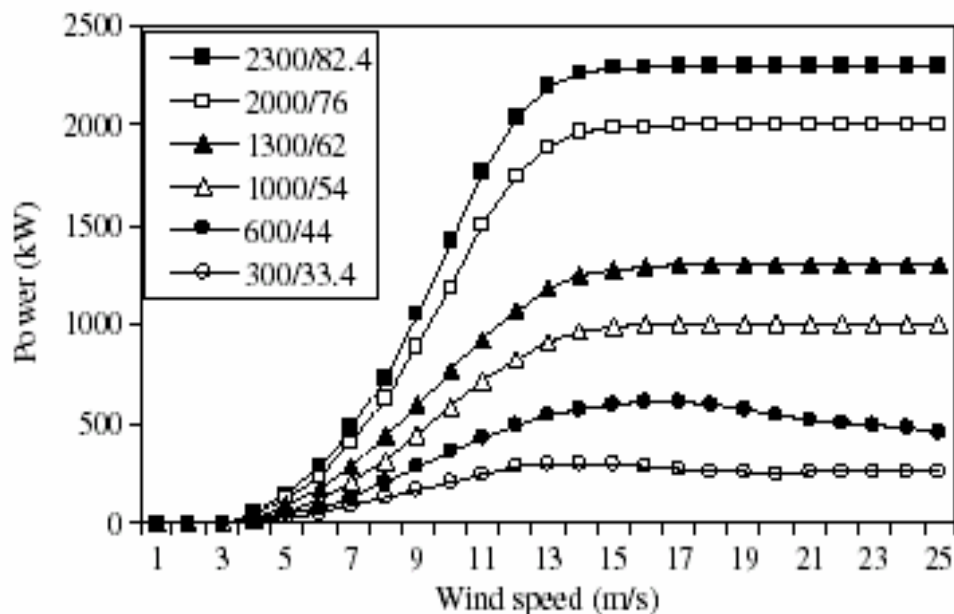


Figure 1. Turbine wind speed-power characteristics [3]

Table 2. Technical data of wind machines used in the analysis [3]

Wind machine	Cut in speed (m/s)	Cut out speed (m/s)	Rated speed (m/s)	Rated output (kW)	Hub height (m)	Rotor diameter (m)
Bonus 2300/82.4	3	25	15	2300	60	82.4
Bonus 2000/76	4	25	15	2000	60	76
Bonus 1300/62	4	25	14	1300	45	62
Bonus 1000/54	3	25	14	1000	45	54
Bonus 600/44	3	25	13	600	35	44
Bonus 300/33.4	3	25	13	300	30	33.4

The turbine performance profiles outlined above do not match well with the Thai monsoonal climate where near still air conditions alternate with high turbulence, giving overall very low average wind speeds. For reference, tables of wind power classes have been developed in the literature [4], as provided in the following examples (Table 3). It is evident from the current review that wind turbine and technology developments in the “low wind speed” zones refer to developments around class 3 – 4 wind speeds indicated in the above table. It seems that such developments are not at sufficiently low wind speeds to be of significant benefit to most potential Thai applications.

However, a detailed economic assessment of the significance of the wind resource potential identified in the DEDP report and table (Table 1) cited previously might be justified. Also, the potential for rural applications where the performance and economics of modern turbine types could be compared with traditional types in applications such as water pumping, battery charging, etc., particularly in remote areas, could usefully be investigated.

Finally, wind power globally is facing increasing obstacles, aside from economic or wind speed considerations. The situation of wind power in Australia, for example, and the climate for investment in this technology has recently become very uncertain as a result of the Australian Federal Government decisions not to increase support for MRET (Mandated Renewable Energy Target) by increasing its

**Table 3.** Wind power classes [4]

Elevation	10m		50m*	
Power class	Wind speed m/s	Power density W/m <sup>2</sup>	Wind speed m/s	Power density W/m <sup>2</sup>
1	0	0	0	0
	4.4	100	5.6	200
2	5.1	150	6.4	300
	5.6	200	7.0	400
3	6.0	250	7.5	500
	6.4	300	8.0	600
4	7.0	400	8.8	800
	9.4	1000	11.9	2000

\* Showing elevation effect based on 1/7 power law

level (the proposed/installed capacity required to meet the original 2% target is already virtually satisfied), and to suspend wind farm project approvals, even where State Government planning approval processes have been successfully negotiated and completed, on the basis of local community group objections on the grounds of landscape unsightliness and possible hazard to migratory birds. Thus Government regulation and attitude together with community consultation have become critical issues in Australia even where technology and wind conditions are favourable.

### Case Study for KMUTT Bangkhuntien Campus

The following simple analysis is based on the premise that suitable low wind speed turbines were to become available for \$US 1,000 per kW installed, and that the performance of the Cape Promthep (Phuket) 150 kW installation can be used as a “model” [5].

Assuming the annual mean wind speed at Bangkhuntien is 3.5 m/s, and taking the data [5] for the 150 kW installation delivering 1300 kWh/kW pa with a mean wind speed of 4.6 m/s (i.e., a 15% availability), and noting that wind power density is a function of wind speed cubed, then for Bangkhuntien, the availability would be approximately 7%, i.e. deliverable energy would be about 600 kWh/kW pa, i.e.  $(3.5/4.6)^3 \times 1300$ .

So, if it is assumed that the annual electricity demand at Bangkhuntien is given by E kWh, then  $(E/600) \times 1000$  (US\$)  $\times 44$  (Baht/US\$) = Installation capital cost = 73E Baht, and the required

installed capacity would be  $73E/(44 \times 1000)$  MW. Now, assuming a 20-year lifetime, and 10% pa of capital cost for operation and maintenance charges, and another 10% pa for interest charges, then the total lifetime costs would be  $73E \times (1 + 20 \times 0.1 + 20 \times 0.1) = 73E \times 5 = 365E$ , and the cost per kWh delivered over the lifecycle would be  $365E/20E = 18.25$  Baht/kWh

The above analysis is very flexible and small changes in any of the assumptions, such as performance, operation/maintenance and financing costs, would make a large difference to the result. Also, since the original study, the exchange rate has varied considerably. It should be noted, however, that with the very intermittent nature of Thai wind, alternative standby power supplies and/or very large storage capability (perhaps by pumped storage?) would be required to ensure continuity of electricity supply. The costs associated with this requirement have not been factored in, but would need to be included in any accurate and complete analysis. The conclusion is thus that electricity costs from wind power generation would be about one order of magnitude greater than electricity purchased from the grid (at around 2.5 Baht/kWh).

## Thailand's Wind Regime and Scenario

### *Wind speeds*

From the Thailand Meteorological Department (Bangkok) and for the river mouth Pilot Station, monthly mean wind speeds taken from climatological data 1966 – 1995 are reported below (min. – max). The figures in { } are taken from “Solar and Wind Energy Potential Assessment of Thailand”, a KMITT (now KMUTT) report from 1984 [7]:-

- Pilot Station: 3.4 – 5.6 m/s (max 60 m/s)
- Bangkok Metropolis: 1.2 – 2.5 m/s (max 45m/s) {2.37 m/s}
- Klong Toey: no data (max 29 m/s)
- Don Muang: 2 – 2.9 m/s (max 53 m/s) {3.13 m/s}
- From the above reference, the highest mean wind speeds reported for any location in Thailand are:
  - Petchaburi: 4.9 m/s
  - Pilot Station: 5.6 m/s
- The further data [6] shown below confirms the generally low wind speeds experienced in Thailand:
  - Mean wind speed: < 5 m/s (range for Ubon 2.20 – 3.74 m/s; Haad Yai 3.6 – 4.35 m/s)
  - Per cent calm period: a maximum of 48% (range from 35%) at Ubon, 93% at Haad Yai, and 35 – 46% at Phuket

### *Power densities*

Exell [6] also includes power density information such as at Prachuapkhirikan, an annual mean of  $92 \text{ W/m}^2$  (seasonal range 43 – 227), Songkhla 160 (80 – 240) and Phuket 168 (40 – 280).

From KMITT report [7], the following comments are made: “... wind speeds < 5m/s may be suitable for water pumping applications...”; “...wind speeds > 5m/s could meet a significant % of the energy needs of the country...”, and also information given: “...that wind power densities >  $500 \text{ W/m}^2$

are available over the ocean.”; “...wind power densities > 200 W/m<sup>2</sup> are available over some limited land areas.”

Note that available wind energy P<sub>a</sub>/A (i.e. the power density x power coefficient = electricity production potential) is expressed by the power law:

$$P_a / A \text{ (W/m}^2\text{)} = 0.5 \times C_p \text{ (power coefficient)} \times \rho \text{ (air density)} \times V^3 \text{ (air speed)}$$

A value for C<sub>p</sub> = 0.4 has been assumed; this is the C<sub>p</sub> achieved by most turbines running optimally. The maximum value obtainable is 0.593 (the Betz limit). An interactive model available at the Australian Wind Energy Association’s (Auswea) website (see Appendix) for a range of turbine sizes at wind speeds probably in excess of those likely at Bangkhuntien has been run with the results as shown in Table 4.

Thus assuming C<sub>p</sub> = 0.4 and taking ρ = 1.16 (from [6]), then P<sub>a</sub> /A = 0.232 x V<sup>3</sup> which becomes, for the following wind speeds,

2 m/s: 1.86 W/m<sup>2</sup> (or, expressed as power density, 4.65)

4 m/s: 14.8 W/m<sup>2</sup> (37)

6 m/s: 50.1 W/m<sup>2</sup> (125)

These figures are in line with, or somewhat below, the mean power densities quoted for Thai locations above. They appear to be below the power densities needed for useful/economic electricity production.

**Table 4.** Auswea interactive wind energy model

Wind speed m/s	Rotor diameter m	Efficiency assumed (optimal ~ 40%)	Power output kW
5	10	40	10
5	50*	40	120 (~1 MW*)
5	5	40	2.5
3	10	50	2.7
4	20	40	20

\* This is approximately the size of turbine being used to generate 1 MW under northern European conditions: thus for Thai wind conditions the power output would be around 10% of rated capacity (see also conclusions for Bangkhuntien campus analysis).

*Selected quotes from relevant reports*

The above statements are supported by a number of reports [5,8-15], from which the following comments have been extracted:

“...analysts...find insufficient wind resources...Thailand...” (p.31 of [8]);

“...it is recognised that there is no useful power output until about 10 mph (about 4.5 m/s)...” (p.5 of [8]);

“...little justification for any extensive promotion of wind power...” (p.2 of [5]);

“...as a rule of thumb...average annual wind speed between 5 and 7 m/s (is required) before it will be profitable to operate with wind energy schemes.” [5];

“...where (an)...average wind speed above 5 – 6 m/s is never reached...avoid investment in wind turbine technology except for test and research...” (private communication received from Ramboll as a follow-up to [5]);

“...money better spent on other technologies...” (follow-up to [5]);

“...based on Phuket wind measurements...and a 600 kW wind turbine...payback period, 37 years.” (p.2 of [5]);

“...average wind speed needed for economically viable projects (even with ‘favourable’ power purchase rates) = 8 m/s...” (p.179 of [9]);

“Wind generation – being reassessed” (p.16 of [10]);

“...In general, winds exceeding 5 m/s are required for cost effective application of small grid-connected wind machines, while wind-farms require wind speeds of 6 m/s...” [11];

“...In general, sites with a Wind Power Class rating of 4 or higher (i.e. > 5.6 m/s at 10 m elevation) are now preferred for large scale wind plants...” [11];

“...The average wind speed in Thailand is moderate to rather low, usually lower than 4 m/s.” [12];

“...constraints affecting wind energy in Thailand:-

- absence of specific financing schemes designed to support wind energy development
- absence of grid for connection in many rural areas
- the lack of wind data which is sufficiently accurate
- industry standards to allow wind site identification
- some existing wind turbines not functioning
- low level of wind technology capacity” [13];

“...As of 2003, a total capacity of 1.5 MW of (wind-driven) water pumps and wind turbines delivering a total capacity of 0.388 MW have been installed mostly by the Electricity Authority of Thailand (EGAT) and DEDE. Currently the production cost of electricity for wind turbines is estimated to be between 0.11 and 0.13 US\$/kWh.” [14,15].

## **The Challenge of Low Wind Speed Regimes**

Clearly the development of wind turbines capable of significant energy extraction at wind speeds below the normal low wind speed regime (i.e. < class 4 wind) is a major challenge. The US Department of Energy [4] states that the research goal of the Low Wind Speed Technology activity is “By 2012 to reduce the cost of electricity from large wind systems in Class 4 winds to 3 c/kWh for onshore systems or 5 c/kWh for offshore systems.” Technology improvements are stated as being needed in the following points:

- Turbine rotor diameters must be larger to harvest the lower energy winds from a larger inflow area without increasing the cost of the rotor.
- Towers must be taller to take advantage of the increasing wind speed at greater heights.
- Generation equipment and power electronics must be more efficient to accommodate sustained light wind operation at lower power levels without increasing electrical system costs.

Under the title “Wind Energy Resource Potential”, it is concluded that areas designated Class 4 or greater are suitable with advanced wind turbine technology under development today and that Class 3

may be suitable for future technology. Class 2 areas are marginal and Class 1 unsuitable for wind energy development.

The paper from which the following comments are drawn [16] addresses some of the issues involved. Comparison is made between the performance of commercially available machines and a postulated hypothetical low wind speed machine. The conclusion drawn is that "...To achieve a large power output in low wind speed areas, a group of small wind machines ...designed for a low cut-in speed might be much more appropriate than a single, large stand-alone high rated power output wind machine.", and "... proper matching between its designed operating wind condition and the frequency distribution of wind speeds at a site is the prime factor..."

Substantial and ongoing R&D effort will be required to support low wind speed studies, including the development of appropriate test facilities such as that reported by Wahab and Tong [17] and investigations of low wind speed performance such as those by Wright and Wood [18]. Of course, for practical installations, the questions of capital and operating cost and service life have to be considered as well as sunk R&D costs. In fact, the technical and the economic aspects would need to be brought together along with social and political considerations for any successful application.

### Overall Economics of Wind Power

There have been many cost comparisons between different electricity generating technologies. A recent example [19] provides the following data based on UK applications ('2004 pUK/kWh):

- Combined cycle gas turbine: 2.2
- Coal (all types): 2.5 – 3.2
- Nuclear power: 2.3
- Onshore wind: 3.7 (rising to 5.4 allowing for back up generating capacity)
- Offshore wind: 5.5 (rising to 7.2 allowing for back up)
- Wave & marine: 6.6
- Biomass: 6.8

An article in *Power Generation World* [20] cited wind power generation costs at US\$/kWh 0.03 – 0.06 compared to approximately US\$/kWh 0.04 for fossil fuels while other reports [14,15] give the wind power generation cost between 0.11 – 0.13 US\$/kWh.

In an article in the *National Geographic Magazine* (2005) (see Appendix for details), approximate power costs in USc/kWh are given as: coal – 5, natural gas – 5.5, wind – 6, nuclear – 7, solar – 22. Another source [21] provides some comparative information on operating, maintenance and fuel costs in USc/kWh (1985) for different electricity generating technologies as follows: wind – 1, coal – 2.3, nuclear – 1.9, gas – 4.2, oil – 5.3. Even if these figures were only very approximate and have changed with the passage of time, they do suggest that the running costs of wind turbines are not insignificant.

Comparisons of generating costs from published data can be difficult because it is not always clear whether the full life cycle costing has been undertaken and all relevant costs have been included. For example, it is not known whether the following have been included in any analysis:

- planning approval and design (including R&D costs where relevant),
- construction costs (including off-site works where required, e.g. strengthening transmission systems, providing for additional generating capacity, etc.),

- operating costs including fuel sourcing, supply and waste disposal, plant maintenance and refurbishment, etc.,
- at the end of service life, the total cost of decommissioning and storage and disposal where required,
- all environmental costs, e.g. climate levies (carbon taxes or credits), land remediation, etc.,
- the cost of financing the necessary investments.

These costs are very site, region and date specific.

### **Commercially Available Wind Turbine Generator Technology**

Wind turbines are commercially available across a very wide range of generator outputs, from a few watts to several megawatts. In this paper there have been several references to data taken from the webpages of wind turbine manufacturers. A listing of a selection of these suppliers is included in the Appendix. Also included is a reference to a provider of software suitable as an aid to designing wind turbine generating systems as well as to providers of more general wind power information.

### **Conclusions**

It would appear from this investigation that there is no justification for investing effort on wind power projects for grid connected electricity production at any scale, and no justification for such an electricity generating installation at the Bangkhuntien campus. There may be some justification for continuing to work on projects intended for remote area applications, where mean wind speeds are at the upper end of reported data for Thailand (e.g. 4–5 m/s), for example for water pumping application.

Thus at Bangkhuntien it could be recommended that studies continue along the path of existing work being undertaken of wind turbines suitable for intermittent loads such as water pumping operating under low wind speed conditions. This work might be immediately applicable to situations such as that at the salt farms to the south-west of Bangkhuntien where traditional windmills are still in use, or for prawn farms.

It should be mentioned that while wind systems may not be currently economically or technically attractive, nonetheless it would be useful for Thailand to have technical capability in this area (as provided by the Cape Promthep installation) and for potential hybrid situations, such as at remote national parks. A continuing watching brief on overseas technology would be appropriate not only to wind turbine developments for low wind speed conditions, but also to developments in such associated equipment as batteries, e.g. versatile systems based on technology similar to fuel cell technology which could simplify the output electrical power conditioning constraints for wind turbines and which could well make some difference to viability.

However, it would be of some concern, based on the low wind potential noted above and in the previous reports from which comments have been drawn, if the statements reported in the Bangkok Post (Business Pages) of late December 2001 were accurate, i.e. that “...energy conservation plan ... key projects ... promoting ... wind power ...” If true, this would appear to be a misallocation of resources.

The correspondence of January 8<sup>th</sup> and 13<sup>th</sup>, 2002 in the same newspaper together with an article profiling the EGAT Governor's views of 21<sup>st</sup> January, 2002 all covered the same ground, with the latter drawing a similar conclusion to that of the authors.

### Acknowledgements

The authors would like to thank the following for their interest and input at various stages during the preparation of the original report and of this paper: Dr. Chullapong Chullabodhi, Mr. Jocelyn Harvey, Professor Robert Exell, Dr. Chumnong Sorapipatana, Dr. Naksitte Coovattanachai and Dr. Bundit Fungtammasan.

### References

1. TrueWind Solutions, "Wind energy resource atlas of Southeast Asia", prepared for The World Bank—Asia Alternative Energy Program, Albany, New York, **2001**.
2. Department of Energy Development and Promotion (DEDP), "Wind resource assessment of Thailand", **2001**. (See also [www.netmeter.org/en/wind](http://www.netmeter.org/en/wind))
3. E. Kavak and S. Alkpinar, "An assessment on seasonal analysis of wind energy characteristics and wind turbine characteristics", Report, Firat University, Turkey, **2004**. (Also from [www.powergeneration.siemens.com](http://www.powergeneration.siemens.com))
4. U.S. Department of Energy, "Wind energy resource potential", Energy Efficiency and Renewable Energy Wind and Hydropower Technologies Program, **2006** ([www.eere.energy.gov/windandhydro](http://www.eere.energy.gov/windandhydro)).
5. Ramboll Consultants (Denmark), "Wind energy – resources and technologies", Report for NEPO/DANCED (National Energy Policy Office, Thailand/Danish Energy Development Consultants), **1998**.
6. R. H. B. Exell, "The wind energy potential of Thailand." *Solar Energy*, **1985**, 35, 3-13.
7. USAID Project Report No. 493-0304, "Solar and wind energy potential assessment of Thailand", **1984**, Ch. 4, p. 4.1. The following are also listed in this reference:-
  - [7A] K. Sitathani, "Analysis of wind energy potential in Thailand", *Masters Thesis*, **1984**, KMITT, Thailand.
  - [7B] B. Ngernswas, "The Analysis of the wind situation in Thailand and design for local turbines", Department of Mechanical Engineering, KMITNB, **1981**.
  - [7C] P. Siripurkpong, B. Suwantragul, B. Ngernswas, and K. Sitathani, "Estimated wind energy potential in Thailand", KMITT – TPA (Thai – Japan), **1981**.
8. "The potential for wind energy in developing countries", Report by Strategies Unlimited (with US Windpower Inc. for DOE/World Bank), **1988** (ISBN 0-88016-073-X and Library of Congress 88-50452).
9. "Wind energy technology", Report, JGSEE Library, TJ 820.W181, **1997**.
10. "Thailand energy strategy and policy", Summary report for NEPO, **1999**.
11. "Wind energy topics", downloaded from the USA DOE website linking to the American Wind Energy Association (AWEA) website (at [www.eren.doe.gov/RE/wind](http://www.eren.doe.gov/RE/wind) and [www.awea.org/faq](http://www.awea.org/faq)).

12. "Thailand – energy and natural resources", report prepared for the National Identity Office by Energy Policy and Planning Office, **2003** ([www.eppo.go.th](http://www.eppo.go.th)).
13. "Renewable energy in Asia – the Thailand report", by Australian Business Council for Sustainable Energy, Melbourne, Australia, **2005**.
14. R. M. Shrestha, S. Kumar, S. Martin, and N. Limjeerajarus, "Report on role of renewable energy for productive uses in rural Thailand", prepared for Global Network on Energy for Sustainable Development (GNESD), Asian Institute of Technology, Thailand, **2006**.
15. "Report on renewable energy development and planning", Department of Alternative Energy Development and Efficiency (DEDE), Ministry of Energy, Thailand, **2004**.
16. C. Sorapipatana, "A method for determining the suitability of commercial wind machines for a given wind regime", *RERIC International Energy Journal*, **1994**, 16, 125-134.
17. A. A. Wahab and C. W. Tong, "Development of an indoor testing facility for low speed wind turbine research activities", *Proceedings of the 2<sup>nd</sup> Regional Conference on Energy Technology Towards a Clean Environment*, Phuket, Thailand, **2003**.
18. A. K. Wright and D. H. Wood, "The starting and low wind speed behaviour of a small horizontal axis wind turbine", Report, University of Newcastle, Australia, **2004**.
19. P. B. Power, "Professional engineering", Report, Royal Academy of Engineering (RAE), UK (referenced from Institution of Mechanical Engineers, UK), 10 March **2004**, p. 5.
20. Power Generation World, "Wind power generation becomes competitive", April **2003** ([www.powergenerationworld.com](http://www.powergenerationworld.com)).
21. "Wind turbine technology", Report, JGSEE Library, call no. TJ 828.W763), **1994**, p. 208.

## Appendix

The following are supplier listings but are not comprehensive:

### 1. Wind power software and general information

- Australian Wind Energy Association, [www.auswea.com.au](http://www.auswea.com.au) , includes a model for power generation estimates (2002).
- "Wind Turbine Technology Briefing Notes", The British Wind Energy Association, 2006, [www.bwea.com](http://www.bwea.com)
- American Wind Energy Association, [www.awea.org](http://www.awea.org)
- HOMER micropower optimization model as an aid to off-grid and grid connected systems, National Renewable Energy Laboratory – NREL, US, [www.nrel.gov/homer](http://www.nrel.gov/homer) (see also the model Windographer @ [www.mistaya.ca/windographer](http://www.mistaya.ca/windographer))
- National Geographic Magazine, August, 2005: p2 "Powering the Future" ([www.nationalgeographic/magazine/0508](http://www.nationalgeographic/magazine/0508))
- BP Global Energy Review – World wind energy and other data at end 2004, ([www.bp.com/sectiongenericarticle](http://www.bp.com/sectiongenericarticle))

### 2. Wind turbine hardware suppliers

- Wind Energy Businesses in the World – from Source Guides – for detailed listings of suppliers by country [www.energy.sourceguides.com/businesses](http://www.energy.sourceguides.com/businesses)

- Siemens Wind Power (previously Bonus @ [www.bonus.dk](http://www.bonus.dk)): 22 kW to 2.3 MW range: (5800 turbines in operation – installed capacity 4500 MW) [www.powergeneration.siemens.com/en/windpower](http://www.powergeneration.siemens.com/en/windpower)
- Swift Silent Rooftop Wind Energy System, UK, 1.5 kW, [www.renewabledevices.com](http://www.renewabledevices.com)
- NEG-MICON: (7,400 turbines in operation – 23% of world generating capacity – 16% annual growth rate in MW installed – future offshore installations in 3 – 5 MW range), Denmark, [www.neg-micon.dk](http://www.neg-micon.dk)
- US Wind Turbine, [www.uswindturbine.com](http://www.uswindturbine.com), 1kW – 5 MW\_range
- Windstream Power Systems, US. ([www.windstreampower.com](http://www.windstreampower.com)), 0.1 kW
- Travers Aerogenerateurs, France, 0.3 kW – 12.5 kW range, [www.travers.com](http://www.travers.com)

### 3. Information on the wind power situation in Thailand

- Electricity Authority of Thailand – [www.egat.or.th](http://www.egat.or.th) - which gives details of the Cape Promthep, Phuket wind power installation – turbines 22 – 150 kW (as at 2002)

*Full Paper*

## **Vehicle jack with wedge mechanism**

**Ademola A. Dare<sup>1</sup> and Sunday A. Oke<sup>2,\*</sup>**

<sup>1</sup> Department of Mechanical Engineering, University of Ibadan, Ibadan, Nigeria

<sup>2</sup> Department of Mechanical Engineering, University of Lagos, Akoka-Yaba, Lagos, Nigeria

\* Author to whom correspondence should be addressed, e-mail: [sa\\_oke@yahoo.com](mailto:sa_oke@yahoo.com)

*Received: 29 November 2007 / Accepted: 28 March 2008 / Published: 31 March 2008*

---

**Abstract:** In many developing countries, particularly Nigeria, the high cost of production of a vehicle jack and the prevailing economic situation has made the commercial production of vehicle jacks difficult. Thus, the development of an appropriate technology for a vehicle jack would be of vital utility to vehicle users. This paper presents the design and construction of a low-price, simple mechanical jack with wedge mechanism to provide a lift of about 160 mm with a self-locking capability for both small- and medium-sized vehicles. The design calculations involve the evaluation of applied force required, the screw shaft design, and the lift head design analysis. The fabricated jack was tested on some small and medium vehicles, which resulted in a good lift without any pre-manual lifting. The jack weighs about 4 kg and costs about ₦1000 per unit.

**Keywords:** vehicle jack, screw system, wedge mechanism, vehicle lifting

---

### **Introduction**

A very important repair tool in the automobile industry is the vehicle jack. Essentially the jack is used in raising a vehicle sufficiently above the ground to remove tyres when required. A vehicle owner without a jack will, at an unguarded moment, suffer loss in time, finance and energy. Although the vehicle jack does not contribute directly to the smooth running of a vehicle engine, yet its availability is crucial during tyre deflation.

There are two broad types of vehicle jack that can be obtained in practice, viz. the mechanical type and the hydraulic type [1, 2]. The mechanical jack can be of the scissors type or of a simple screw jack. When the scissors jack is placed in position under a vehicle, the rotation of the handle causes the frame to rise, thus producing a lift of the vehicle. When it is not in use (unload condition), the handle is

given reverse rotation, which collapses the frame and makes it compact enough for packaging. For a simple screw jack in operation, two gearwheels are meshed so that their shafts are at an angle of  $90^\circ$  to form a bevel gear. One gearwheel locates the handle while the other contains an internal thread in its bore that meshes with the load screw. By rotation of the handle, the driving gearwheel is rotated and this is transmitted to the driven gearwheel, which also induces a lift of the load arm and consequently a lift of the vehicle. The second type of the vehicle jack, the hydraulic type, has its lift provided by hydraulic fluid forced against the load head by a reciprocating motion of the handle. This jack has a higher mechanical advantage compared to mechanical jacks.

Three possible factors militate against the purchase and use of a jack. First the cost is a crucial factor that limits the purchase of a vehicle jack. It is known that in the present circumstances of many developing countries, the prices of imported vehicle jacks are high, thus limiting the number of potential buyers to the few. The second factor relates to the fact that failure encountered in some jacks is more frequent and effective repair difficult. For instance, in the scissors jack excessive load acting on the driving screw frequently causes wear on the screw. Repairs as locally done on this jack involve re-threading the screw and/or welding of the shaft when there is breakage, whereas a more effective approach is to reproduce the square threaded screw shaft or at least order for spares that are not easily disposable to the local metal shop. The third problem confronting the use of vehicle jacks relates to inadequate facilities and personnel. A commercial production fulfilling all design requirements of existing jacks requires special equipment which includes a thread-rolling machine, a gear hobbing machine and other facilities. All these are expensive and technical personnel required are scarce. It is important to note that while vehicle jacks exist in their varieties, a consideration of another option, a wedge jack, that may be used in a developing country is reasonable. The literature on this type of jack seems to be either nonexistent or poorly documented. This is the motivation for the current paper. In particular, this paper presents the design and construction of a low-priced, simple wedge jack to provide a lift of about 160mm with a self-locking capability for both small- and medium-sized vehicles.

## **Design and Development**

By considering all the problems discussed in the previous section, a proposal is now made on the possibility of designing and developing a wedge jack that can be used for vehicles in developing countries. At this stage, it is important to describe the vehicle wedge jack designed and developed. The jack consists of five main parts, viz. the lift head, the sliding wedge, the driving screw, the handle, and the jack body (Figure 1). The lift head is constructed of a mild steel pipe capable of supporting compressive load from the vehicle. The contact surface is cylindrical and coated with high lubricating fluid. In constructing the sliding wedge, a flat steel bar is used with a black hole to locate the drive nut. The slope angle is kept at  $45^\circ$  to minimise space. For the driving screw, the forward and backward movements of the sliding wedge are provided by a threaded shaft that is located via a bushing. The screw is made of hardened steel to withstand excessive wear and loading. At the slotted top of the screw is the handle. The handle transmits motion and energy from the user to the load. By constant clockwise rotation of the handle, the sliding wedge is driven forward and this induces a vertical motion

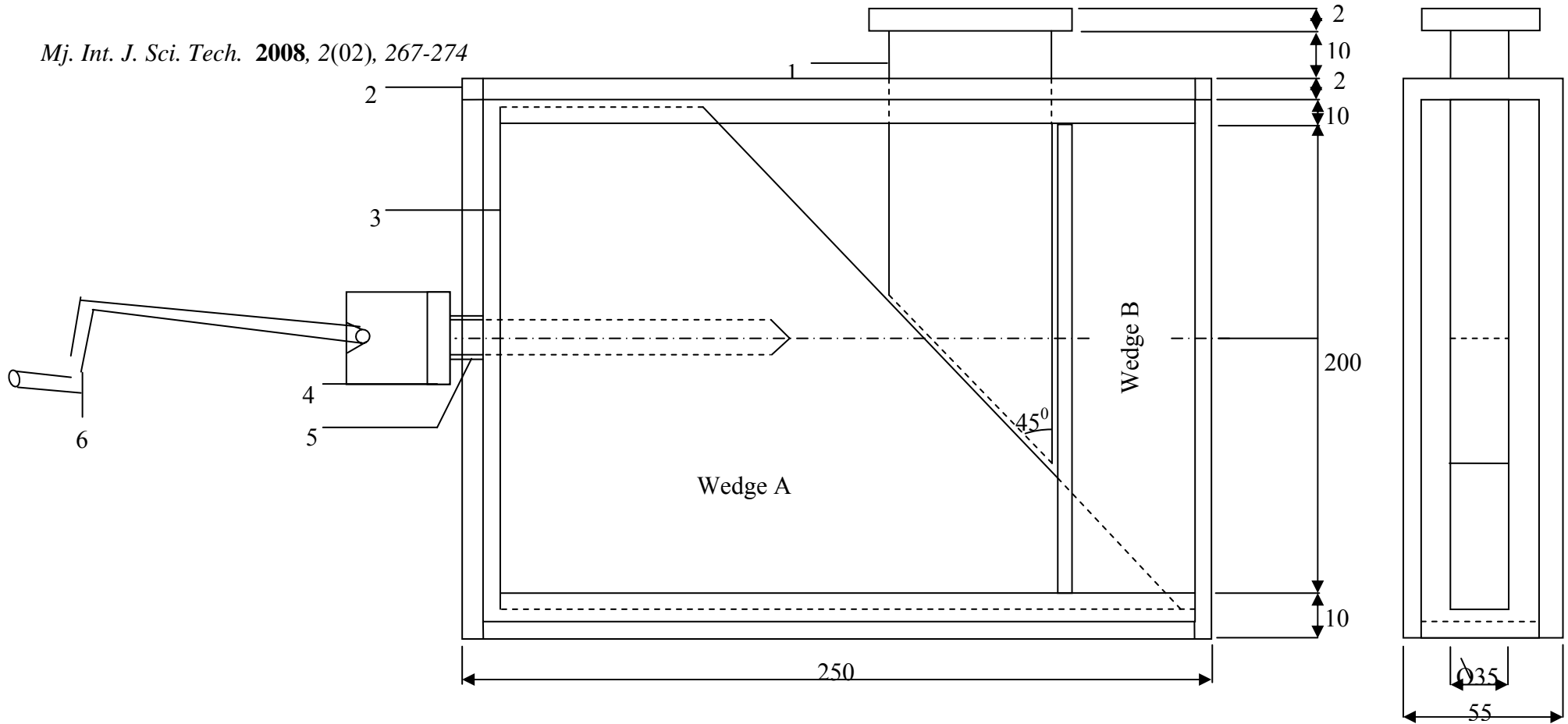


**Figure 1.** Wedge jack and components

All dimensions in millimeters. (For all other unspecified dimensions, use 5 mm.)

Part no.	Description	Quantity
1	Lift head body	1
2	Body	1
3	Sliding wedge	1
4	Slotted screw	1
5	Driving nut	1
6	Handle	1

on the load head giving the desired lift. The handle axis lies at different inclination to the horizontal resulting in the estimated mechanical advantage of about 120 based on ergonomic and other considerations. The handle is made of a steel rod with a welded pin at the end to locate the slot on the driving screw. The jack body is fabricated from a 2-mm flat bar. A back plate locates the bushing from which the screw rotates. The front portion is uncovered to allow the sliding wedge to traverse the whole length. The lift head guide is welded to the top cover of the body.

Consideration is given to the fact that a low technology product is desired for ease of use. It has to be cheap, light, potable, and operated with minimum effort. It is desired that the jack provides a lift of about 160mm. In order to obtain the design data, reference is made to Bosch Automobile Handbook [3]. Tables 1-3 were compiled from Bosch Automobile Handbook 2 [3]. From Table 1, it is observed that the minimum ground clearance for common passenger cars is 120 mm.

**Table 1.** Ground clearance for common passenger cars in Nigeria [3]

Type of car	Ground clearance (mm)
Audi CC	120
BMW 318	125
BMW 524	140
Escort 1.4 cc	140
Sierra 1.8 GL	120
Peugeot 505 GR	120
Peugeot 305 GLD	120
Renault R4 GTL	175
Accord Ex	160
Mazda 323 Lx 1.3	150
Toyota Corolla 1.3 GL	160

Thus, in essence this implies that the maximum height of the jack cannot be more than 120mm, otherwise it will be physically impossible to place the jack directly under the chassis before providing a manual lift. Equally, from Table 2, the maximum inflated tyre thickness which constitutes the minimum lift for clear raising from ground is 130 mm.

**Table 2.** Inflated tyre thickness for some selected passenger cars [3]

Type of car	Inflated tyre thickness (= minimum lift) (mm)
Audi CC	116
BMW 524	123
Peugeot 505 GR	123
Sierra 1.8 GL	116
Accord Ex	130
Mazda	109
Toyota Corolla 1.3 GL	123

This also constitutes a useful guide in jack proportioning in the design data. The maximum weight from the range of vehicles tabulated in Table 3 is 1,660 kg. Since about 2/3 of the weight will

be on the engine side, and this will equally be shared between the two tyres at the engine side, the maximum load on the jack (W) will be 610 kg.

**Table 3.** Curb weight and maximum weight for selected passenger cars in Nigeria [3]

Type of car	Curb weight (kg)	Max weight (kg)
Audi CC	950	1410
BMW 524	1310	1810
Peugeot 505 Sr	1215	1655
Sierra 1.8 GL	1065	1600
Accord Ex	1105	1660
Mazda	880	1450
Toyota Corolla	865	1385

At this stage, an evaluation of applied forces is done. The forces are evaluated from the standpoints of wedges A and B, which are indicated in Figure 1. The basic equations for the evaluation of applied forces, as presented by McGill and King [4] are as follows:

- (Nomenclature:  $\mu$  = coefficient of friction  
 $F_1, F_2$  = frictional forces  
 $N_1, N_2$  = normal forces  
 $P$  = applied load  
 $W$  = vehicle load  
 $D$  = diameter of shaft  
 $D_i$  = linear diameter of shaft  
 $D_o$  = outer diameter of shaft  
 $FS$  = factor of safety  
 $\theta, \alpha$  = angle of inclination  
 $E$  = modulus of elasticity  
 $L$  = lift distance  
 $\pi$  = 3.142  
 $W_{cr}$  = critical load to cause bucking  
 $P_{cr}$  = critical applied load)

For wedge A (see Figure 1), summing up forces along the x-axis yields

$$P - F_1 \cos \theta - N_1 \sin \theta - F_2 = 0 \tag{1}$$

$$F_1 \sin \theta + N_2 - N_1 \cos \theta = 0 \tag{2}$$

$$F_2 = N_2 \tag{3}$$

$$F_1 = \mu N_1 \tag{4}$$

For wedge B (see Figure 1):

$$N_1 \sin \alpha - F_3 - P = 0 \tag{5}$$

$$N_1 \cos \alpha - N_3 = 0 \tag{6}$$

$$F_3 - \mu N_3 = 0 \tag{7}$$

By substituting (3) and (4) into (1) and (2), also substituting equation (7) into (5), four basic equations are obtained as follows:

$$P - \mu N_1 \cos \theta - N_1 \sin \theta - N_2 = 0 \quad (8)$$

$$\mu N_1 \sin \theta + N_2 - N_1 \cos \theta = 0 \quad (9)$$

$$N_1 \sin \alpha - \mu N_3 - W = 0 \quad (10)$$

$$N_1 \cos \alpha - N_3 = 0 \quad (11)$$

These equations are solved for input values of  $\theta$ ,  $\alpha$ ,  $\mu$  and  $W$ . The next stage is to utilise specific design values of  $\theta = 45^\circ$  (for minimum traverse length),  $\alpha = 45^\circ$  (lift head being vertical),  $\mu = 0.20$  (metal to metal contact),  $W = 7982\text{N}$  (actual load x FS) (vehicle load), where FS is the factor of safety given as 1.5. Now, by substituting these values in the set of equations (8) to (11), we obtain  $P = 5096\text{N}$ , which is the load on the screw required to advance the screw in the direction of loading. For the screw shaft design, the screw is treated as a column subjected to the point load  $P$ . The critical load to cause buckling, defined as  $W_{cr}$ , is expressed as

$$W_{cr} = \frac{\pi^3 E D^4}{256 L} = P \quad (12)$$

Given that  $E$  is the modulus of elasticity of the material, and  $L = 160\text{mm}$  (minimum lift + 30 mm), then  $D$  is obtained as 15 mm. This is the required screw diameter to transmit the load applied. The lift head is another item to design. The lift load is treated as a column. Thus, the governing equation used, represented as  $P_{cr}$  or  $W$ , is defined as follows for the hollow section:

$$P_{cr} = W = \frac{\pi^3 E (D_o^4 - D_i^4)}{256 L} \quad (13)$$

By substituting appropriate values and solving iteratively, this yields  $D_o = 35\text{mm}$  and  $D_i = 30\text{mm}$ .

## Product Fabrication and Test

Based on the design proposed above, a model jack was fabricated and tested on some common passenger cars found in Nigeria, which have low and medium ground clearance. The material used for fabrication were mainly steel plates and iron rods. Test results show that the jack gave a good lift without any pre-manual lifting. Also, the jack weighs about 4 kg, which is an acceptable weight in comparison with other kinds of mechanical jacks (Table 4). The information provided in Table 4 also ascertains that a cost of ₦1,000 (\$1 = ₦125) is within the range for other mechanical jacks. However, the large-scale production of this specimen is expected to considerably reduce its production cost to a very competitive price.

**Table 4.** Cost and weight comparison of some jacks [5]

Type of jack	Weights range (kg)	Cost range (₦)
Mechanical	2.5-4	1000-3000
Hydraulic	2.5-5	1000-2500
Designed wedge jack	4	1000

On a careful observation, the merits derivable from the production of the jack fall into three classifications: operation performance, manufacturing techniques, and self-locking capability. For its operational performance, it is noted that failure in the driving screw could not be rampant because the dead load is not directly acting on it, which in turn minimises wear. The basic manufacturing required offers benefits in terms of manufacturing. The techniques required are welding and machining, thus making it easier to produce in a machine shop and consequently reducing the level of skillful personnel required. In addition, on operation the jack is automatically self-locked by the wedge base and has near-zero danger level of unloading the system. This may be induced in some jacks by worm thread or gear teeth.

## Conclusions

A vehicle-lifting technology has been developed, which is an option that might be easily adapted in developing countries. The wedge jack which has been designed, fabricated, and tested offers a comparatively good performance as well as a comparative price range and certain advantages. It is believed that the use of wedge jack will make a positive influence on the vehicle-lifting industry. Since the novelty of the work lies in the fact that this is the first time that the current design is reported in a systematic way, several directions of thoughts needs to be investigated in future studies to make the product mature.

## Acknowledgements

Oturuhoyi Omamerhi and O. E. Akingbemen, who were former students of the first author are gratefully acknowledged for the motivation towards investigating into the area covered by this paper. Many thanks also go to Engineer Adeyinka Oluwo, who assisted with the drawing.

## References

1. P. Gallina, "Vibration in screw jack mechanisms: experimental results", *J. Sound and Vibration*, **2005**, 282, 1025-1041.
2. M. S. Garcia, M. Nouillant, and P. Viot, "Study and improvement of a high speed hydraulic jack", *J. Phys. IV France*, **2006**, 134, 775-781.
3. BOSCH Group, "Automotive Handbook", 1<sup>st</sup> English Edn., Dept. of Technical Publications, Stuttgart, **1976**.
4. D. J. McGill and W. W. King, "Engineering Mechanics-Statics", 2<sup>nd</sup> Edn., PWS-KENT, Boston, **1989**, p. 403-408.
5. O. E. Akingbemen, "Design and construction of mechanical jack using wedge mechanism", Unpublished Final Year Undergraduate Project, University of Ibadan, Nigeria, **1995**.

Full Paper

## **Determination of abscisic acid hormone (ABA), mineral content, and distribution pattern of $^{13}\text{C}$ photoassimilates in bark-ringed young peach trees**

**A. B. M. Sharif Hossain<sup>1\*</sup> and Fusao Mizutani**

The University Experimental Farm, Department of Bioresource Production Science, The United Graduate School of Agricultural Science, Ehime University, Hattanji 498, Matsuyama shi 799-2424, Japan

<sup>1</sup>Present address: Laboratory of Plant Physiology and Biochemistry, Institute of Biological Science, Faculty of Science, University of Malaya, 50603 Kuala Lumpur, Malaysia

\* Corresponding author, e-mail: [sharif@um.edu.my](mailto:sharif@um.edu.my) , [sharifhort@yahoo.com](mailto:sharifhort@yahoo.com)

Received: 1 November 2007 / Accepted: 2 April 2008 / Published: 23 April 2008

---

**Abstract:** Abscisic acid (ABA), mineral content, and  $^{13}\text{C}$  photoassimilates in young leaf, shoot and root of peach trees (*Prunus persica* Batsch cv. Hikawahakuho) as affected by phloemic stress (bark ring) were studied. The trees were treated as control (no phloem ringing), partial phloem ringing (PR) and complete ringing (CR). Phloem ringing was made by peeling out 2 cm length of bark (phloem) from the trunk leaving a connecting 2 mm thickness of phloem strip (a band) while complete ringing (CR) left no phloem strip. Free, bound and total ABA content in peach shoot and leaf were higher in CR and PR treated trees than in control trees. The N and Ca content in the root were higher in PR and CR than in control.  $^{13}\text{C}$  photoassimilates were higher in leaf, shoot and upper trunk in PR and CR than in control. The results show that PR and CR increase ABA content in leaf,  $^{13}\text{C}$  photoassimilate content in shoot and leaf, and mineral content in root. The increase in the hormone (ABA) and mineral content in the leaf and root seems to affect the overall plant nutrition that leads to small-sized peach trees.

**Keywords:** abscisic acid, mineral content,  $^{13}\text{C}$  photoassimilates, dwarfing, partial ringing, complete ringing, peach trees

---

## Introduction

Phloem ringing as represented by partial ringing is a horticultural practice used to manipulate tree growth, development, and fruit growth in a variety of fruit species. Small, compact, dwarfed or size-controlled fruit trees provide for easier pruning, thinning, spraying, harvesting, high production of high-grade fruit and lower cost of production [1]. The primary factor limiting the use of size-controlled rootstocks in stone fruit production is the lack of suitable rootstocks with a wide range of compatibility among cultivars [2]. Jose [3] found that girdling treatments cause lower vegetative growth in relation to control in mango trees.

Arakawa et al. [4] reported that trunk growth of apple trees is significantly increased above the girdling point and reduced below it. Onguso et al. [5] reported that the increase of trunk circumference above the girdle might be caused by swelling of the trunk due to the accumulation of carbohydrates. They also stated that girdling blocks the translocation of sucrose from leaf to root through the phloem bundles. The block decreases the starch content in the root and accumulates sucrose in the leaf. Rose and Smith [6] found that complete girdling of the stems kills the plants and partial girdling weakens the plants.

It has been reported that spraying one-year-old peach shoot with ABA increases their lignin content and dwarfs the plant [7]. A sudden increase in endogenous ABA has been demonstrated for several stress phenomena like salinity, relative humidity, osmotic root stress and wilting [8]. Furthermore, the fruits brought about an increase in leaf ABA levels in soybean within several hours [9]. Goldschmidt et al. [10] observed that accumulation of ABA indeed reflects the tissue response to senescence-inducing stimuli. Davies [11] stated that girdling results in diminished N, P and Ca level in the leaf on the girdled branch compared with ungirdled one. However, there is few available literature on ABA, mineral content and  $^{13}\text{C}$  photoassimilates as affected by bark ringing. This study was undertaken to determine the ABA, mineral, and  $^{13}\text{C}$  photoassimilate content in peach trees and to obtain a quantitative estimation of the changes which occur during senescence as affected by phloem restriction (girdling) on the trunk.

## Materials and Methods

### *Experiment 1*

#### *Site*

The experiment was carried out in an orchard in the Ehime University Farm located in southern Japan.

#### *Plant material*

Two-year-old peach trees (*Prunus persica* Batsch cv. 'Hikawahakuho') grafted on peach seedling stocks (wild form) were used in this experiment during April 2004. The seedling rootstocks were collected from the nursery (potted seedling) and transplanted in the main field on 13 April 2004. The rootstocks were planted by maintaining pit. The pits were spaced at 0.60 m x 1.0 m. The tree height was 1.0 m initially and the trunk circumference and diameter was about 6 cm and 2.3 cm respectively. Weeding was done by maintaining row as required. Compound fertilisers were applied after

transplanting at the rate of 10% (w/v) each of N, P<sub>2</sub>O<sub>5</sub> and K<sub>2</sub>O per tree. Irrigation was applied once a week by hose pipe. Insecticide was applied once a month.

#### Treatment setting

Treatments were set on 13 June 2004. Partial ringing (PR) was done by using a small sharp knife to remove a 2-cm length of partial ring leaving a 2-mm width (thickness) of a connecting strip (bridge) in the trunk 20 cm above the ground (Figure 1). In case of complete ringing (CR) there was no connecting bridge or strip. There were 3 treatments (control, PR, and CR), each performed in quadruplicate. For each replication each individual tree was used. There were thus a total of 48 (4 x 3 x 4) trees used for four dates ((June 20, June 27, July 11 and August 10) for ABA and mineral content analysis.

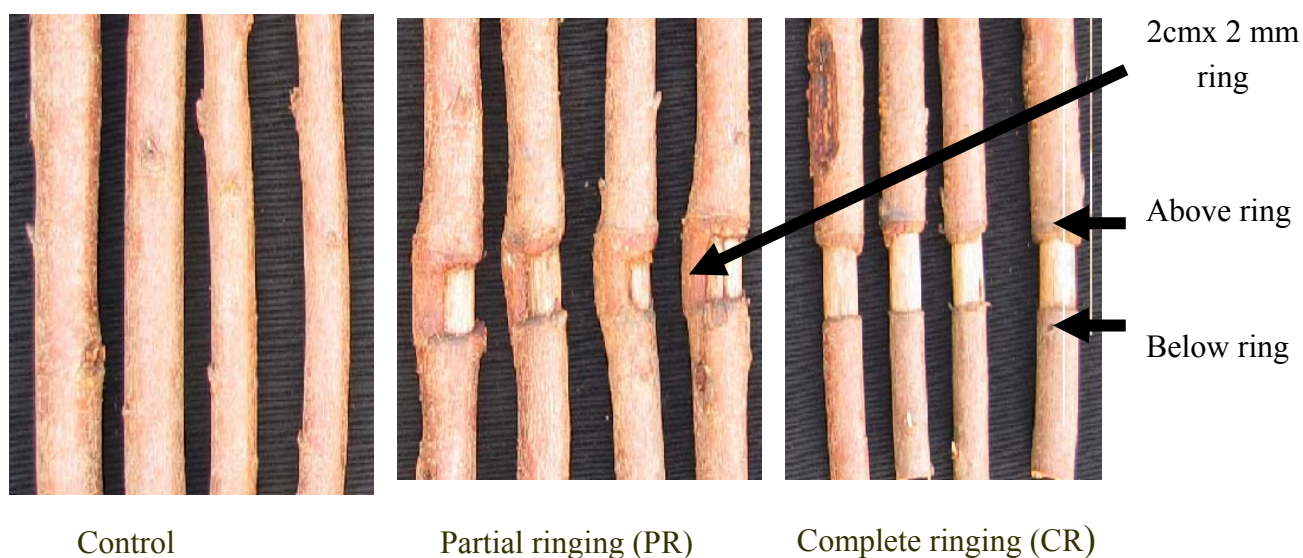


**Figure 1.** Photographs showing ringing structure and trunk circumference of peach trees as affected by partial and complete ringing (PR and CR)

#### Sample collection and preparation for ABA and mineral content analysis

Young leaf (at upper part of ringing), shoot and root samples were collected on the 1st, 2nd, 4th and 8th weeks after treatment (June 20, June 27, July 11 and August 10). Twelve trees were uprooted and washed on each date for ABA and mineral content analysis. Fresh leaves were separated, washed and kept in the freezer immediately after harvest and used for ABA analysis. Shoots and roots were used for mineral analysis.

#### Abscisic acid (ABA) analysis

The analysis was carried out according to the method of Most et al. [12]. A sample (1 g) was homogenised in 80% ethanol and filtered. They were then concentrated in vacuo to the aqueous phase using a rotary evaporator. The aqueous phase was mixed with insoluble polyvinyl pyrrolidone (PVP) (500 mg/5ml H<sub>2</sub>O) and filtered. The pH of the filtrate was adjusted to 8.5 using 5% NH<sub>4</sub>OH followed by partitioning with CH<sub>2</sub>Cl<sub>2</sub> (4 x 10 ml). The organic phase was discarded and the pH of the aqueous phase was adjusted to 3 using 1 M HCl. Partitioning was again repeated four times with CH<sub>2</sub>Cl<sub>2</sub> as

explained above. The organic phase in turn was partitioned four times, each with 10 ml of a bicarbonate buffer (pH 10), and the alkaline aqueous phase was separated. The organic phase, containing free ABA was evaporated to dryness in vacuo.

For hydrolysis of bound ABA, the pH of the acidic aqueous phase was adjusted to 10.5 with 5% NH<sub>4</sub>OH, then heated in a water bath at 60 °C for 45 min. The solution was left to cool at room temperature for 1 h and the pH was adjusted to 3 with 1 N HCl and partitioned four times with CH<sub>2</sub>Cl<sub>2</sub>. The organic phase was retained and evaporated to dryness in vacuo.

The methylation of ABA and the GC conditions were as follows. A prepared sample (1g) containing ABA was dissolved in 5 ml acetone/methanol (9/1) and the methylation with diazomethane was carried out using a method modified from Schlenk and Gellerman [13]. The test tubes were arranged with tube 1 containing acetone, tube 2: carbitol, KOH and NMSA (n-methyl-n-nitroso-p-toluenesulfonamide) (5 g/50 ml acetone), and tube 3: the sample dissolved in acetone/methanol. Nitrogen gas was passed through the sample for 3 min. The sample was evaporated overnight at room temperature with the help of a fan. The sample was taken up in 1ml acetone and 1 µl injected into a Gas Chromatograph (GC-8A, Shimadzu, Kyoto, Japan) equipped with an electron capture detector (<sup>63</sup>Ni) and a glass column packed with Gaschrom Q (80-100 mesh) coated with 2% silicon OV-7. The injection/detector and column temperature were 240 °C and 230 °C respectively. The flow rate of the carrier gas (N<sub>2</sub>) was 40 ml/min.

#### *Mineral content analysis*

One-gram of ground shoot or root samples was placed in a crucible and dry-ashed by heating in a muffle furnace for 5 h at 550° C. One ml of 20% HCl was added to the residue which, after decantation of the acid solution, was rinsed with distilled water (2 x 1 ml). Finally 17 ml distilled water were added to the combined acid and rinses to make a 20 ml solution. This stock solution was used to measure K, Ca and Mg by an atomic absorption spectrophotometer (Shimadzu AA-6200, Kyoto, Japan). Phosphorus (as molybdate-reactive P) was estimated by a colorimetric method at 620 nm (Hitachi U-2001, Tokyo, Japan). For N analysis, 20 mg of leaf samples were taken and analysed by means of a CN coder (Sumitomo NC-80, Tokyo, Japan) [13].

#### *Experiment II*

##### *Plant material*

Potted (φ 30cm) two-year-old peach trees (*Prunus persica* Batsch. var. 'Hikawahakuho') grafted on wild peach rootstocks were used in this experiment in late July 2004. The treatments were the same as in Experiment 1. There were a total of 9 trees used in the experiment.

##### *<sup>13</sup>C labelling experiment*

The trees above the graft union were enclosed inside transparent polyethylene bags. <sup>13</sup>CO<sub>2</sub> was generated by reacting 5.0 g of <sup>13</sup>C-rich BaCO<sub>3</sub> (supplied by Nippon Chemical Industries Co. Ltd, Japan) with 50% lactic acid in a Petri dish inside the bag. A small fan was used to circulate the air in

the bag. The temperature in the bag during  $^{13}\text{CO}_2$  treatment was maintained at 25-30° C by intermittent misting over the bags.

#### *Plant sample collection and $^{13}\text{CO}_2$ analysis*

$^{13}\text{C}$  labeling was carried out for 3 h from 9:00 to 12:00 a.m. on July 31, 2004. The trees were uprooted and washed, and shoots, leaves, trunks and roots were separately collected 24 h after  $^{13}\text{CO}_2$  feeding. The samples were oven-dried (heated at 90° C for 1 h to terminate enzyme activity and dried at 60° C for 3 days), ground and used for analysis of  $^{13}\text{CO}_2$ . One milligram of each sample was used to determine the isotopic ratio between  $^{12}\text{C}$  and  $^{13}\text{C}$  in the sample by combustion using an infrared  $^{13}\text{CO}_2$  analyser (JASCO EX-130S; Japan Spectroscopic Co. Ltd., Tokyo). The % excess of  $^{13}\text{C}$  was calculated by subtracting the concentration of  $^{13}\text{C}$  atoms in nature from the measured concentration in tissues fed with  $^{13}\text{CO}_2$ .

#### *Design and statistical analysis*

Treatments were set following a completely randomised design repeated in different trees. Mean separation was done by Duncan's multiple range test (DMRT) at 5 % level of significance.

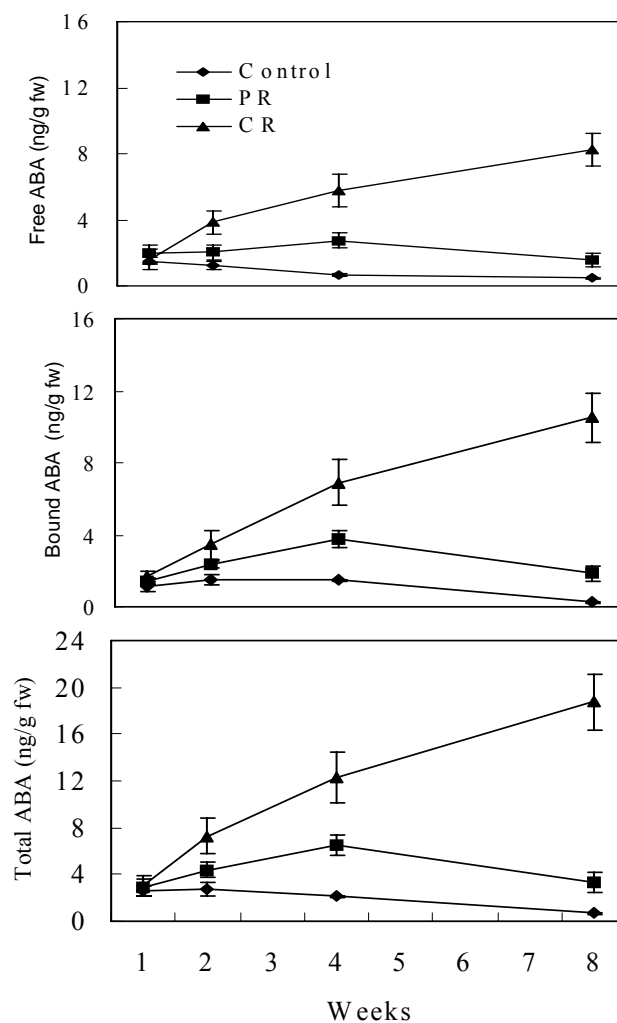
## **Results and Discussion**

Figure 1 shows the effect of partial and complete ringing on the trunk diameter after treatment. In control trees, no changes were observed above and below the ringing girdle. However, the trunk diameter increased above the ring and decreased below the ring in PR- and CR-treated trees compared to control (Table 1). Free ABA content was also higher in PR- and CR-treated trees than in control trees (Figure 2). In CR trees, free ABA content increased during the following 8 weeks, whereas in PR trees free ABA content increased more slowly up to the 4th week, then declined. For bound ABA content a similar trend was observed in both CR and PR trees. Total ABA content was also highest in CR followed by PR trees, both being more than in control trees (Figure 2). The percent nitrogen and calcium were lower in PR and CR trees than in the control for new shoot, old shoot and leaf, but it was higher in CR trees in the case of root (Figures 3-4). This may probably be due to the break in the connection between the upper and lower part of the ring. The percent phosphorous, potassium and magnesium content were found to be lower in the ringing treatments than in the control for shoot, leaf and root (Figures 5-7).

**Table 1.** Trunk circumference of peach trees as affected by PR and CR

Treatment	Trunk circumference (cm)			
	Initial	Above ring (A)	Below ring (B)	Ratio (A/B)
Control (no ringing )	6.2a	6.4b	6.5a	1.01b
PR (partial ringing)	6.1a	6.8a	6.6a	1.03b
CR (complete ringing)	6.1a	6.9a	6.3b	1.09a

Note: Means in column followed by the same letter are not statistically different at 5 % level of significance by Duncan’s multiple range test (DMRT).



**Figure 2.** Free, bound and total ABA content in leaf of peach trees as affected by partial and complete ringing (PR and CR). Vertical bars indicate SE (n = 4).

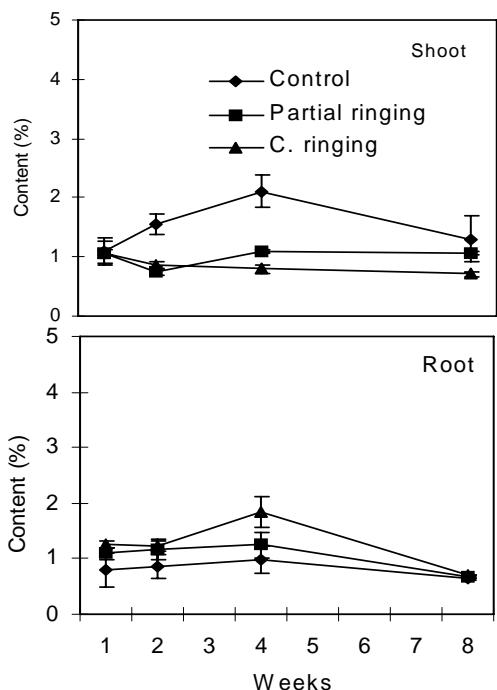


**Figure 3.** Nitrogen content in shoot and root of peach trees as affected by ringing. Vertical bars indicate SE (n = 4).

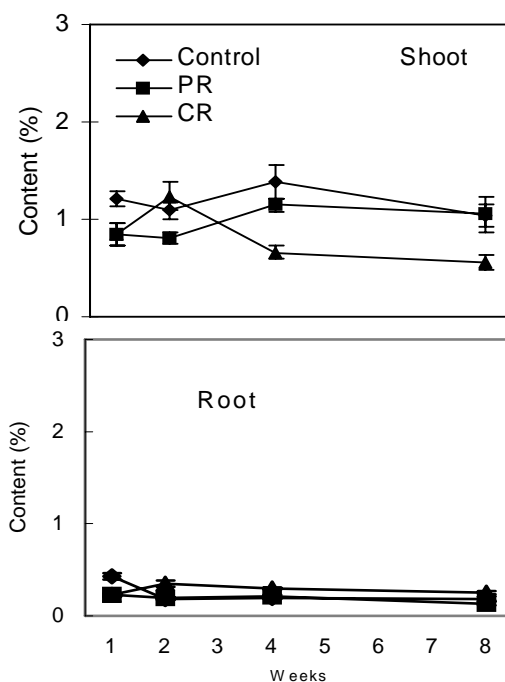


**Figure 4.** Calcium content in shoot and root of peach trees as affected by ringing. Vertical bars indicate SE (n = 4).

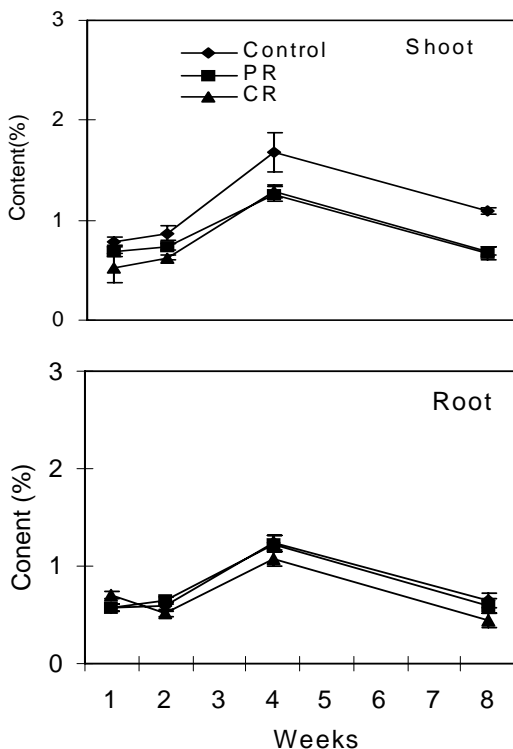


**Figure 5.** Phosphorus content in shoot and root of peach trees as affected by ringing. Vertical bars indicate SE (n = 4).

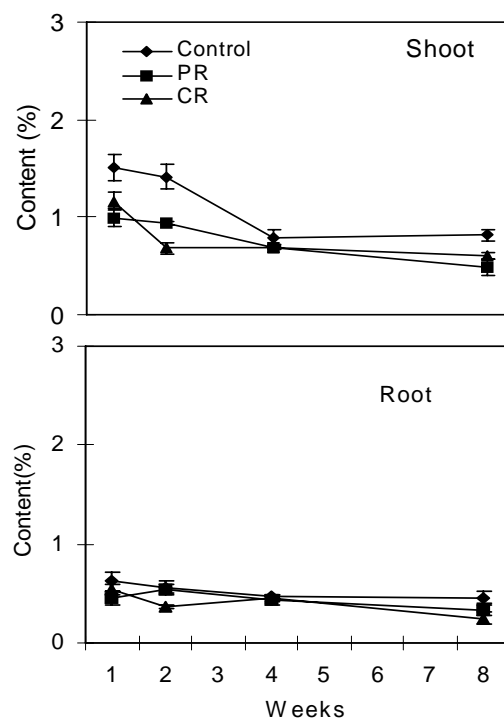


**Figure 6.** Potassium content in shoot and root of peach trees as affected by ringing. Vertical bars indicate SE (n = 4).

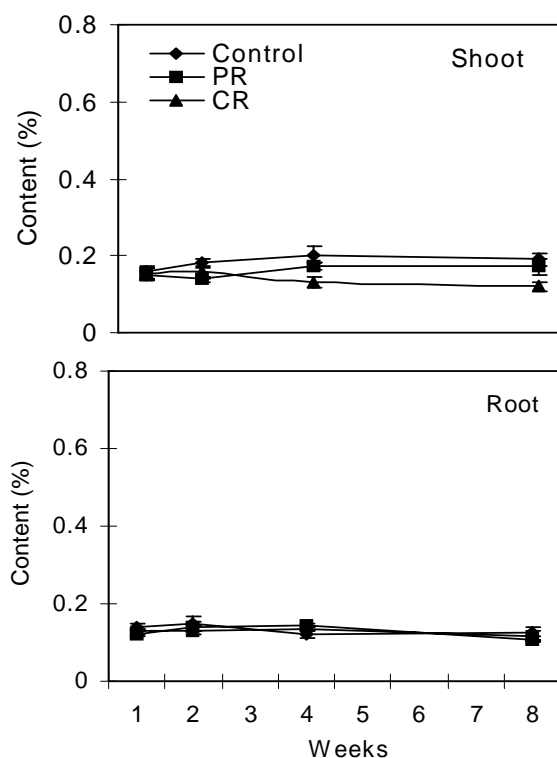


**Figure 7.** Magnesium content in shoot and root of peach trees as affected by ringing. Vertical bars indicate SE (n = 4).

The % excess of  $^{13}\text{C}$  atoms was lower in the control than in CR and PR trees for shoot, upper part of trunk and leaf, but it was only slightly higher in CR and PR trees than in control trees for root (Figure 8). In the lower part of the trunk there was no difference between control and PR treatment. However it was lower in CR trees compared to control and PR trees. Apparently there was no % excess of  $^{13}\text{C}$  atoms in CR trees for the lower trunk and root due to the disconnection between the upper and lower trunk (Figure 8). Figure 9 shows how the  $^{13}\text{CO}_2$  feeding was carried out in potted two-year-old peach trees.

The results show that trunk growth (circumference) is higher above the ring than below it as a result of bark ringing. It is an effective dwarfing technique for young peach trees brought about by the stress phenomenon where bark (phloem) ringing produces more ABA as a result of blocking translocation of photosynthates from leaf to root. Arakawa et al. [4] reported similar results. They observed that trunk growth significantly increases above the girdling point and is reduced below it in apple trees. Onguso et al. [5] also reported a similar result. They stated that the trunk circumference is larger above the ring than below it. They also reported that the sugar and starch content are higher above the ringing than below. The ringing decreases the starch content in the root and accumulates sucrose in the leaf [14-15].

Mullins [16] reported that cytokinin stimulates root growth of young grapes. Antognozzi et al. [17] reported that the cytokinin activating compound,  $N_1$ -(2-chloro-4-pyridyl)- $N_3$ -phenylurea (CPPU), increases the transverse diameter, the size and the fresh weight of olives. Park et al. [18] observed that stem growth in kinetin-treated persimmon trees is higher than in control trees. Cytokinin and other plant growth hormones stimulate cell division (cytokinesis) and influence the pathway of differentiation by stimulating RNA and protein synthesis [7]. They can accumulate in the leaf and cause the stomata to close, reducing transpiration and preventing further water loss. In this way they may affect the physiological processes in tree.

In the case of PR and CR trees, sucrose accumulates in the leaf and causes stomata closure resulting in an increase in ABA and a reduction in cytokinin in leaf, shoot and twig where it exhibits a growth inhibitory effect [8]. A sudden increase in endogenous ABA has also been demonstrated in several stress phenomena [8].

Hossain [19] has shown that the ABA content is higher in PR and CR trees than in control ones when the cytokinin level is lower. This could also be due to stress induced by PR or the cut-off in translocation of photosynthates from the leaf to the root brought about by CR.

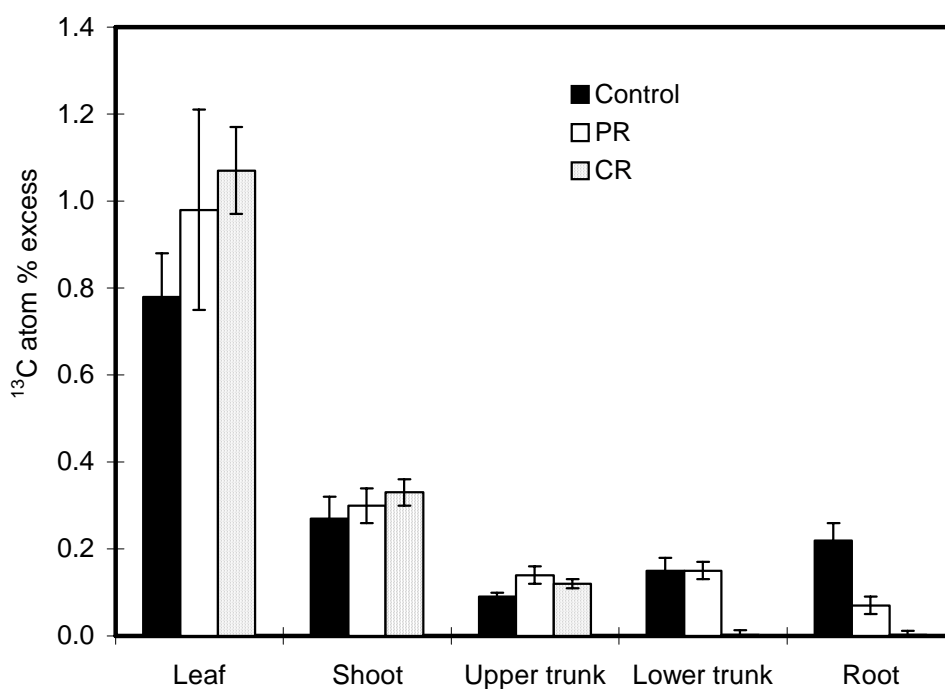


**Figure 8.** Transport of  $^{13}\text{C}$  atoms in different parts of peach trees after  $^{13}\text{CO}_2$  feeding. Vertical bars indicate SE ( $n = 3$ ).

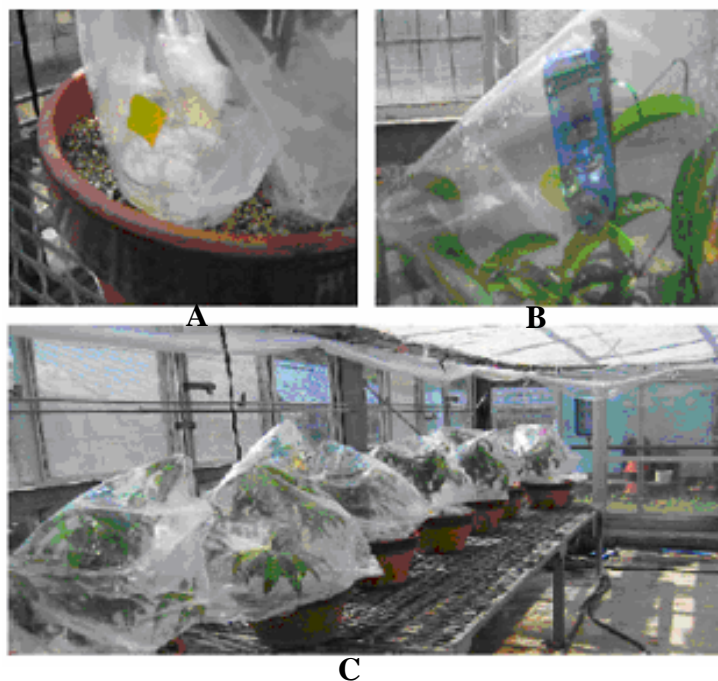


**Figure 9.** Photograph showing  $^{13}\text{CO}_2$  feeding in potted two-year-old peach trees from 9-12 pm on July 31, 2003. A = Petri dish containing  $^{13}\text{C}$ -rich  $\text{BaCO}_3$  with 50% lactic acid, B = Small fan to circulate air in the bag, C= Potted peach trees covered with transplant polythene bags.

## Conclusions

From our results it can be concluded that peach trees with PR produce more ABA hormones, nitrogen, calcium, and  $^{13}\text{C}$  photoassimilates than the unringed (control) trees by causing nutrient and water stresses which can inhibit the trunk growth. As a result, dwarfing is exhibited by the whole tree. This probably can also be effective for other fruit species.

## Acknowledgements

The authors are grateful to the Japanese Ministry of Education, Culture, Sports, Science and Technology for providing the fund for this research and also to Partha Pratim Chowdhury for his technical assistance.

## References

1. H. B. Tukey, "Tree structure, physiology and dwarfing", *Dwarf Fruit Trees*, MacMillan Co., NewYork, **1964**, p.562.
2. D. T. M. De Jong, A. Weibel, W. Tsuji, J. F. Doyle, R. S. Johnson, and D. Ramming. "Evaluation of size controlling rootstocks for California peach production" *Acta Hort.*, **2001**, 557, 103-110.
3. A. Jose, "Effect of girdling treatments on flowering and production of mango", *Acta Hort.*, **1997**, 455,132-134.

4. O. Arakawa, K. Kanno, A. Kanetsuka, and Y. Shiozaki, "Effect of girdling and bark inversion on tree growth and fruit quality of apple", *Acta Hort.*, **1997**, 45, 579-586.
5. J. M. Onguso, F. Mizutani, and A. B. M. S. Hossain, "Effects of partial ringing and heating of trunk on shoot growth and fruit quality of peach trees" *Bot. Bull. Acad. Sin.*, **2004**, 45, 301-306.
6. M. A. Rose and E. Smith, "Overwintering plants in the landscapes", *Horticulture and Crop Science*, Ohio State University Extension, Columbus, **2001**, p. 4.
7. M. Khamis and T. Holubowicz, "Effect of foliar application of alar, etrel, ABA and CCC on the frost resistance of peach trees", *Acta Hort.*, **1978**, 81, 67-72.
8. S. T. C. Wright and R. W. P. Hiron, "Abscisic acid, the growth inhibitor induced in detached leaves and by a period of wilting", *Nature*, **1969**, 224, 719-720.
9. T. L. Setter, W. A. Brun, and M. L. Brenner, "Effect of obstructed translocation of leaf abscisic acid on associated stomatal closure and photosynthesis decline", *Plant Physiol.*, **1980**, 65, 1111-1115.
10. E. E. Goldschmidt, R. Goren, Z. E. Chen, and S. Bittner, "Increase in free and bound abscisic acid during neutral and ethylene induced senescence of citrus fruit peel", *Plant Physiol.*, **1973**, 51, 879-882.
11. P. J. Davies, "The plant hormones: their nature, occurrence, and functions", in "Plant Hormones: Physiology, Biochemistry and Molecular Biology" (Ed. P. J. Davies), Kluwer, Boston, **1995**, pp.13-38.
12. B. H. Most, P. Gaskin, and J. MacMillan, "The identification and quantitative analysis of ABA in plant extracts by gas-liquid chromatography", *Planta*, **1971**, 96, 271-280.
13. F. P. Delia, A. Steudler, and N. Corwin, "Determination of total nitrogen in aqueous samples using persulfate digestion", *Limnol. Oceanogr.*, **1977**, 22, 760-764.
14. H. Schneider, "Effect of trunk girdling on phloem of trunk of sweet orange trees on sour orange rootstocks", *Hilgardia*, **1969**, 22, 593-601.
15. Z. Plaut and L. Reinhold, "The effect of water stress on the movement of <sup>14</sup>C-sucrose tritiated water within the supply of leaves of young bean plants", *Aus. J. Biol. Sci.*, **1967**, 20, 297-307.
16. M. G. Mullins, "Morphogenetic effects of roots and some synthetic cytokinins in *Vitis vinifera* L.", *J. Exptl. Bot.*, **1967**, 18, 206-214.
17. E. Antognozzi, P. Proietti, and M. Boco, "Effect of CPPU (cytokinin) on table olive cultivars", *Acta Hort.*, **1993**, 329, 153-155.
18. M-J. Park, B. Kim, and S. Kang, "Effect of kinetin and B9 on the growth and carbohydrate partitioning in one -year-old trees of persimmon", Proc. 1<sup>st</sup> Int. Persimmon Symposium. *Acta Hort.*, **1997**, 436, 365-373.
19. A. B. M. S. Hossain, "Dwarfing peach trees grafted on vigorous rootstock by summer pruning and partial ringing", *PhD. Thesis*, **2006**, Ehime University, Japan.

Full Paper

## Elementary theory of quantum Hall effect

Keshav N. Shrivastava

Department of Physics, University of Malaya, Kuala Lumpur 50603, Malaysia

E-mail: [keshav\\_shri@yahoo.com](mailto:keshav_shri@yahoo.com)

Received: 7 January 2008 / Accepted: 5 April 2008 / Published: 23 April 2008

---

**Abstract:** The Hall effect is the generation of a current perpendicular to both the direction of the applied electric as well as magnetic field in a metal or in a semiconductor. It is used to determine the concentration of electrons. The quantum Hall effect with integer quantization was discovered by von Klitzing and fractionally charged states were found by Tsui, Stormer and Gossard. Robert Laughlin explained the quantization of Hall current by using “flux quantization” and introduced incompressibility to obtain the fractional charge. We have developed the theory of the quantum Hall effect by using the theory of angular momentum. Our predicted fractions are in accord with those measured. We emphasize our explanation of the observed phenomena. We use spin to explain the fractional charge and hence we discover spin-charge locking.

**Keywords:** Hall effect, Dirac equation, magnetic moments, effective charge

---

### Introduction

The ordinary Hall effect was discovered by Edwin Hall in 1879 [1]. In 1978 von Klitzing and Englert found a plateau in the Hall effect [2]. In 1980 von Klitzing et al. found the value of  $h/e^2$  from the plateau in the Hall effect [3]. In 1982, Tsui et al. discovered the steps at fractional numbers [4]. The force is  $\mathbf{F} = e \mathbf{v} \times \mathbf{B}$  so that the Hall voltage is,  $V = IB/necd$  where  $I$  is the Hall current,  $B$  is the magnetic induction,  $n$  is the electron concentration,  $e$  is the electron charge,  $c$  is the velocity of light and  $d$  is the thickness of the sample as shown in Figure 1.

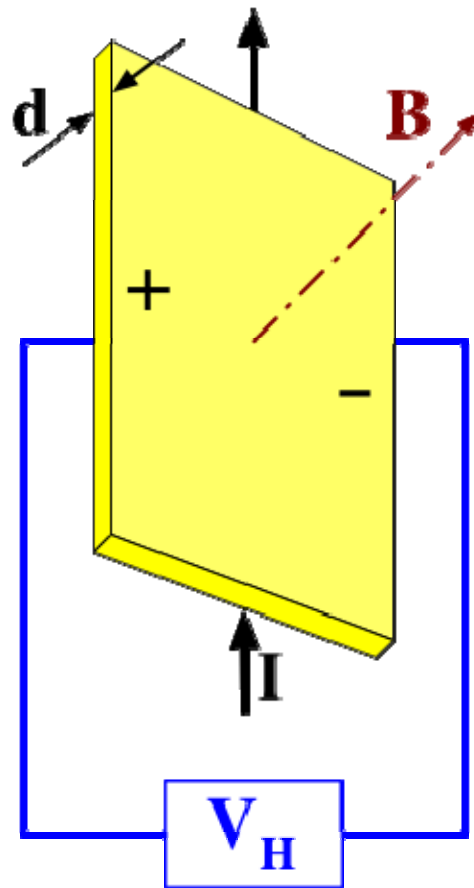


**Figure 1.** The Hall voltage is measured orthogonal to both the electric as well as the applied magnetic field.

### Two Dimensional Electron Systems

A two dimensional electron system is formed in a heterostructure which has layers of GaAs over AlGaAs. The energy gap of GaAs increases upon Al doping. When GaAs is doped with donors at zero temperature the Fermi level lies higher than the bottom of the conduction band. The electrons bound to donors move into GaAs conduction band and the process stops when some proportion of electrons have moved. The electrons in the inversion layer are two dimensional as shown in Figure 2.

The average drift velocity of the electron subjected to the electric field is,

$$V_d = -eE\tau/m \tag{1}$$

where E is the electric field, m is the electron mass and  $\tau$  is the mean life time so that the current density is,

$$j = -neV_d = \sigma_0 E \tag{2}$$

where

$$\sigma_0 = ne^2\tau/m \tag{3}$$

where n is the electron density. In the presence of a steady magnetic field, the conductivity and resistivity become matrices,

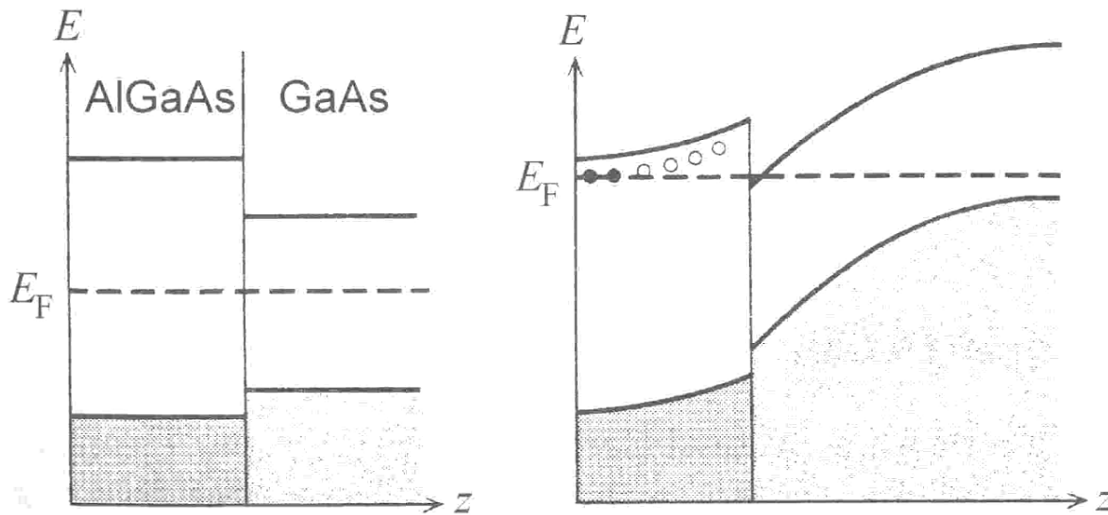


**Figure 2.** The two dimensional electrons are formed in between AlGaAs and GaAs.

$$\sigma = \begin{pmatrix} \sigma_{xx} & \sigma_{xy} \\ \sigma_{yx} & \sigma_{yy} \end{pmatrix}, \quad \rho = \begin{pmatrix} \rho_{xx} & \rho_{xy} \\ \rho_{yx} & \rho_{yy} \end{pmatrix}. \tag{4}$$

We take x and y axes in the 2-dimensional plane, to obtain,

$$\begin{aligned} i_x &= \sigma_{xx} E_x + \sigma_{xy} E_y, \\ i_y &= \sigma_{yy} E_x + \sigma_{yx} E_y. \end{aligned} \tag{5}$$

Owing to the isotropy,  $\sigma_{xx}=\sigma_{yy}$  and  $\sigma_{xy}=-\sigma_{yx}$ . The first one is called the diagonal conductivity and the second one is called the Hall conductivity. The relation between conductivity and resistivity is,

$$\rho_{xx} = \rho_{yy} = \frac{\sigma_{xx}}{\sigma_{xx}^2 + \sigma_{xy}^2} \tag{6}$$

for the diagonal resistivity and

$$\rho_{xy} = -\rho_{yx} = -\frac{\sigma_{xy}}{\sigma_{xx}^2 + \sigma_{xy}^2} \tag{7}$$

for the Hall resistivity. We measure these quantities by connecting various leads as given in Figure 3. In the case of homogeneous current in the y direction,  $i_x=I/W$  and  $i_y=0$ . The electric field is given by,  $E_x=V_{12}/L$  and  $E_y=V_{13}/W$  so we have,  $\rho_{xx}=V_{12}W/IL$  and  $\rho_{yx}=V_{13}/I=R_H$  where  $R_H$  is the Hall coefficient. According to the Drude (ordinary non-interacting metals) theory,  $\rho_{xx}=1/\sigma_o=m/ne^2\tau$  and  $\sigma_{xy}=B/nec$  in a weak magnetic field. The Hall resistivity is inversely proportional to the electron density and independent of mean scattering life time. In a strong magnetic field, there are new phenomena. Von Klitzing et al. [3] found the plateau in the Hall resistivity which gave the correct value of  $h/e^2$ . One of the plateaus is given in Figure 4. We see from the plot that (i) there is a plateau region in which the Hall resistivity remains constant. As the electron density is varied in this region the diagonal resistivity is almost zero, and (ii) the value of the Hall resistivity in the plateau regions is exactly equal to  $h/e^2$  divided by an integer. Therefore, the Hall conductivity  $\sigma_{xy}$  in the plateau region is “quantised” into integer multiples of  $e^2/h$ . This phenomenon was called the “integer quantised Hall effect” (IQHE).

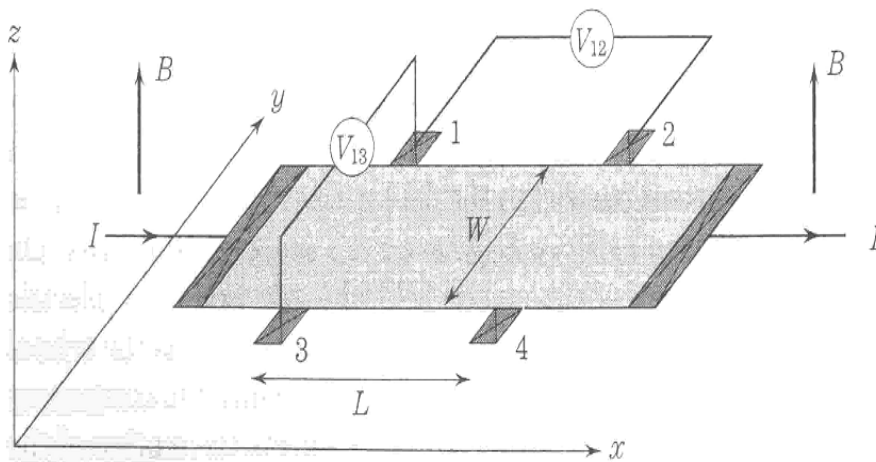


**Figure 3.** The sample with the magnetic field  $B$  and the current  $I$  perpendicular to it. The wires are connected to measure Hall voltage perpendicular to both  $I$  and  $B$  in various directions.  $W$  is the width of the sample and  $L$  is the length.

**Flux Quantisation and the Hall Effect**

Introduction of the flux quantisation immediately explains the integer quantised Hall effect. The Hall resistivity is,

$$\rho = B/nec \tag{8}$$

where  $B$  is the magnetic field. According to the flux quantisation, the field in a certain area,  $A$ , is quantised,

$$B.A = m\phi_0 \tag{9}$$

where the magnetic flux quantum is,  $\phi_0=hc/e$ . Substitution of (9) into (8) gives the integer quantised Hall effect as,

$$\rho = \frac{\frac{mhc}{Ae}}{\frac{N_o}{A}ec} = \frac{m}{N_o} \frac{h}{e^2} \tag{10}$$

The quantum Hall effect thus is the quantisation of Hall resistivity as,

$$\rho = \frac{h}{ie^2} \tag{11}$$

Hence the charge of the quasiparticle is  $ie$ . Here  $i$  = integer. The charge thus becomes  $1e, 2e, 3e, \dots, ie, \dots$ . Von Klitzing obtained the correct value of the charge for  $i=1$ . So the value of  $h/1e^2$  became “one von Klitzing”. When this experiment was repeated with cleaner samples with higher electron mobility, with higher magnetic fields and lower temperatures, it led to the discovery of plateau at  $i = 1/3$  which gave birth to the fractional charge. We show the data in Figure 4 with plateau at  $1/3$ . Since this fractional value occurred in the middle of various highly degenerate Landau levels, where no gap is apparent, the observation could not be explained by the experimentalists by using the non-interacting quantum mechanical theory. It was thought that the observation is a result of the many-body effects of

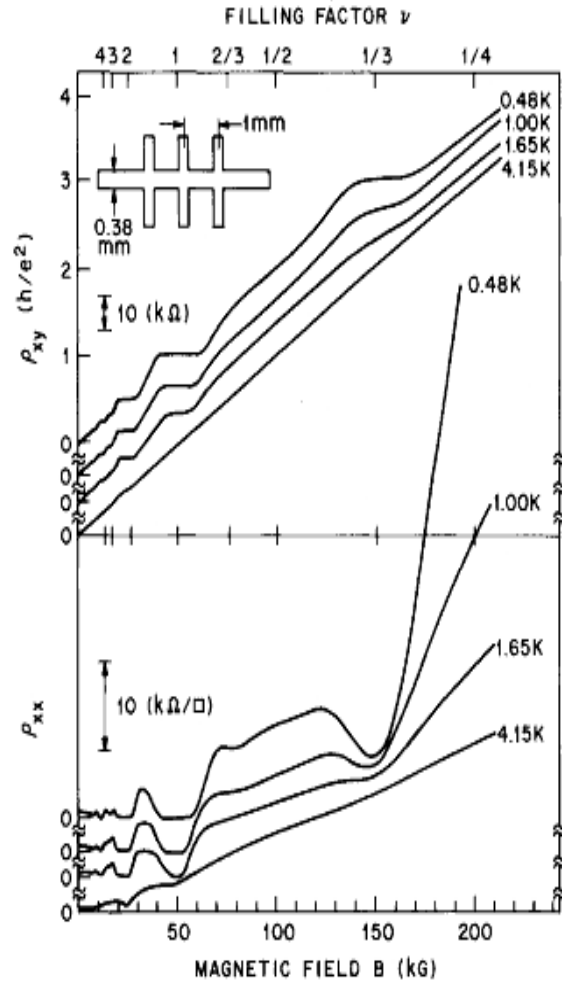


**Figure 4.** The data of experimentally measured Hall resistivity showing the plateau at  $\nu = 1/3$

electron interactions. Subsequent experimental work showed a lot many more plateaus which are displayed in Figure 5. We will see that there is no need of any interaction to explain the plateau at  $1/3$ .

### Laughlin's Theory

Laughlin made the first efforts to explain the quantum Hall effect [5]. The flux quantisation was immediately found to explain at least the integer quantised Hall effect. Subsequently, Laughlin started from first principles using the Hamiltonian,

$$H = \sum_j \{ |(\hbar/i)\nabla_j - (e/c)\vec{A}_j|^2 + V(z_j) \} + \sum_{j>k} e^2 / |z_j - z_k| \tag{12}$$

where  $j$  and  $k$  sum over  $N$  particles and  $V$  is the potential due to nuclei. The repulsive Coulomb interactions can produce the plateaus only when flux quantisation is considered. A trial wave function of the form given below,

$$|\Psi(z_1, \dots, z_N)\rangle^2 = e^{-\beta(\phi+\gamma)} \tag{13}$$

with  $\beta=1/m$ ,

$$\phi = -2m^2 \sum_{j<k} \ln|z_j - z_k| + m/2 \sum_{\ell}^N |z_{\ell}|^2 \tag{14}$$

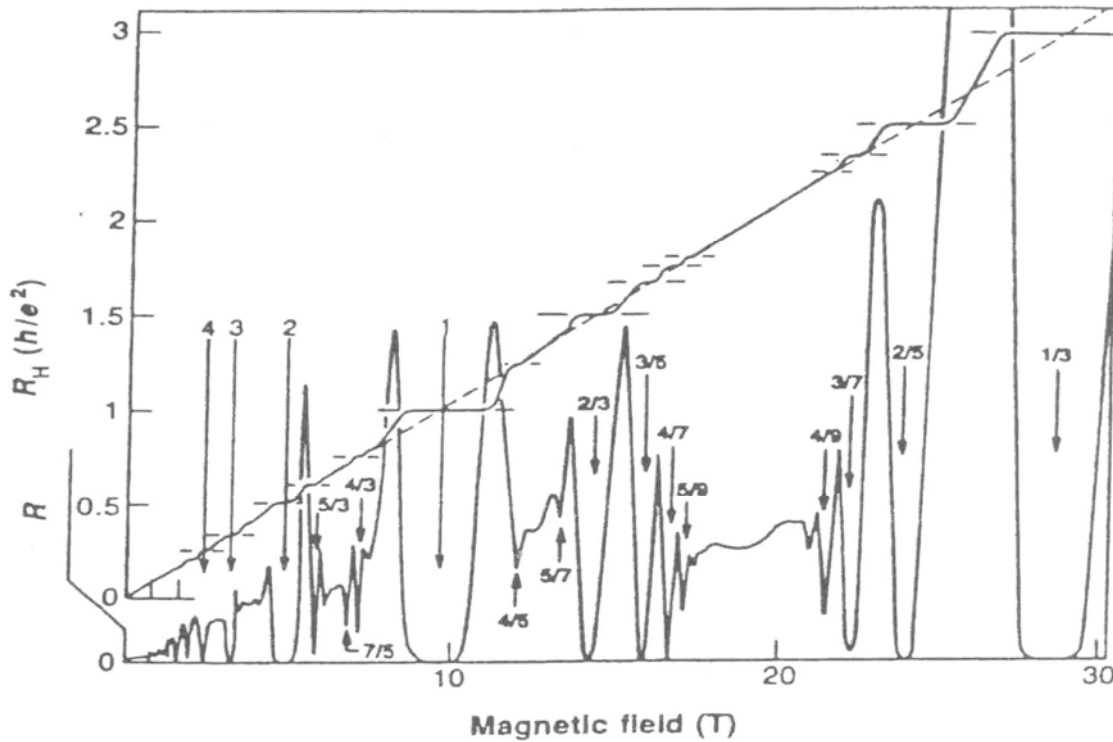


**Figure 5.** The data of quantum Hall effect showing many plateaus including the one at 1/3

is used to solve the Schrodinger equation to find the ground state. Laughlin obtained the approximate energy expression in terms of  $m$  as well as computed the energy by using the exact density of states. By using “incompressibility” the charge of the particles is fixed at 1/3 and 1/5. Unfortunately there is area in the flux quantisation which must also be fixed, otherwise the charge will leak. Laughlin thus laid the foundation for the study of fractional charges from the first principles by using only the Coulomb interactions. The Hamiltonian then consists of the kinetic energies and the Coulomb potentials and the correlations produce the fractional charges. Unfortunately the problem requires incompressibility due to the area in flux quantisation.

**Shrivastava’s Theory [6-17]**

We consider that electrons have spin as well as the orbital angular momentum so that,

$$g_j j = g_s \vec{s} + g_l \vec{l} = \frac{1}{2}(g_l + g_s)\vec{j} + \frac{1}{2}(g_l - g_s)(\vec{l} - \vec{s}) . \tag{15}$$

Multiplying both sides by  $j = l + s$  and taking eigen values,

$$g_j j(j+1) = (1/2)(g_l + g_s)j(j+1) + (1/2)(g_l - g_s)[\vec{l}(l+1) - s(s+1)]. \tag{16}$$

Substituting  $s=1/2$  and  $j = l \pm (1/2)$  we get,

$$g_j = g_l \pm \frac{g_s - g_l}{2l+1} . \tag{17}$$

For  $g_s=2, g_l = 1$ , we find,

$$g_{\pm} = 1 \pm \frac{1}{2l+1} \quad (18)$$

The equation (17) has both the signs for the spin. The cyclotron frequency is,

$$\omega = \frac{eB}{mc} \quad (19)$$

From the charge, e in the cyclotron frequency, we generate the charge of a particle. It is also possible to obtain the charge from the e in Bohr magneton. Corresponding to the cyclotron frequency, the voltage along y direction is,

$$\hbar\omega = eV_y \quad (20)$$

or,

$$\hbar \frac{eB}{mc} = eV_y.$$

Multiplying this expression by e/h, we get,

$$\frac{e^2 B}{2\pi mc} = \frac{e^2}{h} V_y \quad (21)$$

which is the current in x direction, so that the resistivity,

$$\rho_{xy} = \frac{h}{e^2} \quad (22)$$

The  $S_z=1/2$ , and the energy in a magnetic field is  $g\mu_B H.S$ , so correcting B in the cyclotron frequency we find,

$$I_x = \frac{1}{2} g \frac{e^2 B}{2\pi mc} = \frac{1}{2} g \frac{e^2 V_y}{h} \quad (23)$$

For  $l=0$ ,  $g=2$ ,

$$I_x = \frac{e^2}{h} V_y \quad (24)$$

which describes the quantised current correctly for  $\nu=1$ . From the above equations we have  $\nu = \frac{1}{2} g_{\pm}$

which gives the filling factor, one for + sign and the other for – sign as in (18). For  $l=0$ , we obtain  $(1/2)g_+=1$  and  $(1/2)g_-=0$  and other values as given in Table 1. The Landau levels are introduced by multiplying the above values by n so that

$$\nu = n \left( \frac{1}{2} g_{\pm} \right)$$

so we can multiply the tabulated values by an integer when needed. The values of  $\rho_{xx}$  and  $\rho_{xy}$  for a single interface of GaAs/AlGaAs have been measured at 150 mK. The values predicted in Table 1 are exactly the same as in the experimental data shown in Figure 5. The values shown in the figure occur in two sets: 2/5, 3/7, 4/9, 5/11, 6/13, ... etc. and 2/3, 3/5, 4/7, 5/9, 6/11 etc. Using the Table 1, when we multiply the values by n, we can interpret all of the experimentally measured values correctly. The columns of Table 1 belong to two Kramers conjugates, one belonging to +1/2 and the other one to -1/2 spin and the experimental data also display them in two sets.

For the cyclotron frequency  $\hbar\omega_c = g\mu_B B$  where  $\mu_B = e\hbar/2mc$  is the Bohr magneton. Therefore,  $(1/2)g_{\pm}$  can be considered to be the effective charge,  $e_{\text{eff}} = \frac{1}{2} g e = \nu e$ . In Table 1, we see two series,

$$\nu_- = \frac{l}{2l+1} \quad \text{and} \quad \nu_+ = \frac{l+1}{2l+1} \quad \text{which can be used to explain the high Landau levels easily.}$$

**Table 1.** Predicted values of the fractional charge

$l$	$(1/2)g_{-} = \frac{l}{2l+1}$	$(1/2)g_{+} = \frac{l+1}{2l+1}$
0	0	1
1	1/3	2/3
2	2/5	3/5
3	3/7	4/7
4	4/9	5/9
5	5/11	6/11
6	6/13	7/13
$\infty$	1/2	1/2

For the higher values of the Landau level quantum number,  $n$ , the number of fractions observed are much less than at the lowest Landau level. At the magnetic field of 4 or 5 Tesla only a small number of fractions are observed, the strongest ones being at: 8/3, 5/2 and 7/3. The series  $l/(2l+1)$  is the particle-hole conjugate of  $(l+1)/(2l+1)$ . For  $l=7$ , two values, 7/15 and 8/15, are predicted and for  $l=\infty$  the value is 1/2. When the same particle occurs in different levels its charge remains unchanged. We can multiply the values by  $n=5$  so that the predicted values of 1/2, 7/15 and 8/15 become 5/2, 7/3 and 8/3. These predicted values are exactly the same as those observed experimentally. Thus, 7/3 is the particle-hole conjugate of 8/3 as seen in Table 2 for  $n=5$ . For a long time only odd denominators were reported which show that even denominators are weak. After that even denominators as well as even

numerators with odd denominators are found. We go back to the same formula,  $\frac{l + \frac{1}{2} \pm s}{2l+1}$ . When  $s=1, l=0$ ,  $(1/2)+1=3/2$  has even denominator.

**Table 2.** The fractions produced for high Landau levels

$l$	$l/(2l+1)$	$(l+1)/(2l+1)$	$n l/(2l+1)$	$n(l+1)/(2l+1)$
$\infty$	1/2	1/2	5/2	5/2
7	7/15	8/15	7/3	8/3

The predicted fraction for  $l=0$  is 3/2 and for  $l=1$  it is 5/2. Hence for electron clusters or pairs the fraction has even denominator. Since the number of particles is larger than one its probability becomes small so these plateaus are weak but the same theory explains the even denominators. There is a limiting value of the series which also gives 1/2. One can introduce a Fermi surface at  $n/2$ , thus 1/2, 2/2, 3/2, 4/2, 5/2, 6/2 and 7/2 are predicted which are the same values as observed. The effective mass and  $g$  factor of some of the fractions are equal to those of others. We have shown that the effective mass can be equal only when the two quasiparticles are particle-hole conjugates. The particle-hole conjugates should obey the following relation,

$$v_p + v_h = 1 \tag{25}$$

The values given in Table 1 always obey this relation [8].

### Half-filled Landau Level

The  $l = \infty$  in the two series produces,

$$\lim_{l \rightarrow \infty} \nu_+ = \frac{1}{2}(+) \tag{26}$$

$$\lim_{l \rightarrow \infty} \nu_- = \frac{1}{2}(-)$$

One  $\frac{1}{2}$  comes from the right and the other from the left when magnetic field is varied, i.e. one while increasing the field and the other while reducing. One can go from  $\frac{1}{3}$  to  $\frac{1}{2}$  by reducing the field while from  $\frac{2}{3}$  to  $\frac{1}{2}$  is obtained by increasing the field. We can go from  $\frac{1}{3}$  to  $\frac{3}{5}$  by reversing the spin and increasing  $l$ , and similarly from  $\frac{2}{3}$  to  $\frac{2}{5}$  by reducing the spin and increasing  $l$ . In this way angular momentum is conserved. One of the  $\frac{1}{2}$  values is like an electron  $(\frac{1}{2})A$  and the other is like a hole,  $(\frac{1}{2})B$ , (A for + series and B for – series). Since the electron and the hole are separated by a distance, this state is compressible. When we multiply this result by  $n$ , the Landau level quantum number, we obtain:  $\frac{1}{2}, 2/2, 3/2, 4/2, 5/2, \dots$ , which are in agreement with data.

### Effective Charge

We discussed the Laughlin’s wave function earlier. Here the repulsive Coulomb interactions cannot give rise to a fractional charge of  $\frac{1}{3}$ . It is first assumed on the basis of experimental data and then substituted in the theory. Laughlin’s charge is independent of spin but in our theory it depends. In Laughlin’s theory a particle of charge  $\frac{1}{3}$  is produced but in our theory splitting occurs in fractions of  $\frac{1}{3}$  and  $\frac{2}{3}$ , etc. In Laughlin’s theory,  $\frac{1}{3}$  charge arises due to incompressibility and the Hamiltonian first principles. In our theory  $\frac{1}{3}$  charge can arise only when  $\frac{2}{3}$  also arises as depicted in Figure 6. There is a difference between Laughlin’s and our theory. The fractionalisation in Laughlin’s theory is independent of spin whereas in our theory spin plays an important role in determining the fraction.

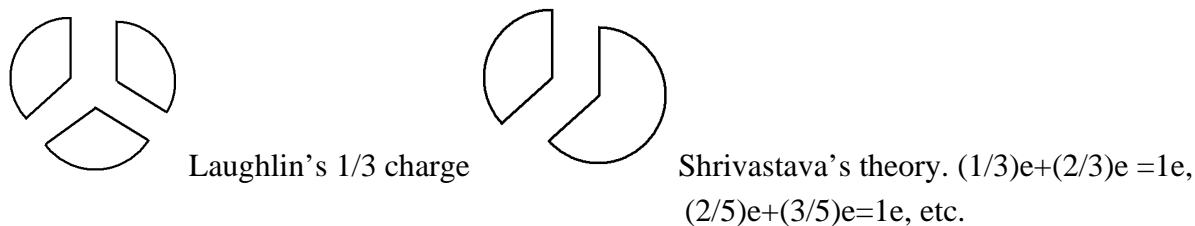


**Figure 6.** Pictorial display of the difference between the two theories

### Dirac Equation

The basic idea of Dirac equation is to have space-time symmetry and the constancy of velocity of light, so that instead of  $p^2/2m$ , the kinetic energy appears as  $c\alpha \cdot p$  and the wave equation becomes,

$$(c\alpha.p + \beta mc^2)\Psi(x,t) = i\hbar \frac{\partial}{\partial t} \Psi(x,t) , \quad (27)$$

the free particle solutions of which are,

$$E_{\pm} = \pm(c^2 p^2 + m^2 c^4)^{1/2} . \quad (28)$$

This equation gives the correct magnetic moments for the proton as well as for the neutron, subject to using the mass of the respective particle and an appropriate g value. In the case of electron Lande's formula,

$$g = 1 + \frac{j(j+1) - l(l+1) + s(s+1)}{2j(j+1)} \quad (29)$$

with positive spin is used. In our case, the effective charge and hence the magnetic moment is determined by the g values. Hence, our method of defining the charge is the same as that for the magnetic moments of proton and neutron.

### Shubnikov-de Haas Effect

At low temperatures, the integration over the Fermi distribution leads to  $x/\sinh x$  type expression which is called Dingle's formula. The spin symmetry is found to modify this formula which determines the oscillation amplitude of resistivity as a function of magnetic field, called the Shubnikov-de Haas effect. Our theory introduces the effective charge so that the cyclotron frequency gets fractionalised resulting in  $m/v_{\pm}$  which for  $v_{\pm}=1$  becomes  $m$ , the electron mass. Thus, we have taken into account the spin-charge fractions to obtain the correct mass. For example, at certain magnetic field  $1.5 m$  is found instead of  $m$ . The mass of the electron relative to band value as a function of carrier density has been deduced from Shubnikov-de Haas effect in GaAs/AlGaAs heterostructures. The factors 1 and  $2/3$  are found to arise from the spin-charge effect of Shrivastava. The experimental data are obtained from Tan et al.[18]. The dashed line is found by Kwon et al. [19] on the basis of small self energy corrections due to many body perturbative interactions. The factors of 1 and  $2/3$  in the mass are found by us. The mass of the free electron is  $m_e$  and the screening radius is deduced from the density,  $n$ , per unit area. We find that  $m/v_{\pm}$  occurs in place of  $m$  for the mass of the electron in the Shubnikov-de Haas (SdH) effect. In fact, many other fractions of the mass of the electron given in Table 1, become allowed so that the electron really "falls apart". The oscillations due to flux quantisation allow the measurement of  $m/h^2$ . The flux quantisation in the Shubnikov-de Haas effect leads to "quantised Shubnikov-de Haas effect". Therefore, we observe consequences of the effect of flux quantisation on the Shubnikov-de Haas oscillations. There are zeroes in the resistivity at certain fields. There is a spin-charge effect so that the spin flip corresponds to a change in the charge. The Shubnikov-de Haas effect uses quantisation of Landau levels but not the flux quantisation. Hence, we find that there is a "quantised Shubnikov-de Haas effect" which measures the  $m/h^2$ . We find that when fractional values of  $v_{\pm}$  are taken into account, the mass of the electron, equal to band mass in GaAs/AlGaAs, is obtained. When the magnetic field is varied, the different values of  $n$  cross the Fermi energy at different fields resulting in oscillations in the resistivity as a function of magnetic field. The oscillating resistivity is given by,

$$\delta\rho_{xx}(\varepsilon)_{\pm} = \rho_o \sum_p \gamma_{th} c_{\alpha,\beta} \exp\left(-\frac{p\pi}{v_{\pm}\omega_c\tau_q}\right) \cos\left[2\pi p\left(\frac{\varepsilon}{v_{\pm}\hbar\omega_c} - \frac{1}{2}\right)\right] \tag{30a}$$

where

$$\gamma_{th} = \frac{2\pi^2 p k_B T / (\hbar\omega_c v_{\pm})}{\sinh\left[2\pi^2 p k_B T / (\hbar\omega_c v_{\pm})\right]} \tag{30b}$$

The cosine factor also leads to zero resistivity whenever,

$$2\pi p\left(\frac{\varepsilon}{v_{\pm}\hbar\omega_c} - \frac{1}{2}\right) = \frac{\pi}{2} \tag{31}$$

so that the resistivity vanishes when B satisfies the above formula. We introduce the flux quantisation so that the exponential factor in (30) becomes,

$$\exp\left(-\frac{P\pi mc}{v_{\pm}\tau_c eB}\right) = \exp\left(-\frac{\pi mA}{v_{\pm}\tau_c h}\right) \tag{32}$$

so that m/h will be measured from the oscillations. Introducing the flux quantisation in the argument of Sinh factor, we obtain,

$$\hbar v_{\pm}\omega_c = \frac{\hbar v_{\pm} n_2 h}{mA} \tag{33}$$

which does not have the charge but measures m/h. In the experiments the factor measured is m\*g\*/n so it is clear that the mass and g get mixed [14].

### Spin-Charge Locking

The charge of the electron may be described by matrices just as the angular momentum is. When the spin is aligned along the charge, such as  $s_x$  parallel to  $e_x$ , the arrangement is called the spin-charge locking. Taking our effective charge expression for  $e_{eff}/e=(1/2)g_{\pm}$  we find the dot product of spin and charge to find,

$$e^* .s' = (2l+1)^{-1}\left(l + \frac{1}{2}\pm s\right).s' = (2l+1)^{-1}\left(1.s' + \frac{1}{2}(1).s' + s.s\right) \tag{34}$$

which produces spin-orbit and spin-spin interactions and there is spin divided by 2l+1. That is what makes it difficult to detect this type of effect.

### Conclusions

We have found the correct explanation of the experimentally observed quantum Hall effect. We find that angular momentum gives rise to fractional charge. Therefore, there is a spin-charge effect, i.e. under high magnetic fields the spin determines the charge.

## References

1. E. Hall, "On a new action of the magnet on electric current", *Am. J. Math.*, **1879**, 11, 287-292.
2. T. Englert and K. von Klitzing, "Analysis of  $\rho_{xx}$  minima in surface quantum oscillations on (100) n-type silicon inversion layers", *Surface Sci.* **1978**, 73, 70-80.
3. K. von Klitzing, G. Dorda, and M. Pepper, "New method for high-accuracy determination of the fine-structure constant based on quantized Hall resistance", *Phys. Rev. Lett.*, **1980**, 45, 494-497.
4. D. C. Tsui, H. L. Stormer, and A. C. Gossard, "Two-dimensional magnetotransport in the extreme quantum limit", *Phys. Rev. Lett.*, **1982**, 48, 1559-1562.
5. R. B. Laughlin, "Anomalous quantum Hall effect: an incompressible quantum fluid with fractionally charged excitations", *Phys. Rev. Lett.*, **1983**, 50, 1395-1398.
6. K. N. Shrivastava, "Rational numbers of the fractionally quantized new states and their observation in fractionally quantized Hall effect", *Phys. Lett. A*, **1986**, 113, 435-436 ;**1986**, 115, 459(errata).
7. K. N. Shrivastava, "Negative-spin quasiparticles in quantum Hall effect", *Phys. Lett. A*, **2004**, 326, 469-472.
8. K. N. Shrivastava, "Particle-hole symmetry in quantum Hall effect", *Mod. Phys. Lett. B*, **1999**, 13, 1087-1090.
9. K. N. Shrivastava, "Theory of quantum Hall effect and high Landau levels", *Mod. Phys. Lett. B*, **2000**, 14, 1009-1013.
10. K. N. Shrivastava, "The fractional charges in the quantized Hall effect", *Nat. Acad. Sci. Lett.(India)*, **1986**, 9, 145-146.
11. K. N. Shrivastava, "Spin-dependent charge of a quasiparticle in clusters in quantum Hall effect", *Nat. Acad. Sci. Lett. (India)*, **2003**, 26, 159-161.
12. K. N. Shrivastava, "Unification of charge of the electron with proton and neutron through Hall effect", *Nat. Acad. Sci. Lett. (India)*, **2004**, 27, 435-440.
13. K. N. Shrivastava, "Microwave absorption in Wigner crystals at high magnetic fields", *Nat. Acad. Sci. Lett. (India)*, **2005**, 28, 199-203.
14. H. A. Kassim, I. A. Jalil, N. Yusof, and K. N. Shrivastava, "The mass of the electron in GaAs/AlGaAs by Shubnikov-de Haas effect and the spin-charge locking", *Amer. Inst. Phys. Conf. Proc. (U.S.A.)*, **2007**, 909, 43-49.
15. H. A. Kassim, I. A. Jalil, N. Yusof, and K. N. Shrivastava, "The quantum Hall effect: spin-charge locking", *Amer. Inst. Phys. Conf. Proc. (U.S.A.)*, **2007**, 909, 50-56.
16. K. N. Shrivastava, "Interpretation of quantum Hall effect from angular momentum theory and Dirac equation", *Bull. Amer. Phys. Soc.*, **2007**, 52, Paper No. S40-12.
17. K. N. Shrivastava, "The quantum Hall effect in spin quartets in grapheme", *Bull. Amer. Phys. Soc.*, **2008**, 53, Paper No. V37-14.

18. Y. W. Tan, J. Zhu, and H. L. Stormer, "Measurement of the density-dependent many-body electron mass in two dimensional GaAs/AlGaAs heterostructure", *Phys. Rev. Lett.*, **2005**, 94, 016405-1-4.
19. Y. Kwon, D. M. Ceperly, and R. M. Martin, "Quantum Monte Carlo calculation of the Fermi-liquid parameters in the two-dimensional electron gas", *Phys. Rev. B*, **1994**, 50, 1684-1694.

© 2008 by Maejo University, San Sai, Chiang Mai, 50290 Thailand. Reproduction is permitted for noncommercial purposes.

*Full Paper*

## **Characterisation of sewage wastewater and assessment of downstream pollution along Huluka River of Ambo, Ethiopia**

**Padanilly Chidambaram Prabu\***, Zerihun Teklemariam, Tadele Nigusse, Sevanan Rajeshkumar, Lakew Wondimu, Alemayehu Negassa, Ephrem Debebe, Esayas Aga, Asfaw Andargie, and Asefa Keneni

Department of Biology, P.O.Box.19, Ambo University College, Ambo, Ethiopia

\*Corresponding author, e-mail: [prabu\\_22@yahoo.com](mailto:prabu_22@yahoo.com)

*Received: 18 December 2007/ Accepted 16 April 2008 / Published 23 April 2008*

---

**Abstract:** This study was conducted to assess the downstream pollution profiles of Huluka River due to sewage water contamination, and to provide the data on the physico-chemical properties and nutrient content of Huluka River in Ethiopia. The water quality indices, viz. temperature, pH, electrical conductivity, carbon dioxide content, total dissolved solids (TDS), hardness, dissolved oxygen (DO), biological oxygen demand (BOD), chemical oxygen demand (COD), calcium, magnesium, chloride, nitrate, sulphate, and phosphate were determined. Results reveal a worsening trend in the variations of most of these parameters from upstream to downstream areas of the river, which indicates an introduction of pollution load from domestic sewage and agricultural activities. For example, TDS and DO values for some downstream water samples do not conform to the accepted standards, and these samples also have eight to ten times higher values of BOD and COD compared to those for the upstream samples. Progressing downstream, the majority of the measured ions also show an increasing trend. All of these findings indicate that the quality of the water of Huluka River is declining.

**Keywords:** Huluka River, downstream pollution, Ambo, Ethiopia

---

### **Introduction**

Ambo, one of the biggest developing towns in West Shoa zone of Ethiopia, is located 110 km from the western direction of Addis Ababa, the capital city. The town has three kebeles (villages) with a population of approximately 65,000. The place is endowed with one river, known as Huluka River,

which separates the town into two major parts. Huluka River starts from Dendi Lake near the town of Wonchi, which is 39 km from Ambo, and flows from the southern pole of Ambo towards the northern direction of the town. The water content of the river varies from season to season with a mean daily water flow of about 15,000 and 75,000 m<sup>3</sup>/day during dry and rainy season respectively [1]. In rural areas, the river water is used for drinking, sanitation, livestock, and agricultural purposes. However, sewage from residential areas near the river is directly expelled into the river and dense weeds have occupied the riverside, thus affecting the water flow.

Despite of its foul odour and toxicity caused by intensive exploitation by domestic and agricultural activities, the river is still used for various purposes including irrigation, recreation, and cattle washing. These observations may reveal the absence of policies protecting the water systems and/or overt monitoring studies on Huluka River. At present limited or no reports dealing with the water quality of Huluka River have appeared in the literature. Hence, with the aims of assessing temporal variations and thereby encouraging public awareness of the water quality of the Huluka River, the present physico-chemical analysis study is conducted to evaluate the pollution caused by human influences along the river.

## **Materials and methods**

### *Sampling location*

To determine the pollution load from sewage wastewater, four representative samples were collected from domestic and municipal sources which discharge wastewater into Huluka River. The volume of the wastewater discharged into the river varies between 10,000 to 15,000 L/day [2]. The five sampling sites in the river are designated as S1 to S5 (Figure 1) as they reflect different activities along the watercourse of the river. Sampling site S1 represents the upper stream where the river enters into the town while S5 represents the lower stream of the river ending at Ambo. Sampling sites S2 to S4 are selected in between S1 and S5. The selected sampling sites are based on accessibility, safety, potential sources of pollution, and waste disposal activities. The sites are evenly distributed along the course of the river with more emphasis on polluted sites. The sampling sites span 10 km from upper to lower stream of the river.

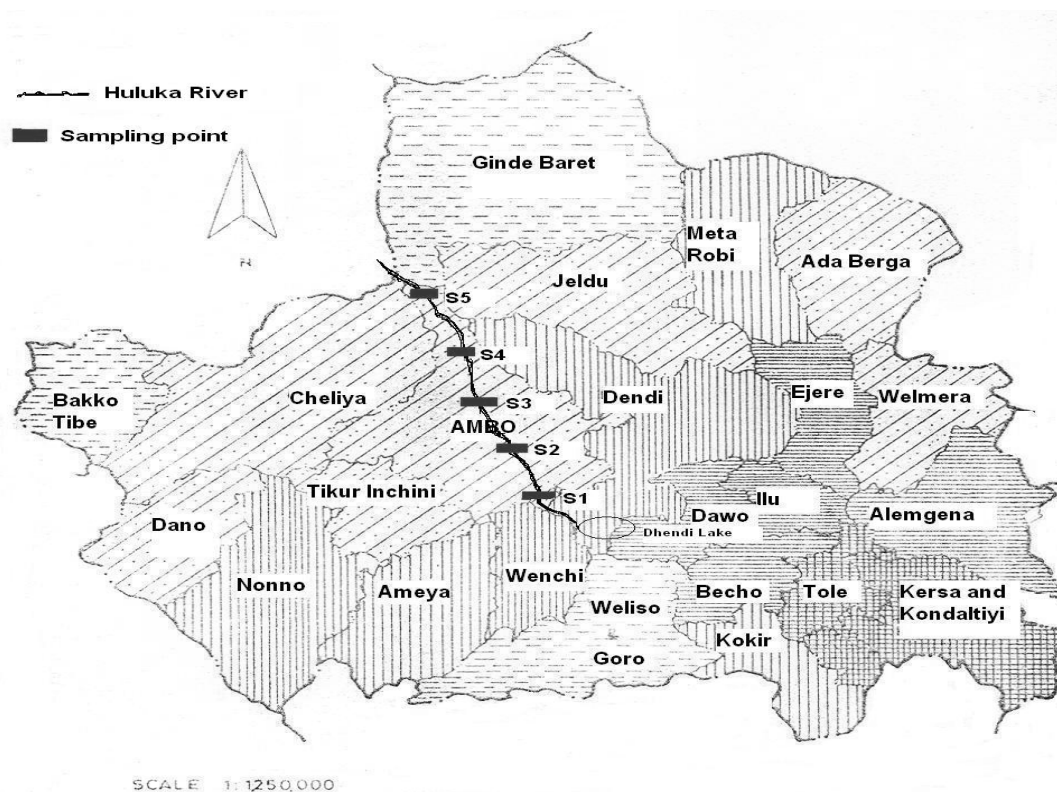


**Figure 1.** Map showing sampling points along Huluka River

#### *Sampling procedures and methods of analysis*

Samplings were carried out for a period of 6 months from February to July 2007, covering both dry and rainy seasons. Water samples (number of samples,  $n = 5$ ) were collected in polyethylene cans at monthly intervals, and transported to the Department of Biology, Ambo College for further characterisation. The samples were analysed for temperature, pH, electrical conductivity (EC), carbon dioxide, TDS, hardness (as  $\text{CaCO}_3$ ), DO, BOD, COD, calcium, magnesium, chloride, sulphate, nitrate, and phosphate, using standard methods for the examination of wastewater outlined in the APHA manual [3] and WHO/UNEP guidelines [4].

#### **Results and Discussion**

A detailed characterisation of sewage wastewater and downstream water samples has been carried out to determine the downstream pollution load in Huluka River. The composite raw sewage water in the town of Ambo which enters Huluka River at various points had the following characteristics: pH = 7.9, EC =  $1420 \mu\text{S}/\text{cm}$ ; total solids, DO, BOD, and COD = 850, 3.2, 250, and  $540 \text{ mgL}^{-1}$  respectively; nutrients: Ca, Mg, chloride, nitrate, phosphate and sulfate = 115, 95, 350, 9.28, 5.50, and  $55 \text{ mgL}^{-1}$  respectively. As for the Huluka River water samples, the results of analysis of the physico-chemical properties and the major ions and nutrients are summarised in Tables 1-2.

The temperature of the water samples range between  $15.2\text{-}23.2^\circ \text{C}$ , which is noted to be above the maximum permissible limit ( $15^\circ \text{C}$ ) of the Canadian Council of Ministers for Environment (CCME) guidelines for community water used as aesthetic object (Table 3), and is found to vary during the

rainy and dry season. During the dry season (February to May), the temperature of Huluka River ranges between 22.4-23.2° C while it is 15.2-17.8° C during the rainy season. The pH of Huluka River is slightly alkaline in nature and ranges between a minimum of 7.40 in the rainy season and a maximum of 8.18 in the dry season (Table 1), which is the usual range of river waters [5]. The slight alkalinity could be due to the calcium bedrock weathering which reflects the importance of dissolution of limestone and dolomites in the watershed. This finding confirms the result of an earlier study on Tinishu Akaki River [6]. The pH is much lower at the entry point of the river to the town (S1) and increases to a maximum furthest downstream (S5). The increase could be due to the intermixing of the sewage wastewater whose pH value is greater than 8 at the downstream sampling points (S3-S5), thus indicating the possible presence of free ammonia, which is likely to pose problems when the water is to be used for drinking and fishing by the downstream users. Ammonia is much more toxic in alkaline water than in acidic one, being toxic to aquatic biota than when it is in the oxidised form [7]. However, all the values are still within the limit of CCME and WHO guidelines for livestock watering and irrigation water.

The electrical conductivity (EC) of water is a useful and convenient indicator of its salinity or total salt content, and the values for the water of Huluka River are between 168.6-597.1  $\mu\text{S}/\text{cm}$  during the dry season and 125.4-541.2  $\mu\text{S}/\text{cm}$  during the rainy season. The lowest and highest EC values are within the recommended value of EC of potable water (750  $\mu\text{S}/\text{cm}$ ). Generally, the EC increases going downriver (S1 to S5) apparently due to the accumulation of domestic and sewage wastewater and also to the enrichment of electrolytes from mineralisation or weathering of sediment. This observation is supported by a similar study of Tinishu Akaki River [6], in which it was found that the water quality downstream was strongly degraded resulting in low dissolved oxygen and high conductivity. As for  $\text{CO}_2$  content, there is also a marked increase going downstream in both seasons, varying between 3-20  $\text{mgL}^{-1}$  and tends to be higher during the dry season (Table 1).

The value of total dissolved solids (TDS) is an important property used to evaluate the suitability of water for irrigation since the solids might clog both pores and components of the water distribution system. TDS is noted to be high during the dry season (109.6-388.1  $\text{mgL}^{-1}$ ) as compared to the rainy season (81.5-351.8  $\text{mgL}^{-1}$ ). Maximum values of TDS are obtained furthest downstream (S5) during both seasons. However, even the values for S4 water are larger than 283  $\text{mgL}^{-1}$ , the mean value of TDS for the world's large rivers [6]. The increase in TDS can probably be related to pollution through discharge of domestic and sewage wastewater into the river. However, although some TDS values are higher than normal, it is found to be below the CCME guidelines for drinking water, i.e. 500  $\text{mgL}^{-1}$  [8].

The increase in water hardness generally decreases metal toxicity, which is possibly due to Ca competition on the cell surface [9]. The total hardness of water samples from Huluka River is found to be within the maximum permissible limit according to the Environmental Protection Authority (EPA), i.e. 500  $\text{mgL}^{-1}$  (Table 3). The total hardness as  $\text{CaCO}_3$  varies from 12 (at S1) to 68 (at S5), which is classified as soft and moderately soft (Table 4) for all samples, based on hardness description used in the UK [10]. Although these values are within the acceptable ranges of the provisional discharge limits set by the EPA, the downstream samples are about three times harder compared to the upstream samples.

**Table 1.** Physico-chemical properties of water samples from Huluka River

Sample	Temperature (°C)						pH						Electrical conductivity (µS/cm)					
	Feb	Mar	Apr	May	Jun	Jul	Feb	Mar	Apr	May	Jun	Jul	Feb	Mar	Apr	May	Jun	Jul
S1	22.4	22.6	22.8	22.8	17.5	16.9	7.90	7.85	7.91	7.69	7.40	7.45	168.6	174.1	169.1	178.5	138.1	125.4
S2	22.4	22.6	23.1	22.8	17.5	16.8	7.97	7.97	7.95	7.89	7.41	7.45	171.2	172.2	175.2	165.9	148.3	145.9
S3	22.4	22.8	23.1	23.2	17.8	16.0	8.02	8.15	8.12	8.14	7.50	7.56	395.0	385.1	398.2	401.3	325.2	315.2
S4	22.6	22.4	23.2	23.1	16.0	16.2	8.10	8.05	8.04	8.05	7.71	7.71	553.6	561.2	578.2	545.5	498.2	481.5
S5	22.4	22.4	23.2	23.1	16.2	15.2	8.14	8.15	8.18	8.12	8.14	8.01	580.2	574.0	580.3	597.1	541.2	520.1
Sample	CO <sub>2</sub> (mgL <sup>-1</sup> )						TDS (mgL <sup>-1</sup> )						Hardness (mgL <sup>-1</sup> CaCO <sub>3</sub> )					
	Feb	Mar	Apr	May	Jun	Jul	Feb	Mar	Apr	May	Jun	Jul	Feb	Mar	Apr	May	Jun	Jul
S1	5	5	6	6	3	3	109.6	113.2	109.9	116.0	89.8	81.5	20	21	21	20	15	12
S2	7	8	9	8	5	5	111.3	111.9	113.8	107.8	96.4	94.8	28	25	26	24	26	21
S3	8	8	13	10	8	7	256.8	250.3	258.8	260.9	211.4	204.9	60	59	58	50	58	58
S4	12	10	13	10	10	8	359.8	364.8	375.8	354.6	323.8	312.9	52	52	54	65	50	55
S5	20	15	15	13	18	12	377.1	373.1	377.2	388.1	351.8	338.1	68	67	65	54	58	60
Sample	Temperature (°C)						pH						Electrical conductivity (µS/cm)					
	Feb	Mar	Apr	May	Jun	Jul	Feb	Mar	Apr	May	Jun	Jul	Feb	Mar	Apr	May	Jun	Jul
S1	6.5	6.2	6.5	7.2	7.8	7.9	5.8	6.7	8.5	10.0	5.5	5.8	23	28	31	35	25	28
S2	5.0	5.0	5.1	5.4	6.8	6.9	7.0	7.6	8.0	11.0	6.1	5.9	94	102	105	95	90	95
S3	3.9	3.8	3.9	3.9	4.5	4.2	9.0	10.0	12.0	15.0	8.4	9.6	76	75	81	86	85	92
S4	3.5	3.5	3.2	3.1	4.1	4.0	25.0	31.0	22.0	23.0	21.0	18.0	150	165	157	184	168	152
S5	3.2	3.1	3.0	3.0	3.4	3.6	42.0	46.0	37.0	42.0	37.0	41.0	265	245	285	255	240	215

**Table 2.** Concentration of major ions and nutrients in water samples from Huluka River

Sample	Ca (mgL <sup>-1</sup> )						Mg (mgL <sup>-1</sup> )						Cl (mgL <sup>-1</sup> )					
	Feb	Mar	Apr	May	Jun	Jul	Feb	Mar	Apr	May	Jun	Jul	Feb	Mar	Apr	May	Jun	Jul
S1	15	14	18	15	14	12	5.2	4.8	5.4	4.9	3.4	3.2	12.1	13.9	12.8	12.4	8.0	7.5
S2	28	25	29	28	22	20	13.9	14.0	13.2	12.7	8.1	8.9	20.8	20.2	21.0	22.3	15.2	15.4
S3	48	45	46	47	35	23	17.1	17.8	17.9	18.1	12.3	11.9	29.9	29.5	28.4	31.2	24.9	23.5
S4	55	58	59	60	35	34	18.3	19.1	21.0	17.6	13.1	12.1	38.6	35.6	35.1	38.2	31.9	28.7
S5	68	60	59	72	40	41	25.4	23.4	24.5	25.3	20.4	18.9	45.4	46.0	45.0	46.3	35.2	33.2
Sample	Nitrate (mgL <sup>-1</sup> )						Phosphate (mgL <sup>-1</sup> )						Sulphate (mgL <sup>-1</sup> )					
	Feb	Mar	Apr	May	Jun	Jul	Feb	Mar	Apr	May	Jun	Jul	Feb	Mar	Apr	May	Jun	Jul
S1	0.88	0.76	0.89	0.91	1.12	1.35	0.12	0.15	0.12	0.15	0.20	0.30	16.2	15.2	15.8	15.5	16.5	18.5
S2	0.96	0.94	0.99	1.10	1.25	1.46	0.28	0.21	0.25	0.30	0.35	0.53	19.4	19.8	19.5	20.1	20.8	22.8
S3	1.07	1.23	1.35	1.25	1.32	1.57	0.62	0.65	0.67	0.81	0.65	0.80	22.6	22.6	23.0	23.2	25.3	25.9
S4	1.76	1.81	1.92	1.96	2.25	2.75	0.81	0.84	0.90	0.92	0.90	1.05	25.3	26.0	25.1	26.2	30.1	30.1
S5	2.64	2.60	2.81	2.89	3.15	3.58	1.20	1.20	1.28	1.45	1.40	1.60	28.9	29.5	29.0	21.1	32.3	33.4

As shown in Table 1, traversing downstream the value of dissolved oxygen (DO) steadily decreases with values ranging from 7.9-3.4 and 6.5-3.0 mgL<sup>-1</sup> during the rainy and dry season respectively, which is an indicator that the quality of water increasingly worsens as it travels further downstream. Except for those at S1 and partly at S2, all other samples are found critically low in DO and do not conform to the value in the CCME guideline for the protection of aquatic life, i.e. 5.5-9.5 mgL<sup>-1</sup>. The low DO level causes anaerobic conditions resulting in foul odour of the Huluka River. The lower levels of DO downstream may be attributed to the microbial utilisation of DO in the breakdown of organic compounds introduced by the discharge of domestic and sewage wastewater.

The pollution profile as indicated by BOD and COD is depicted graphically in Figure 2. They range from 5.5 to 46.0 mgL<sup>-1</sup> and 23 to 285 mgL<sup>-1</sup> respectively (Table 1). These values are within acceptable ranges (BOD ≤ 200 mgL<sup>-1</sup>, COD ≤ 500 mgL<sup>-1</sup>) according to the provisional discharge limits set by Ethiopian EPA [11]. However, the downstream samples (S4 and S5) are approximately eight times higher in BOD, and ten times higher in COD than the upstream samples and their BOD values exceed 15 mgL<sup>-1</sup>, which is categorised as bad according to the UK general water quality assessment criteria (Table 4).

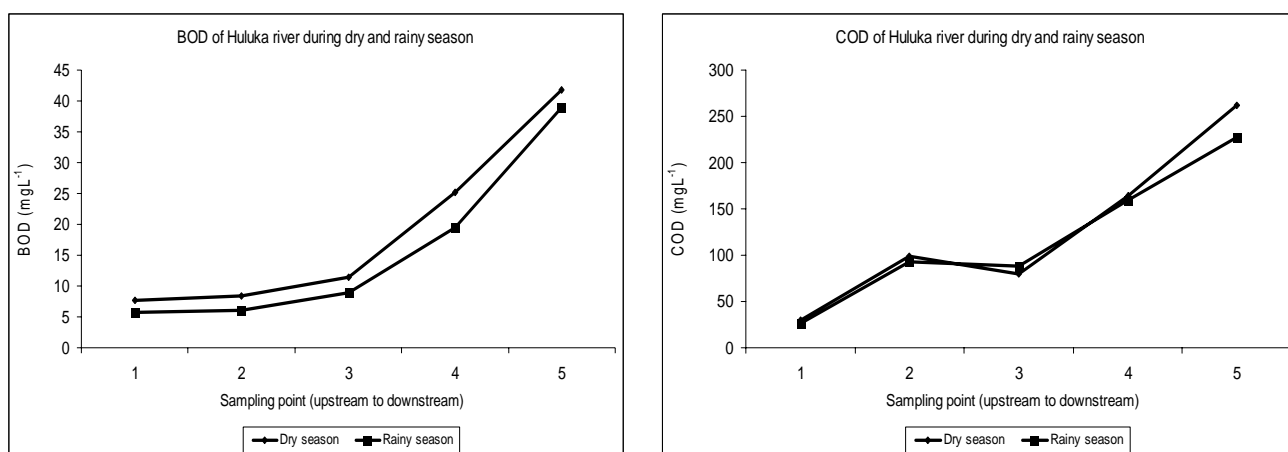


**Figure 2.** BOD and COD values of water samples from Huluka River

The measurement of Ca and Mg ion content of Huluka River registers 14-72 mgL<sup>-1</sup> and 3.2-25.4 mgL<sup>-1</sup> respectively (Table 2). As usual with most other indices, the Ca and Mg concentration increases progressively going downstream. However, the base cations are associated with the weathering of the bedrock and groundwater discharges. The extent of weathering in turn is associated with the reactivity of the rock and the surface area of contact between the rock and the river water [12].

The chloride ion concentrations in the river (7.5-35.2 mgL<sup>-1</sup> during the rainy season and 12.1-46.3 mgL<sup>-1</sup> during the dry season) are considered to be within the limit of the CCME for use as irrigation water and domestic purposes (Table 3). The probable sources of chloride could be the domestic and municipal sewage wastewater. The chloride concentration in downstream samples is up to four times that of the upstream ones and denotes the levels of pollution due to domestic and sewage wastewater intrusion.

**Table 3.** Water quality standards given by different organisations/bodies

Parameter	Desirable limit	Maximum permissible limit	Organisation/Body
Temperature ( $^{\circ}\text{C}$ )	-	15	CCME [8]
pH	7.0-8.5		WHO [13]
EC ( $\mu\text{S}/\text{cm}$ )	750	2500	WHO
DO ( $\text{mgL}^{-1}$ )	5.5-9.5	-	CCME
TDS ( $\text{mgL}^{-1}$ )	500	1500	ICMR [14]
Nitrate ( $\text{mgL}^{-1}$ )	25	50	EC [15]
	-	45	WHO
Chloride ( $\text{mgL}^{-1}$ )	100-700	1000	CCME
Phosphate ( $\text{mgL}^{-1}$ )	0.35	6.1	EC
	1	-	WHO
Calcium ( $\text{mgL}^{-1}$ )	1000 - Livestock	-	CCME
Total hardness ( $\text{mgL}^{-1}$ )	100	500	EPA [16], ICMR
Sulphate ( $\text{mgL}^{-1}$ )	<1000- Livestock	-	CCME

Note: CCME = Canadian Council of Minister for Environment; WHO = World Health Organization; ICMR = Indian Council of Medical Research; EC = European Community; EPA = Environmental Protection Agency

**Table 4.** The UK General Quality Assessment (GQA) for rivers and hardness description used in UK [6]

GQA grade	Description	BOD ( $\text{mgL}^{-1}$ )	Hardness ( $\text{mgL}^{-1} \text{CaCO}_3$ )	Description
A	Very good	2.5	0-50	Soft
B	Good	4.0	50-100	Moderately soft
C	Fairly good	6	100-150	Slightly hard
D	Fair	8	150-200	Moderately hard
E	Poor	15	200-300	Hard
F	Bad	>15	>300	Very hard

The variation of the nitrate concentrations ( $0.76\text{-}3.58 \text{ mgL}^{-1}$ ) in the water of Huluka River follows the same trend described above. The recommended maximum concentration of nitrate for public water supplies which is  $45 \text{ mgL}^{-1}$  [13]. Although the values are still well within the maximum permissible limits (e.g.  $25 \text{ mgL}^{-1}$  for drinking water—Table 3), an elevated amount of nitrate pollution may cause blue baby syndrome [17]. On the other hand the phosphate concentrations ( $0.12\text{-}1.60 \text{ mgL}^{-1}$ ) although somewhat low upstream are above the desirable limits ( $0.35\text{-}1 \text{ mgL}^{-1}$ ) further downriver by European Community and WHO standards. The increase in nitrate and phosphate content is most probably a consequence of urban and/or agricultural activities, mainly from the use of fertilisers and phosphate-containing detergents [6].

The sulphate ion content in the river ( $15.2$  to  $33.4 \text{ mgL}^{-1}$ ) is well within the limit given by CCME for livestock use ( $<1000 \text{ mgL}^{-1}$ ). Sulphate ions are often the result of dissolution of gypsum, oxidation of sulfides, and atmospheric input [6].

Elevated concentrations of these ions are mostly attributed by domestic and municipal sewage water, whereby, proper measures should be administered before release into the receiving Huluka

river. Though national standards for management of water quality in Ethiopia are in the process of enactment, the direct discharge of these pollutants to downstream of Huluka river could entail negative effects on the water quality river, as well as serious harm to the aquatic life and the downstream users.

## Conclusions

As the water of Huluka River flows through Ambo, its quality is found to steadily deteriorate. All measured values for parameters relating to the water quality (except temperature) are found to have a worsening trend as one goes further downstream. Particularly, the levels of TDS, DO, BOD, and phosphate concentration determined for some of the downstream water samples are found to be outside the desirable ranges.

## References

1. S. B. Awulachew., A. D. Yilma., M. Loulseged., W. Loiskandl., M. Ayana, and T. Alamirew, "Water Resources and Irrigation Development in Ethiopia", International Water Management Institute, Working Paper 123, Colombo, 2007.
2. Z. Gebre-Mariam, in "Conservation, Ecology, and Management of African Fresh Waters". (Ed. T. L. Crisman., L. J. Chapman., C. A. Chapman, and L. S. Kaufman), University Press, Florida, 2006, Ch.6.
3. APHA (American Public Health Association), "Standard Methods for the Examination of Water and Wastewater", 18<sup>th</sup> Edn., Washington DC, 1992.
4. WHO/UNEP, "Water Quality Monitoring: A Practical Guide to the Design and Implementation of Fresh Water Quality Studies and Monitoring Programs", UN publication series III, Paris, 1996.
5. G. Han and C. O. Liu, "Alteration of physical and chemical characteristics of rivers due to topography, geology and water/rock interaction", *Chem. Geology*, 2004, 204, 1-8.
6. S. Melaku, T. Wondimu, R. Dams, and L. Moens, "Pollution status of Tinishu Akaki River and its tributaries (Ethiopia) evaluated using physico-chemical parameters, major ions and nutrients", *Bull. Chem. Soc. Ethiop.*, 2007, 21, 13-22.
7. S. Leta., F. Assefa, and G. Dalhammar, "Characterization of tannery wastewater and assessment of downstream pollution profiles along Modjo River in Ethiopia", *Ethiop. J. Biol. Sci.*, 2003, 2, 157-168.
8. Canadian Council of Ministers of the Environment (CCME-online), <http://www.ccme.ca/publications.html>, 1999.
9. C. Gueguen, R. Gilbin, M. Padros, and J. Dominik, "Relationship between water hardness and metal toxicity", *Appl. Geochem.*, 2004, 19, 153-159.
10. R. Reeve, "Introduction to Environmental Analysis", Wiley Publications, London, 2002.
11. Environmental Protection Authority, "Provisional Standards for Industrial Sector: Ecologically Sustainable Industrial Development Project", US/ETH/99/068 Ethiopia, EPA/UNIDO, Addis Ababa, 2003.

12. H. P. Jarvie, C. Neal, D. V. Leach, G. P. Ryland, W. A. House, and A. J. Robinson, "An analysis on association of base cations (Ca and Mg) and alkalinity", *Sci. Total. Environ.*, **1997**, 194/195, 285-294.
13. WHO, "Assessment of Freshwater Quality--Global Environmental Monitoring System (GEMS)", Report on the related environmental monitoring, **1988**.
14. Indian Council of Medical Research, "Manual of Standards of Quality for Drinking Water Supplies", Special report, No. 44:275-98, **1975**.
15. European Community (EC), "Protection of the environment" *Official Gazette of European Union*, No.L.229/11-229/29, **1980**.
16. Environmental Protection Agency (EPA), "Handbook for Capacity Development. Developing Water System Capacity under the Safe Drinking Water Act", Office of Water (WH-550), Washington, DC, **1989**.
17. J. K. Tufuor, D. K. Dodoo, A. K. Armah, G. A. Darpaah, and D. K. Essumang, "Some chemical characteristics of the River Pra estuary in the western region of Ghana", *Bull. Chem. Soc. Ethiop.*, **2007**, 21, 341-348.

**Maejo International**  
**Journal of Science and Technology**

Full Paper

**Theoretical analysis and design of double implanted MOSFET on 6H silicon carbide wafer for low power dissipation and large breakdown voltage**

Munish Vashishath<sup>1,\*</sup> and Ashoke Kumar Chatterjee<sup>2</sup>

<sup>1</sup> Department of Electrical and Electronics Engineering, YMCA Institute of Engineering, Faridabad, India 121006.

<sup>2</sup> Department of Electronics and Communication Engineering, Thapar Institute of Engineering and Technology, Patiala, India 147004

\*Author to whom correspondence should be addressed, e-mail: munish276@yahoo.com, akchatterjee@tiet.ac.in

Received: 2 February 2008 / Accepted: 26 April 2008 / Published: 1 May 2008

---

**Abstract:** This paper analyses the device structure of a 6H-SiC vertical double-implanted MOSFET (DIMOSFET) in order to provide a high breakdown voltage of about 10 kV and a low power dissipation for a rise in device temperature of 600 °C. Analysis of an 800 W power dissipation for stable device operation corresponding to this temperature rise shows optimum doping levels of the drift region lying between  $5 \cdot 10^{13} \text{ cm}^{-3}$  and  $5 \cdot 10^{15} \text{ cm}^{-3}$  for a breakdown voltage of 10 kV.

**Keywords:** silicon carbide, DIMOSFET, power dissipation

---

## Introduction

Silicon Carbide (SiC) has been recently given renewed attention as a potential material for the high power and high frequency applications requiring high temperature operation. Some of the possible applications of SiC as a material of power electronic devices are for advanced turbine engines, propulsion systems, automotive and aerospace electronics and applications requiring large radiation damage resistance. Properties such as large breakdown electric field strength and large saturated electron drift velocity, small dielectric constant, reasonably high electron mobility, and high thermal conductivity make SiC attractive for fabrication of power devices with reduced power losses and die sizes. High thermal conductivity and breakdown electric field also suggest that integration of devices

made from SiC make possible higher packing densities and thus improvement in the current handling capability of these devices can be achieved. In spite of these advantages, research pertaining to SiC power devices and their practical application has been hampered by lack of reproducible techniques to grow semiconductor-quality single crystals and epilayers. However, recent developments in the growth of mono crystalline thin films of SiC by chemical vapour deposition and significant advancement in the growth of 6H-SiC single crystal boules, have stimulated a renewed interest in the SiC devices for a wide gamut of high-temperature and high-power device applications. Developments in the areas of the growth of the large area SiC bulk single crystal of 6H-SiC, improvement in the quality of SiC epilayers on Si and 6H-SiC substrates, high temperature ion implantation and doping of p and n types dopant, thermal oxidation reactive ion etching, discovery of ohmic contact materials, study of the electrical properties of grown and the doped films and their dependence on the temperature and advancements in the characterization techniques of the CVD-grown SiC films have made fabrication of high voltage SiC power devices a realistic possibility in the near future.

The SiC lattice consists of alternating planes of silicon and carbon items, and the stacking sequence of these planes defines different polytypes of the material identified by the repeat distance of the stacking sequence (e.g. 3C,4H & 6H). The lattice constant in the basal plane is virtually identical for all polytypes, but important electrical properties such as band gap energy, electron mobility and critical field differ significantly between the polytypes [1-5]. The high thermal and chemical stability of SiC makes certain types of fabrication difficult. Diffusion coefficients for dopant atoms are extremely low at the temperatures typically used for silicon device processing and for this reason selective doping of SiC are accomplished by ion implantation. Implant activation typically requires annealing at temperatures between 1000 and 1700°C. Chemical etching is impractical owing to the high chemical stability of SiC and selective etching is accomplished by reactive ion etching (RIE) using fluorinated gases.

SiC offers significant advantages for power electronics applications such as lamp ballasts, motor controls, medical electronics, automotive electronics, high-density high-frequency power supplies and smart-power application-specific integrated circuits. Hence, silicon carbide-based MOSFET can be used in high power application and hence MOSFETs require a high breakdown voltage. The one-step field plate termination can enhance the breakdown voltage to 910 V, embedded mesa termination can increase it to 1350 V and the embedded mesa with step field plating can give a breakdown voltage of 1100 V [6]. However, 6H-SiC DIMOSFETs in practice have attained a maximum blocking voltage of 760 V [7]. The specific on-resistance of the drift region of the MOSFET can be significantly reduced by enhancing the inversion channel mobility using pyrogenic re-oxidation annealing [8] thereby reducing the power dissipation. The present work aims at estimating theoretically the breakdown voltages, power dissipation and specific on-resistance at various doping levels by varying the drain voltage.

### **Status of SiC-Based MOSFETs**

In late 1980s it had been observed that power silicon devices were approaching their theoretical limits [9,7] and that these limits could be significantly extended by fabricating power devices in the materials with higher breakdown electric fields, such as silicon carbide. For the majority of vertically

oriented carrier devices, the theoretical minimum value of the resistance-area product which is specific on-resistance under punch-through condition is:

$$R_{\text{on-sp}} = \left(\frac{3}{2}\right)^3 \frac{V_B^2}{\mu_n \epsilon_s E_C^3} = \frac{3.375 V_B^3}{\mu_n \epsilon_s E_C^3} \quad (1)$$

where  $R_{\text{on-sp}}$  is the specific on-resistance in  $\Omega \text{ cm}^2$ ,  $\mu_n$  is the electron mobility perpendicular to the surface,  $\epsilon_s$  is the permittivity of the semiconductor,  $E_C$  is the critical field for avalanche breakdown perpendicular to the surface and  $V_B$  is the designed blocking voltage of the drift region. Although it varies with doping, the critical field  $E_C$  in SiC is almost an order of magnitude higher than in silicon. Even allowing for the lower electron mobility, the specific resistance in SiC at a given blocking voltage is about 400 times that of the silicon.

The first MOSFETs in SiC were reported in late 1980s and the first power MOSFETs in 1994. The power devices were the vertical trench MOSFETs or UMOSFETs. UMOSFETs are attractive because the base and source regions are formed epitaxially without the need for ion implantation and associated high temperature annealing. In UMOSFETs, the MOS channel is formed on the sidewalls of trenches created by RIE. However, SiC UMOSFETs have been reported to have two serious problems: a) a high electric field occurs in the gate oxide caused by higher electric fields in the SiC drift region. This problem occurs at the trench corners leading to catastrophic failure of the gate oxide at higher drain voltages, thus restricting the maximum operating voltage to less than 40% of ideal breakdown voltage, and b) the low inversion layer mobility along the trench sidewalls results in high specific on-resistance, which nullifies the advantage of low drift region in SiC. By 1995, UMOSFETs fabricated on the carbon face of SiC had achieved the breakdown voltage of about 260V.

In 1997, Northrop Grumman Science and Technology Center introduced and fabricated the 4H-SiC UMOSFETs at the blocking voltages of 1.1 kV [10] and 1.4 kV[11]. In the same year it also introduced and fabricated the 4H-SiC DIMOSFETS at the blocking voltages of 900 V [12]. Also in the same year, Denso Corporation Japan introduced UMOSFET, which produced the blocking voltage of 450 V, specific resistance of  $10.9 \text{ m}\Omega\text{cm}^2$  and  $V_B^2/R_{\text{on-sp}}$  of  $18.6 \text{ MW/cm}^2$  [13]. In 1998, Purdue University reported a SiC accumulation-channel UMOSFET with new structural features that shield the trench oxide from high electric fields in the blocking state. The new features consist of a p-type region formed in the trench bottom by self-aligned ion implantation and a thin n-type epilayer incorporated between the n-drift region and the p-type base [14].

A way to avoid the problem with oxide breakdown at the trench corners is to eliminate the trenches. This was accomplished in 1996 with the introduction of planar implanted DMOSFETs [15]. Since impurity diffusion is impractical in SiC, the base and source regions are formed by selective ion implantation using aluminum or boron for the p-type base and nitrogen for n+ source. Because p-type implants are conducted at temperatures between 1600 and 1700 °C, self-aligned implant process using polysilicon gates are not practical in SiC and realignment tolerances must be allowed between the base, the source and the gate features. Due to these disadvantages, the elimination of the trench corners resulted in a threefold improvement in device blocking voltage to 760 V. This blocking voltage was achieved using 6H-SiC [16].

### Theoretical Analysis of Silicon Carbide High-Voltage DIMOSFET

DMOS transistors are common in silicon power device technology where the p-base and n+ source regions are formed by diffusion of impurities through a common mask opening. However, impurity diffusion is impractical in SiC because of the very low diffusion coefficients at any temperature. The Purdue group fabricated the first DMOS transistors in SiC using ion implantation to introduce dopants for the p-base and the n+ source [16]. The implanted DMOSFET requires that separate masks be used to define p-base and the n+ source. The construction is a vertical structure with a drift layer built on a highly conductive n+ layer. The n-drift region is designed to give the forward blocking capabilities as shown in Figure 1. The forward blocking capability is achieved by the pn junction between p-base region and n-drift region.

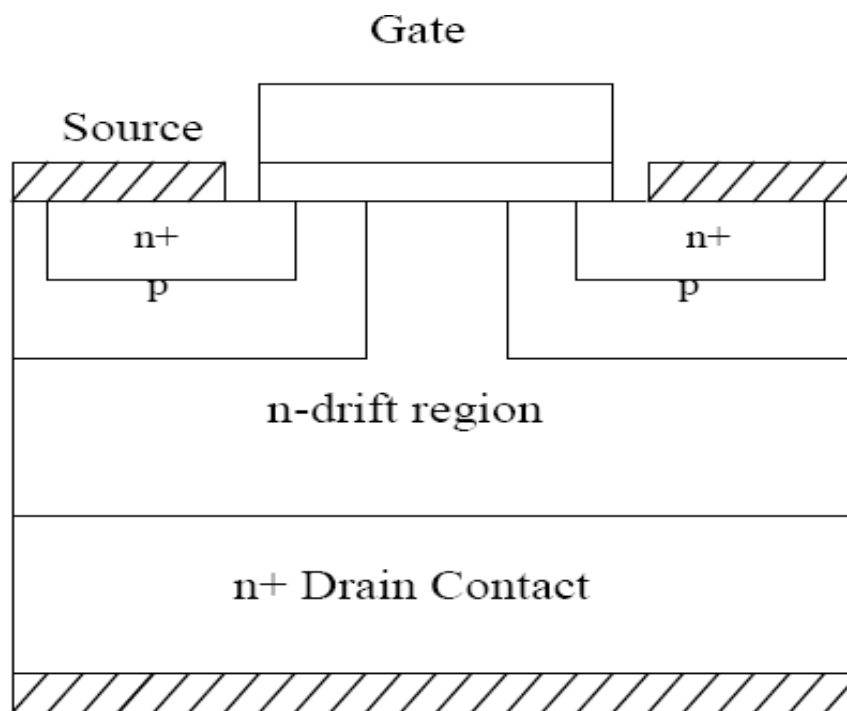


**Figure 1.** Structure of DIMOSFET

During the device operation, a fixed potential to the p-base region is established by connecting it to the source metal by the break in the n+ source region. By short-circuiting the gate to the source and applying a positive bias to the drain, the p-base/n-drift region junction becomes reverse-biased and this junction supports the drain voltage by the extension of depletion layer on both sides. However, due to the higher doping level of the p-base layer, the depletion layer extends primarily into the n-drift region. On applying the positive bias to the gate electrode, the conductive path between n+ source region and the n-drift region is formed. The application of positive drain voltage results in a current flow between drain and source through the n-drift region and conductive channel. The conductivity of the channel is modulated by the gate bias voltage and the current flow is determined by the resistance of various resistive components. The total specific on-resistance is determined as:

$$R_{\text{on-sp}} = R_{\text{n}^+} + R_{\text{C}} + R_{\text{A}} + R_{\text{J}} + R_{\text{D}} + R_{\text{S}} \quad (2)$$

where  $R_{on-sp}$  is the specific on resistance,  $R_{n+}$  is the contribution from the n+ source,  $R_C$  is the channel resistance,  $R_A$  is the accumulation layer resistance,  $R_J$  is the resistance from the drift region between the p-base regions due to JFET pinchoff action,  $R_D$  is the drift region resistance, and  $R_S$  is the substrate resistance.

In a power MOSFET, the blocking voltage is supported across the drift layer, and thus the drift-region resistance is considered to be the minimum possible theoretical limit for the on-resistance of a MOSFET. For an ideal DIMOSFET, the resistances associated with the n+ source, the n-channel, the accumulation region and the n+ substrate are assumed to be negligible and the specific on-resistance of the power MOSFET is determined by the drift region only. This assumption is not accurate at lower breakdown voltages where the drift region resistance  $R_D$  is comparable to the other resistive components and these resistances should be included in calculating  $R_{on-sp}$ . However, at higher breakdown voltages,  $R_D$  is significantly higher than other resistances and  $R_{on-sp}$  can be approximated by  $R_D$ . The details of the device structure are shown in Figure 2.

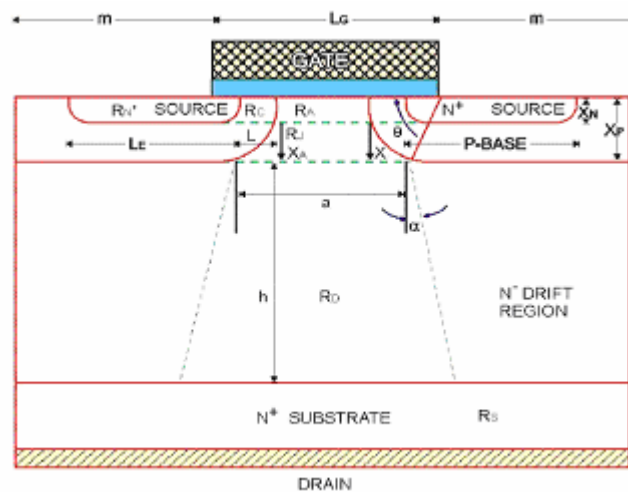


Figure 2. Cross section of power MOSFET

### Basic device equations

Consider the depletion region between the p-base region and the n-drift region as a one-dimensional abrupt p-n junction. It can be shown that the doping level  $N_B$  (/cm<sup>3</sup>) [17] that can support a given breakdown voltage  $V_B$  (V) and the depletion width  $W$  (cm) [18] at breakdown can be given as:

$$N_B = \frac{\epsilon E_c^2}{2qV_B} \quad (3)$$

and  $W = \frac{2V_B}{E_C} \quad (4)$

where  $q$  is the electron charge.

The specific on-resistance,  $R_{on-sp}$  ( $\Omega\text{-cm}^2$ ) [19] of the drift layer to support  $V_B$  is

$$R_{on-sp} = \frac{W}{qN_B\mu_n} \quad (5)$$

Substituting the values of eqs.(3) and (4) in eq.(5),

$$R_{on-sp} = \frac{4V_B^2}{\epsilon E_C^3 \mu_n} \quad (6)$$

where  $\epsilon$  is the permittivity (F/cm),  $E_C$  is the critical field of breakdown (V/cm) and  $\mu_n$  is the electron mobility in  $cm^2/V$ -sec.

The equation connecting the breakdown electric field strength  $E_C$  on the doping level  $N_B$  for a pn diode of 6H-SiC has been derived. Based on these results the relationship between  $E_C$  and  $N_B$  was obtained [20]:

$$E_C = 1.95 \times 10^4 \times N_B^{0.131} \text{ V/cm} \quad (7)$$

Eliminating  $E_C$  between eqs.(7) and (3),

$$N_B = \left( \frac{1.02 \times 10^{15}}{V_B} \right)^{1.35} \quad (8)$$

This gives for  $R_{on-sp}$  from eq. (5),

$$R_{on-sp} = (5.93 \times 10^{-9}) V_B^{2.5} \quad (9)$$

Finally the power dissipation  $P_D$  (W) [20] for the device for a 50% duty cycle can be evaluated using the equation,

$$P_D = \frac{1}{2} (J_{on}^2 A R_{on-sp} + J_L A V_B) \quad (10)$$

where  $J_{on}$  is the on-state current density in the linear region of ( $I_{DS}$ - $V_{DS}$ ) characteristics of the device in  $A/cm^2$ , and  $A$  is the device cross-sectional area in  $cm^2$ .

$R_{on-sp}$  can be determined by the slope of  $I_{DS}$ - $V_{DS}$  curve in the linear region. In our calculations we have set  $J_{on} = \frac{I_{DS}}{A}$  to calculate the maximum power dissipation for a MOSFET, which is the maximum value corresponding to  $J_{on}$  for a given gate bias. Again  $J_L \ll J_{on}$  and the second term in eq.(8) can be neglected. Hence eq.(10) can be written as:

$$P_D = \frac{1}{2} (J_{on}^2 A R_{on-sp}) \quad (11)$$

The exact equations for  $I_{DS}$  (current between drain and source),  $\rho_D$  (resistivity in drift region) and  $R_{on-sp}$  (specific on-resistance) [21-23] can be given by:

$$I_{DS} = \frac{Z \mu_n C_{ox} [2(V_G - V_T) - V_D^2]}{2L} \quad (12)$$

$$\rho_D = \frac{1}{\mu_n q N_B} \quad (13)$$

$$R_{on-sp} = \frac{\rho_D (L_G + 2m) \ln(1 + 4 \tan 26^\circ) 10^{-4}}{\tan 26^\circ} \quad (14)$$

with

$$J_{on} = \frac{I_D}{200 \times 10^{-8}} \text{ Ampere/cm}^2 \quad (15)$$

$$V_f = R_{on-sp} \times J_{on} \quad (16)$$

where we have evaluated  $I_{DS}$  for  $V_{GS} = 40$  volts, the threshold voltage  $V_T$  having been set equal to 1V as is usually the case.  $Z$  and  $L$  are the device dimensions shown in Figure 2,  $C_{OX}$  is the oxide

capacitance, and  $J_f$  and  $V_f$  are the forward current density and forward drop respectively. The rise in temperature of the device  $\Delta T$  °K is proportional to  $P_D$ , the power dissipated:

$$\Delta T = \theta_{th} P_D \tag{17}$$

where  $\theta_{th}$  is the thermal resistance associated with the device in Kelvin /Watt, its value depending on the state of the art device packaging technology. With today's technology  $\theta_{th}$  is about 1°K/W giving

$$\Delta T = P_D \tag{18}$$

For all calculations we have used an average value of  $\mu_n$ [24,20] of 530 cm<sup>2</sup>/ V sec.

*Calculations and related graphs*

In calculating the current  $I_{DS}$  and power dissipation  $P_D$ , we have used the following parameters with the value quoted against each one of them:  $L_G=20\mu m$ ,  $m=10 \mu m$ ,  $Z= 10\mu m$ ,  $L=3 \mu m$ ,  $A=200 \times 10^{-8} \text{ cm}^2$ ,  $C_{ox}=\epsilon_s/0.1$ ,  $V_G=40V$ ,  $V_D=2V$ ,  $V_T=1V$ ,  $\mu_n=530 \text{ cm}^2/V\text{-sec}$ ,  $h=30 \mu m$ , and  $a=15 \mu m$ . The set of the calculations were made on the basis of eqs. (1) to (15). By using these equations the following graphs (Figures 3-7) are plotted.

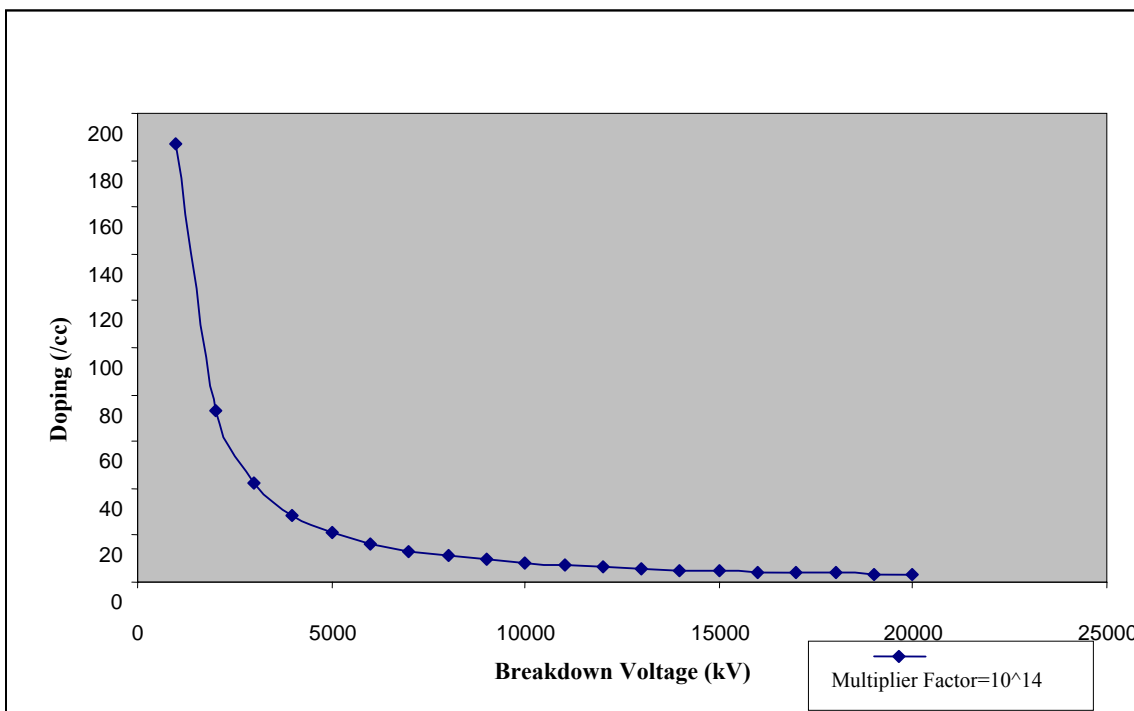


**Figure 3.** Plot of doping vs. breakdown voltage

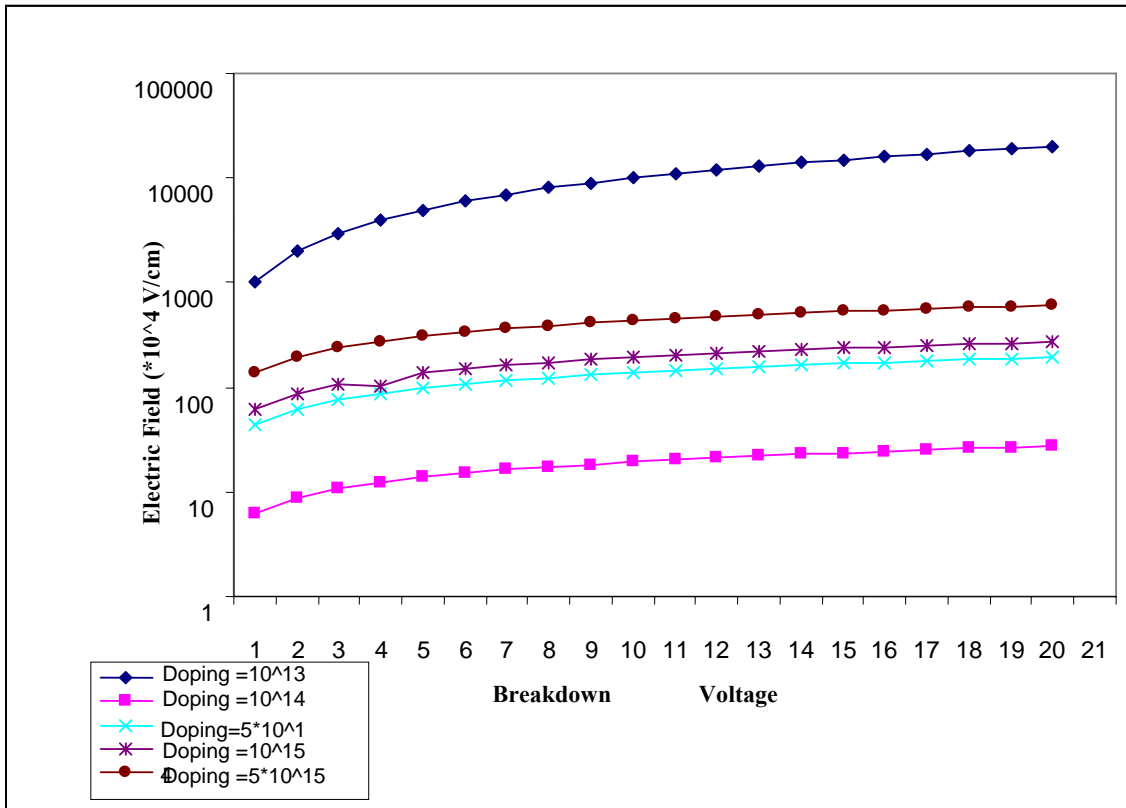


Figure 4. Plot of electric field vs. breakdown voltage

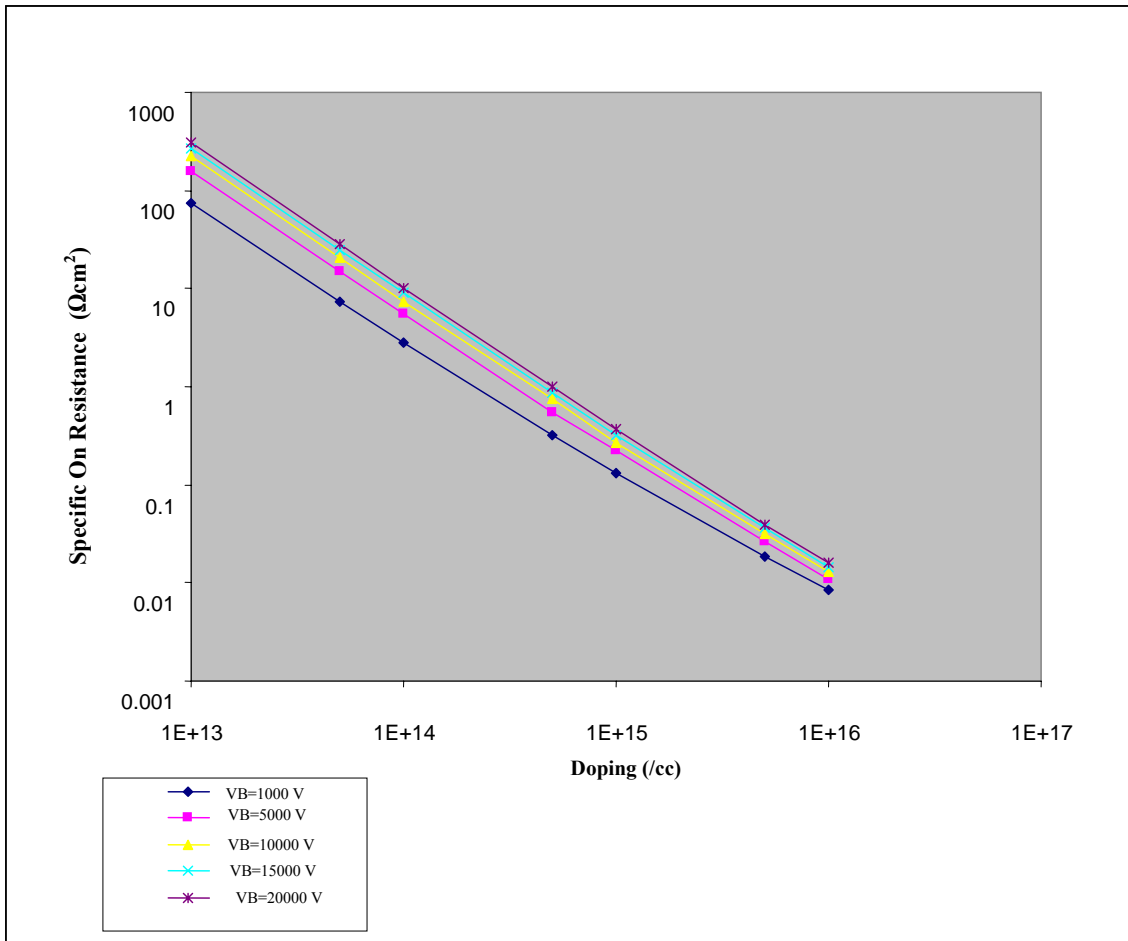


Figure 5. Plot of specific on-resistance vs. doping

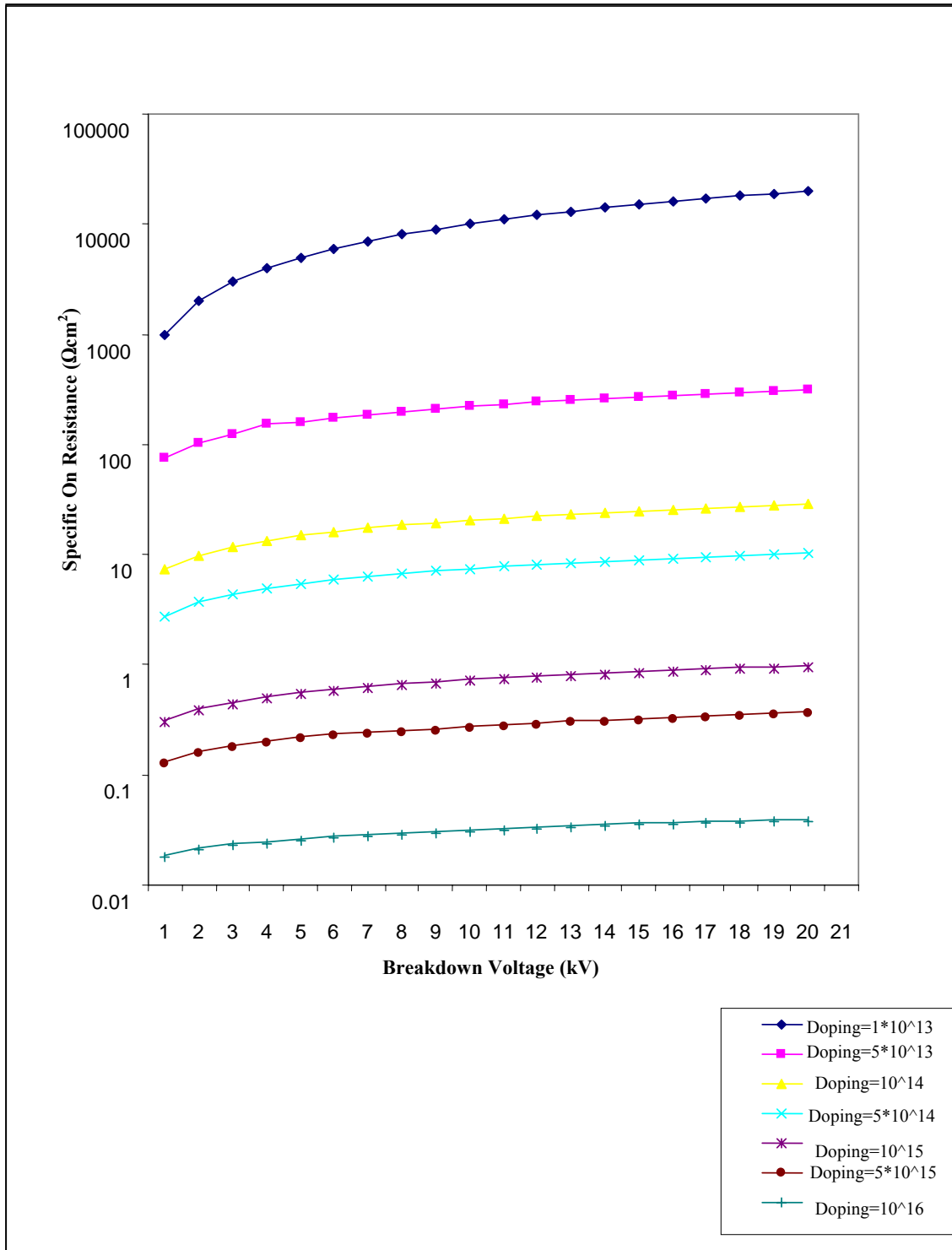


Figure 6. Plot of specific on-resistance vs. breakdown voltage

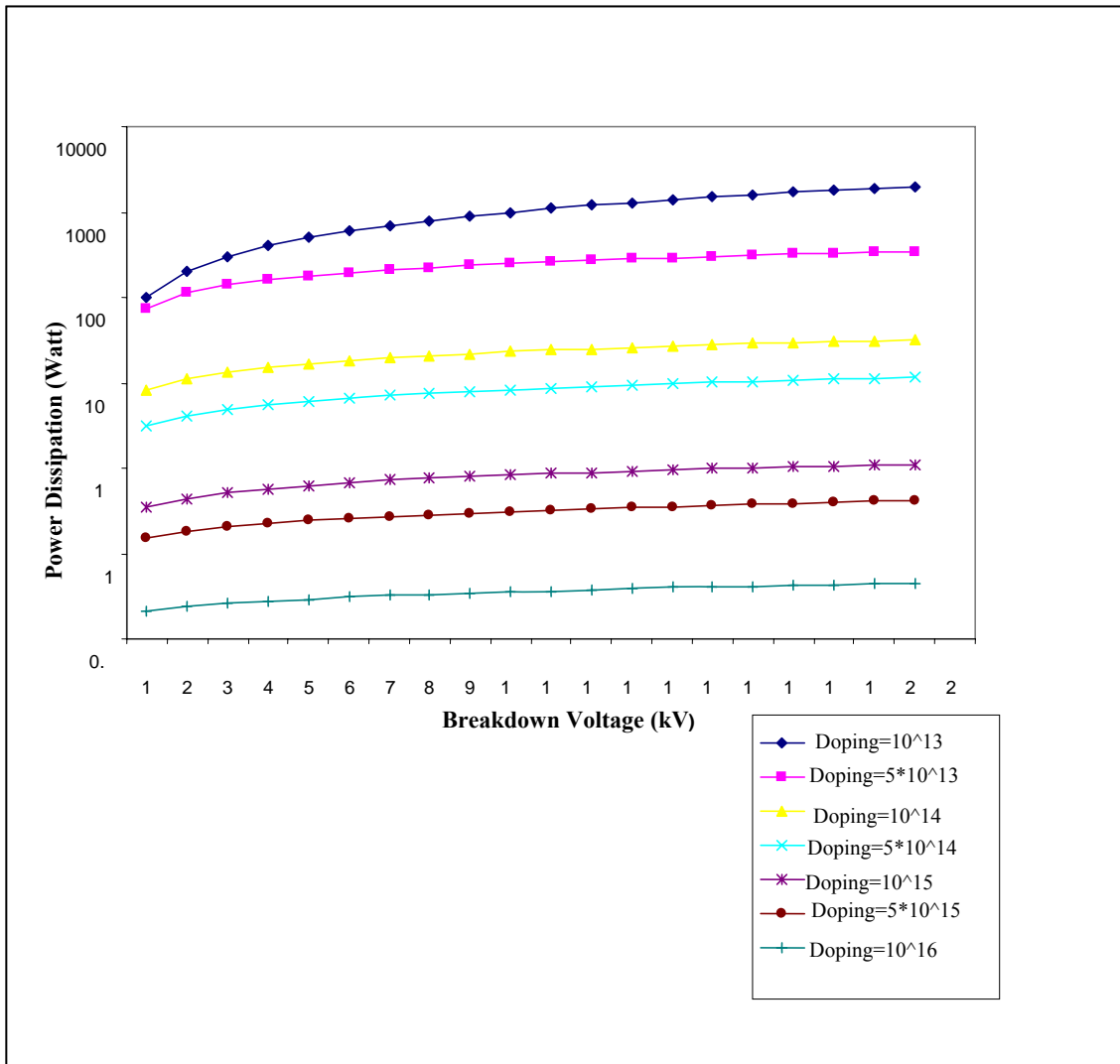


Figure 7. Plot of power dissipation vs. breakdown voltage

### Results and Discussion

Having set the device dimension as above, we began by considering the graph of Figure 3 wherein it is seen that the high breakdown voltage  $\cong 10$  kV can be attained by using the low doping level of the order of  $10^{15}/\text{cm}^3$  or less. However very low doping levels can give rise to a large parasitic drop across the drift region. Hence we needed to reduce this parasitic loss. We began with the design rule that a maximum value of the temperature rise  $\Delta T_{\text{max}}$  of  $600^\circ\text{C} \cong 800$  K for power dissipation is permissible with the latest packaging technology. This gives  $\Delta T_{\text{max}} = P_{\text{Dmax}} = 800$  W. From Figure 7 we noted that at  $V_B \geq 10$  kV,  $P_{\text{Dmax}}$  of 400 W can be attained with a doping level of  $5 \cdot 10^{13} \text{cm}^{-3}$ . Making allowance for an increase in the  $R_{\text{on-sp}}$  to twice its room temperature value over this range of the temperature rise for SiC power MOSFET, the safe margin would be to set  $N_B = 5 \cdot 10^{13}/\text{cm}^3$ . At  $V_B = 10$  kV and  $N_B = 5 \cdot 10^{13}/\text{cm}^3$ , the  $R_{\text{on-sp}} = 205 \Omega\text{-cm}^2$  (see Figure 6). Hence doubling of  $R_{\text{on-sp}}$  at  $N_B = 5 \cdot 10^{13}/\text{cm}^3$  with rise in temperature could lead to doubling the level of permissible power dissipation to 800 W. This value of  $R_{\text{on-sp}}$  can be checked from Figure 5, which gives plot of  $R_{\text{on-sp}}$  vs.  $N_B$  for different values of  $V_B$ . Finally for  $V_B = 10$  kV,  $N_B = 5 \cdot 10^{13}/\text{cm}^3$ , the critical field for breakdown, i.e.

$E_c$  can be obtained from Figure 4 giving  $E_c \cong 4.3 \cdot 10^5 \text{ V/cm}$ . Thus, apart from the device dimensions quoted above, we recommend a doping level of  $5 \cdot 10^{13} / \text{cm}^3$  for an n-drift layer of  $30 \mu\text{m}$  thickness for the safe operation of a 6H-SiC power MOSFET with a breakdown voltage of 10 kV and a maximum rise in the device temperature of  $600^\circ\text{C}$ . However, in order to reduce parasitic loading effect of  $R_{\text{on-sp}}$  of the drift region, it is recommended that either  $5 \cdot 10^{13} / \text{cm}^3$  or  $10^{15} / \text{cm}^3$  values for  $N_B$  can be safely used. Hence, the limit of  $N_B$  for a safe operation of 6H-SiC power MOSFET for 800W power dissipation in Figure 7 can be obtained by setting any value of  $N_B$  between  $5 \cdot 10^{13} / \text{cm}^3$  and  $10^{15} / \text{cm}^3$  for  $V_B = 10 \text{ kV}$  with  $E_c$  lying between  $4.3 \cdot 10^5 \text{ V/cm}$  and  $4.3 \cdot 10^6 \text{ V/cm}$  respectively.

## Conclusions

The results of this paper are based primarily on the variation of specific on-resistance with temperature and its effect on the power dissipation using the concept of field independent mobility, which help to estimate the optimum doping levels of the drift region. The 6H-SiC power MOSFET designed in the paper has a low specific on-resistance, a high breakdown voltage of 10 kV, not-too-high electric field of  $E_c \cong 10^6 \text{ V/cm}$ , and a low power dissipation much less than a maximum limit of 800W. In our analysis we have used an average value of carrier mobility of  $530 \text{ cm}^2/\text{V}\cdot\text{sec}$ . However, for still more accurate work it is advisable to use the field dependent mobility given by the equation:  $\mu = \mu_0 / [1 + (\mu_0 E / v_{\text{sat}})^\beta]^{1/\beta}$  where  $\mu_0 =$  low field mobility of  $530 \text{ cm}^2/\text{V}\cdot\text{sec}$  at  $N_B = 10^{14} / \text{cm}^3$  with an electric field of about 1000 V/cm. However, experimental verification of such a device designed along the lines given in the paper remains to be done.

## References

1. M. Ostling and N. Lundberg, "Low Ohmic Cobalt Silicide contacts to p-type 6H-SiC", IEEE Device Research Conf., Santa Barbara, CA, USA, June 1996, p.157.
2. T. Ouisse, N. Becourt, F. Templier, J. Vuiolld, S. Cristoloveanu, T. Billon, and F. Mondon, "Noise in 6H-SiC ion implanted  $p-n$  diodes", 5th Int. Conf. on Silicon Carbide and Related Materials, Conf. Ser. No. 137, September 1995, pp.683-686.
3. S. Sridevan, P. K. Mclarty, and B. J. Baliga, "On the presence of aluminum in thermally grown oxides on 6H-silicon carbide [power MOSFETs]", *IEEE Electron Device Lett.*, 1996, 17, 136-138.
4. J. A. Cooper Jr., "Recent advances in silicon carbide MOS technology", 6th Int. Conf. on Silicon Carbide and Related Materials, Kyoto, Japan, September 1995, pp.186-188.
5. J. W. Palmour, Cree Research, private communication, 1996.
6. S. Hu and K. Shan, "A new edge termination technique for SiC power devices", *Solid State Electronics*, 2004, 48, 122-123.
7. J. A. Cooper, M. R. Melloch, R. Singh, A. Aggarwal, and J. W. Palmour, "Status and prospect for SiC MOSFET", *IEEE Trans. Electron Devices*, 2002, 49, 658-664.
8. R. Kosugi, S. Suzuki, M. Okamoto, S. Harada, J. Senzaki, and K. Fukuda, "Strong dependence of the inversion channel mobility of 4H and 6H SiC (0001) MOSFETs on the water content in pyrogenic re-oxidation annealing", *IEEE Electron Device Lett.*, 2002, 23, 136-138.

9. B. J. Baliga, "Power semiconductor device figure of merit for high-frequency applications", *IEEE Electron Device Lett.*, **1989**, *10*, 455-457.
10. J. B. Casady, A. K. Agarwal, L. B. Rowland, S. Seshadri, P. A. Sanger, and C. D. Brandt, "Silicon carbide MOSFET technology", IEEE Int. Symposium on Compound Semiconductors, San Diego, USA, September **1997**, pp.359-362.
11. A. K. Agarwal, J. B. Casady, L. B. Rowland, W. F. Valek, M. H. White, and C. D. Brandt, "1.1 kV 4H-SiC Power UMOSFET's", *IEEE Trans. Electron Device Lett.*, **1997**, *18*, 586-588.
12. J. B. Casady, A. K. Agarwal, L. B. Rowland, W. F. Valek, and C. D. Brandt, "900V DMOS and 1100 V UMOS 4H-SiC Power FET's", IEEE Device Research Conf., Fort Collins, USA, June **1997**, pp 32-33.
13. P. M. Shenoy and B. J. Baliga, "The planar 6H-SiC ACCFET: a new high-voltage power MOSFET structure," *IEEE Trans. Electron Device Lett.*, **1997**, *18*, 589-591.
14. Y. Sugawara and K. Asano, "1.4 kV 4H-SiC UMOSFET with low specific on-resistance", Int. Symposium on Power Semiconductor Devices & ICs, Kyoto, Japan, June 1998, pp.119-122.
15. J. N. Shenoy, J. A. Cooper, and M. R. Melloch, "High-voltage double-implanted MOS power transistors in 6H-SiC", IEEE Device Research Conf., Santa Barbara, CA, June **1996**, pp. 202-204.
16. J. N. Shenoy, J. A. Cooper, and M. R. Melloch, "High-voltage double-implanted power MOSFET's in 6H-SiC", *IEEE Trans. Electron Device Lett.*, **1997**, *18*, 93-95.
17. K. Shenai, R. S. Scott, and B. J. Baliga, "Optimum semiconductors for high power electronics", *IEEE Trans. Electron Devices*, **1989**, *36*, 1811-1823.
18. C. Weitzel, J. Palmour, C. Carter, K. Moore, K. Nordquist, S. Allen, C. Thero, and M. Bhatnagar, "Silicon carbide high-power devices", *IEEE Trans. Electron Devices*, **1996**, *43*, 1732-1741.
19. B. J. Baliga, "Trends in power semiconductor devices", *IEEE Trans. Electron Devices*, **1996**, *43*, 1717-1731.
20. M. Bhatnagar and B. J. Baliga, "Comaparison of 6H-SiC, 3C-SiC and Si for power devices", *IEEE Trans. Electron Devices*, **1993**, *40*, 645-655.
21. S. M. Sze, "Physics of Semiconductor Devices", 2nd Edn., John Wily & Sons, New York, **1985**.
22. M. Ruff, H. Mitlehner, and R. Helbig, "SiC devices: physics and numerical simulation", *IEEE Trans. Electron Devices*, **1994**, *41*, 1040-1054.
23. M. Hasanuzzaman, S. K. Islam, and L. M. Tolbert, "Model simulation and verification of vertical double implanted (DIMOSFET) transistor in 6H-SiC", *Int. J. Modelling and Simulation*, **2003**, *4*, 1-4.
24. R. B. Hillborn and H. Kang, "Charge carrier concentration and mobility in n-type 6H polytypes of SiC", in "Special Reports for the Performance of Silicon Carbide", University of South Carolina Press, **1973**, pp. 337-339.

Full Paper

## Changes in viscoelastic properties of longan during hot-air drying in relation to its indentation

Jatuphong Varith\*, Chanisara Noochuay, Tipaporn Khamdang, and Adisorn Ponpai

Department of Agricultural and Food Engineering, Maejo University, Chiang Mai, 50290, Thailand

\* Author to whom correspondence should be addressed, e-mail: [jatuphon@mju.ac.th](mailto:jatuphon@mju.ac.th)

Received: 3 October 2007 / Accepted: 30 April 2008 / Published: 1 May 2008

---

**Abstract:** Changes in viscoelastic properties are related to the indentation of whole longan (*Dimocarpus longan* Lour.) in the drying process. The objective of this research is to determine parameters from a creep test to characterise the viscoelastic properties of on-progress dried longan. During 65°C hot-air drying, the whole longan was sampled every 2 hours to perform the creep test with a constant stress of 44 kPa using a texture analyser. Viscoelastic properties, viz. retardation time ( $\lambda_{ret}$ ), instantaneous compliance ( $J_0$ ), retarded compliance ( $J_1$ ), creep compliance ( $J$ ), Newtonian viscosity ( $\eta_0$ ), and modulus of elasticity ( $E$ ) were analysed using the four-element Burger's model. The  $\lambda_{ret}$  and  $E$  decreased linearly as the moisture content decreased from approximately 70% to 64-57%, then they linearly increased as the moisture content further decreased to 11%. The  $J$  and  $J_1$  increased linearly and then decreased linearly as the moisture content decreased, showing the transition moisture content of 64%. The  $J_0$  decreased as the moisture content decreased. There was no marked change in  $\eta$ , thus it was not involved in the indentation of dried longan. The moisture content of 64-57% was found to be the critical range leading to the indentation of longan during the drying process.

Keywords: longan, drying, creep test, viscoelastic properties, indentation

---

### Introduction

Longan (*Dimocarpus longan* Lour.) is one of the most important crops of Thailand with an export value of 2.4 billion Baht in 2006 [1]. Concentrated production of longan in a short season causes the depreciation of the fresh produce selling price. The most popular method to prolong the longan shelf

life is to dry the longan with a hot-air stream. Drying the longan with peel, referred to as 'whole longan', is generally more popular than drying the longan flesh because the drying process can be operated in large scale. However, the problem associated with whole longan large-scale drying is the incident of indentation of the finished product. Indented longan is considered as a low-grade product and lowers the selling price as much as 50%. Therefore, a study to characterise the viscoelastic properties of whole longan is necessary for the basic understanding of how indentation takes place during the hot-air drying.

Generally, drying of whole longan is accomplished with hot-air at 60-75°C for 60-72 hr. As drying progresses, the moisture content decreases slowly, resulting in shrinkage of the internal tissue. At the initial stage, the longan peel is softened, but toward the final stage, the peel becomes hardened. Indentation often occurs between these two drying stages but has never been defined in terms of a critical drying period or moisture content. It is comprehensible that the indentation of longan occurs due to the loading compression of longan in the drying cabinet. The nearly constant loading can be simulated using a creep test. Previously, the creep test was effectively used as a tool to characterise the viscoelastic properties of biological materials. Ru et al. [2] studied the nonlinear behaviour of apple flesh under uniaxial creep loading condition and found that the power law equation was adequate to predict the creep behaviour of apple flesh. The non-linear creep formulation predicted the creep behaviour of apple flesh to within 2.7% at 67.2 kPa loading level. Ru and Puri [3] further studied the nonlinear behaviour of apple and potato flesh under uniaxial and triaxial creep tests using the four material property functions in a nonlinear three-dimensional constitutive equation based on the Green-Rivlin theory. The nonlinear constitutive equation predicted the results which were comparable to the experimental data. The nonlinearity of both apple and potato flesh increased with loading time and became significant after an initial loading period of 90 sec. Datta and Morrow [4] studied the creep behaviour of biological materials with graphical and computational method. Both methods were based upon the assumption of linear viscoelasticity, and the four element Burger's model was applied to the biological materials. The computational method was effective for determining the accurate magnitude of material constant and well described the experimental creep behaviour of apple, potato and cheese. On the other hand, the graphical method provided approximate values for the material constants used as initial values for available curve fitting.

Previous work about creep test applied on biological materials was reported on some products addressed above. However, the report on creep test being applied on longan has not been found. The objective of this study is to evaluate changes in viscoelastic properties of longan during hot-air drying in relation to the indentation of whole longan. Information obtained from this work should provide the drying strategy to minimise the indentation problem and improve the quality of dried longan.

## Materials and Methods

### *Critical spot susceptible to indentation*

This preliminary experiment aims to explore a critical spot on fresh longan where indentation often occurs. Grade AA, off-season longan cv. Dor, with an average diameter of 25 mm freshly harvested from orchard in Lumphun province, Thailand, was used in this work. The flat surface probe with a

diameter of 60 mm was applied in compression mode by a texture analyser model TA-XT Plus (Texture Technologies, Inc., UK) with a cross-head speed of 1 mm/s on the longan fruit at 3 specific locations (Figure 1), providing the quasi-static load while the data acquisition sensitivity following ASAE Standards S368.4 [5] was ensured. Compression test was ended at the target strain of 20% of initial fruit height or equivalent to 5.2 mm to ensure an occurrence of longan indentation. The force-distance profile from the compression test was obtained and analysed. The test was accomplished with 6 replications. The location on the fruit which exhibited the lowest force at 20% strain was identified as the critical spot of indentation.

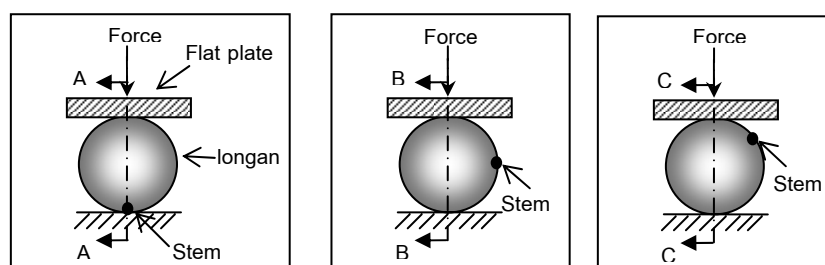


**Figure 1.** Test of critical spot of indentation on longan fruit: Plane A-A – at stem, Plane B-B – at 90° from stem, Plane C-C – at 45° from stem

#### *Drying apparatus setup*

A laboratory-scale hot-air dryer without air recirculation was used for the experiment (Figure 2). The dryer consisted of an axial fan, an electric heater and a drying basket with a capacity of 3 kg (20x25x10 cm: height x length x width) connected to an electric balance, model CP3202S (Satorius AG, Goettingen, Germany), for data acquisition (DAQ). The RS232 port of the electric balance was connected to a personal computer providing DAQ every 5 min. Two additional baskets (size 20x25x25 cm) without DAQ were placed in the front and back of the basket with DAQ to provide the creep test for the longan sample during drying. Overall length of the three baskets was 60 cm, equivalent to the thickness of the longan bed in industrial hot-air drying. A hot-air stream at 65°C with a velocity of 0.7 m/s, an optimum drying velocity reported by Achariyaviriya et al. [6], was employed to dry the longan. For each batch, the fruits were dried for 60 hr to the final moisture content of about 11%. The initial and intermediate moisture content of fresh longan was determined using the hot-air oven method at 103±1°C for 72 hr following ASAE Standards S325.2 [7].

#### *Creep test analysis*

The creep test was performed on the on-progress dried longan with a texture analyser model TA-XT Plus (Texture Technologies, Inc., UK). During drying with the hot-air apparatus, three longans from the front and back baskets without DAQ (Figure 2) were sampled every 2 hr to perform the creep test. Each longan was quickly placed on the texture analyser platform inside the temperature-controlled cabinet which provided a testing temperature of 65°C, similar to that in the hot-air dryer. A cross-head

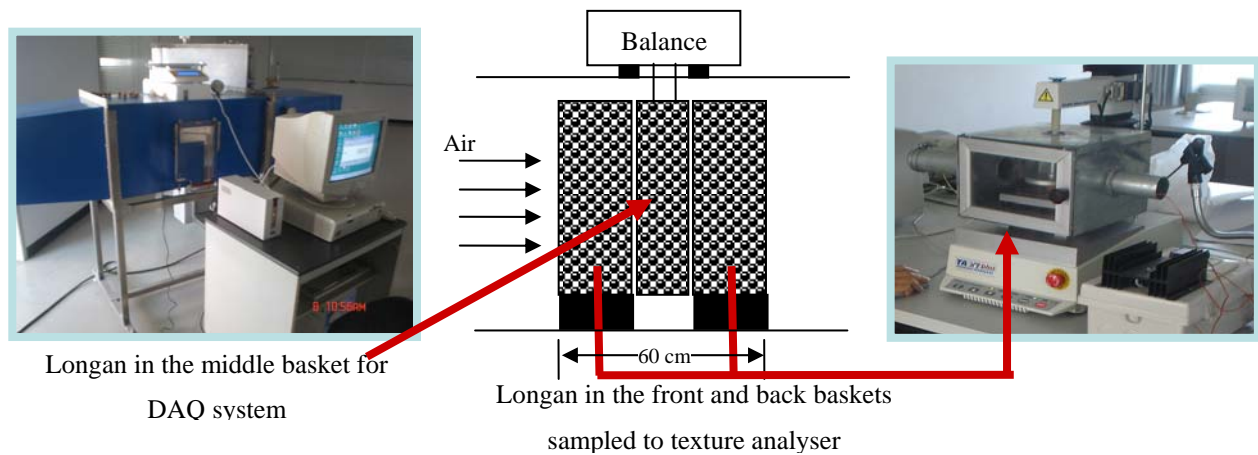


**Figure 2.** Laboratory-scaled tray dryer with DAQ system (left); Schematic diagram of longan basket setup inside drying chamber (middle); Texture analyser used for creep test (right)

speed of the 60-mm diameter flat-plate probe was set at 1 mm/s. For the creep test, the longan fruit was compressed and held with a constant stress of 44 kPa for 3 min (details of stress estimation are discussed later). Compression was performed on the fruit at the critical spot determined in the previous section. To analyse the data, assumptions of creep test were applied as follows:

- a. A constant stress of 44 kPa was estimated from the stress on a single longan derived from the vertical load onto the bottom plane of longan in a commercial longan drying bed with a height of 60 cm, according to Figure 3.
- b. The cross-sectional area used for stress calculation was assumed fixed at 0.639 cm<sup>2</sup> (Figure 3). Using a fixed area for stress calculation provided the approximate rather than the accurate magnitude of stress since the compressing area could change during constant loading. However, this approximate stress provided sufficient information to characterise the viscoelastic properties of longan in this work.
- c. The stress applied on longan was assumed as a nominal stress [8], meaning that an internal integrity of longan was uniform and the effect of internal hole on stress was included in the assumption.
- d. The strain applied on longan in this work, defined as a change in height compared to the original height of longan fruit, was assumed as an axial strain. The transverse strain on longan during compression was negligible.

After each test, the strain versus time profile of the creep test was analysed with four element Burger's model (Figure 4) following Eq (1):

$$J = J_0 + J_1 \left( 1 - \exp \left( \frac{-t}{\lambda_{ret}} \right) \right) + \frac{t}{\eta_0} \quad (1)$$

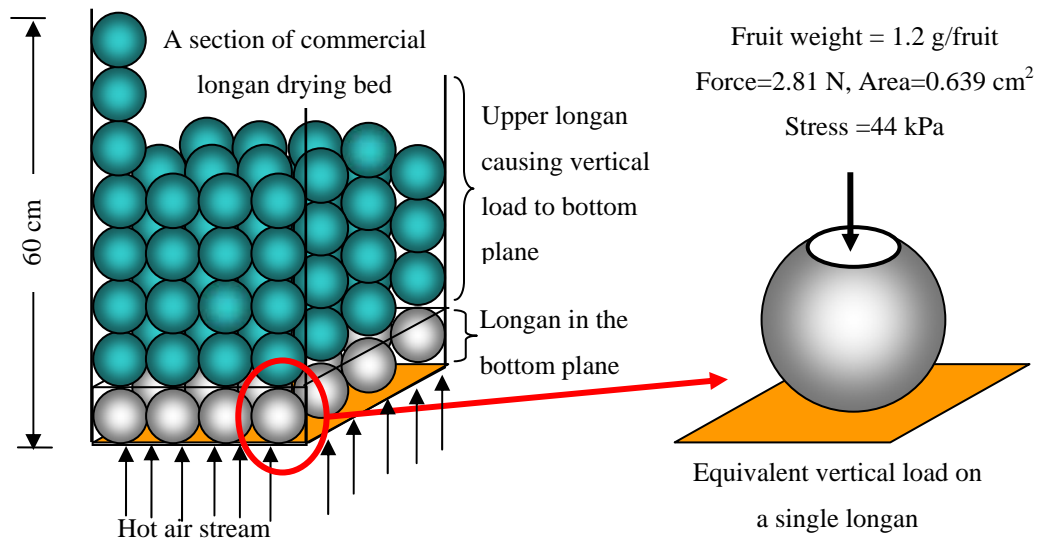


**Figure 3.** Schematic diagram of estimation of stress on longan for creep test analysis

where  $J$  is creep compliance which is a function of time ( $t$ ), expressed by  $\gamma/\sigma_{constant}$  or  $1/E$  ( $E$  is elastic modulus,  $\gamma$  is strain, and  $\sigma_{constant}$  is constant stress);  $J_0$  is instantaneous compliance defined as  $1/E_0$  ( $E_0$  is elastic modulus of free spring);  $J_1$  is retarded compliance defined as  $1/E_1$  ( $E_1$  is elastic modulus of compound spring);  $\lambda_{ret}$  is retardation time defined as a ratio of  $\eta_1/E_1$  ( $\eta_1$  is Newtonian viscosity of compound dashpot); and  $\eta_0$  is Newtonian viscosity of free dashpot. The complete derivation of Burger’s model was described by Steffe [9].

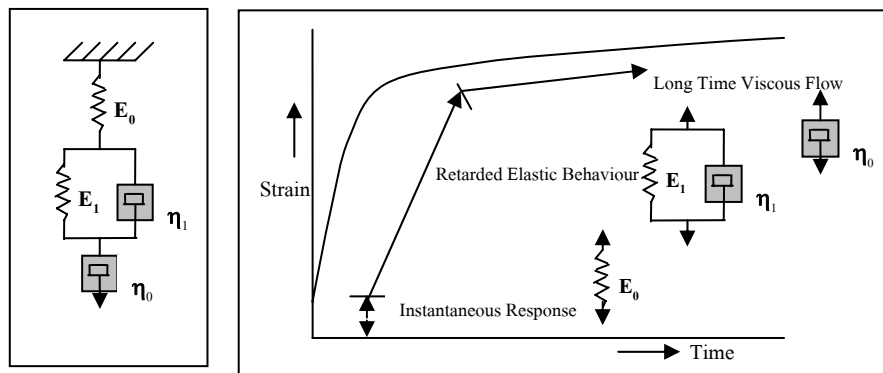


**Figure 4.** Mechanical analogy of four element Burger’s model for the creep test of longan

The creep parameters, e.g.  $J_0$ ,  $J_1$ ,  $\lambda_{ret}$  and  $\eta_0$  from Eq (1) were determined using generalised reduced gradient nonlinear optimisation embedded in Microsoft Excel™ (Frontline Systems, Inc. NV) with a prediction tolerance of  $10^{-4}$  and 95% confident interval. Once  $J_0$ ,  $J_1$ ,  $\lambda_{ret}$  and  $\eta_0$  were obtained from the optimisation,  $J$  was calculated using Eq (1) for each drying time ( $t$ ). Plots of  $J_0$ ,  $J_1$ ,  $\lambda_{ret}$ ,  $\eta_0$ ,  $J$ , and  $E$  (a reciprocal of  $J$ ) versus moisture content were obtained to characterise the changes in viscoelastic properties as well as the critical moisture content of longan susceptible to indentation during drying with hot air.

## Results and Discussion

### Critical indentation spot evaluation

Figure 5 shows that fresh longan compressed on plane A-A (at the stem) requires greater force to reach 20% of the original fruit height than that for plane B-B (90° from stem) and plane C-C (45° from stem). Greater compression force implies more resistance of the longan to external force. At a deformation of 5.2 mm (20% of initial height), compressing the longan at the stem requires a force of approximately 60 N while compressing the longan at 90° and 45° from the stem requires about 10 and 30 N respectively. It can be implied that the spot at 90° from the stem is the critical spot susceptible to indentation of longan due to the lowest compression force used. This result agrees with the observation that most dried longan fruits sampled from two industrial drying sites exhibited indentation, more than 80% of which were on the spot 90° from the stem. Therefore, for further creep test all samples were tested at the spot 90° from the stem.

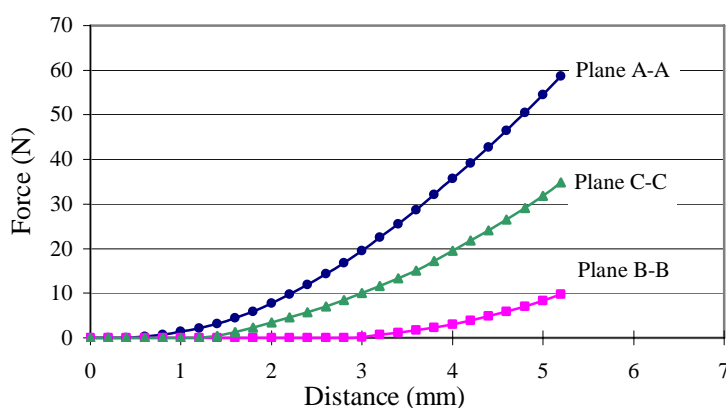


**Figure 5.** Average force-distance profiles to evaluate the critical indentation spot of fresh longan

### Drying characteristics of whole longan

The drying curves of whole longan are different for the three locations of drying (Figure 6). The front basket, located near the heater, was subjected to direct 65°C hot air exposure, therefore it exhibited the fastest moisture decrease. The drying curve of the longan in the front basket fits well with an exponential model ( $r^2$  of 0.99). On the other hand, the fruits in the middle (DAQ) and the back basket were subjected to indirect hot air after passing through the front basket. Thus the drying curves of longan in the middle (DAQ) and the back basket exhibited a slower moisture decrease. Both curves fit well with the 3<sup>rd</sup> degree polynomial models rather than the exponential model. The reason for these differences is the thickness of the basket. As hot air passes through the front basket, there is a pressure drop of air stream across the middle and back baskets. Heat is transferred to the longan in the front basket to remove moisture. Thus, the hot air is moistened and the enthalpy of the hot air stream is reduced resulting in a lower capacity to remove moisture from longan. So the drying rate decreases drastically as apparent in the drying curves of longan in the middle (DAQ) and back baskets. Since

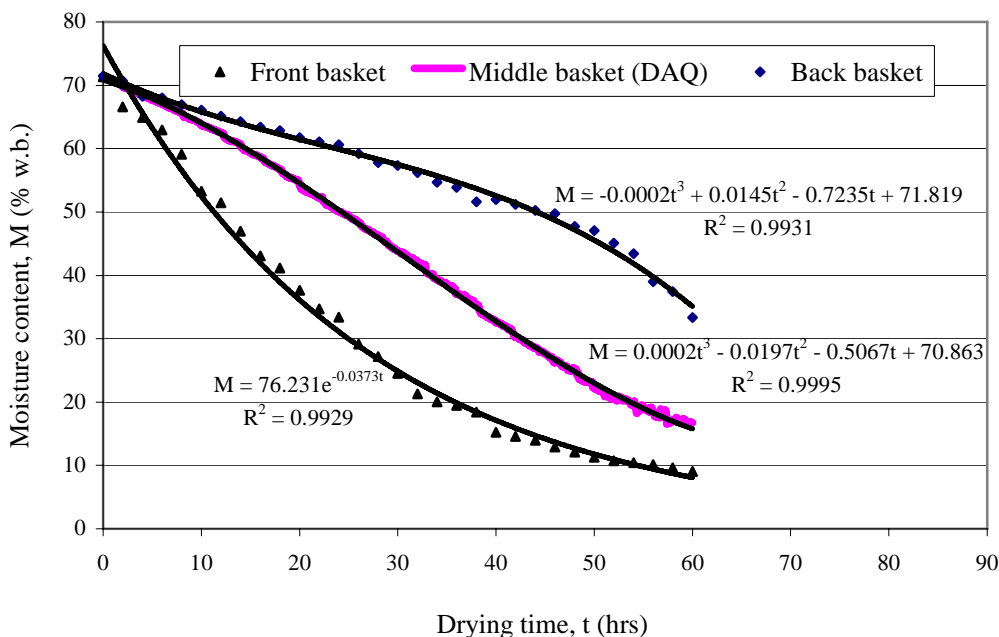
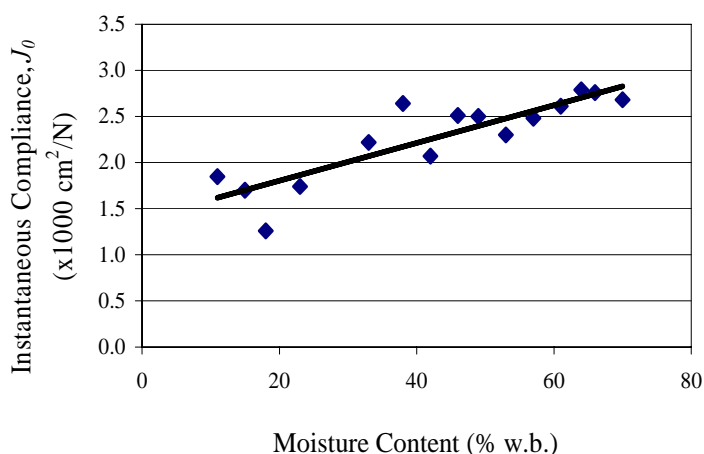


**Figure 6.** Drying curves of whole longan using hot-air (65°C) at velocity of 0.7 m/s

further experiments on the viscoelastic characteristics of longan during the drying process were done on the longan sampled from the front and back baskets, it is more appropriate to characterise the viscoelastic properties in relation to the moisture content rather than drying time.

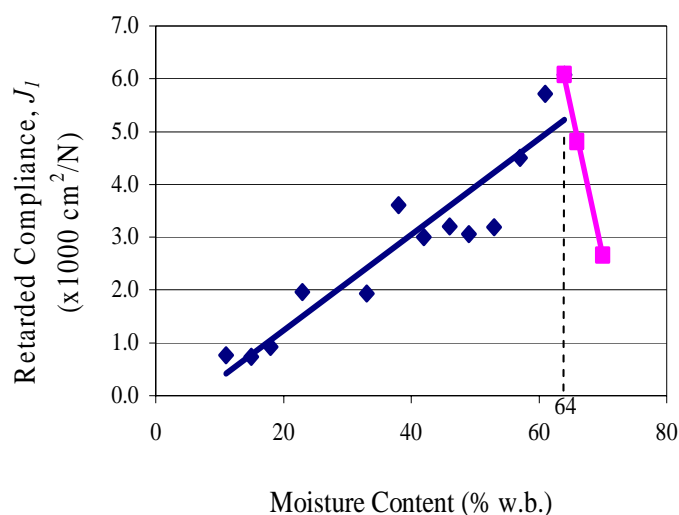
*Changes in viscoelastic properties*

Figure 7 shows that the instantaneous compliance ( $J_0$ ), representing the elastic part of longan, decreases with a decrease in moisture content. A decrease in  $J_0$  suggests that longan loses its elastic behaviour, resulting in a slower response in resisting external loading. At the beginning of drying, the whole internal space of fresh longan is filled with longan flesh, therefore its elastic behaviour is evident. As the drying progresses, the flesh of longan shrinks markedly, thus air void becomes larger inside the dried longan. Consequently, it loses its capacity to react to the sudden external loading resulting in a decrease of its elastic behaviour.



**Figure 7.** Relationship between instantaneous compliance ( $J_0$ ) and moisture content of longan

Figures 8 and 9 indicate that the retarded compliance ( $J_I$ ) and retardation time ( $\lambda_{ret}$ ) of longan during drying are divided into two periods. The first period is identified by moisture content reduction from 71% to 64-57% (w.b.) while the second period is from 64-57% to 11% (w.b.) reduction of moisture content. The  $J_I$  value represents the retarded elastic behaviour during constant loading. In relation to moisture content,  $J_I$  during moisture reduction from 71 to 64% increases and then gradually decreases as longan continues to dry at moisture content below 64%. The  $\lambda_{ret}$  value, representing the time under constant loading until the strain reaches asymptotic plateau, exhibits the response to constant loading in a similar manner to  $J_I$ , with the transition moisture content of about 57%. Therefore the moisture content in the range of 57-64% is the critical range of viscoelastic changes during the drying of longan. However, the Newtonian viscosity ( $\eta_0$ ) does not change during drying (Figure 10), implying that the changes in viscoelastic properties of longan during drying are not influenced by  $\eta_0$ . The creep compliance ( $J$ ) in Figure 11 exhibits a similar trend of change to that of  $J_I$ , while the elastic modulus ( $E$ ) in Figure 12 which is in inverse relationship to  $J_I$  exhibits an opposite trend.



**Figure 8.** Relationship between retarded compliance ( $J_I$ ) and moisture content of longan

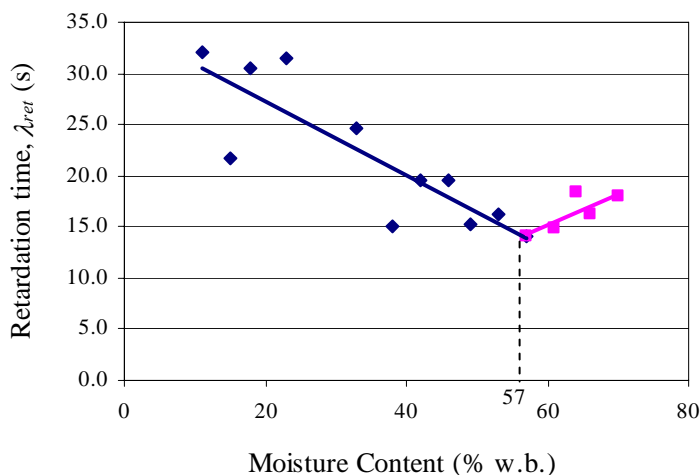


**Figure 9.** Relationship between retardation time ( $\lambda_{ret}$ ) and moisture content of longan

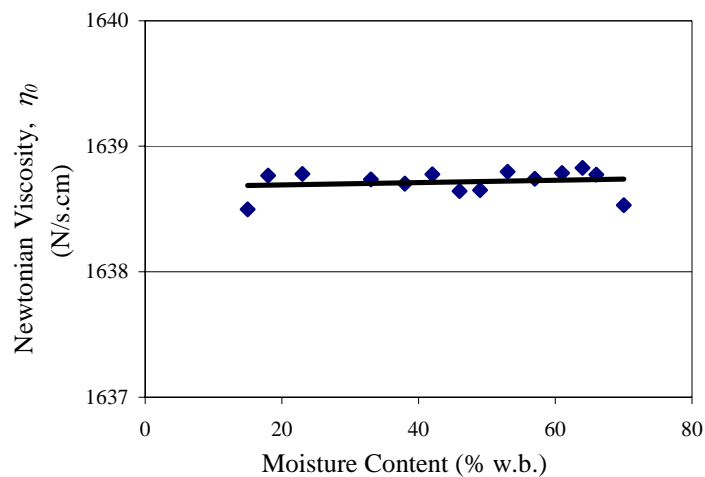


**Figure 10.** Relationship between Newtonian viscosity ( $\eta_0$ ) and moisture content of longan

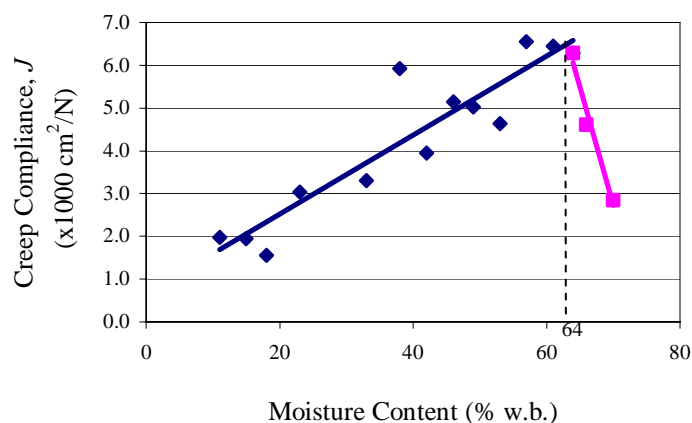


**Figure 11.** Relationship between creep compliance ( $J$ ) and moisture content of longan

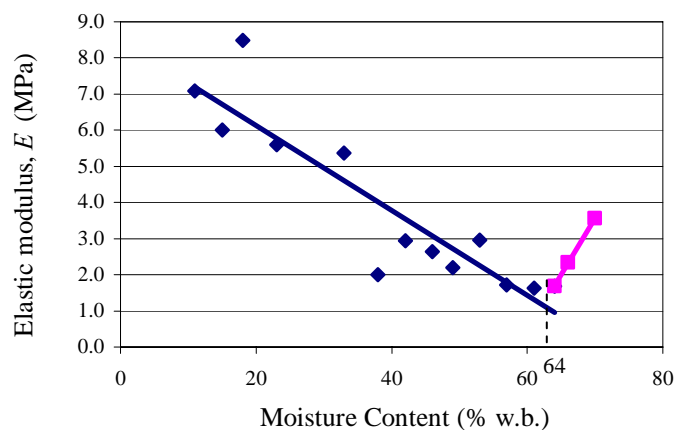


**Figure 12.** Relationship between elastic modulus ( $E$ ) and moisture content of longan

The moisture content in the range of 57-64% is a critical range susceptible to indentation of longan because  $E$  and  $\lambda_{ret}$  are minimal while  $J$ , and  $J_I$  are maximal. The minimum  $E$  at the critical

moisture content also means minimal resistance of longan to the external force. In implementing the findings to the industrial drying process, care should then be taken during the critical moisture content range of 57-64% when the on-progress dried longan will be weakest and easily indented. If the constant load due to the weight of the drying bed is too high, longan at the bottom layer of the drying bed may be indented, especially at the critical moisture content. Once the drying progresses toward the final moisture content of 11% (w.b.), the peel will harden, in agreement with increasing  $E$ . However, the longan loses its ability to regain the original spherical shape, which is explained by the increasing of  $\lambda_{ret}$ . This results in a permanently indented longan, which drastically lowers the market value of the final product. Our findings also agree with the observation of the longan drying processors that special care must be taken during the 15-20 hours of drying (corresponding to the moisture content of about 60% w.b. in Figure 6) when the softening of longan in the drying cabinet tends to occur. Therefore our analyses are compatible with the practical guidelines from the longan drying processor, and also provide an in-depth explanation on how the viscoelastic properties influence the indentation of longan.

## Conclusions

In this work, changes in viscoelastic properties of longan during hot air drying have been determined. Some important parameters derived from the creep test, including  $J$ ,  $J_1$ ,  $E$  and  $\lambda_{ret}$ , indicate that longan indentation is related to its moisture content. At the beginning of the drying process, the fruit is softened (less firm) until moisture content is lowered to about 57-64%, when it starts to harden. Changes in the creep compliance ( $J$ ), the retarded compliance ( $J_1$ ), the elastic modulus ( $E$ ) and the retardation time ( $\lambda_{ret}$ ) correspond well with changes in viscoelastic properties during the drying process. Critical moisture content has been determined to be in the range of 57-64% (w.b.), at which  $J$  and  $J_1$  are maximal and  $E$  and  $\lambda_{ret}$  are minimal. These findings could be a useful guide that helps to minimise permanent indentation of longan.

## References

1. Office of Agricultural Economic, Thailand, online from <http://www.oae.go.th/statistic/export/1301LOD.xls> (in Thai), 2007.
2. R. Ru, V. M. Puri., and C. T. Morrow, "Nonlinear Viscoelastic Properties of Apple Flesh Under Creep", ASAE Paper No. 88-6504. St. Joseph, MI, USA, 1988.
3. R. Ru and V. M. Puri, "Characterization of Nonlinear Behavior of Apple and Potato Flesh Under Creep", ASAE Paper No. 91-6023. St. Joseph, MI, USA, 1991.
4. A. K. Datta and C. T. Morrow, "Graphical and computational analysis of creep curves", *Transac. ASAE*, 1983, 26, 1870-1874.
5. ASABE Standards, "Compression Test of Food Materials of Convex Shape" St. Joseph, MI, USA, 2006a, pp. 608-616.
6. A. Achariyaviriya, S. Sophonronarit, and J. Tiansuwan, "Study of longan flesh drying", *Drying Technology*, 2001, 19, 2315-2329.
7. ASABE Standards, "Moisture Measurement—Unground Grain and Seeds", St. Joseph, MI, USA, 2006b, pp. 605-606.

8. N. N. Mohsenin, "Physical Properties of Plant and Animal Materials", 2nd Edn., Gordon and Breach Publishers, New York, **1996**.
9. J. F. Steffe, "Rheological Methods in Food Process Engineering", 2nd Edn., Freeman Press, East Lansing, **1996**.

© 2008 by Maejo University, San Sai, Chiang Mai, 50290 Thailand. Reproduction is permitted for noncommercial purposes.

*Full Paper*

## **A survey on the energy consumption and demand in a tertiary institution**

**Adekunle O. Adelaja, Olatunde Damisa, Sunday A. Oke\*, Akinwale B. Ayoola, and Allen O. Ayeyemitan**

Department of Mechanical Engineering, University of Lagos, Nigeria

\* Author to whom correspondence should be addressed, e-mail: [sa\\_oke@yahoo.com](mailto:sa_oke@yahoo.com)

*Received: 15 December 2007 / Accepted: 5 May 2008 / Published: 12 May 2008*

---

**Abstract:** The need for energy supply, particularly electricity, has been on the increase in the last two decades in developing countries such as Nigeria. Economic and industrial developments have led to this increase in demand for electricity. In universities, much of the electricity consumption is consumed in air conditioning systems, which are used to overcome the indoor thermal discomfort during harsh seasons. An amount of electricity is also consumed by laboratory equipment and machinery used for practical and demonstrations. Thus, if universities are to achieve the goals of teaching, research and community service, then proper management of electricity supplied to the system is needed in view of its limited availability. Since electrical energy in Nigeria is highly subsidised by the government, monitoring and controlling the energy consumption pattern in a university is a major aim in the country. However, there is still a lack of information about electricity end-use consumption in Nigerian universities. This paper presents the results of a walk-through energy audit conducted in a university and recommends means of tackling the problem from the demand end by focusing on the areas of potential savings flagged by the energy audit. It was noted that tackling the problem of energy demand from the users' end is quite challenging, but it might be the only hope of the school in view of inflexibility of supply.

**Keywords:** energy, energy demand, energy consumption

---

## **Introduction**

Reduction of energy consumption in domestic buildings and commercial settings has been a major aim worldwide in view of the limiting of the growing demand for electricity and the efforts to reduce CO<sub>2</sub> emissions [1-4]. Investigations have been extensive with active researches carried out in major countries such as Kuwait [2], Sweden [3], Namibia [5], USA [6], Syria [7], Brazil [8] and India [9], among others.

Several energy demand/consumption predictive models have aided in a proper understanding of energy dynamics in both residential and industrial/organisational settings. For instance, Azadeh et al. [10] integrated genetic algorithm (GA) and artificial neural network (ANN) to estimate and predict electricity demand using stochastic procedures. The application of Bayesian approach to energy demand is also an accepted technique in the literature [11]. The use of computer software has also been encouraged. For instance, practical applications using plant simulation programmes as a design tool for carrying out or confirming the performance of building designs encoded within the TRNSYS-IISIBAT environment have been reported [2]. The projection of electricity consumption for the industrial sector based on time series forecasting (multivariate linear regression model) has also been established in the literature [12].

Apart from these mathematical predictive models, an entirely empirical approach has also been used to monitor the energy consumption. An approach involves using a questionnaire survey, supported by the annual gas and electricity meter data and floor-area estimates [13]. Another approach is the use of Model of Analysis of the Energy Demand (MAED). This method has been improved upon by the Grey Prediction with Rolling Mechanism (GPRM) approach, which produces high prediction accuracy, is applicable in limited data environments and requires little computational effort [14].

On a general note, Muneer and Arif [15] studied energy consumption in Pakistan and the issue of security of electrical energy supply. Hossain and Badr [16] considered the prospects of renewable energy utilisation for electricity generation in Bangladesh. Tommerup et al. [17] studied the energy-efficient houses built according to energy performance requirements introduced in Denmark. Yohanis et al. [18] investigated the real-life energy use in the UK with a focus on how occupancy and dwelling characteristics affect domestic electricity use. Ensinas et al. [19] studied the analysis of process stem demand reduction and electricity generation in sugar and ethanol production from sugarcane. Becerra-Lopez and Golding [20] studied the dynamic energy analysis for capacity expansion of regional power-generation systems using the case study of far West Texas. Cai et al. [21] performed a scenario analysis on CO<sub>2</sub> emission reduction potential in China's electricity sector. Trygg and Amiri [22] presented the European perspective on absorption cooling in a combined heat and power system using a case study of energy utility and industries in Sweden.

Furthermore, Kaldellis and Zafirakis [23] studied the present situation and future prospects of electricity generation in Aegean Archipelago Islands and Kaldellis [24] made a critical evaluation of the hydropower applications in Greece. Bahaj et al. [25] considered the influence of micro wind turbine output on electricity consumption in buildings while Ozturk et al. [26] reviewed the past, present, and future status of electricity in Turkey. Fung et al. [27] studied the impact of urban

temperature on energy consumption of Hong Kong. The study by Peacock and Newborough [28] focused on the impact of micro-combined heat-and-power systems on energy flows in the UK electricity supply industry. McAllister and Farrel [6] investigated electricity consumption by battery-powered consumer electronics using a household-level survey. The impact of ICT investment and energy price on industrial electricity demand was investigated by Cho et al. [29].

The power outage in universities is common in recent times, particularly in developing countries where these outages are closely linked to peak times since electricity is a non-storable commodity and must be supplied at the same time that it is being used. However, there is also a long gestation period associated with adding new capacity. Obviously, advancements in technology have changed the world over the last few years thereby suggesting the obvious need for new methods as regards energy utilisation. One major resource of effective energy management is the actions taken by the end users themselves. In the past, there was little incentive for more efficient energy use due to the availability of energy at low cost. However, the situation is changing and universities have to adjust its energy use habits in order to cope with the current situation of inadequacy of supply as well as rising costs. Since energy demand is a choice, it could be assumed that system outages can be greatly minimised by the use of peak demand-reducing strategies without any increase in energy supply [30]. Having considered the diverse studies on energy demand and consumption, it seems obvious that investigations relating to academic institutions, particularly universities, in developing countries are missing. The need to bridge this important gap has provided the impetus for the current study. This study surveys the consumption of electric energy in the environment of a university whose goal is to achieve excellence in teaching, research and community service.

### **Analogue Models of Energy Demand in the University of Lagos**

The forms of energy consumed in the University of Lagos for uses other than transportation are electricity, kerosene, charcoal, gas (LPG), firewood and diesel, among which electricity accounts for a major part of the energy used. A walk-through energy audit was conducted in the school to determine the peak energy demand of the school as well as flagged areas for potential savings.

#### *Categorisation of demand sectors*

For the purpose of simplicity of the study, the University of Lagos is classified into three sectors. These are:

- Faculty and service areas: these comprise all faculty buildings, administrative buildings, buildings for health and other essential services (library, power, etc), general purpose buildings and outdoor lighting.
- Residential area: this comprises the staff quarters and students' hostels.
- Commercial centres: this comprises all commercial buildings on the campus.

### *End use categorisation*

The electrical energy end use in the University of Lagos is categorised [31] as follows:

1. Space cooling – This includes all the energy used for ventilation and air conditioning equipment such as room fans, air conditioners and extractor fans.
2. Refrigeration – Refrigeration comprises energy used by food and drink cooling equipment such as water dispensers, fridges and freezers.
3. Water heating – This category considers energy used by water heaters of all kinds.
4. Cooking – This includes energy utilised by cooking equipment such as electric cookers, gas cookers, electric toasters, microwave ovens, and kerosene stove, as well as those other methods of cooking which utilise the other forms of energy.
5. Personal computer – This includes all computer systems, printers and servers.
6. Office machines – The category of office machines includes all equipment that are typical in office environment, e.g. typewriters, fax machines, photocopy machines, and scanners.
7. Laboratory machines – This takes into consideration energy used by all laboratory equipment and machines. The energy can be in the form of electricity, gas or kerosene.
8. Lighting – This comprises all forms of lighting appliances ranging from incandescent lamps to fluorescent lamps, halogen lamps, rechargeable lamps, street lights and large stage lights.
9. Electronics – This category considers all electronic appliances such as television sets, radio sets, video cassette players, video compact disc players, and decoders.
10. Ordinary machines – This group of machines are the common machines that are not used in laboratories such as water pumps, grinding machines, sewing machines, and washing machines.
11. Others – The category of others comprises those appliances which are not considered in any of the aforementioned categories. They include pressing irons, hair dryers, blenders, etc.

The data obtained during the energy audit are presented in tables and charts in the next section. The strategies for reducing this demand are also discussed.

### **Energy Demand in the University of Lagos**

The energy demand in the University of Lagos is shown in Figure 1. Electricity accounts for about 97% of the energy demand in the school. At 16.602 terajoules, it stands at about five times the average monthly energy demand for the year 2005. Figure 2 gives the proportion of this energy demand for different end uses. Since energy demand is a choice, we therefore pursue means of reducing demand. Figure 2 will assist in pointing out areas on which these strategies will be focused.

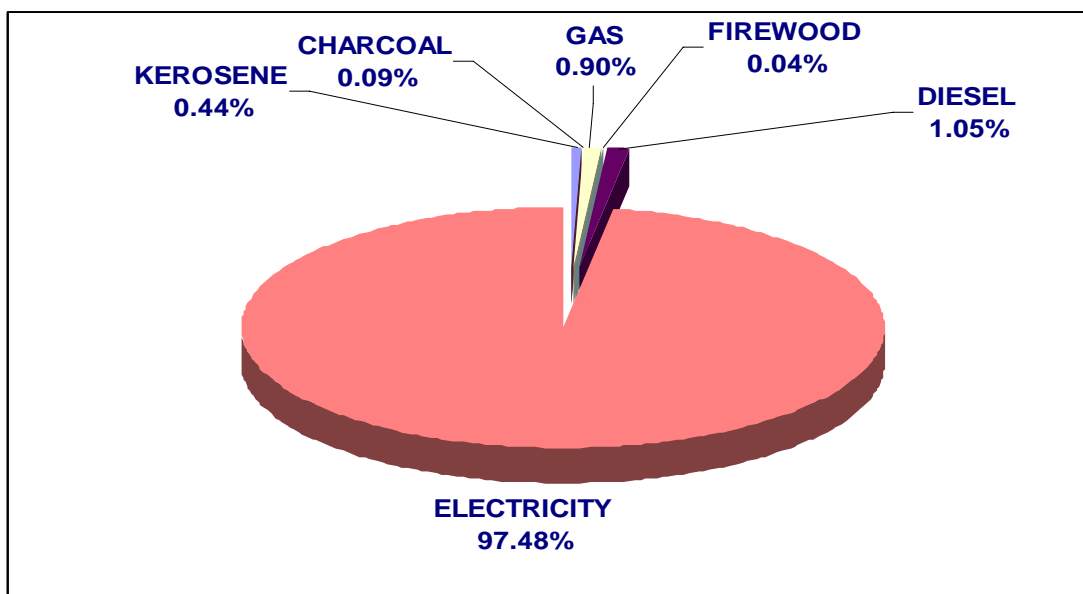


Figure 1. Demand for various forms of energy in the University of Lagos

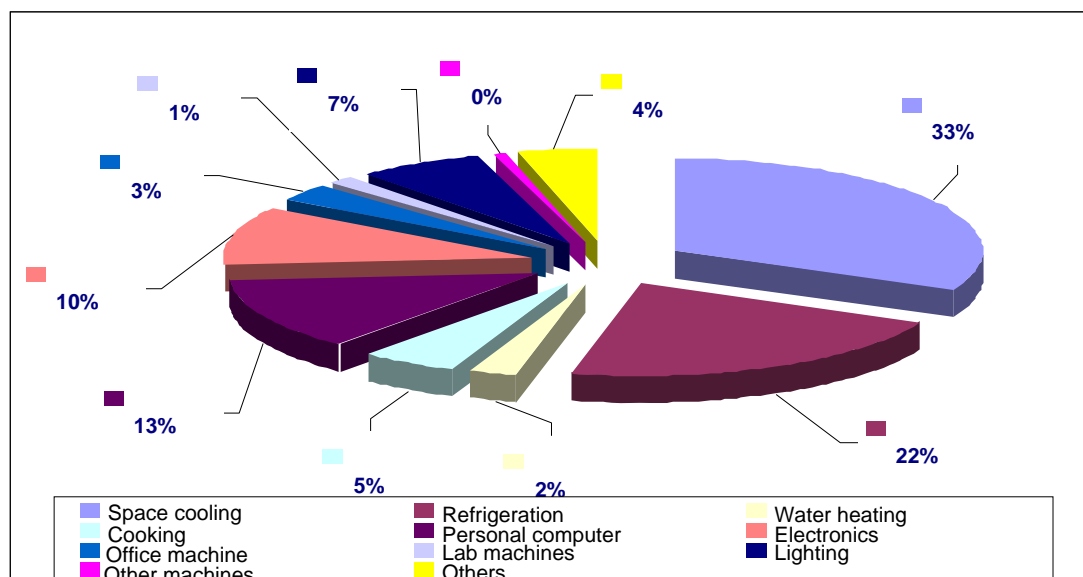


Figure 2. Electrical energy demand for different end uses in the University of Lagos

### Peak Demand Reduction Strategies

Four major strategies for reducing peak demand are: load reducing strategies, high efficiency equipment, energy source substitution, and on-site heat and electricity generation [32]. These methods are discussed here.

#### Load reducing strategies

These are strategies that reduce service demands without affecting the economic benefit derived from that energy use, such as load controls for buildings and equipment and behavioural changes such as turning off lights. Lighting, which is the easiest load to reduce, accounts for 17% of

the energy demand in the faculty and service area as seen in Figure 3, 7% of the energy demand in the residential sector (Figure 4), and 7% of the total electric energy demand of the University of Lagos (Figure 2).

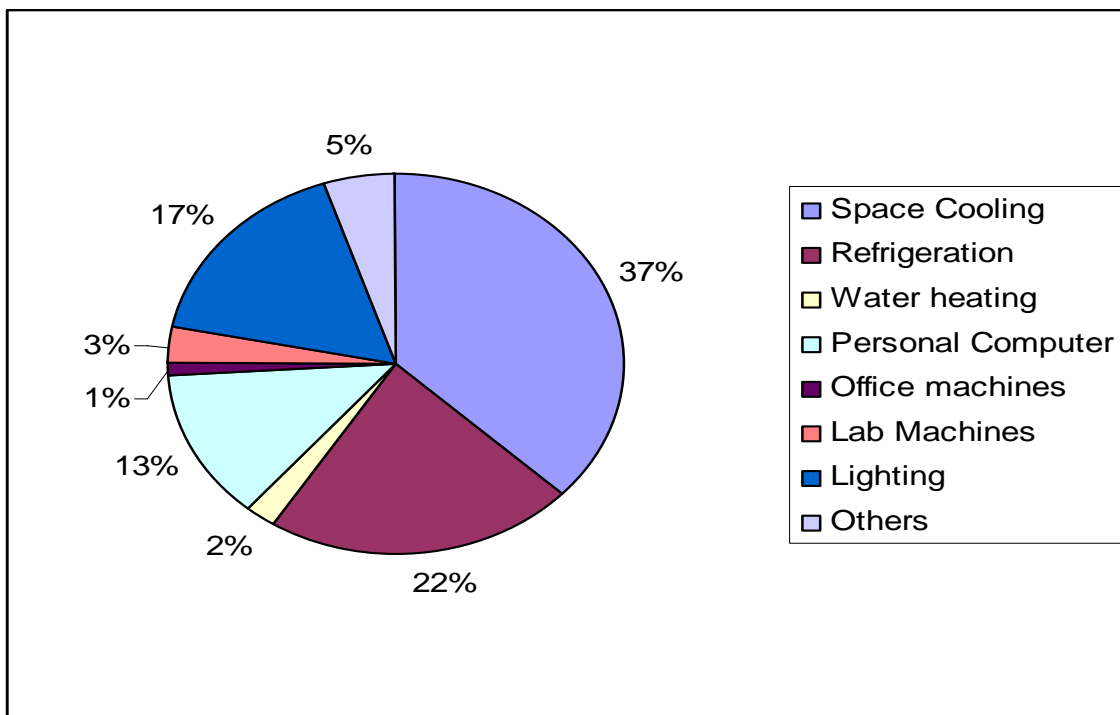


**Figure 3.** Electricity demand in the faculty and service area for various end-uses

Two methods are most common for the reduction of the lighting load, viz. installation of building automation systems and use of daylighting. The traditional on-off toggle switch has been the lighting control of choice in homes. But experience shows that even with convenient light switch locations, lights are often left on when rooms are unoccupied. Building automation systems can help solve this problem. They can be used to automatically turn on, turn off, or dim electric lights around a building. These include occupancy sensors, timers and motion sensors. Daylighting is the use of windows and skylights to bring sunlight into the building. When properly designed and effectively integrated with the electric lighting system, it can offer significant energy savings by offsetting a portion of the electric lighting load.

*High efficiency equipment*

High efficiency equipment reduces the energy needed to deliver a given level of energy services or produces more energy service per unit of energy. A careful observation of Figure 2 shows that space cooling, refrigeration and lighting are items which consume the bulk of the energy supplied to the school, thus flagged areas for potential improvement of efficiency.

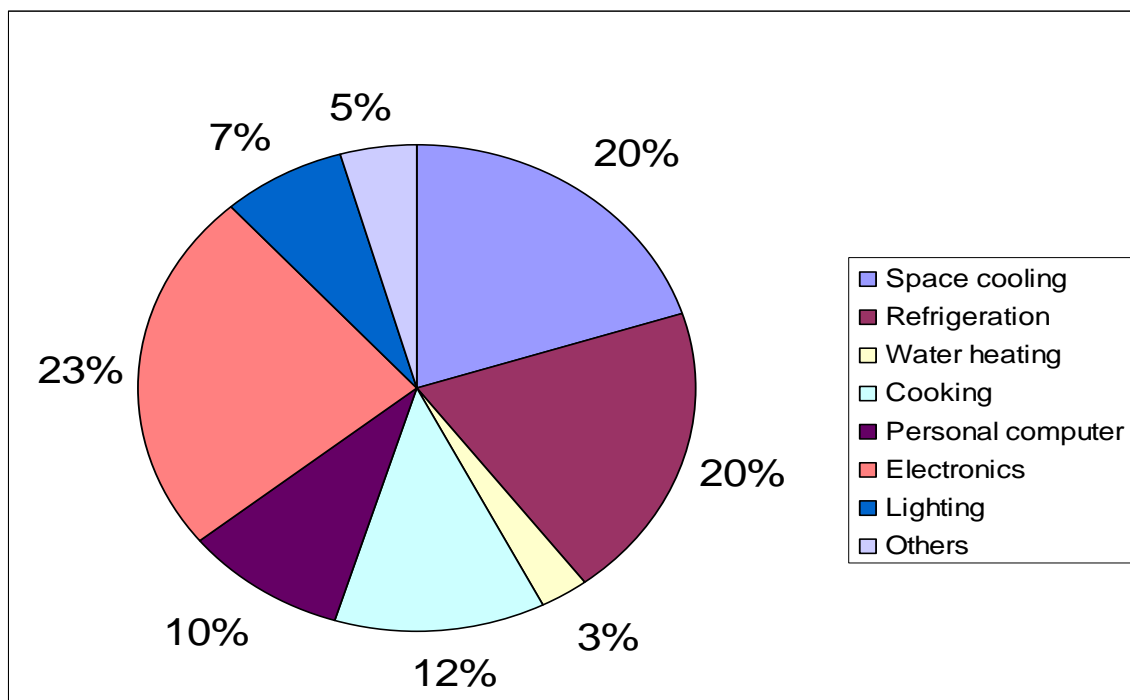


**Figure 4.** Residential energy demand for different end-uses

What lends further credence to this is the fact that the Faculty of Arts and Social Sciences places a higher demand for energy than the Engineering and Science Faculties (Figure 5) even though the latter two make extensive use of laboratory machines that exert heavy loads on the supply system. These machines, however, are only on for a short period of time, in contrast to the extensive use of air conditioning and refrigeration devices that exert smaller loads on the supply system but are on for a longer period of time.

**Efficient lighting:**

The principal lamp types of interest to the energy manager are incandescent, fluorescent, mercury vapour, metal halide, sodium vapour lamps and sodium lamps. The last three are used for outdoor lighting and fall under the category of high-intensity discharge lamps. In this case, efficient lighting can be achieved by introduction of energy-saving bulbs as replacements of traditional incandescent bulbs. This will reduce the energy consumed by the lighting system as well as the heat generated in the enclosure.

**Efficient air conditioning:**

Air-conditioning accounts for 37% of the electrical energy demand in the faculty and service area (Figure 3), 20% of the demand in the residential sector (Figure 4) and 42% of the commercial sector's demand (Figure 6). So in almost all cases, it accounts for the largest demand for any single end use and marks a crucial area in the demand for energy services in the University. Measures that are

needed to provide an economical, efficient and comfortable heating and cooling system are proper installation, proper sizing, and proper design and sealing of the duct system.

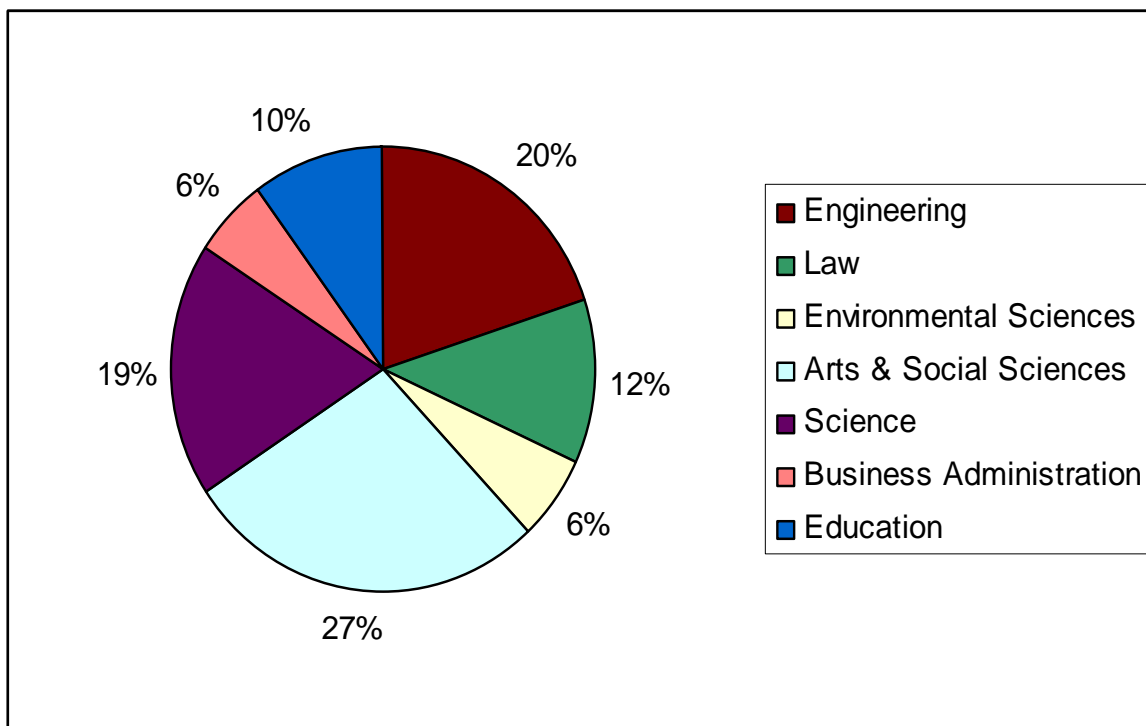


Figure 5. Electricity demand by each Faculty

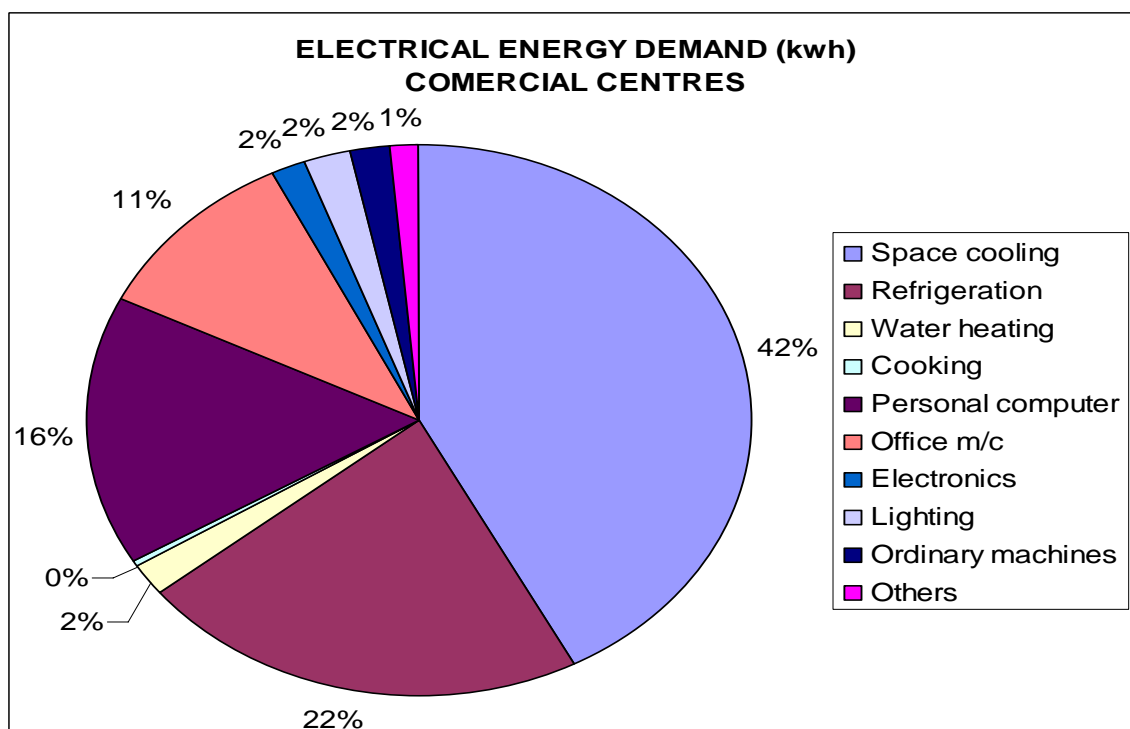


Figure 6. Commercial electrical energy demand for different end-uses

### Efficient refrigeration:

The demand for energy in the end-use can be minimised by certain no-cost practices such as regular cleaning of the evaporator and condenser coils, proper maintenance of door seals, and immediate loading of items that need refrigeration.

### Energy source substitution

Due to the relatively low efficiency of energy conversion to electricity (often 30-35 percent), other primary energy sources such as charcoal and gas should be used wherever possible for heating. This will help reduce the demand on the electric power system for the purposes of cooking and water heating. Cooking and water heating account for 15% of the energy demand by the residential sector (Figure 4), a sharp contrast with the commercial sector which demands less than 1% of its electrical energy for cooking and about 2% for water heating (Figure 6). This is obviously reflected in the greater demand of the commercial sector for charcoal (97% as seen in Table 1) and kerosene (65% as seen in Figure 7).

**Table 1.** Monthly demand for charcoal by various sectors of the University of Lagos

Sector	Total charcoal demand (kg)	Percentage
Faculty and service area	0	0.00%
Commercial center	922	97.36%
Residential area	25	2.64%
Total	947	100%

However, care should also be taken to ensure the cost effectiveness when taking this measure. For instance, the data obtained during a walk-through energy audit indicated that much of the commercial cooking in the University of Lagos is done by charcoal. However, commercial operators and residents who do not have the charcoal pots assume that kerosene is a cheaper option compared to butane gas. Charcoal is rightly considered an economical source of energy but the assumption that kerosene is more economical than cooking gas (butane) is false. Based on this survey, a family of five, for instance, who cooks on a fairly regular basis will exhaust a 12.5-kg gas cylinder in two months. The cost of the 12.5-kg gas is about ₦2200. The initial cost of the cylinder and a gas cooker with two faces is about ₦15, 000. After the initial spending, the consumer will only need to be refilling his cylinder. A family of five who uses kerosene will spend about ₦500 on a weekly basis to buy kerosene. This will amount to ₦4,000 in two months. The initial cost of buying a stove is just about ₦2000. However, most of the stoves that are sold in Nigeria are not durable and the consumer may find himself changing

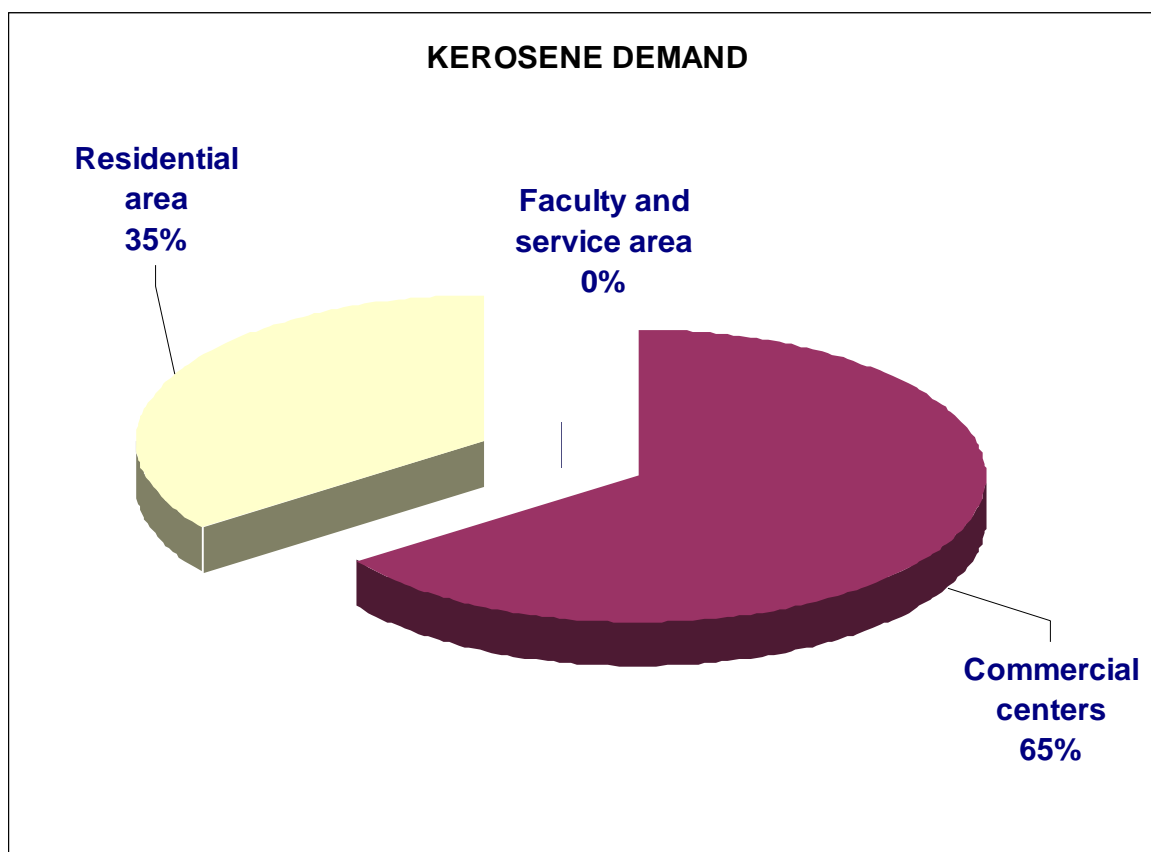


**Figure 7.** Monthly kerosene demand by various sectors in the University of Lagos

the stove after a short time. Furthermore, kerosene cooks slowly as well as blackens the bottom of the pot and leaves the kitchen in a messy form. There is also a higher risk of explosion in the use of kerosene. The monthly demand for gas by the various sectors in the University of Lagos is shown in Figure 8, with residential and commercial sectors placing the highest demand.

#### *On-site heat and electricity generation*

This method reduces the demands seen by the utility grid, although it does require additional energy input. Examples of application of this method include the use of solar energy for heating purposes and photovoltaic cells for electricity generation.

Figure 9 gives the total peak demand for electrical energy by the various sectors of the University. From Figure 9, it can be seen that the residential sector has the potential to consume as much electricity as the faculty and service area and even more electricity than the commercial sector. Yet the commercial sector pays over 200% more per kilowatt-hour of energy used than the residential sector. The hostel residents do not pay for the energy they use. This perhaps might be a plausible cause as to the reason why the demand from this sector is so high. Another cause could also be that the commercial services rendered in university are not major and so require a minimal amount of energy.

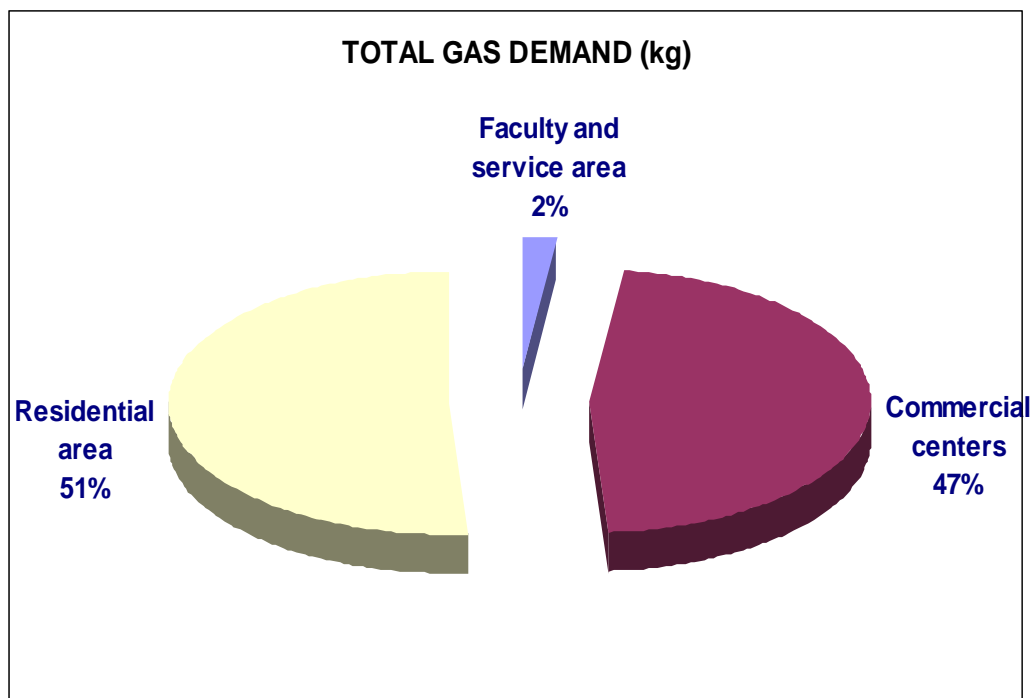


Figure 8. Monthly demand for gas (LPG) by various sectors of the University of Lagos

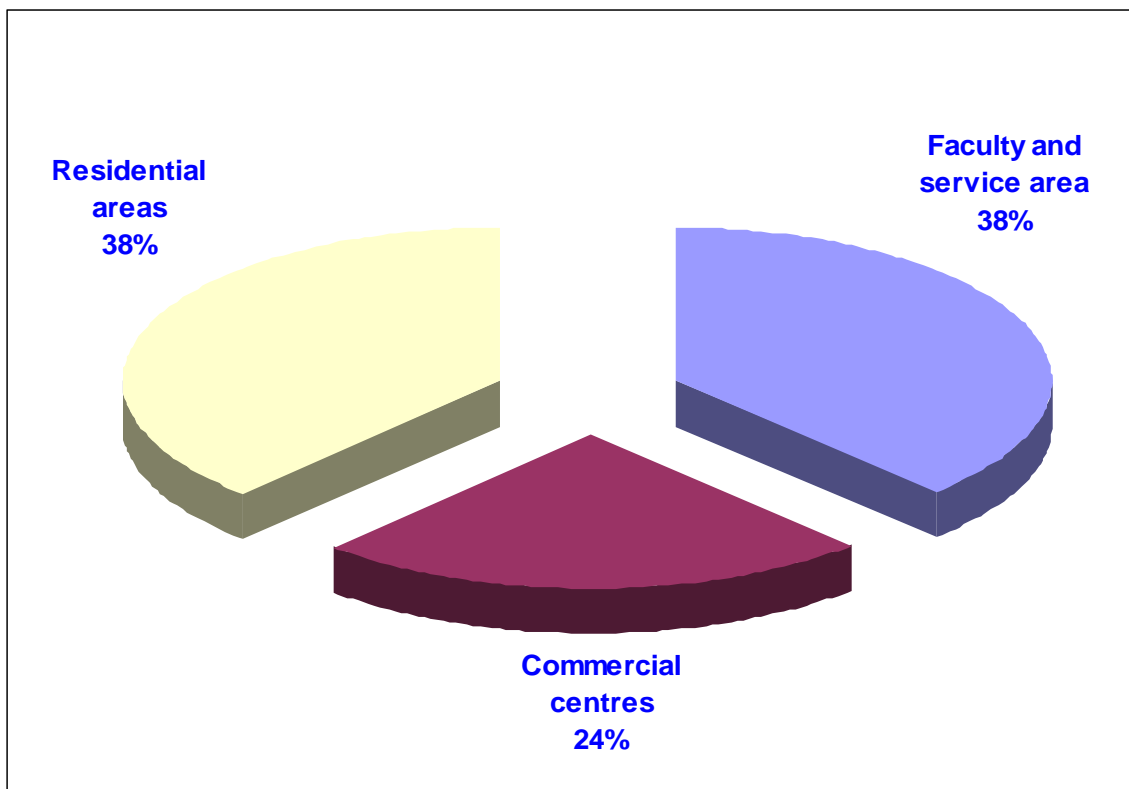


Figure 9. Electrical energy demand of different sectors in the University of Lagos

## Concluding Remarks

The need for a proper control of energy consumption has motivated the current study. Thus, this study has provided a walk-through energy audit through a survey conducted in the University of Lagos. To reduce the strain on the school's electrical supply systems and hence prevent system outages, it is recommended that the peak demand reducing strategies highlighted in this study be implemented. Furthermore, improvements in metering systems and energy data processing and storage would help to ensure the effectiveness of this measure. In conclusion, tackling the problem of energy demand from the users end is quite challenging but might be the only hope of the school in view of inflexibility of supply.

## References

1. B. Atanasiu and P. Bertoldi, "Residential electricity consumption in new member states and candidate countries", *Energy and Buildings*, **2008**, *40*, 112-125.
2. F. F. Al-ajmi and V. I. Hanby, "Simulation of energy consumption for Kuwaiti domestic buildings", *Energy and Buildings*, **2007** (in press).
3. D. Henning and L. Trygg, "Reduction of electricity use in Swedish industry and its impact on national power supply and European CO<sub>2</sub> emissions", *Energy Policy*, **2007** (in press).
4. P. A. Steenhof and W. Fulton, "Factors affecting electricity generation in China: current situation and prospects", *Technological Forecasting and Social Change*, **2007**, *74*, 663-681.
5. D. G. Vita, K. Endresen, and L. C. Hunt, "An empirical analysis of energy demand in Namibia", *Energy Policy*, **2006**, *34*, 3447-3463.
6. J. A. McAllister and A. E. Farrell, "Electricity consumption by battery-powered consumer electronics: a household-level survey", *Energy*, **2007**, *32*, 1177-1184.
7. A. Hainoun, M. K. Self-Eldin, and S. Almoustafa, "Analysis of the Syrian long-term energy and electricity demand projection using the end-use methodology", *Energy Policy*, **2006**, *34*, 1958-1970.
8. A. S. Szklo, J. B. Soares and M. T. Tolmasquim, "Energy consumption indicators and CHP technical potential in the Brazilian hospital sector", *Energy Conversion and Management*, **2004**, *45*, 2075-2091.
9. R. Devi, V. Singh, R. P. Dahiya, and A. Kumar, "Energy consumption pattern of a decentralized community in northern Haryana", *Renewable and Sustainable Energy Reviews*, **2007** (in press).
10. A. Azadeh, S. F. Ghaderi, S. Tarverdian, and M. Saberi, "Integration of artificial neural networks and genetic algorithm to predict electrical energy consumption", *Applied Mathematics and Computation*, **2007**, *186*, 1731-1741.
11. N. Xiao, J. Zarnikau, and P. Damien, "Testing functional forms in energy modelling: an application of the Bayesian approach to U.S. electricity demand", *Energy Economics*, **2007**, *29*, 158-166.
12. A. Al-Ghandoor, I. Al-Hinti, J. O. Jaber, and S. A. Sawalha, "Electricity consumption and associated GHG emissions of the Jordanian industrial sector: empirical analysis and future projection", *Energy Policy*, **2008**, *36*, 258-267.

13. K. J. Baker and R. M. Rylatt, "Improving the prediction of UK domestic energy demand using annual consumption data", *Applied Energy*, **2007** (in press).
14. D. Akay and M. Atak, "Grey prediction with rolling mechanism for electricity demand forecasting of Turkey", *Energy*, **2007**, 32, 1670-1675.
15. T. Muneer and M. Asif, "Prospects for secure and sustainable electricity supply for Pakistan", *Renewable and Sustainable Energy Reviews*, **2007**, 11, 654-671.
16. A. K. Hossain and O. Badr, "Prospects of renewable energy utilization for electricity generation in Bangladesh", *Renewable and Sustainable Energy Reviews*, **2006**, 11, 8, 1617-1649.
17. H. Tommerup, J. Rose, and S. Svenden, "Energy-efficient houses built according to energy performance requirements introduced in Denmark in 2006", *Energy and Buildings*, **2006**, 39, 1123-1130.
18. Y. G. Yohanis, J. D. Mondol, A. Wright, and B. Norton, "Real-life energy use in the UK: how occupancy and dwelling characteristics affect domestic electricity use", *Energy and Buildings*, **2007** (in press).
19. A. V. Ensinas, S. A. Nebra, M. A. Lozano, and L. M. Serra, "Analysis of process steam demand reduction and electricity generation in sugar and ethanol production from sugarcane", *Energy Conversion and Management*, **2007**, 48, 2978-2987.
20. H. R. Becerra-Lopez and P. Golding, "Dynamic energy analysis for capacity expansion of regional power-generation systems: case study of far west Texas", *Energy*, **2007**, 32, 2167-2186.
21. W. Cai, C. Wang, K. Wang, Y. Zhang, and J. Chen, "Scenario analysis on CO2 emissions reduction potential in China's electricity sector", *Energy Policy*, **2007**, 35, 6445-6456.
22. L. Trygg and S. Amiri, "European perspective on absorption cooling in a combined heat and power system – a case study of energy utility and industries in Sweden", *Applied Energy*, **2007**, 84, 1319-1337.
23. J. K. Kaldellis and D. Zafirakis, "Present situation and future prospects of electricity generation in Aegean Archipelago Islands", *Energy Policy*, **2007**, 25, 4623-4639.
24. J. K. Kaldellis, "Critical evaluation of the hydropower applications in Greece", *Renewable and Sustainable Energy Reviews*, **2008**, 12, 218-234.
25. A. S. Bahaj, L. Myers, and P. A. B. James, "Urban energy generation; influence of micro-wind turbine output on electricity consumption in buildings", *Energy and Buildings*, **2007**, 39, 154-165.
26. H. K. Ozturk, A. Yilanci, and O. Atalay, "Past, present and future status of electricity in Turkey and the share of energy sources", *Renewable and Sustainable Energy Reviews*, **2007**, 11, 183-209.
27. W. Y. Fung, K. S. Lam, W. T. Hung, S. W. Pang, and Y. L. Lee, "Impact of urban temperature on energy consumption of Hong Kong", *Energy*, **2006**, 31, 2623-2637.
28. A. D. Peacock and M. Newborough, "Impact of Micro-combined heat and power systems on energy flows in the UK electricity supply industry", *Energy*, **2006**, 31, 1804-1818.
29. Y. Cho, J. Lee, and T. Kim, "The impact of ICT investment and energy price on industrial electricity demand: dynamic growth model approach", *Energy Policy*, **2007**, 35, 4730-4738.
30. A. W. L. Yao and S. C. Chi, "Analysis and design of a Taguchi-Grey based electricity demand predictor for energy management systems", *Energy Conversion and Management*, **2004**, 45, 1205-1217.

31. R. A. Zogg and D. L. Alberino, "Electricity consumption by small end uses in residential buildings", Report prepared by Arthur D. Little, **1998**, [www.eere.energy.gov/buildings/info/documents/pdfs/lbnl-42393.pdf](http://www.eere.energy.gov/buildings/info/documents/pdfs/lbnl-42393.pdf) (retrieved 19-12-07).
32. R. E. Brown and J. G. Kooney, "Electricity use in California: past trends and present usage patterns", *Energy Policy*, **2003**, *31*, 849-864.

© 2008 by Maejo University, San Sai, Chiang Mai, 50290 Thailand. Reproduction is permitted for noncommercial purposes.

**Maejo International**  
**Journal of Science and Technology**

ISSN 1905-7873

Available online at [www.mijst.mju.ac.th](http://www.mijst.mju.ac.th)

*Full Paper*

**Abundance, food habits, and breeding season of exotic *Tilapia zillii* and native *Oreochromis niloticus* L. fish species in Lake Zwai, Ethiopia**

**Alemayehu Negassa and Padanillay C. Prabu\***

Department of Biology, Ambo University College, P. O. Box 19, Ambo, Ethiopia

\* Author to whom correspondence should be addressed, e-mail: [prabu\\_22@yahoo.com](mailto:prabu_22@yahoo.com)

*Received: 31 December 2007 / Accepted: 4 June 2008 / Published:*

---

**Abstract:** Relative abundance, diet and breeding season overlap in the reproduction of exotic *Tilapia zillii* and native *Oreochromis niloticus* in Lake Zwai were studied from samples collected over 12 months. Younger fish of both species collected were also evaluated for food composition. Food items from stomachs of both species were collected and analysed using the frequency of occurrence method. In terms of number, *T. zillii* dominated *O. niloticus* at the sampling sites. In both species, macrophytes, detritus, blue green algae, diatoms, green algae, *Ceratium*, *Euglena*, and *Phacus* constituted foods of plant origin, whereas chironomid larvae, Copepoda, Cladocera, Rotifera, Nematoda, fish eggs, and fish scales constituted foods of animal origin. Foods of the latter type such as Ephemeroptera and mollusks were also noted in the diet of adult *T. zillii*. Despite the extensive overlap in food habits of the two species, however, the food items were found in the diet of the species with different average percentage frequencies of occurrence. The level of gonad maturation and gonadosomatic index (GSI) values showed that in Lake Zwai breeding was year-round for both *T. zillii* and *O. niloticus*, with a peak during April-September and February-August respectively, indicating extended breeding season overlap in reproduction. The two species were always found together in the catches from the sampling sites, which indicated some niche overlap between them.

**Keywords:** breeding season, *Oreochromis niloticus*, *Tilapia zillii*, Lake Zwai, Ethiopia

---

## Introduction

Though fishes are the most diverse among the major vertebrate groups [1], they are faced with considerable threats which are generally associated with a combination of factors summarised in the acronym HIPO (habitat destruction, introduced species, pollution, and over-exploitation) [2]. As elsewhere, a number of attempts have been made to introduce exotic freshwater fish species into Ethiopia. *Tilapia zillii* is one of such species and has been particularly released into several water bodies including Lake Zwai [3]. *T. zillii* and *Oleochromis niloticus* are widely distributed and have a very wide common range. However, in East Africa while *O. niloticus* is widely distributed and supports important commercial fisheries, *T. zillii* is indigenous only to Lake Albert and Lake Rudolf.

*T. zillii* is essentially a macrophyte-feeder. The adult feeds preferentially on aquatic macrophytes and vegetable matter of terrestrial origin [4], whereas *O. niloticus* is among the many phytoplanktivorous species. and is also known to include animals in its diet consisting of zooplankton and benthic organisms like insect larvae, crustaceans, and mollusks [5]. *T. zillii* is a monogamous biparental guarder as opposed to *O. niloticus* which is a polygamous maternal mouth brooding species. It is both economically and ecologically important in the country as a whole, but its population in Lake Zwai is currently declining.

It is clear that the knowledge on the complex interaction between the fish species and the impact of introduced species on native ones is imperative for management of the ecosystem and the fisheries. Yet limited information is known about how these different species are performing in all of the water bodies in general and in Lake Zwai in particular. Accordingly, the present study was conducted to determine the status of *T. zillii* and assess its relations in feeding and breeding with the native *O. niloticus* species in Lake Zwai.

## Materials and Methods

### *Study area: Lake Zwai*

Lake Zwai (Figure 1) is located in the most northerly part of the upper rift lakes in the country of Ethiopia. The lake is situated at 7° 52' to 8° 8'N latitude and 38° 40' to 38° 56'E longitude and lies at an altitude of 1636 m, with a surface area of 434 km<sup>2</sup> and mean depth of 2.5 m [6]. The lake is fed by a number of rivers, the major two being Meki and Katar, and outflows south from its southwest corner via the Bulbula River. The lake lies in a region with an almost constant semi-arid climate characterised by the rainy season period (mid-June to mid- September), the dry season period (October to February), and a "small" rainy season with occasional

precipitation in March. Significant rainfall was also noted in May during the study period (Figure 2).

The sampling sites, Edo Kontella (Site 1) and Kontella (Site 2), were located in the littoral zone at the southwestern end of the lake and characterised by extensive macrophyte vegetation and sandy substratum. The littoral zone of the lake is fringed by emergent and submergent vegetation. The most common emergent plants are *Scripus* spp., *Cyperus* spp., *Typha angustifolia*, *Paspalidium geminatum*, and *Phragmites* sp., whereas the floating and submerged vegetation is represented by *Nymphaea coerulea* and *Potamogeton* spp.

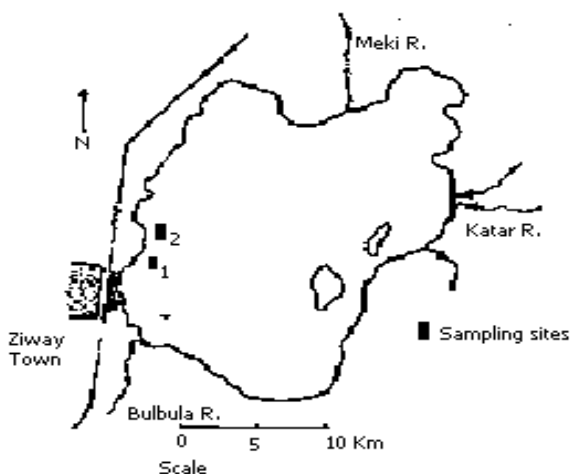


Figure 1. Map of Lake Zwai showing the sampling sites

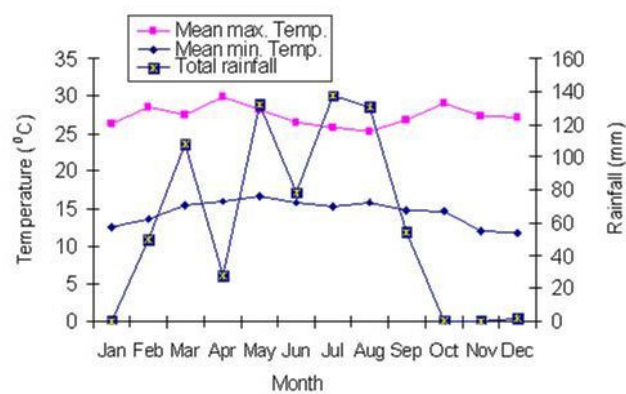


Figure 2. Meteorological data of Lake Zwai during 2001

The phytoplankton community is dominated by blue-green algae, of which *Lyngbia limnetica*, *Microsystis aeruginosa* and *Synechococcus elongatus* are the major species in terms of biomass. The diatoms, *Melosira granulata*, *Navicula* spp. and *Surirella* spp., and the green algae, *Straurastrum leptocladum* and *Pediastrum boryannum* are also important. The zooplankton community of the lake is composed of cyclopoids (*Mesocyclops* spp., *Microcyclops* spp., and *Afroscyclops* spp.), cladocerans (*Diaphanosoma excisum* and *Alona davidii*), and rotifers (*Keratella* sp., *Brachionus* spp., *Filinia* spp., *Hexarthra* spp., *Lecane* spp., and *Trichocerca* spp.). The bottom fauna comprises gastropod and chironomid larvae. The fish community is composed of both native and introduced species. The native species comprise *O. niloticus* and some *Barbus* species, whereas the introduced ones are *T. zillii*, *Clarias gariepinus* and *Carassius auratus*. The potential yield of all species combined is estimated to be in the range of 1,000 to 6,000 tons per year [7].

### *Collection of samples*

Adult fish samples of *T. zillii* and *O. niloticus* were collected from the two sampling sites over a twelve-month period during the year 2001 using gill nets (60 x 100 mm stretched mesh). Younger fish of both species were collected in October, November, and December 2001, in shallow waters less than 1m in depth using a 5-mm stretched mesh beach seine. Fish caught were sorted according to species and counted. The fish samples were then taken to the Zwai Fisheries Resources Development Research Center laboratory soon after capture for stomach content analysis. The stomach of each fish was removed and preserved in a plastic bag containing 5% formalin. Sex determination of each adult specimen was done through examination of the gonad, and the maturity level of the gonad was determined through visual examination following maturity keys for *T. zillii* [8] and *O. niloticus* [9]. Accordingly, five-point and six-point maturity scales were used for *T. zillii* and *O. niloticus* respectively. Each gonad was weighed to the nearest 0.1 g, and stomach samples were then transported to Addis Ababa University for further laboratory studies.

### *Relative abundance*

The relative abundance of *T. zillii* and *O. niloticus* was estimated from catch per unit effort (CPUE) records. Catch per unit effort was recorded as the number of fish in each species caught per trap per set during the sampling occasions.

### *Food habits*

A study on the natural food of *T. zillii* was made based on stomach contents of 703 adults (394 M and 309 F, 12.5-32 cm total length), and 150 young fish (5.5-12 cm total length). Similarly, assessment on the food of *O. niloticus* was made from stomach contents of 591 adults (291 M and 300 F, 13.5-40 cm total length), and 120 young fish (6-13 cm total length). The basis for categorising *T. zillii* into two-length groups in diet study was the change in the major component of the diet, whereas in *O. niloticus* it was the association of the fish with *T. zillii* belonging to either of the length groups in the catches. The stomach contents preserved in 5% formalin were examined either macroscopically or microscopically at several levels of magnification. The food items, excluding macrophytes and detritus, were then identified to the lowest taxonomic level possible using descriptions, illustrations, and keys from various sources [10-12]. The results were then analysed using the frequency of occurrence method in which the number of stomach samples containing one or more of a given food item was expressed as a percentage of non-empty stomachs examined.

*Breeding season*

Breeding seasons of *T. zillii* and *O. niloticus* were determined based on the frequency of the various gonad stages identified and the gonadosomatic index (GSI) values. GSI was calculated as gonad weight as percentage of total body weight (including the gonad):

$$\text{GSI} = \frac{\text{Gonad wt} \times 100}{\text{Body wt}}$$

The percentage frequency of breeding fish and GSI were then plotted monthly, and the time of the year when the frequency and GSI were high was considered as the peak-breeding season for the fish.

**Results***Relative abundance*

Throughout the sampling periods, *T. zillii* was always more abundant than *O. niloticus* in the catches from both sampling sites in Lake Zwai (Figure 3). The former species constituted 74% and 82.8% of the total collections of 709 and 1038 fish made from Edo Kontella and Kontella respectively.

*Food habits*

**Adult and young *T. zilli*.** Of the total 703 adult fish examined for food composition, 605 or 86% had food in their stomachs which contained diverse items of both plant and animal origins (Table 1). Foods of plant origin were made of macrophytes (unidentified) and phytoplankton belonging to blue-green algae, diatoms, and green algae. Foods of animal origin comprised chironomid larvae, copepoda (*Mesocyclopes* sp.), cladocera (*Alona* sp. and *Diaphanosoma* sp), Rotifera (*Brachionus* sp., *Keratella* sp. and *Lecane* sp.), Ephemeroptera, mollusks, and eggs and scales of unidentified fish. Other components of the diet were plant detritus and unidentified broken parts of animal body. However, these food items occurred in the diet of the fish with different average percentage frequency (Table 1).

Of all elements of the diet of adult *T. zillii*, macrophytes were the most frequent and occurred in all of the stomachs examined. As a group, blue green algae, diatoms, green algae, and plant detritus were found in 64%, 54%, 38%, and 10% of the stomachs respectively. Among blue green algae, *Microcystis* spp. and *Lyngbya* spp. were found to be frequent (59% and 33% of the stomachs respectively), whereas *Navicula* (48%) and *Cymbella* (15%) were the diatoms noted with high frequency of occurrence. *Spirogyra* and *Staurastrum* were the most frequently occurring green algae, each with 16% occurrence of the stomachs examined. Among foods of

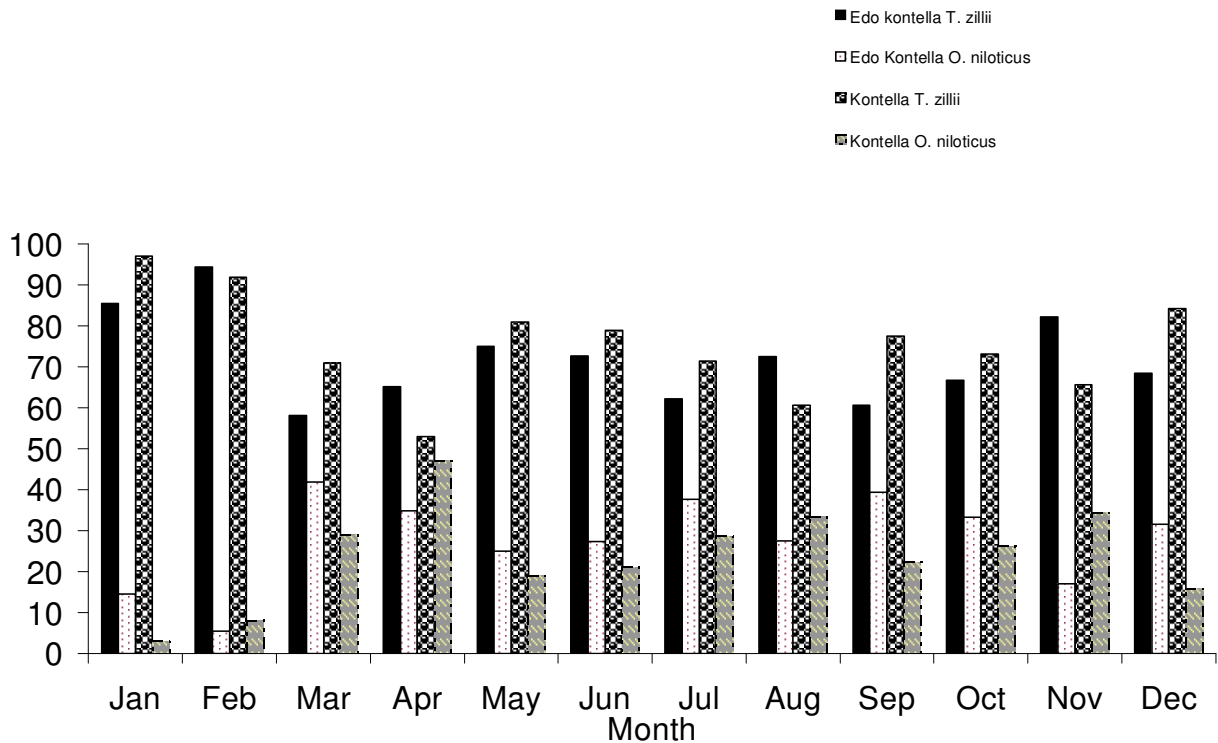


Figure 3. Relative abundance of the two species at the two sites

animal origin, chironomid larvae were most frequently found (at 10% occurrence), followed by fish scales (at 5% occurrence). The other remaining components were noted to be less frequent in occurrence.

All young *T. zillii* examined for diet composition had food in their stomachs. Analysis based on these food contents showed that the foods of this group of fish in the lake were diverse, consisting of both plants and animals (Table 1). Foods of plant origin were composed of diatoms, blue-green algae, green algae, plant detritus, macrophytes, *Ceratium*, *Phacus*, and *Euglena*, whereas chironomid larvae, copepoda, rotifera, and fish scales formed the foods of animal origin. These food items had different frequencies of occurrence in the diet of the young fish (Table 1). As a group, diatoms, blue-green algae and green algae occurred in 96%, 86%, and 59% respectively of the total stomachs. For diatoms, *Navicula* (84%), *Rhopalodia* (78%) and *Cymbella* (59%), and for blue-green algae, *Microcystis* (91%), *Lyngbya* (55%) and *Oscillatoria* (54%) were the most frequent food items. Among green algae, *Scenedesmus* (32%) and *Closterium* (21%) were relatively frequent. Plant detritus were found at 83% and macrophytes at 40% of the stomachs. Of animal-originated food components, chironomid larvae occurred at 58% of the stomachs examined and the rest were less frequent.

**Table 1.** List of food items identified in the stomachs of adult and young *T. zillii* and *O. niloticus* collected from Lake Zwai during the year 2001 with their percentage frequency range of occurrence (% occurrence). Number in parenthesis indicates average value.

Food category	% Occurrence ( <i>T. zillii</i> )		% Occurrence ( <i>O. niloticus</i> )	
	Adult	Young	Adult	Young
A. Macrophytes	100	35-65(40)	11-100(84)	2-42(11)
B. Phytoplankton				
i. Cyanophyta	12-100(64)	78-92(86)	100	100
<i>Anabaena</i>	0-51(18)	16-47(32)	5-95(58)	45-50(48)
<i>Anabaenopsis</i>	--	--	0-11(6)	--
<i>Chroococcus</i>	0-9(7)	0-12(8)	10-71(46)	45-55(50)
<i>Gloeocapsa</i>	0-2 (0.4)	0-8 (4)	0-7 (1)	--
<i>Lyngbya</i>	2-52(33)	47-63(55)	48-100(89)	55-68(62)
<i>Merismopedia</i>	0-27(11)	21-34(28)	0-80(33)	33-75(74)
<i>Microcystis</i>	12-100(59)	84-92(91)	97-100(100)	100
<i>Oscillatoria</i>	0-40(33)	39-89(54)	33-100(89)	20-64(62)
<i>Spirulina</i>	0-5(1)	0-8(3)	0-16(4)	0-5(1)
ii. Bacillariophyta	2-82(54)	84-100(96)	100	95-100(98)
<i>Achnanthes</i>	0-5(0.4)	0-61(25)	0-84(30)	32-45(38)
<i>Amphora</i>	--	--	--	0-5(2)
<i>Cyclotella</i>	8-28(11)	5-39(30)	5-43(22)	0-5(2)
<i>Cymbella</i>	5-36(15)	5-71(59)	19-91(66)	73-75(74)
<i>Denticula</i>	--	0-9(5)	0-21(9)	5-23(14)
<i>Frustulia</i>	--	0-13(7)	0-33(11)	14-20(17)
<i>Gomphonema</i>	0-4(0.2)	--	0-89(44)	36-45(40)
<i>Navicula</i>	4-84(48)	63-97(84)	40-100(75)	60-91(76)
<i>Nitzschia</i>	2-8(2)	8-32(18)	0-33(12)	18-60(24)
<i>Opephora</i>	0-3(0.4)	--	0-89(16)	0-6(2)
<i>Pinullaria</i>	--	--	0-89(33)	28-85(36)
<i>Rhoicosphenia</i>	2-9(4)	0-8(4)	0-20(5)	--
<i>Rhopalodia</i>	8-41(10)	47-87(78)	0-80(29)	86-90(88)
<i>Surirella</i>	--	8-11(9)	0-16(10)	10-18(14)
<i>Synedra</i>	6-18(13)	--	0-98(61)	0-50(16)
iii. Chlorophyta	13-83(38)	58-61(59)	87-100(96)	100
<i>Ankistrodesmus</i>	2-6(2)	--	0-53(18)	9-35(21)
<i>Botryococcus</i>	2-8(2)	--	0-41(14)	0-9(5)
<i>Coelastrum</i>	2-12(6)	0-8(5)	0-29(4)	0-14(7)
<i>Closterium</i>	2-24(8)	16-26(21)	0-67(23)	9-50(28)
<i>Cosmarium</i>	2-6(3)	2-5(3)	0-58(20)	10-18(14)
<i>Euastrum</i>	0-8(2)	0-3(1)	0-32(9)	0-14(7)
<i>Pediastrum</i>	2-19(4)	0-3(2)	0-84(46)	27-30(28)
<i>Scendesmus</i>	2-23(6)	24-39(32)	10-87(71)	60-82(71)
<i>Selenastrum</i>	--	--	0-16(2)	--
<i>Spirogyra</i>	4-26(16)	5-12(10)	5-95(41)	5-41(24)
<i>Staurastrum</i>	2-71(16)	0-13(10)	0-84(36)	75-77(76)
<i>Tetradron</i>	0-3(0.2)	--	--	--

C. Detritus	2-37(10)	20-88(83)	0-38(9)	0-15(11)
D. Chironomid larvae	2-48(10)	39-68(58)	0-14(3)	0-9(5)
E. Zooplankton				
Copepoda	0-3(1)	0-4(3)	0-50(8)	0-5(2)
Cladocera	0-4(0.6)	--	0-20(4)	--
Rotifera	0-2(0.9)	--	0-43(13)	0-13(2)
F. Others				
<i>Ceratium</i>	0-29(8)	0-12(4)	0-27(7)	0-8(3)
<i>Euglena</i>	0-5(1)	0-2(0.3)	0-47(14)	27-35(31)
<i>Phacus</i>	0-2(0.2)	(0-0.2)	0-63(17)	23-25(24)
Nematoda	0-3(0.4)	--	--	0-5(1)
Ephemeroptera	0-4(0.4)	--	--	--
Molluscs	0-8(0.4)	--	--	--
Fish egg	0-5(0.6)	--	0-10(0.8)	--
Fish scale	0-9(5)	10-16(13)	0-8(2)	4-5(5)
Unidentified species	0-6(0.8)	--	--	--

**Adult and young *O. niloticus*.** Adult *O. niloticus* in Lake Zwai was found to utilise quite a wide range of food material particularly phytoplankton which were distributed among three major groups consisting of blue-green algae, diatoms and green algae (Table 1). The blue green algae consisted mainly of *Microcystis* (100% occurrence), *Lyngbya* (89%) and *Oscillatoria* (49%). Occurrence of the green algae was noted to be 41% for *Spirogyra* and 36% for *Staurastrum*, while *Navicula* (75%), *Cymbella* (66%) and *Synedra* (61%) were among those of the diatoms that were frequent. Macrophytes, plant detritus, *Ceratium*, *Phacus*, and *Euglena* were also noted to be among the components of the diet. Foods of animal origin included chironomid larvae, crustacea (Copepoda and Cladocera), Rotifera, and fish scales.

The diet of young *O. niloticus* in the lake was very similar to the food items of the adults both in terms of food composition and diversity and included blue-green algae, diatoms, green algae, plant detritus, *Ceratium*, *Euglena*, and *Phacus* (Table 1). Foods of animal origin were encountered and consisted of chironomid larvae, Copepoda, Cladocera, Rotifera, Nematoda, and fish scales. The blue-green algae (100% *Microcystis*, 62% *Lyngbya* and 50% *Chroococcus*), the green algae (76% *Staurastrum* and 71% *Scenedesmus*), and the diatoms (88% *Rhopalodia*, 76% *Navicula* and 74% *Cymbella*) were items with high frequency of occurrence. These food items were numerically more important in the diet.

#### *Breeding season of T. zillii and O. niloticus*

Monthly variation of GSI of both sexes was evident for *T. zillii* (Figure 4) as well as for *O. niloticus* (Figure 6). The mean monthly GSI  $\pm$  SE of female *T. zillii* ranged from  $0.32 \pm 0.02$  (in

January) to  $3.58 \pm 0.31$  (in August), while that of the males ranged from  $0.15 \pm 0.02$  to  $0.34 \pm 0.04$ . *T. zillii* had its highest GSI values from February to September, while lower values were recorded between October and January. The percentage of mature females and males ranged from 5-68% and 6-76% respectively, with high values between April and September (Figure 5).

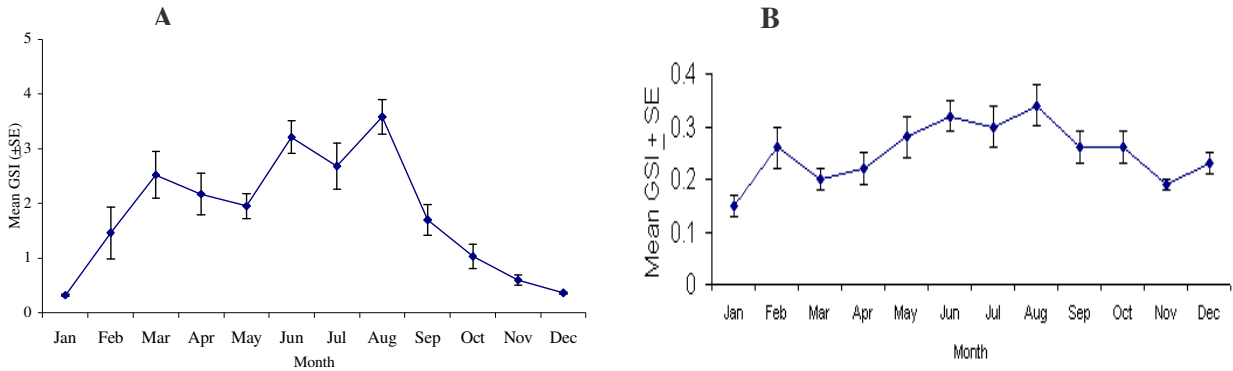


**Figure 4.** Gonadosomatic index (mean  $\pm$  SE) of *T. zillii* (A: female, B: male) in Lake Zwai during 2001

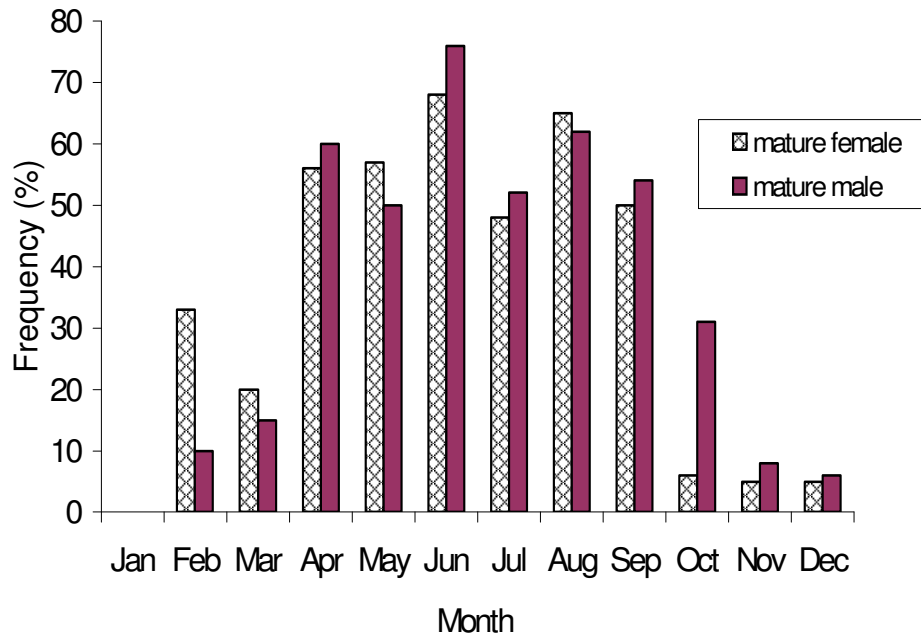


**Figure 5.** Percentage of mature female and male *T. zillii* in Lake Zwai during the year 2001

In *O. niloticus* the mean monthly GSI  $\pm$  SE of females ranged from  $0.30 \pm 0.03$  (in October-November) to  $2.02 \pm 0.46$  (in August), whereas that of males ranged from  $0.09 \pm 0.01$  (in September-December) to  $0.50 \pm 0.10$  (in May and August). High GSI values extended from February to August, whereas low GSI values were recorded between September and January

(Figure 6). The percentage of mature females and males ranged from 3-42% and 3-45% respectively, with higher values between February and August (Figure 7).

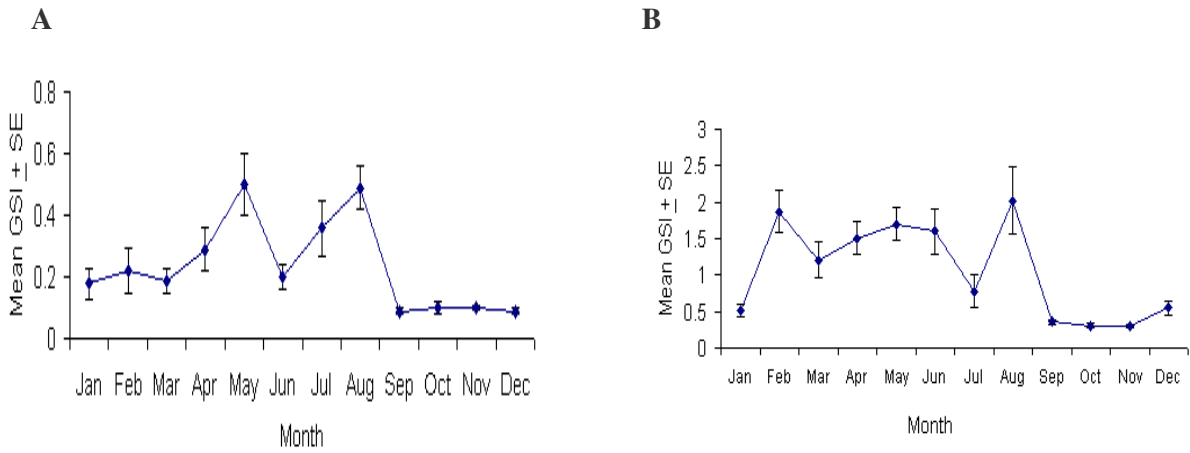


**Figure 6.** Gonadosomatic index (mean ± SE) of *O. niloticus* (A: female, B: male) in Lake Zwai during 2001

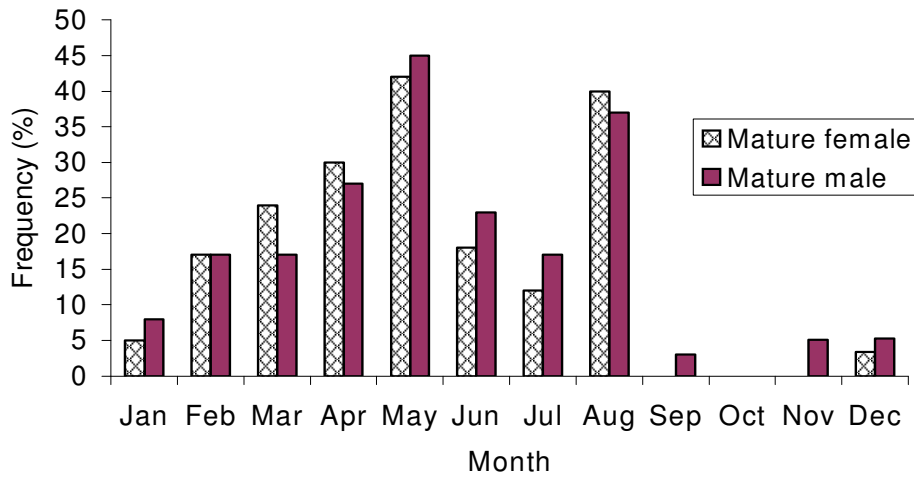


**Figure 7.** Percentage of mature female and male *O. niloticus* in Lake Zwai during 2001

From the above observations it was evident that the reproduction of *T. zillii* and *O. niloticus* in Lake Zwai was continuous throughout the year and was most active between April-September and February-August respectively.

## Discussion

At the sampling sites in Lake Zwai, *T. zillii* regularly appeared in the catches during the sampling periods. The fish were also noted to be present in many places around the shallow marginal water of the lake, which indicated that this particular species has successfully established itself in the lake. *O. niloticus*, however, was always associated with *T. zillii* in the catches, including the ones with mature gonads from both species, which indicated a niche overlap. Young fish of the two species were also found together in collections employing beach seine net. Results from catch per unit effort records indicated that *T. zillii* was more abundant than *O. niloticus* (Figure 3). On the contrary, *T. zillii* was rarely encountered in the catches far from the lakeshore. Thus, the catch records from the sampling sites alone may not reflect the exact abundance of the species in the whole lake.

*T. zillii* was observed to be more dependent on shoreline habitat compared to *O. niloticus*, and differences in the distribution of the species in the lake might be due to their habitat preferences. This is in agreement with the findings conducted in Lake Victoria [13]. McConnell [14] also pointed out that substrate-spawners with macrophyte feeding habit (e.g. *T. zillii*) are more dependent on shoreline habitat than are the mouth brooders with their microphagous feeding and more pelagic habitat, (e.g. *O. niloticus*), especially in waters rich in plankton. Thus, *T. zillii* may be an important component of the Zwai ecosystem because of its abundance in shallow waters as required by spawning fish including *O. niloticus*.

Stomach content analysis based on the occurrence method showed that both *T. zillii* and *O. niloticus* exploited diverse food sources of both plant and animal origins (Table 1). Similar findings have been reported for the two species in Lake Victoria [13] and Nile canal [15]. Nevertheless, foods of plant origin were the major components of the diet in both species and comprised macrophytes, plant detritus, and phytoplankton consisting of blue-green algae, green algae, diatoms, *Ceratium*, *Phacus*, and *Euglena*. On the other hand, chironomid larvae, Ephemeroptera, mollusks, Copepoda, Cladocera, Rotifera, and eggs and scales of unidentified fish were foods of animal origin. Of these, Ephemeroptera, mollusks and unidentified animal pieces of larger size were noted exclusively in the diet of adult *T. zillii*.

Though not quantified, the diet of *T. zillii* in Lake Zwai varied depending on the size of the fish as the adult chiefly fed on macrophytes and the young on phytoplankton. This may be due to difference in the degree of development of the feeding organs and the habitat occupied by the fish. Philipart and Ruwet [4] also reported the variation in the feeding regime of fish species depending on size, age and the microhabitat occupied by the fish in a given water body.

In adults, higher plant tissues including large portions of roots, leaves and stems of aquatic vegetation and seeds occurred in all of the stomachs examined. Several authors [5,13,15] also reported that *T. zillii* feeds essentially on plant materials, which is consistent with the present observation, in which blue-green algae, diatoms, and green algae were found in 64%, 54%, and 38% respectively of the stomachs examined. These items were also reported to be ingested by the fish from Lake Quarun [16], Lake Kinnert [17], and Nile canal [15]. The occurrence of planktonic material in the guts of fish with no filter feeding mechanism, as is the case in *T. zillii*, is a strange phenomenon. However, Welcomme [13] suggested that the source of planktonic material in the diet of *T. zillii* in Lake Victoria was a flocculent deposit offshore.

Adult *T. zillii* were also known to ingest benthic invertebrates [16], insect larvae and crustacea [15] in other water bodies, and the observation from Lake Zwai also supports this findings. The occurrence larger animals like mollusk in the diet of adult *T. zillii*, but not *O. niloticus*, may be due to the relatively greater tendency of the former species to exploit animal foods, whereas their exclusion from the diet of young ones may be attributed to prey-predator size relationship. Abdel-Malek [16] also associated to the change in composition of the diet as the fish grows with an increase in the minimum size of the organism eaten. Diet composition of young *T. zillii* in Lake Zwai was similar to what has been reported [8] for Lake Quarun for fish whose total length ranged from 4.5-9 cm.

From analysis using the frequency of occurrence and personal observations on the abundance of the food items, it was clear that phytoplankton (blue greens, diatoms and greens) were the principal foods of both adult and young *O. niloticus* in the length range considered. Previous reports of some Ethiopian rift valley lakes including Zwai also showed that adult *O. niloticus* mainly feeds on phytoplankton [17-18]. On the other hand, juvenile *O. niloticus* was known to be an omnivore feeding on algae, zooplankton and insect larvae [19]. These reports further stated that young *O. niloticus* in the length range considered in the present study feeds primarily on phytoplankton. Thus, the food composition of young *O. niloticus* in the present observation (mainly phytoplankton) could have resulted from a possible ontogenetic diet shift.

Analysis of the food habits of *T. zillii* and *O. niloticus* in Lake Zwai revealed extensive diet overlap (Table 1). However, the food items utilised by both species varied in their contribution to the diet. There was a clear tendency for adult *T. zillii* to feed mainly on macrophytes while phytoplankton was found to be the principal food of young *T. zillii* and *O. niloticus* (adult and young). This observation is contrary to the conclusion by Bowen [20] who stated that tilapias in general feed on any food particle small enough to pass through the esophagus. Consequently, the

diet overlap between adult *T. zillii* and the remaining groups (young *T. zillii* and *O. niloticus* in both length groups) might be moderated by their food preferences.

On the other hand, differences in feeding site and habitat could be important for resource partitioning between adult *O. niloticus* and the young of both species. The preferred habitat of adult *O. niloticus* is the pelagic zone and that of the young is the lakeshore. Ribbink et al. [21] emphasised the importance of feeding site to resource partitioning rather than the foods they take in coexisting related species of cichlids in the African Great Lakes. Nevertheless, the young of both *T. zillii* and *O. niloticus* having a similarity in diet preference were found to share similar habitat as they were collected together from the same fishing ground. Thus, spatial relation and overlap in the major diet of the young of *T. zillii* and *O. niloticus* indicate possible competition for food resources.

The seasonal variation in GSI and percentage of mature fish of both sexes of *T. zillii* (Figures 4-5) and *O. niloticus* (Figures 6-7) was quite apparent. The seasonal pattern of gonad development and variation in percentage of mature fish of both sexes were more or less similar for *T. zillii* and *O. niloticus*. Indeed, fish with well-developed gonads and mature eggs in both species were noted almost throughout the year. GSI values and percentages of mature fish indicated that breeding in both species was year-round with its peak during April-September for *T. zillii* and February-August for *O. niloticus*.

The presence of breeding fish in Lake Zwai throughout the year may be attributed to the low seasonal fluctuation in temperature and photoperiod (Figure 2). It is a well-established fact that in the tropics seasonal fluctuation in temperature and photoperiod is generally very low and this might be favourable for fish species to spawn any time of the year. The annual peaks of reproductive activity in both species are coincident with the rainy season (Figure 2). With the advent of the rainy season the lake level rises and due to the flooding of land nutrients are flushed into the lake. As a result, habitat and food resource for fish expand greatly and this may trigger reproduction. McConnell [14] also concluded that breeding among tilapias often occurs sporadically year-round but has a distinct peak just before or at the onset of the rainy season, which is in accordance with the present findings. Rainfall increases production [22] and water level, which in turn provides suitable spawning grounds for adults, and feeding and nursery grounds for the young [23].

## Conclusions

The level of gonad maturation and mean gonadosomatic index (GSI) values indicated extended breeding season overlap in reproduction between *T. zillii* and *O. niloticus*. The reproduction of young fish that share similar habitat by the two species during similar seasons might have had some effect on the population of *O. niloticus* due to possible competition on nursery grounds. Such phenomenon, in which the young of *T. zillii* were introduced into Lake Victoria, has displaced the young of a native tilapia species from crucial nursery areas, causing a severe decline in the native species. The competitive interaction in feeding and on nursery grounds between young *T. zillii* and young *O. niloticus* may therefore have been one of the factors that contributes to the decline in the population of *O. niloticus* in Lake Zwai and should be further studied in detail.

## Acknowledgements

We would like to thank the Swedish Agency for Research and Education for Developing Countries (SAREC) and the Rockefeller Foundation (Grant No. 2001AR 002) for financial support and the National Meteorology Services Agency for providing the meteorological data. We also extend our sincere thanks to the fishermen of the Lake who helped us in sample collection, of whom Gezahegn Tilinti and Mulatu Galato deserve especial consideration.

## References

1. P. B. Moyle and J. J. Cech, "Fishes: An Introduction to Ichthyology.", 3<sup>rd</sup> Edn., Prentice Hall, New York, **1996**.
2. A. Getahun and M. L. J. Stiassny, "The freshwater biodiversity crisis: the case of the Ethiopian fish fauna", *SINET: Ethiop. J. Sci.*, **1998**, 21, 207-230.
3. S. Tedla and F. HaileMeskel, "Introduction and transplantation of freshwater fish species in Ethiopia", *SINET: Ethiop. J. Sci.*, **1981**, 4, 69-72.
4. J. C. L. Philipart and J. C. L. Ruwet, in "The Biology and Culture of Tilapias", (Ed. R. S. V. Pullin and R. H. Lowe-McConnell), Cambridge University Press, London, **1982**, Ch.1.
5. J. D. Balarin and T. J. Hatton, "Tilapia: A Guide to Their Biology and Culture in Africa", Stirling University Press, Scotland, **1979**.
6. R. Schroder, "An attempt to estimate the fish stock and sustainable yield of Lake Zwai and Lake Abaya in Ethiopian Rift Valley", *Arch. Hydro-Biologia, Suppl. Bd.*, **1984**, 69, 411-441.
7. Lake Fisheries Development Project (LFDP), "Fisheries Report", Department of Animal and Fisheries Resources Development, Phase II Report, Addis Ababa, **1998**.

8. S. E. El-Zarka, "Tilapia fisheries investigation in Egyptian lakes: Maturity, spawning and sex ratio of *Tilapia zillii* (Gerv.) in Lake Quarun", Extension and Publication section- Notes and Memories No. 67, Cairo, **1962**.
9. M. M. Babiker and H. Ibrahim, "Studies on the reproduction of the cichlid *Tilapia nilotica* (L) gonadal maturation and fecundity", *J. Fish Biol.*, **1979**, 14, 437-448.
10. R. Schroder, "An attempt to estimate the fish stock and sustainable yield of Lake Zwai and Lake Abaya, Ethiopian Rift valley", *Arch. Hydrobiologia Suppl.*, **1984**, 69, 411-441.
11. R. W. Pennak, "Freshwater Invertebrates of the United States", John Wiley and Sons, New York, **1978**.
12. D. Defaye, "Contribution a la connaissance des crustaces copepods d'Ethiopie", *Hydrobiologia*, **1988**, 164, 103-147.
13. R. L. Welcomme, "Observations on the biology of the introduced species of tilapia in Lake Victoria", *Rev. Zool. Bot. Afr.*, **1967**, XXVI, 3-4.
14. R. H. Lowe-McConnell, "Ecological Studies in Tropical Fish Communities", Cambridge University Press, London, **1987**.
15. E. A. Khallaf and A. A. Alne-na-ei, "Feeding ecology of *Oreochromis niloticus* (Linnaes) and *Tilapia zillii* (Gervais) in a Nile canal", *Hydrobiologia*, **1987**, 146, 57-62.
16. S. A. Abdel-Malek, "Food and feeding habits of some Egyptian fishes in Lake Quarun: *Tilapia zillii* (Gerv.) B. according to different length groups", *Bull. Institute of Oceanography and Fisheries*, **1972**, 205-213.
17. G. Teferra and C. H. Fernando, "The food habits of an herbivorous fish (*Oreochromis niloticus* L.) in Lake Awassa, Ethiopia", *Hydrobiologia*, **1989**, 174, 195-200.
18. G. Teferra, "The composition and nutritional status of the diet of *Oreochromis niloticus* in Lake Chamo, Ethiopia", *J. Fish Biol.*, **1993**, 42, 865-874.
19. Z. Tadesse, *M.Sc. Thesis*, **1988**, Addis Ababa University, Ethiopia.
20. S. H. Bowen, in "The Biology and Culture of Tilapias", (Ed. R. S. V. Pullin and R. H. Lowe-McConnell), Cambridge University Press, London, **1982**, Ch.3.
21. A. J. Ribbink, B. A. Marsh, A. C. Marsh, A. C. Ribbink, and B. J. Sharp, "A preliminary survey of the cichlid fishes of rocky habitats in Lake Malawi", *S. Afr. J. Zool.*, **1983**, 18, 149-310.
22. E. Kebede, Z. GebreMariam, and I. Ahlgren, "The Ethiopian rift valley lakes: chemical characteristics of a salinity-alkalinity series", *Hydrobiologia*, **1994**, 288, 1-12.
23. C. Tudorancea, Z. GebreMariam, and E. Dadebo, in "Limnology in Developing Countries", (Ed. R. G. Wetzel and B. Gopal), Vol. 2, International Association for Limnology, India, **1999**, pp. 63-118.

**Maejo International**  
**Journal of Science and Technology**

ISSN 1905-7873

Available online at [www.mijst.mju.ac.th](http://www.mijst.mju.ac.th)

*Full Paper*

**Abundance, food habits, and breeding season of exotic *Tilapia zillii* and native *Oreochromis niloticus* L. fish species in Lake Zwai, Ethiopia**

**Alemayehu Negassa and Padanillay C. Prabu\***

Department of Biology, Ambo University College, P. O. Box 19, Ambo, Ethiopia

\* Author to whom correspondence should be addressed, e-mail: [prabu\\_22@yahoo.com](mailto:prabu_22@yahoo.com)

*Received: 31 December 2007 / Accepted: 4 June 2008 / Published: 13 June 2008*

---

**Abstract:** Relative abundance, diet and breeding season overlap in the reproduction of exotic *Tilapia zillii* and native *Oreochromis niloticus* in Lake Zwai were studied from samples collected over 12 months. Younger fish of both species collected were also evaluated for food composition. Food items from stomachs of both species were collected and analysed using the frequency of occurrence method. In terms of number, *T. zillii* dominated *O. niloticus* at the sampling sites. In both species, macrophytes, detritus, blue green algae, diatoms, green algae, *Ceratium*, *Euglena*, and *Phacus* constituted foods of plant origin, whereas chironomid larvae, Copepoda, Cladocera, Rotifera, Nematoda, fish eggs, and fish scales constituted foods of animal origin. Foods of the latter type such as Ephemeroptera and mollusks were also noted in the diet of adult *T. zillii*. Despite the extensive overlap in food habits of the two species, however, the food items were found in the diet of the species with different average percentage frequencies of occurrence. The level of gonad maturation and gonadosomatic index (GSI) values showed that in Lake Zwai breeding was year-round for both *T. zillii* and *O. niloticus*, with a peak during April-September and February-August respectively, indicating extended breeding season overlap in reproduction. The two species were always found together in the catches from the sampling sites, which indicated some niche overlap between them.

**Keywords:** breeding season, *Oreochromis niloticus*, *Tilapia zillii*, Lake Zwai, Ethiopia

---

## Introduction

Though fishes are the most diverse among the major vertebrate groups [1], they are faced with considerable threats which are generally associated with a combination of factors summarised in the acronym HIPO (habitat destruction, introduced species, pollution, and over-exploitation) [2]. As elsewhere, a number of attempts have been made to introduce exotic freshwater fish species into Ethiopia. *Tilapia zillii* is one of such species and has been particularly released into several water bodies including Lake Zwai [3]. *T. zillii* and *Oleochromis niloticus* are widely distributed and have a very wide common range. However, in East Africa while *O. niloticus* is widely distributed and supports important commercial fisheries, *T. zillii* is indigenous only to Lake Albert and Lake Rudolf.

*T. zillii* is essentially a macrophyte-feeder. The adult feeds preferentially on aquatic macrophytes and vegetable matter of terrestrial origin [4], whereas *O. niloticus* is among the many phytoplanktivorous species. and is also known to include animals in its diet consisting of zooplankton and benthic organisms like insect larvae, crustaceans, and mollusks [5]. *T. zillii* is a monogamous biparental guarder as opposed to *O. niloticus* which is a polygamous maternal mouth brooding species. It is both economically and ecologically important in the country as a whole, but its population in Lake Zwai is currently declining.

It is clear that the knowledge on the complex interaction between the fish species and the impact of introduced species on native ones is imperative for management of the ecosystem and the fisheries. Yet limited information is known about how these different species are performing in all of the water bodies in general and in Lake Zwai in particular. Accordingly, the present study was conducted to determine the status of *T. zillii* and assess its relations in feeding and breeding with the native *O. niloticus* species in Lake Zwai.

## Materials and Methods

### *Study area: Lake Zwai*

Lake Zwai (Figure 1) is located in the most northerly part of the upper rift lakes in the country of Ethiopia. The lake is situated at 7° 52' to 8° 8' N latitude and 38° 40' to 38° 56' E longitude and lies at an altitude of 1636 m, with a surface area of 434 km<sup>2</sup> and mean depth of 2.5 m [6]. The lake is fed by a number of rivers, the major two being Meki and Katar, and outflows south from its southwest corner via the Bulbula River. The lake lies in a region with an almost constant semi-arid climate characterised by the rainy season period (mid-June to mid- September),

the dry season period (October to February), and a "small" rainy season with occasional precipitation in March. Significant rainfall was also noted in May during the study period (Figure 2).

The sampling sites, Edo Kontella (Site 1) and Kontella (Site 2), were located in the littoral zone at the southwestern end of the lake and characterised by extensive macrophyte vegetation and sandy substratum. The littoral zone of the lake is fringed by emergent and submergent vegetation. The most common emergent plants are *Scripus* spp., *Cyperus* spp., *Typha angustifolia*, *Paspalidium geminatum*, and *Phragmites* sp., whereas the floating and submerged vegetation is represented by *Nymphaea coerulea* and *Potamogeton* spp.

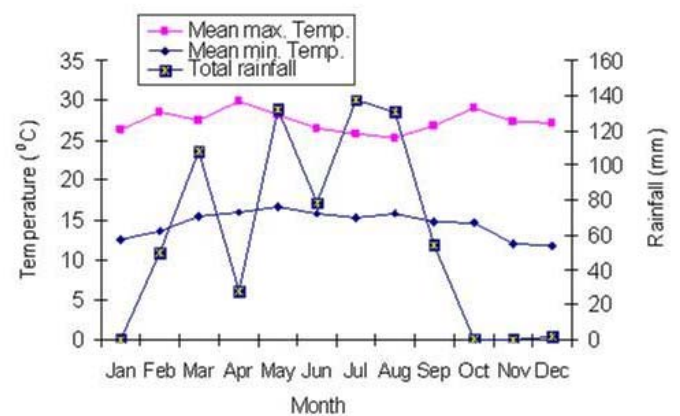
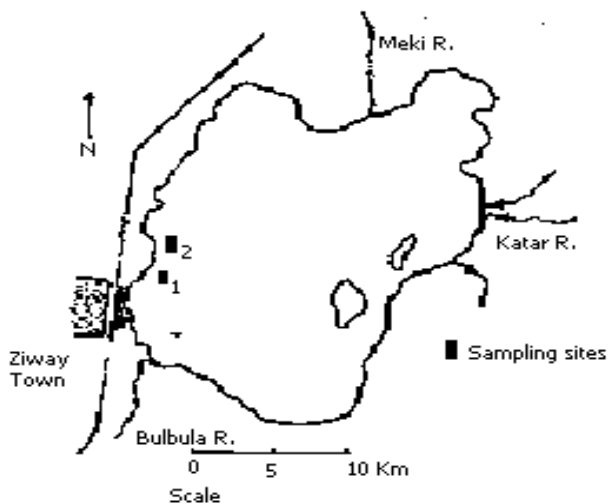


**Figure 1.** Map of Lake Zwai showing the sampling sites **Figure 2.** Meteorological data of Lake Zwai during 2001

The phytoplankton community is dominated by blue-green algae, of which *Lyngbia limnetica*, *Microsystis aeruginosa* and *Synechococcus elongatus* are the major species in terms of biomass. The diatoms, *Melosira granulata*, *Navicula* spp. and *Surirella* spp., and the green algae, *Straurastrum leptocladum* and *Pediastrum boryannum* are also important. The zooplankton community of the lake is composed of cyclopoids (*Mesocyclops* spp., *Microcyclops* spp., and *Afroscyclops* spp.), cladocerans (*Diaphanosoma excisum* and *Alona davidii*), and rotifers (*Keratella* sp., *Brachionus* spp., *Filinia* spp., *Hexarthra* spp., *Lecane* spp., and *Trichocerca* spp). The bottom fauna comprises gastropod and chironomid larvae. The fish community is composed of both native and introduced species. The native species comprise *O. niloticus* and some *Barbus* species, whereas the introduced ones are *T. zillii*, *Clarias gariepinus* and *Carassius auratus*. The potential yield of all species combined is estimated to be in the range of 1,000 to 6,000 tons per year [7].

### *Collection of samples*

Adult fish samples of *T. zillii* and *O. niloticus* were collected from the two sampling sites over a twelve-month period during the year 2001 using gill nets (60 x 100 mm stretched mesh). Younger fish of both species were collected in October, November, and December 2001, in shallow waters less than 1m in depth using a 5-mm stretched mesh beach seine. Fish caught were sorted according to species and counted. The fish samples were then taken to the Zwai Fisheries Resources Development Research Center laboratory soon after capture for stomach content analysis. The stomach of each fish was removed and preserved in a plastic bag containing 5% formalin. Sex determination of each adult specimen was done through examination of the gonad, and the maturity level of the gonad was determined through visual examination following maturity keys for *T. zillii* [8] and *O. niloticus* [9]. Accordingly, five-point and six-point maturity scales were used for *T. zillii* and *O. niloticus* respectively. Each gonad was weighed to the nearest 0.1 g, and stomach samples were then transported to Addis Ababa University for further laboratory studies.

### *Relative abundance*

The relative abundance of *T. zillii* and *O. niloticus* was estimated from catch per unit effort (CPUE) records. Catch per unit effort was recorded as the number of fish in each species caught per trap per set during the sampling occasions.

### *Food habits*

A study on the natural food of *T. zillii* was made based on stomach contents of 703 adults (394 M and 309 F, 12.5-32 cm total length), and 150 young fish (5.5-12 cm total length). Similarly, assessment on the food of *O. niloticus* was made from stomach contents of 591 adults (291 M and 300 F, 13.5-40 cm total length), and 120 young fish (6-13 cm total length). The basis for categorising *T. zillii* into two-length groups in diet study was the change in the major component of the diet, whereas in *O. niloticus* it was the association of the fish with *T. zillii* belonging to either of the length groups in the catches. The stomach contents preserved in 5% formalin were examined either macroscopically or microscopically at several levels of magnification. The food items, excluding macrophytes and detritus, were then identified to the lowest taxonomic level possible using descriptions, illustrations, and keys from various sources [10-12]. The results were then analysed using the frequency of occurrence method in which the number of stomach samples containing one or more of a given food item was expressed as a percentage of non-empty stomachs examined.

*Breeding season*

Breeding seasons of *T. zillii* and *O. niloticus* were determined based on the frequency of the various gonad stages identified and the gonadosomatic index (GSI) values. GSI was calculated as gonad weight as percentage of total body weight (including the gonad):

$$\text{GSI} = \frac{\text{Gonad wt} \times 100}{\text{Body wt}}$$

The percentage frequency of breeding fish and GSI were then plotted monthly, and the time of the year when the frequency and GSI were high was considered as the peak-breeding season for the fish.

**Results***Relative abundance*

Throughout the sampling periods, *T. zillii* was always more abundant than *O. niloticus* in the catches from both sampling sites in Lake Zwai (Figure 3). The former species constituted 74% and 82.8% of the total collections of 709 and 1038 fish made from Edo Kontella and Kontella respectively.

*Food habits*

**Adult and young *T. zillii*.** Of the total 703 adult fish examined for food composition, 605 or 86% had food in their stomachs which contained diverse items of both plant and animal origins (Table 1). Foods of plant origin were made of macrophytes (unidentified) and phytoplankton belonging to blue-green algae, diatoms, and green algae. Foods of animal origin comprised chironomid larvae, copepoda (*Mesocyclopes* sp.), cladocera (*Alona* sp. and *Diaphanosoma* sp), Rotifera (*Brachionus* sp., *Keratella* sp. and *Lecane* sp.), Ephemeroptera, mollusks, and eggs and scales of unidentified fish. Other components of the diet were plant detritus and unidentified broken parts of animal body. However, these food items occurred in the diet of the fish with different average percentage frequency (Table 1).

Of all elements of the diet of adult *T. zillii*, macrophytes were the most frequent and occurred in all of the stomachs examined. As a group, blue green algae, diatoms, green algae, and plant detritus were found in 64%, 54%, 38%, and 10% of the stomachs respectively. Among blue green algae, *Microcystis* spp. and *Lyngbya* spp. were found to be frequent (59% and 33% of the stomachs respectively), whereas *Navicula* (48%) and *Cymbella* (15%) were the diatoms noted

with high frequency of occurrence. *Spirogyra* and *Staurastrum* were the most frequently occurring green algae, each with 16% occurrence of the stomachs examined. Among foods of

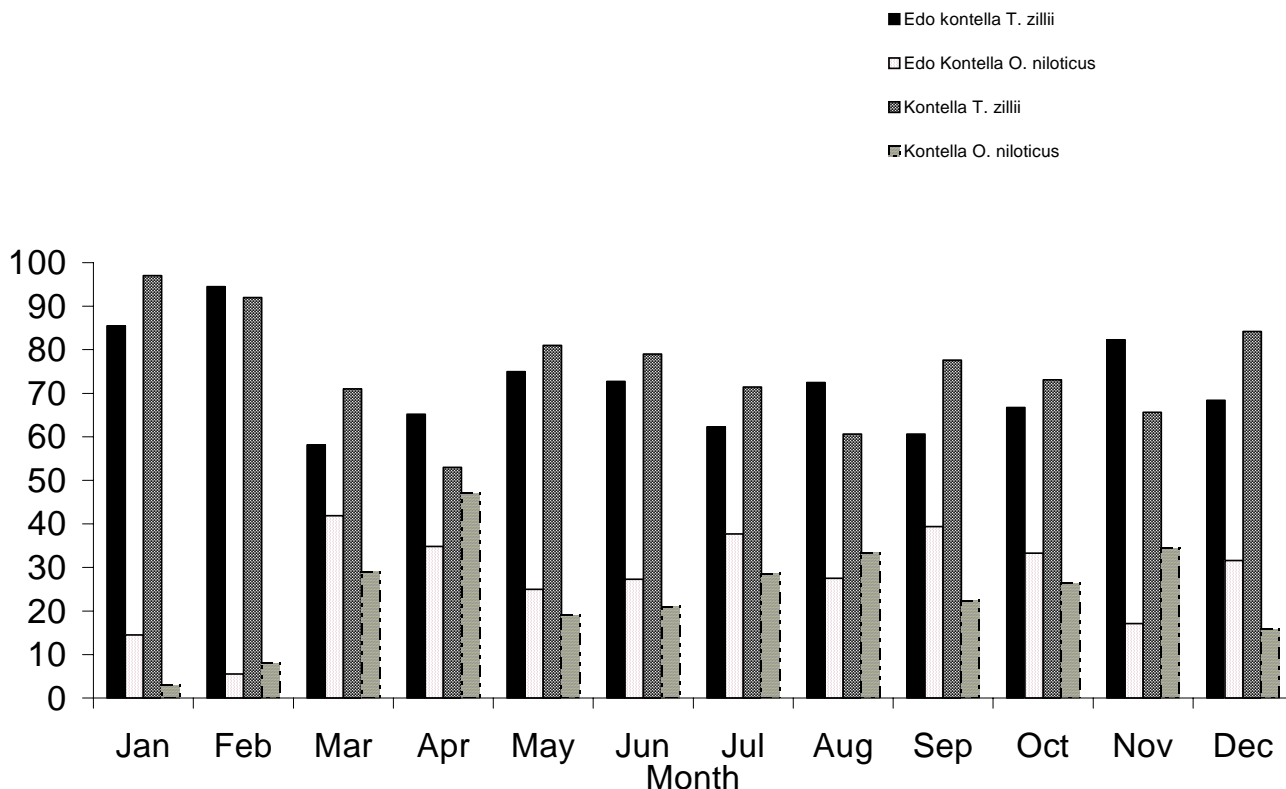


Figure 3. Relative abundance of the two species at the two sites

animal origin, chironomid larvae were most frequently found (at 10% occurrence), followed by fish scales (at 5% occurrence). The other remaining components were noted to be less frequent in occurrence.

All young *T. zillii* examined for diet composition had food in their stomachs. Analysis based on these food contents showed that the foods of this group of fish in the lake were diverse, consisting of both plants and animals (Table 1). Foods of plant origin were composed of diatoms, blue-green algae, green algae, plant detritus, macrophytes, *Ceratium*, *Phacus*, and *Euglena*, whereas chironomid larvae, copepoda, rotifera, and fish scales formed the foods of animal origin. These food items had different frequencies of occurrence in the diet of the young fish (Table 1). As a group, diatoms, blue-green algae and green algae occurred in 96%, 86%, and 59% respectively of the total stomachs. For diatoms, *Navicula* (84%), *Rhopalodia* (78%) and *Cymbella* (59%), and for blue-green algae, *Microcystis* (91%), *Lyngbya* (55%) and *Oscillatoria* (54%) were the most frequent food items. Among green algae, *Scenedesmus* (32%) and *Closterium* (21%) were

relatively frequent. Plant detritus were found at 83% and macrophytes at 40% of the stomachs. Of animal-originated food components, chironomid larvae occurred at 58% of the stomachs examined and the rest were less frequent.

**Table 1.** List of food items identified in the stomachs of adult and young *T. zillii* and *O. niloticus* collected from Lake Zwai during the year 2001 with their percentage frequency range of occurrence (% occurrence). Number in parenthesis indicates average value.

Food category	% Occurrence ( <i>T. zillii</i> )		% Occurrence ( <i>O. niloticus</i> )	
	Adult	Young	Adult	Young
A. Macrophytes	100	35-65(40)	11-100(84)	2-42(11)
B. Phytoplankton				
i. Cyanophyta	12-100(64)	78-92(86)	100	100
<i>Anabaena</i>	0-51(18)	16-47(32)	5-95(58)	45-50(48)
<i>Anabaenopsis</i>	--	--	0-11(6)	--
<i>Chroococcus</i>	0-9(7)	0-12(8)	10-71(46)	45-55(50)
<i>Gloeocapsa</i>	0-2 (0.4)	0-8 (4)	0-7 (1)	--
<i>Lyngbya</i>	2-52(33)	47-63(55)	48-100(89)	55-68(62)
<i>Merismopedia</i>	0-27(11)	21-34(28)	0-80(33)	33-75(74)
<i>Microcystis</i>	12-100(59)	84-92(91)	97-100(100)	100
<i>Oscillatoria</i>	0-40(33)	39-89(54)	33-100(89)	20-64(62)
<i>Spirulina</i>	0-5(1)	0-8(3)	0-16(4)	0-5(1)
ii. Bacilliarophyta	2-82(54)	84-100(96)	100	95-100(98)
<i>Achnanthes</i>	0-5(0.4)	0-61(25)	0-84(30)	32-45(38)
<i>Amphora</i>	--	--	--	0-5(2)
<i>Cyclotella</i>	8-28(11)	5-39(30)	5-43(22)	0-5(2)
<i>Cymbella</i>	5-36(15)	5-71(59)	19-91(66)	73-75(74)
<i>Denticula</i>	--	0-9(5)	0-21(9)	5-23(14)
<i>Frustulia</i>	--	0-13(7)	0-33(11)	14-20(17)
<i>Gomphonema</i>	0-4(0.2)	--	0-89(44)	36-45(40)
<i>Navicula</i>	4-84(48)	63-97(84)	40-100(75)	60-91(76)
<i>Nitzschia</i>	2-8(2)	8-32(18)	0-33(12)	18-60(24)
<i>Opephora</i>	0-3(0.4)	--	0-89(16)	0-6(2)
<i>Pinullaria</i>	--	--	0-89(33)	28-85(36)
<i>Rhoicosphenia</i>	2-9(4)	0-8(4)	0-20(5)	--
<i>Rhopalodia</i>	8-41(10)	47-87(78)	0-80(29)	86-90(88)
<i>Surirella</i>	--	8-11(9)	0-16(10)	10-18(14)
<i>Synedra</i>	6-18(13)	--	0-98(61)	0-50(16)
iii. Chlorophyta	13-83(38)	58-61(59)	87-100(96)	100
<i>Ankistrodesmus</i>	2-6(2)	--	0-53(18)	9-35(21)
<i>Botryococcus</i>	2-8(2)	--	0-41(14)	0-9(5)
<i>Coelastrum</i>	2-12(6)	0-8(5)	0-29(4)	0-14(7)
<i>Closterium</i>	2-24(8)	16-26(21)	0-67(23)	9-50(28)
<i>Cosmarium</i>	2-6(3)	2-5(3)	0-58(20)	10-18(14)

<i>Euastrum</i>	0-8(2)	0-3(1)	0-32(9)	0-14(7)
<i>Pediastrum</i>	2-19(4)	0-3(2)	0-84(46)	27-30(28)
<i>Scendesmus</i>	2-23(6)	24-39(32)	10-87(71)	60-82(71)
<i>Selenastrum</i>	--	--	0-16(2)	--
<i>Spirogyra</i>	4-26(16)	5-12(10)	5-95(41)	5-41(24)
<i>Staurastrum</i>	2-71(16)	0-13(10)	0-84(36)	75-77(76)
<i>Tetradron</i>	0-3(0.2)	--	--	--
C. Detritus	2-37(10)	20-88(83)	0-38(9)	0-15(11)
D. Chironomid larvae	2-48(10)	39-68(58)	0-14(3)	0-9(5)
E. Zooplankton				
Copepoda	0-3(1)	0-4(3)	0-50(8)	0-5(2)
Cladocera	0-4(0.6)	--	0-20(4)	--
Rotifera	0-2(0.9)	--	0-43(13)	0-13(2)
F. Others				
<i>Ceratium</i>	0-29(8)	0-12(4)	0-27(7)	0-8(3)
<i>Euglena</i>	0-5(1)	0-2(0.3)	0-47(14)	27-35(31)
<i>Phacus</i>	0-2(0.2)	(0-0.2)	0-63(17)	23-25(24)
Nematoda	0-3(0.4)	--	--	0-5(1)
Ephemeroptera	0-4(0.4)	--	--	--
Molluscs	0-8(0.4)	--	--	--
Fish egg	0-5(0.6)	--	0-10(0.8)	--
Fish scale	0-9(5)	10-16(13)	0-8(2)	4-5(5)
Unidentified species	0-6(0.8)	--	--	--

**Adult and young *O. niloticus*.** Adult *O. niloticus* in Lake Zwai was found to utilise quite a wide range of food material particularly phytoplankton which were distributed among three major groups consisting of blue-green algae, diatoms and green algae (Table 1). The blue green algae consisted mainly of *Microcystis* (100% occurrence), *Lyngbya* (89%) and *Oscillatoria* (49%). Occurrence of the green algae was noted to be 41% for *Spirogyra* and 36% for *Staurastrum*, while *Navicula* (75%), *Cymbella* (66%) and *Synedra* (61%) were among those of the diatoms that were frequent. Macrophytes, plant detritus, *Ceratium*, *Phacus*, and *Euglena* were also noted to be among the components of the diet. Foods of animal origin included chironomid larvae, crustacea (Copepoda and Cladocera), Rotifera, and fish scales.

The diet of young *O. niloticus* in the lake was very similar to the food items of the adults both in terms of food composition and diversity and included blue-green algae, diatoms, green algae, plant detritus, *Ceratium*, *Euglena*, and *Phacus* (Table 1). Foods of animal origin were encountered and consisted of chironomid larvae, Copepoda, Cladocera, Rotifera, Nematoda, and fish scales. The blue-green algae (100% *Microcystis*, 62% *Lyngbya* and 50% *Chroococcus*), the green algae

(76% *Staurastrum* and 71% *Scenedesmus*), and the diatoms (88% *Rhopalodia*, 76% *Navicula* and 74% *Cymbella*) were items with high frequency of occurrence. These food items were numerically more important in the diet.

*Breeding season of T. zillii and O. niloticus*

Monthly variation of GSI of both sexes was evident for *T. zillii* (Figure 4) as well as for *O. niloticus* (Figure 6). The mean monthly GSI  $\pm$  SE of female *T. zillii* ranged from  $0.32 \pm 0.02$  (in January) to  $3.58 \pm 0.31$  (in August), while that of the males ranged from  $0.15 \pm 0.02$  to  $0.34 \pm 0.04$ . *T. zillii* had its highest GSI values from February to September, while lower values were recorded between October and January. The percentage of mature females and males ranged from 5-68% and 6-76% respectively, with high values between April and September (Figure 5).

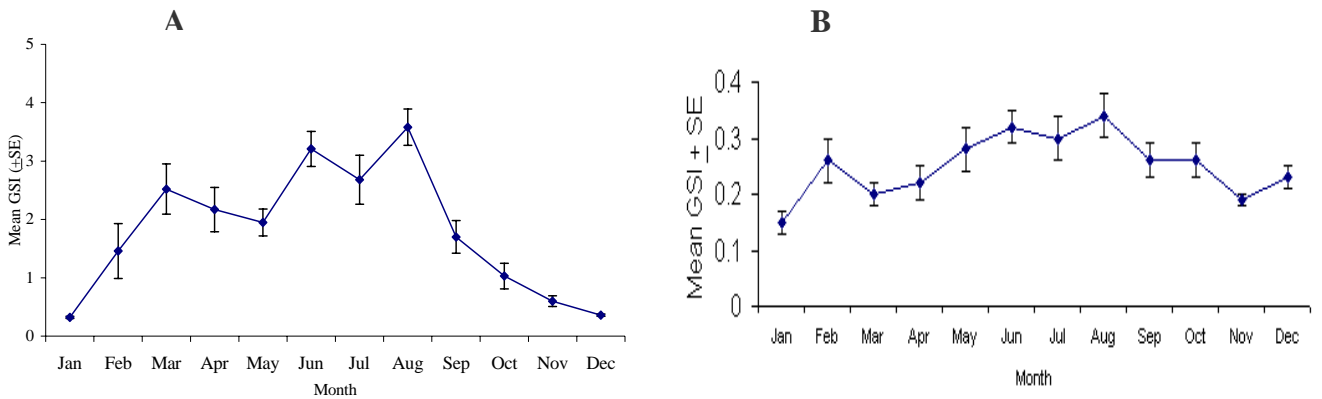


**Figure 4.** Gonadosomatic index (mean  $\pm$  SE) of *T. zillii* (A: female, B: male) in Lake Zwai during 2001

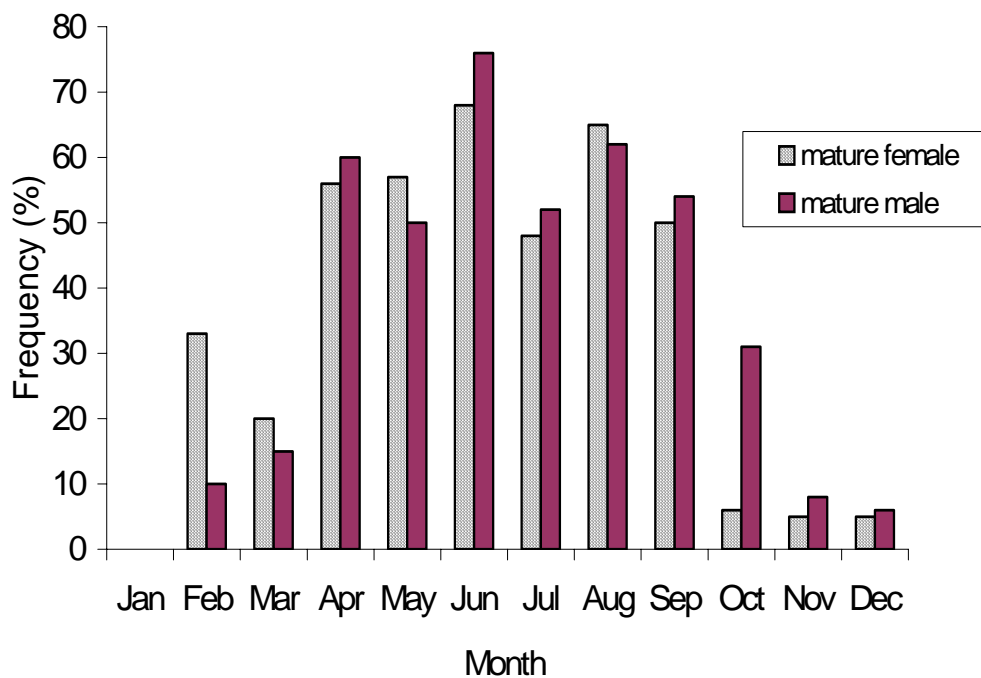


**Figure 5.** Percentage of mature female and male *T. zillii* in Lake Zwai during the year 2001

In *O. niloticus* the mean monthly GSI  $\pm$  SE of females ranged from  $0.30 \pm 0.03$  (in October-November) to  $2.02 \pm 0.46$  (in August), whereas that of males ranged from  $0.09 \pm 0.01$  (in September-December) to  $0.50 \pm 0.10$  (in May and August). High GSI values extended from February to August, whereas low GSI values were recorded between September and January (Figure 6). The percentage of mature females and males ranged from 3-42% and 3-45% respectively, with higher values between February and August (Figure 7).

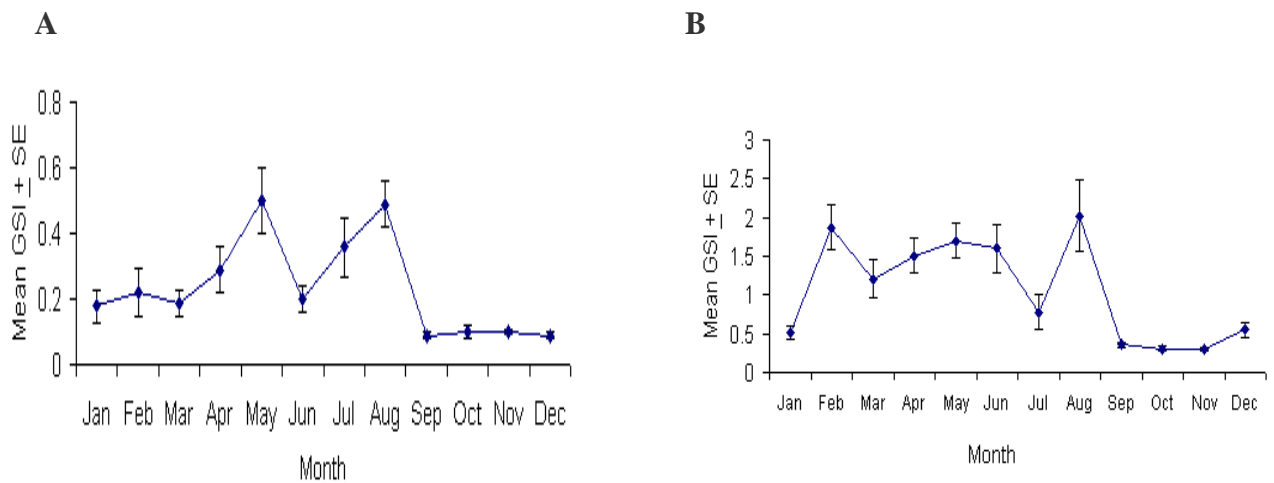


**Figure 6.** Gonadosomatic index (mean  $\pm$  SE) of *O. niloticus* (A: female, B: male) in Lake Zwai during 2001

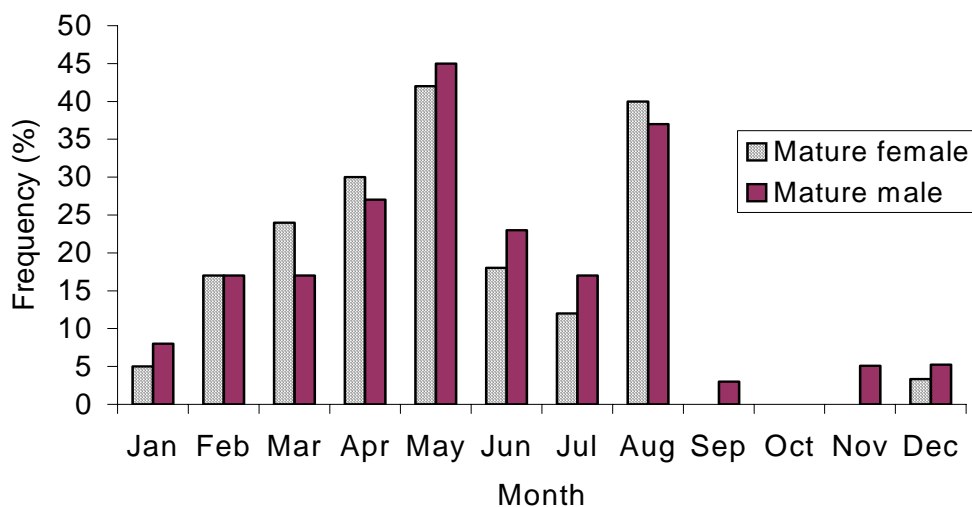


**Figure 7.** Percentage of mature female and male *O. niloticus* in Lake Zwai during 2001

From the above observations it was evident that the reproduction of *T. zillii* and *O. niloticus* in Lake Zwai was continuous throughout the year and was most active between April-September and February-August respectively.

## Discussion

At the sampling sites in Lake Zwai, *T. zillii* regularly appeared in the catches during the sampling periods. The fish were also noted to be present in many places around the shallow marginal water of the lake, which indicated that this particular species has successfully established itself in the lake. *O. niloticus*, however, was always associated with *T. zillii* in the catches, including the ones with mature gonads from both species, which indicated a niche overlap. Young fish of the two species were also found together in collections employing beach seine net. Results from catch per unit effort records indicated that *T. zillii* was more abundant than *O. niloticus* (Figure 3). On the contrary, *T. zillii* was rarely encountered in the catches far from the lakeshore. Thus, the catch records from the sampling sites alone may not reflect the exact abundance of the species in the whole lake.

*T. zillii* was observed to be more dependent on shoreline habitat compared to *O. niloticus*, and differences in the distribution of the species in the lake might be due to their habitat

preferences. This is in agreement with the findings conducted in Lake Victoria [13]. McConnell [14] also pointed out that substrate-spawners with macrophyte feeding habit (e.g. *T. zillii*) are more dependent on shoreline habitat than are the mouth brooders with their microphagous feeding and more pelagic habitat, (e.g. *O. niloticus*), especially in waters rich in plankton. Thus, *T. zillii* may be an important component of the Zwai ecosystem because of its abundance in shallow waters as required by spawning fish including *O. niloticus*.

Stomach content analysis based on the occurrence method showed that both *T. zillii* and *O. niloticus* exploited diverse food sources of both plant and animal origins (Table 1). Similar findings have been reported for the two species in Lake Victoria [13] and Nile canal [15]. Nevertheless, foods of plant origin were the major components of the diet in both species and comprised macrophytes, plant detritus, and phytoplankton consisting of blue-green algae, green algae, diatoms, *Ceratium*, *Phacus*, and *Euglena*. On the other hand, chironomid larvae, Ephemeroptera, mollusks, Copepoda, Cladocera, Rotifera, and eggs and scales of unidentified fish were foods of animal origin. Of these, Ephemeroptera, mollusks and unidentified animal pieces of larger size were noted exclusively in the diet of adult *T. zillii*.

Though not quantified, the diet of *T. zillii* in Lake Zwai varied depending on the size of the fish as the adult chiefly fed on macrophytes and the young on phytoplankton. This may be due to difference in the degree of development of the feeding organs and the habitat occupied by the fish. Philipart and Ruwet [4] also reported the variation in the feeding regime of fish species depending on size, age and the microhabitat occupied by the fish in a given water body.

In adults, higher plant tissues including large portions of roots, leaves and stems of aquatic vegetation and seeds occurred in all of the stomachs examined. Several authors [5,13,15] also reported that *T. zillii* feeds essentially on plant materials, which is consistent with the present observation, in which blue-green algae, diatoms, and green algae were found in 64%, 54%, and 38% respectively of the stomachs examined. These items were also reported to be ingested by the fish from Lake Quarun [16], Lake Kinnert [17], and Nile canal [15]. The occurrence of planktonic material in the guts of fish with no filter feeding mechanism, as is the case in *T. zillii*, is a strange phenomenon. However, Welcomme [13] suggested that the source of planktonic material in the diet of *T. zillii* in Lake Victoria was a flocculent deposit offshore.

Adult *T. zillii* were also known to ingest benthic invertebrates [16], insect larvae and crustacea [15] in other water bodies, and the observation from Lake Zwai also supports this findings. The occurrence larger animals like mollusk in the diet of adult *T. zillii*, but not *O. niloticus*, may be due to the relatively greater tendency of the former species to exploit animal foods, whereas their

exclusion from the diet of young ones may be attributed to prey-predator size relationship. Abdel-Malek [16] also associated to the change in composition of the diet as the fish grows with an increase in the minimum size of the organism eaten. Diet composition of young *T. zillii* in Lake Zwai was similar to what has been reported [8] for Lake Quarun for fish whose total length ranged from 4.5-9 cm.

From analysis using the frequency of occurrence and personal observations on the abundance of the food items, it was clear that phytoplankton (blue greens, diatoms and greens) were the principal foods of both adult and young *O. niloticus* in the length range considered. Previous reports of some Ethiopian rift valley lakes including Zwai also showed that adult *O. niloticus* mainly feeds on phytoplankton [17-18]. On the other hand, juvenile *O. niloticus* was known to be an omnivore feeding on algae, zooplankton and insect larvae [19]. These reports further stated that young *O. niloticus* in the length range considered in the present study feeds primarily on phytoplankton. Thus, the food composition of young *O. niloticus* in the present observation (mainly phytoplankton) could have resulted from a possible ontogenetic diet shift.

Analysis of the food habits of *T. zillii* and *O. niloticus* in Lake Zwai revealed extensive diet overlap (Table 1). However, the food items utilised by both species varied in their contribution to the diet. There was a clear tendency for adult *T. zillii* to feed mainly on macrophytes while phytoplankton was found to be the principal food of young *T. zillii* and *O. niloticus* (adult and young). This observation is contrary to the conclusion by Bowen [20] who stated that tilapias in general feed on any food particle small enough to pass through the esophagus. Consequently, the diet overlap between adult *T. zillii* and the remaining groups (young *T. zillii* and *O. niloticus* in both length groups) might be moderated by their food preferences.

On the other hand, differences in feeding site and habitat could be important for resource partitioning between adult *O. niloticus* and the young of both species. The preferred habitat of adult *O. niloticus* is the pelagic zone and that of the young is the lakeshore. Ribbink et al. [21] emphasised the importance of feeding site to resource partitioning rather than the foods they take in coexisting related species of cichlids in the African Great Lakes. Nevertheless, the young of both *T. zillii* and *O. niloticus* having a similarity in diet preference were found to share similar habitat as they were collected together from the same fishing ground. Thus, spatial relation and overlap in the major diet of the young of *T. zillii* and *O. niloticus* indicate possible competition for food resources.

The seasonal variation in GSI and percentage of mature fish of both sexes of *T. zillii* (Figures 4-5) and *O. niloticus* (Figures 6-7) was quite apparent. The seasonal pattern of gonad

development and variation in percentage of mature fish of both sexes were more or less similar for *T. zillii* and *O. niloticus*. Indeed, fish with well-developed gonads and mature eggs in both species were noted almost throughout the year. GSI values and percentages of mature fish indicated that breeding in both species was year-round with its peak during April-September for *T. zillii* and February-August for *O. niloticus*.

The presence of breeding fish in Lake Zwai throughout the year may be attributed to the low seasonal fluctuation in temperature and photoperiod (Figure 2). It is a well-established fact that in the tropics seasonal fluctuation in temperature and photoperiod is generally very low and this might be favourable for fish species to spawn any time of the year. The annual peaks of reproductive activity in both species are coincident with the rainy season (Figure 2). With the advent of the rainy season the lake level rises and due to the flooding of land nutrients are flushed into the lake. As a result, habitat and food resource for fish expand greatly and this may trigger reproduction. McConnell [14] also concluded that breeding among tilapias often occurs sporadically year-round but has a distinct peak just before or at the onset of the rainy season, which is in accordance with the present findings. Rainfall increases production [22] and water level, which in turn provides suitable spawning grounds for adults, and feeding and nursery grounds for the young [23].

## Conclusions

The level of gonad maturation and mean gonadosomatic index (GSI) values indicated extended breeding season overlap in reproduction between *T. zillii* and *O. niloticus*. The reproduction of young fish that share similar habitat by the two species during similar seasons might have had some effect on the population of *O. niloticus* due to possible competition on nursery grounds. Such phenomenon, in which the young of *T. zillii* were introduced into Lake Victoria, has displaced the young of a native tilapia species from crucial nursery areas, causing a severe decline in the native species. The competitive interaction in feeding and on nursery grounds between young *T. zillii* and young *O. niloticus* may therefore have been one of the factors that contributes to the decline in the population of *O. niloticus* in Lake Zwai and should be further studied in detail.

## Acknowledgements

We would like to thank the Swedish Agency for Research and Education for Developing Countries (SAREC) and the Rockefeller Foundation (Grant No. 2001AR 002) for financial support and the National Meteorology Services Agency for providing the meteorological data. We also extend our sincere thanks to the fishermen of the Lake who helped us in sample collection, of whom Gezahegn Tilinti and Mulatu Galato deserve especial consideration.

## References

1. P. B. Moyle and J. J. Cech, "Fishes: An Introduction to Ichthyology.", 3<sup>rd</sup> Edn., Prentice Hall, New York, **1996**.
2. A. Getahun and M. L. J. Stiassny, "The freshwater biodiversity crisis: the case of the Ethiopian fish fauna", *SINET: Ethiop. J. Sci.*, **1998**, *21*, 207-230.
3. S. Tedla and F. HaileMeskel, "Introduction and transplanted of freshwater fish species in Ethiopia", *SINET: Ethiop. J. Sci.*, **1981**, *4*, 69-72.
4. J. C. L. Philipart and J. C. L. Ruwet, in "The Biology and Culture of Tilapias", (Ed. R. S. V. Pullin and R. H. Lowe-McConnell), Cambridge University Press, London, **1982**, Ch.1.
5. J. D. Balarin and T. J. Hatton, "Tilapia: A Guide to Their Biology and Culture in Africa", Stirling University Press, Scotland, **1979**.
6. R. Schroder, "An attempt to estimate the fish stock and sustainable yield of Lake Zwai and Lake Abaya in Ethiopian Rift Valley", *Arch. Hydro-Biologia, Suppl. Bd.*, **1984**, *69*, 411-441.
7. Lake Fisheries Development Project (LFDP), "Fisheries Report", Department of Animal and Fisheries Resources Development, Phase II Report, Addis Ababa, **1998**.
8. S. E. El-Zarka, "Tilapia fisheries investigation in Egyptian lakes: Maturity, spawning and sex ratio of *Tilapia zillii* (Gerv.) in Lake Quarun", Extension and Publication section- Notes and Memories No. 67, Cairo, **1962**.
9. M. M. Babiker and H. Ibrahim, "Studies on the reproduction of the cichlid *Tilapia nilotica* (L) gonadal maturation and fecundity", *J. Fish Biol.*, **1979**, *14*, 437-448.
10. R. Schroder, "An attempt to estimate the fish stock and sustainable yield of Lake Zwai and Lake Abaya, Ethiopian Rift valley", *Arch. Hydrobiologia Suppl.*, **1984**, *69*, 411-441.
11. R. W. Pennak, "Freshwater Invertebrates of the United States", John Wiley and Sons, New York, **1978**.
12. D. Defaye, "Contribution a la connaissance des crustaces copepods d'Ethiopie", *Hydrobiologia*, **1988**, *164*, 103-147.
13. R. L. Welcomme, "Observations on the biology of the introduced species of tilapia in Lake Victoria", *Rev. Zool. Bot. Afr.*, **1967**, *XXVI*, 3-4.
14. R. H. Lowe-McConnell, "Ecological Studies in Tropical Fish Communities", Cambridge University Press, London, **1987**.
15. E. A. Khallaf and A. A. Alne-na-ei, "Feeding ecology of *Oreochromis niloticus* (Linnaeus) and *Tilapia zillii* (Gervais) in a Nile canal", *Hydrobiologia*, **1987**, *146*, 57-62.

16. S. A. Abdel-Malek, "Food and feeding habits of some Egyptian fishes in Lake Quarun: *Tilapia zillii* (Gerv.) B. according to different length groups", *Bull. Institute of Oceanography and Fisheries*, **1972**, 205-213.
17. G. Teferra and C. H. Fernando, "The food habits of an herbivorous fish (*Oreochromis niloticus* L.) in Lake Awassa, Ethiopia", *Hydrobiologia*, **1989**, 174, 195-200.
18. G. Teferra, "The composition and nutritional status of the diet of *Oreochromis niloticus* in Lake Chamo, Ethiopia", *J. Fish Biol.*, **1993**, 42, 865-874.
19. Z. Tadesse, *M.Sc. Thesis*, **1988**, Addis Ababa University, Ethiopia.
20. S. H. Bowen, in "The Biology and Culture of Tilapias", (Ed. R. S. V. Pullin and R. H. Lowe-McConnell), Cambridge University Press, London, **1982**, Ch.3.
21. A. J. Ribbink, B. A. Marsh, A. C. Marsh, A. C. Ribbink, and B. J. Sharp, "A preliminary survey of the cichlid fishes of rocky habitats in Lake Malawi", *S. Afr. J. Zool.*, **1983**, 18, 149-310.
22. E. Kebede, Z. GebreMariam, and I. Ahlgren, "The Ethiopian rift valley lakes: chemical characteristics of a salinity-alkalinity series", *Hydrobiologia*, **1994**, 288, 1-12.
23. C. Tudorancea, Z. GebreMariam, and E. Dadebo, in "Limnology in Developing Countries", (Ed. R. G. Wetzel and B. Gopal), Vol. 2, International Association for Limnology, India, **1999**, pp. 63-118.

© 2007 by Maejo University, San Sai, Chiang Mai, 50290 Thailand. Reproduction is permitted for noncommercial purposes.

***Maejo International***  
***Journal of Science and Technology***

ISSN 1905-7873

Available online at [www.mijst.mju.ac.th](http://www.mijst.mju.ac.th)

*Full Paper*

## **Water quality of Wenchi Crater Lake in Ethiopia**

**Malairajan Singanan<sup>\*</sup>, Lakew Wondimu, and Mitiku Tesso**

Ecotoxicology Research Center, Ambo University College, P.O.Box.19, Ambo Town,  
Western Shoa, Ethiopia

\* Author to whom correspondence should be addressed, e-mail: [swethasivani@yahoo.co.in](mailto:swethasivani@yahoo.co.in),  
[msinganan@yahoo.com](mailto:msinganan@yahoo.com)

*Received: 5 February 2008 / Accepted: 4 June 2008 / Published: 13 June 2008*

---

**Abstract:** Determination of physico-chemical properties of water samples from Wenchi Crater Lake in Ethiopia was carried out. Selected heavy metals in water, sediment, and plant samples from the lake were also comparatively determined. The results indicated that most general physico-chemical properties of the lake water fell within those recommended for drinking water. However, the lake water was found to be high in some heavy metals, which also accumulated in the sediment. Bioconcentration of these metals was also observed in the plant samples.

**Key words:** Wenchi Crater Lake, water quality, heavy metals, sediment, *Typha latifolia*

---

## Introduction

Wenchi Crater Lake is one of the important lakes in Ethiopia. The lake is located in Western Shoa region, which extends between latitude  $15^{\circ}$  N -  $3^{\circ}$  S and longitudes  $48^{\circ}$  E -  $33^{\circ}$  W. It is situated at the major topographic feature in the country, being 130 km south-west of the capital city, Addis Ababa. It is surrounded by Kelela region in the north, Dera region in the east, Goro Wenchi region in the south and Haro Gebeya region in the west. This lake, 1,600 square metres in total area, is ecologically, recreationally, and aesthetically important as well as a popular place for tourists. The topographical location of the lake is presented in Figures 1 and 2.

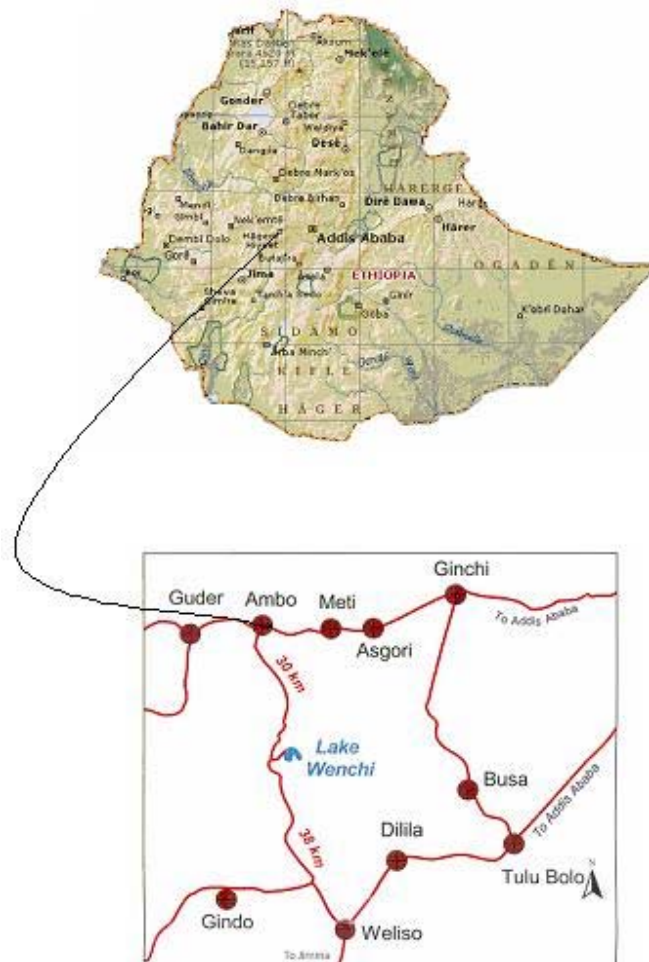


**Figure 1.** Location of Wenchi Crater lake in Ethiopia



Figure 2. Topography of Wenchi Crater Lake

The health of a lake is governed by the quantity of nutrients it receives from various streams. Nutrient recycling and proper productivity are necessary for sustenance and balance of the system. Due to nutrient enrichment, the system may lose its balance and may turn eutrophic. Thus, water quality studies are necessary to ascertain the suitability of water for various beneficial uses and to assess the trophic level of the lake.

In aquatic systems, the natural concentrations of metal ions are principally dependent on the ambient distribution, weathering and leaching of the elements from the soil in the catchment area, while heavy metals are carried to the lakes through atmospheric deposition and other man made activities. The characteristics of the water, such as acidity and the amount of organic matter, are known to be important factors in determining the fate of heavy metals in lakes [1-3].

The sediment of the aquatic environment acts as a major reservoir of metals [4] and also as a source of contaminants. Enrichment of heavy metals due to industrialisation and urbanisation was recorded in the sediment of coastal areas all over the world [5-9]. The monitoring of the heavy metal resulting from anthropogenic activities are particularly important for the assessment of environmental quality and protection. Heavy metal distribution in lagoonal and intertidal sediment has frequently been used to investigate chronological inputs [10-12].

Increased loading of heavy metals into lakes may have several ecological consequences. Elevated trace metal concentrations may lead, for example, to toxic effects or biomagnification in the aquatic environment. Accumulation of heavy metals in the food web can occur either by bioconcentration from the surrounding medium such as water or sediment, or by bioaccumulation from the food source.

In the following study, no attempts were made to investigate the environmental health of Wenchi Crater Lake. The main objective of this study, the first performed for this lake, is to monitor the water quality of the lake with reference to standard water quality parameters and heavy metals in its water and sediment, and in *Typha latifolia*, a major aquatic plant present in the lake.

## **Materials and Methods**

The water, sediment and *Typha latifolia* samples were collected bimonthly between January-December 2007 from eight sampling points (Figure 2) in the lake in cleaned polythene containers. The water quality parameters, viz. pH, electrical conductivity (EC), total dissolved solids (TDS), total hardness (TH), total alkalinity (ALK), common metal ions ( $\text{Ca}^{2+}$ ,  $\text{Mg}^{2+}$ ,  $\text{Na}^+$ , and  $\text{K}^+$ ), anions chloride ( $\text{Cl}^-$  and  $\text{SO}_4^{2-}$ ), and dissolved oxygen (DO) were analysed employing standard experimental protocols outlined in the literature [13-14]. In case of heavy metals, Cd, Cu, Ni, Cr, Pb, Mn, and Zn were selected and analysed as per the standard experimental protocols outlined in the literature [13] using a Shimadzu AA 6200 atomic absorption spectrophotometer. All the chemicals and reagents used in the experiments were of analytical grade. All the results were statically significant at  $p < 0.05$ .

## **Results and Discussion**

The results of the physico-chemical analysis of the water samples collected from all the sampling points were presented in Table 1.

### *pH and dissolved oxygen (DO)*

The pH of Wenchi Crater Lake water (7.4-7.6) fell within the desirable range (6.5-8.5) for drinking water as per the WHO guideline [16]. This result indicated that there were no human influences in the lake area and the responsible factor for the slightly alkaline value of the pH was only through the chemical composition of the bed rock sediment.

Dissolved oxygen is very essential for all living organisms in any water bodies. The recorded level of dissolved oxygen in the water of Wenchi Crater Lake ranged between 7.4- to 7.6 mg/L (WHO range: 4.5-7.5 mg/L). A similar result was also reported for Lake Naivasha, Kenya [15]. In the lake, the population of phytoplankton was relatively more than that of the zooplankton. The overgrowth of the plankton species and other aquatic plants might cause eutrophication in the lake in due course of time.

**Table 1.** Physico-chemical characteristics of the lake water

Water quality parameter	Sample collection point in the Crater Lake								WHO guideline value for drinking water [16]
	S1	S2	S3	S4	S5	S6	S7	S8	
	Mean value								
pH	7.5	7.6	7.6	7.4	7.5	7.5	7.6	7.6	6.5 – 8.5
EC ( $\mu\text{mhos/cm}$ )	1180	1182	1179	1180	1183	1182	1181	1183	1500
TDS (mg/L)	767	768.30	766.35	767	768.95	768.30	767.65	768.95	1000
TH (mg/L)	282	283	280	282	285	284	282	284	400
Ca (mg/L)	135	137	135	136	134	135	136	135	200
Mg (mg/L)	105	102	105	104	106	105	103	105	100
Na (mg/L)	48	52	50	49	48	50	48	47	200
K (mg/L)	26	28	27	28	26	28	29	27	20
Cl <sup>-</sup> (mg/L)	458	460	458	462	460	457	459	460	400
SO <sub>4</sub> <sup>2-</sup> (mg/L)	390	394	392	390	392	394	392	390	400
DO (mg/L)	7.4	7.6	7.5	7.5	7.6	7.5	7.6	7.5	4.5 – 7.5

**Note:** The analytical results were statistically significant at  $p < 0.05$ .

#### *Electrical conductivity (EC) and total dissolved solids (TDS)*

The conductivity of the water samples registered 1179-1183  $\mu\text{mhos/cm}$ . This is well below the WHO guideline value prescribed for drinking purpose (1500  $\mu\text{mhos/cm}$ ). The TDS present in the water affects its aesthetic value as well as its physico-chemical and biological properties. The TDS values found (766.35-768.95 mg/L) were also below the drinking water standard (1,000 mg/L).

#### *Total hardness (TH), calcium and magnesium*

The lake water samples recorded a low level of total hardness (280-285 mg/L). The total hardness has no known adverse effects on human health, and the recorded values were well below the guideline value for drinking purpose (400 mg/L).

Primarily, the calcium and magnesium present are responsible for the hardness of the water. The desirable limit for calcium in water is (75 mg/L) and the maximum permissible limit is (200 mg/L), and for magnesium these values are 30 and 100 mg/L

respectively. In the present investigation, we have observed that the values for calcium were 134-137 mg/L and those for magnesium, 102-106 mg/L.

#### *Sodium and potassium*

Sodium and potassium are the monovalent cations commonly present in water. These ions do not produce hardness to water. However, significantly high amounts of these ions in water create problem in its taste as well as make the water unsuitable for irrigation purpose. In the present study, the concentration of sodium (47-52 mg/L) was well below the listed value in Table 1, while that of potassium (26-29 mg/L) exceeded the allowed value (20 mg/L). This might be due to the presence of potash minerals in the area. A further geological investigation of the studied area is necessary.

#### *Chloride and sulphate*

The presence of chloride and sulphate in water in excess amounts is not desirable. Its origin is mainly from mineral weathering of bed rocks as well as from anthropogenic source. In the present investigation, the concentrations of chloride and sulphate ranged 457-462 mg/L and 390-394 mg/L respectively. The desirable limit of chloride is 250mg/L and the maximum permissible limit is 400 mg/L and for sulphate, it is 200 and 400 mg/L respectively. The concentration of chloride was thus somewhat higher than the permissible limit for drinking purpose.

#### *Heavy metals in water*

The concentrations of Cd, Cu, Ni, Cr, Pb, Mn, and Zn were determined in water samples from eight sampling points in the lake. The analytical results are presented in Figure 3. The drinking water standards (WHO guidelines) for the trace inorganic contaminants such as Cd, Cu, Ni, Cr, Pb, Mn and Zn are 0.003, 2.0, 0.02, 0.05, 0.01, 0.5 and 5.0 mg/L respectively [16]. The results indicate that only the levels of Cu, Mn and Zn in the lake water were well within the allowable concentrations. The concentrations of all other metals were significantly increased in the lake water.

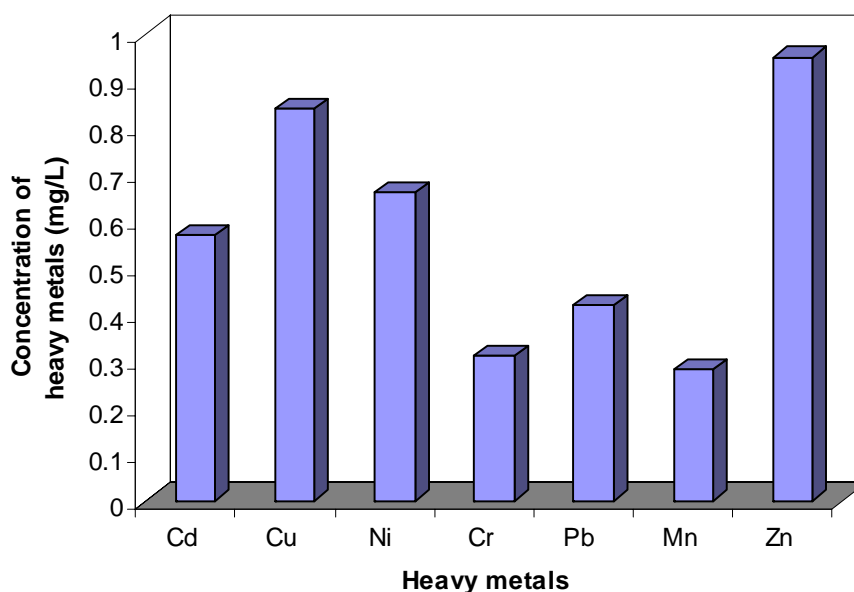


**Figure 3.** Levels of heavy metals in the lake water

#### *Heavy metals in sediment*

Sediment samples were collected in the same eight locations in the lake and were analysed for the concentration of Cd, Cu, Ni, Cr, Pb, Mn and Zn. Two sediment samples were fine-grained and others were coarse-grained. The sediment samples registered significantly higher amounts of heavy metals than the water samples (Figure 4).

#### *Heavy metals in plant samples (Typha latifolia)*

*Typha latifolia* was the major aquatic plants in the lake. Their roots were collected near the water sampling points and analysed for heavy metal concentrations, the average values of which are presented in Figure 5. The result shows that the plants accumulated significantly higher amounts of heavy metals compared to the sediment. Since heavy metals present in water and sediment are slowly absorbed by the aquatic plants and thereby concentrated in the root metabolism, the plants can be used as a bioindicator of heavy metal pollution in the lake.

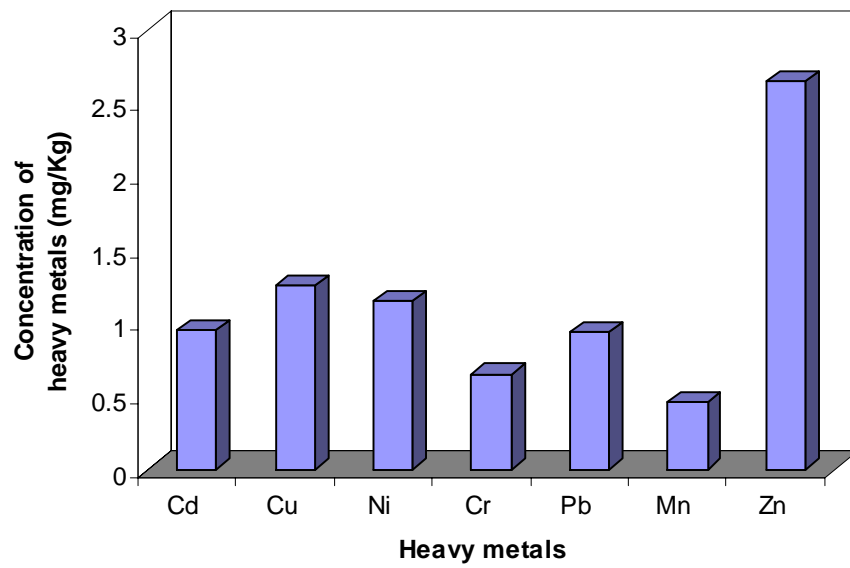


Figure 4. Levels of heavy metals in lake sediment

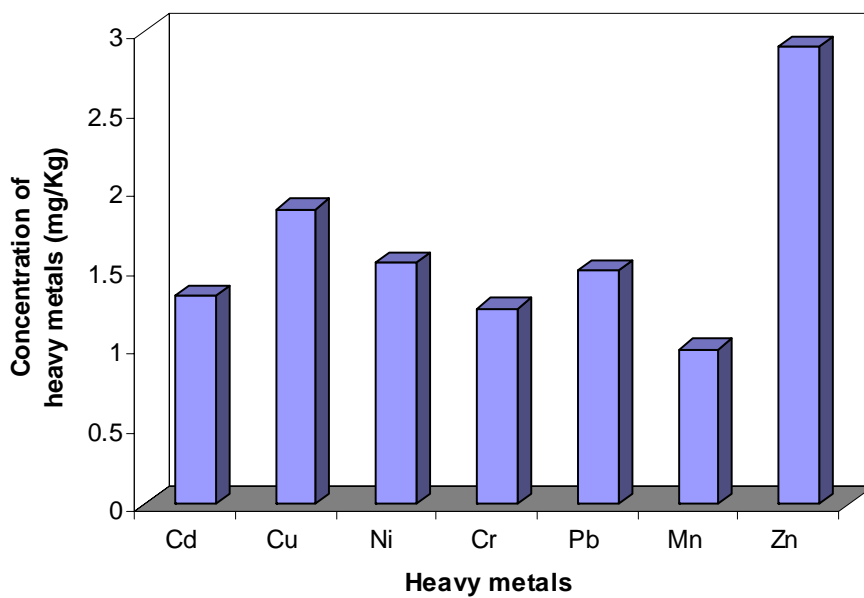


Figure 5. Levels of heavy metals in roots of *Typha latifolia*

Notably the three sampled items show distinct variation in metal contents. The concentration gradients (plant root > sediment > water) exist for all the heavy metals in the lake and it might be possible that the sedimental particles were transported towards the lower reach of the lake. Parallel gradients of organic matter contents and grain size distribution of the sediment are also likely to influence the heavy metal concentration in the lake [17-18]. The fine-grained sediment is reported to have a greater influence on the adsorption of heavy metals from the water [19].

It is also observed in many estuaries across the world that the concentration of heavy metals from known anthropogenic input generally increases [10,20]. In Wenchi Crater Lake area there are three inlets and two outlets. However, the outlet points are present only in the upper part of the lake and the volume of water discharge is comparatively small while the bulk of the lake water is lost through evaporation and absorption. Therefore the lake area becomes a large sink for heavy metals. The concentration factor is the main cause of sediment toxicity while this factor through bioaccumulation by plants (*Typha latifolia* in this case) is apparently more pronounced. Land erosion and natural weathering of bedrocks of the lake are probably the main factors responsible for the accumulation of heavy metals in the lake ecosystem.

### **Conclusions**

Most physico-physical properties of Wenchi Crater Lake conformed to the standards set out by WHO for drinking water, except for the level of magnesium, chloride, and sulphate ions, which just overstepped the borderlines. As for heavy metals, it was observed that only Cu, Mn, and Zn were well within the allowable concentrations while Cd, Ni, Cr, and Pb were significantly higher than the set limits allowable for potable water. Moreover, the lake sediment was found to be enriched with these heavy metals compared to the lake water. However, heavy metal enrichment through bioconcentration by plants in the lake was even more conspicuous.

The presence of increased amounts of heavy metals may have a direct impact on the health of humans as well as aquatic animals. Visibly the water looks very clean with no

contamination. The volume of water in the lake is very high and can potentially be used for various purposes by employing artificial recharging technologies and special purification methods. However, there is a dense population of macrophytes in the lake. Further research work is necessary to study them and their impact on the water quality of the lake.

### **Acknowledgement**

The authors wish to acknowledge the research and publication coordination office of the Ambo University College, Ambo Town, Ethiopia for the financial support.

### **References**

1. J. Mannio, M. Verta, and O. Jarvinen, "The trace metal concentrations in the water of small lakes, Finland", *Appl. Geochem. Suppl.*, **1993**, 2, 57-59.
2. B. L. Skjelkvale, T. Andersen, E. Fjeld, J. Mannio, A. Wilander, K. Johansson, J. P. Jensen, and T. Moiseeko, "Heavy metal survey in Nordic lakes: concentrations, geographic patterns and relation to critical limits", *Ambio*, **2001**, 30, 2-10.
3. T. Tulonen, M. Pihlstrom, L. Arvola, and M. Rask, "Concentration of heavy metals in food web components of small boreal lake", *Boreal Environ. Res.*, **2006**, 11, 185-194.
4. V. G. Caccia, F. J. Millero, and A. Palanques, "The distribution of trace metals in Florida Bay sediments", *Mar. Pollut. Bull.*, **2003**, 46, 1420-1433.
5. H. Feng, X. Han, W. Zhang, and L. Yu, "A Preliminary study of heavy metal concentration in Yangtze River intertidal zone due to urbanization", *Mar. Pollut. Bull.*, **2004**, 49, 910-915.
6. J. L. Gallasso, F. R. Siegel, and J. H. Kravitz, "Heavy metals in eight 1965 cores from the Novaya Zemlya Trough, Kara Sea, Russian Arctic", *Mar. Pollut. Bull.*, **2000**, 40, 839-852.
7. D. S. Manta, M. Angelone, and A. Bellanca, "Heavy metals in urban soils: a case study from the city of Palermo (Sicily), Italy", *Sci. Total Environ.*, **2002**, 300, 229-243.

8. H. Pekey, "The distribution and sources of heavy metals in Izmit Bay surface sediments affected by a polluted stream", *Mar. Pollut. Bull.*, **2006**, 52, 1197-1208.
9. C. P. Priju and A. C. Narayana, "Heavy and trace metals in Vembanad Lake sediments", *Int. J. Environ. Res.*, **2007**, 1, 280-289.
10. E. H. De Carlo and S. A. Anthony, "Spatial and temporal variability of trace element concentrations in an urban subtropical watershed, Honolulu, Hawaii", *Appl. Geochem.*, **2002**, 17, 475-492.
11. R. B. Owen and N. Sandhu, "Heavy metal accumulation and anthropogenic impacts on Tolo Harbour, Hong Kong", *Mar. Pollut. Bull.*, **2000**, 40, 174-180.
12. K. L. Spenser, "Spatial variability of metals in the inter-tidal sediments of the Medway Estuary, Kent, U.K", *Mar. Pollut. Bull.*, **2002**, 44, 933-944.
13. APHA, "Standard Methods for the Examination of Water and Wastewater." 20<sup>th</sup> Edn., American Public Health Association, Washington, DC, **1998**.
14. R. K. Trivedy and P. K. Goel, "Chemical and Biological Methods for Water Pollution Studies", Environmental Publications, Karad, India, **1984**, pp. 2-55.
15. W. Njenga, A. L. Ramanathan, and V. Subramanian, "Comparative studies of water chemistry of three tropical lakes in Kenya and India", Proceedings of the International Conference on Water and Environment (WE-2003), December 15-18, **2003**, Bhopal, India, pp. 51 – 61.
16. WHO, "Guidelines for Drinking Water Quality, Recommendations", World Health Organization, Geneva, **1984**, p. 130.
17. E. R. Daka, J. R. Allen, and S. J. Hawkins, "Heavy metal contamination in sediment biomonitors from sites around the Isle of Man", *Mar. Pollut. Bull.*, **2003**, 46, 784-794.
18. W. Halcrow, D. W. Mackay, and I. Thorton, "The distribution of trace metals and fauna in the firth of Clyde in relation to the disposal of sewage sludge", *J. Mar. Biol. Ass. U.K.*, **1973**, 53, 721-739.

19. J. C. Wasserman, F. B. L. Oliveira, and M. Bidarra, "Cu and Fe associated with humic acids in sediments of a tropical coastal lagoon, Organ", *Geochem.*, **1998**, 28, 813-822.
20. A. R. Karbassi, G. R. Nabi-Bidhendi, and I. Bayati, "Environmental geochemistry of heavy metals in a sediment core off Bushehr, Persian Gulf", *Iran J. Environ. Health. Sci. Eng.*, **2005**, 2, 255-260.

© 2007 by Maejo University, San Sai, Chiang Mai, 50290 Thailand. Reproduction is permitted for noncommercial purposes.

***Maejo International***  
***Journal of Science and Technology***

**ISSN 1905-7873**

Available online at [www.mijst.mju.ac.th](http://www.mijst.mju.ac.th)

*Full Paper*

## **Water quality of Wenchi Crater Lake in Ethiopia**

**Malairajan Singanan<sup>\*</sup>, Lakew Wondimu, and Mitiku Tesso**

Ecotoxicology Research Center, Ambo University College, P.O.Box.19, Ambo Town,  
Western Shoa, Ethiopia

\* Author to whom correspondence should be addressed, e-mail: [swethasivani@yahoo.co.in](mailto:swethasivani@yahoo.co.in),  
[msinganan@yahoo.com](mailto:msinganan@yahoo.com)

*Received: 5 February 2008 / Accepted: 4 June 2008 / Published: 13 June 2008*

---

**Abstract:** Determination of physico-chemical properties of water samples from Wenchi Crater Lake in Ethiopia was carried out. Selected heavy metals in water, sediment, and plant samples from the lake were also comparatively determined. The results indicated that most general physico-chemical properties of the lake water fell within those recommended for drinking water. However, the lake water was found to be high in some heavy metals, which also accumulated in the sediment. Bioconcentration of these metals was also observed in the plant samples.

**Key words:** Wenchi Crater Lake, water quality, heavy metals, sediment, *Typha latifolia*

---

## Introduction

Wenchi Crater Lake is one of the important lakes in Ethiopia. The lake is located in Western Shoa region, which extends between latitude  $15^{\circ}$  N -  $3^{\circ}$  S and longitudes  $48^{\circ}$  E -  $33^{\circ}$  W. It is situated at the major topographic feature in the country, being 130 km south-west of the capital city, Addis Ababa. It is surrounded by Kelela region in the north, Dera region in the east, Goro Wenchi region in the south and Haro Gebeya region in the west. This lake, 1,600 square metres in total area, is ecologically, recreationally, and aesthetically important as well as a popular place for tourists. The topographical location of the lake is presented in Figures 1 and 2.

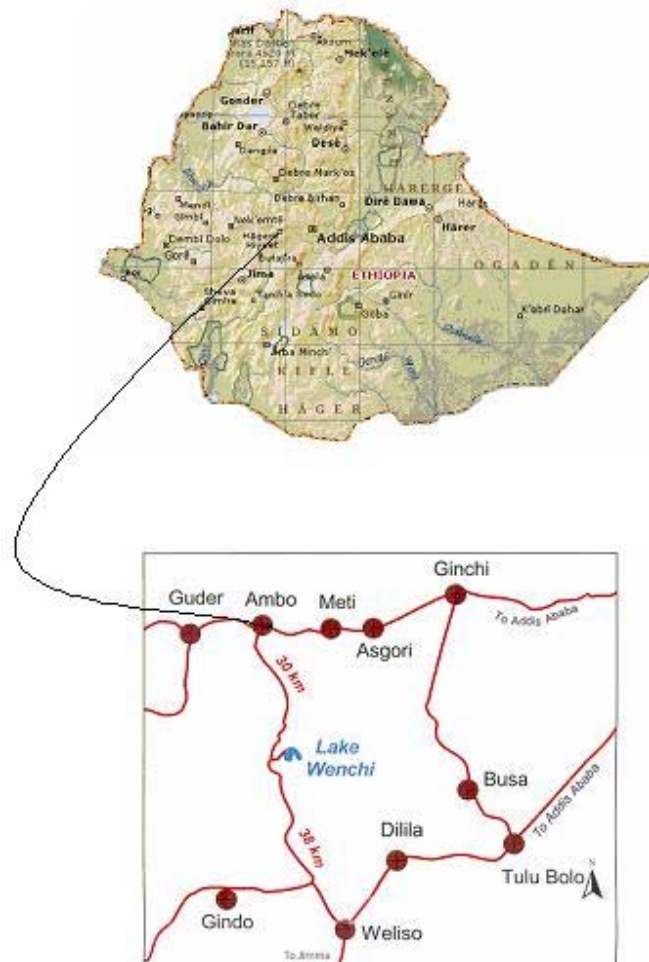


**Figure 1.** Location of Wenchi Crater lake in Ethiopia



Figure 2. Topography of Wenchi Crater Lake

The health of a lake is governed by the quantity of nutrients it receives from various streams. Nutrient recycling and proper productivity are necessary for sustenance and balance of the system. Due to nutrient enrichment, the system may lose its balance and may turn eutrophic. Thus, water quality studies are necessary to ascertain the suitability of water for various beneficial uses and to assess the trophic level of the lake.

In aquatic systems, the natural concentrations of metal ions are principally dependent on the ambient distribution, weathering and leaching of the elements from the soil in the catchment area, while heavy metals are carried to the lakes through atmospheric deposition and other man made activities. The characteristics of the water, such as acidity and the amount of organic matter, are known to be important factors in determining the fate of heavy metals in lakes [1-3].

The sediment of the aquatic environment acts as a major reservoir of metals [4] and also as a source of contaminants. Enrichment of heavy metals due to industrialisation and urbanisation was recorded in the sediment of coastal areas all over the world [5-9]. The monitoring of the heavy metal resulting from anthropogenic activities are particularly important for the assessment of environmental quality and protection. Heavy metal distribution in lagoonal and intertidal sediment has frequently been used to investigate chronological inputs [10-12].

Increased loading of heavy metals into lakes may have several ecological consequences. Elevated trace metal concentrations may lead, for example, to toxic effects or biomagnification in the aquatic environment. Accumulation of heavy metals in the food web can occur either by bioconcentration from the surrounding medium such as water or sediment, or by bioaccumulation from the food source.

In the following study, no attempts were made to investigate the environmental health of Wenchi Crater Lake. The main objective of this study, the first performed for this lake, is to monitor the water quality of the lake with reference to standard water quality parameters and heavy metals in its water and sediment, and in *Typha latifolia*, a major aquatic plant present in the lake.

## **Materials and Methods**

The water, sediment and *Typha latifolia* samples were collected bimonthly between January-December 2007 from eight sampling points (Figure 2) in the lake in cleaned polythene containers. The water quality parameters, viz. pH, electrical conductivity (EC), total dissolved solids (TDS), total hardness (TH), total alkalinity (ALK), common metal ions ( $\text{Ca}^{2+}$ ,  $\text{Mg}^{2+}$ ,  $\text{Na}^+$ , and  $\text{K}^+$ ), anions chloride ( $\text{Cl}^-$  and  $\text{SO}_4^{2-}$ ), and dissolved oxygen (DO) were analysed employing standard experimental protocols outlined in the literature [13-14]. In case of heavy metals, Cd, Cu, Ni, Cr, Pb, Mn, and Zn were selected and analysed as per the standard experimental protocols outlined in the literature [13] using a Shimadzu AA 6200 atomic absorption spectrophotometer. All the chemicals and reagents used in the experiments were of analytical grade. All the results were statically significant at  $p < 0.05$ .

## **Results and Discussion**

The results of the physico-chemical analysis of the water samples collected from all the sampling points were presented in Table 1.

### *pH and dissolved oxygen (DO)*

The pH of Wenchi Crater Lake water (7.4-7.6) fell within the desirable range (6.5-8.5) for drinking water as per the WHO guideline [16]. This result indicated that there were no human influences in the lake area and the responsible factor for the slightly alkaline value of the pH was only through the chemical composition of the bed rock sediment.

Dissolved oxygen is very essential for all living organisms in any water bodies. The recorded level of dissolved oxygen in the water of Wenchi Crater Lake ranged between 7.4- to 7.6 mg/L (WHO range: 4.5-7.5 mg/L). A similar result was also reported for Lake Naivasha, Kenya [15]. In the lake, the population of phytoplankton was relatively more than that of the zooplankton. The overgrowth of the plankton species and other aquatic plants might cause eutrophication in the lake in due course of time.

**Table 1.** Physico-chemical characteristics of the lake water

Water quality parameter	Sample collection point in the Crater Lake								WHO guideline value for drinking water [16]
	S1	S2	S3	S4	S5	S6	S7	S8	
	Mean value								
pH	7.5	7.6	7.6	7.4	7.5	7.5	7.6	7.6	6.5 – 8.5
EC ( $\mu\text{mhos/cm}$ )	1180	1182	1179	1180	1183	1182	1181	1183	1500
TDS (mg/L)	767	768.30	766.35	767	768.95	768.30	767.65	768.95	1000
TH (mg/L)	282	283	280	282	285	284	282	284	400
Ca (mg/L)	135	137	135	136	134	135	136	135	200
Mg (mg/L)	105	102	105	104	106	105	103	105	100
Na (mg/L)	48	52	50	49	48	50	48	47	200
K (mg/L)	26	28	27	28	26	28	29	27	20
Cl <sup>-</sup> (mg/L)	458	460	458	462	460	457	459	460	400
SO <sub>4</sub> <sup>2-</sup> (mg/L)	390	394	392	390	392	394	392	390	400
DO (mg/L)	7.4	7.6	7.5	7.5	7.6	7.5	7.6	7.5	4.5 – 7.5

**Note:** The analytical results were statistically significant at  $p < 0.05$ .

#### *Electrical conductivity (EC) and total dissolved solids (TDS)*

The conductivity of the water samples registered 1179-1183  $\mu\text{mhos/cm}$ . This is well below the WHO guideline value prescribed for drinking purpose (1500  $\mu\text{mhos/cm}$ ). The TDS present in the water affects its aesthetic value as well as its physico-chemical and biological properties. The TDS values found (766.35-768.95 mg/L) were also below the drinking water standard (1,000 mg/L).

#### *Total hardness (TH), calcium and magnesium*

The lake water samples recorded a low level of total hardness (280-285 mg/L). The total hardness has no known adverse effects on human health, and the recorded values were well below the guideline value for drinking purpose (400 mg/L).

Primarily, the calcium and magnesium present are responsible for the hardness of the water. The desirable limit for calcium in water is (75 mg/L) and the maximum permissible limit is (200 mg/L), and for magnesium these values are 30 and 100 mg/L

respectively. In the present investigation, we have observed that the values for calcium were 134-137 mg/L and those for magnesium, 102-106 mg/L.

#### *Sodium and potassium*

Sodium and potassium are the monovalent cations commonly present in water. These ions do not produce hardness to water. However, significantly high amounts of these ions in water create problem in its taste as well as make the water unsuitable for irrigation purpose. In the present study, the concentration of sodium (47-52 mg/L) was well below the listed value in Table 1, while that of potassium (26-29 mg/L) exceeded the allowed value (20 mg/L). This might be due to the presence of potash minerals in the area. A further geological investigation of the studied area is necessary.

#### *Chloride and sulphate*

The presence of chloride and sulphate in water in excess amounts is not desirable. Its origin is mainly from mineral weathering of bed rocks as well as from anthropogenic source. In the present investigation, the concentrations of chloride and sulphate ranged 457-462 mg/L and 390-394 mg/L respectively. The desirable limit of chloride is 250mg/L and the maximum permissible limit is 400 mg/L and for sulphate, it is 200 and 400 mg/L respectively. The concentration of chloride was thus somewhat higher than the permissible limit for drinking purpose.

#### *Heavy metals in water*

The concentrations of Cd, Cu, Ni, Cr, Pb, Mn, and Zn were determined in water samples from eight sampling points in the lake. The analytical results are presented in Figure 3. The drinking water standards (WHO guidelines) for the trace inorganic contaminants such as Cd, Cu, Ni, Cr, Pb, Mn and Zn are 0.003, 2.0, 0.02, 0.05, 0.01, 0.5 and 5.0 mg/L respectively [16]. The results indicate that only the levels of Cu, Mn and Zn in the lake water were well within the allowable concentrations. The concentrations of all other metals were significantly increased in the lake water.

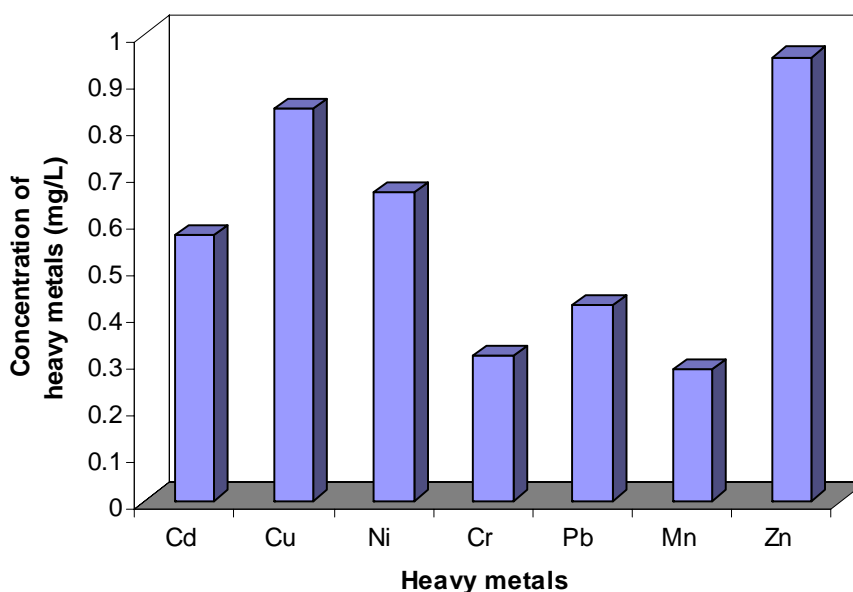


**Figure 3.** Levels of heavy metals in the lake water

#### *Heavy metals in sediment*

Sediment samples were collected in the same eight locations in the lake and were analysed for the concentration of Cd, Cu, Ni, Cr, Pb, Mn and Zn. Two sediment samples were fine-grained and others were coarse-grained. The sediment samples registered significantly higher amounts of heavy metals than the water samples (Figure 4).

#### *Heavy metals in plant samples (Typha latifolia)*

*Typha latifolia* was the major aquatic plants in the lake. Their roots were collected near the water sampling points and analysed for heavy metal concentrations, the average values of which are presented in Figure 5. The result shows that the plants accumulated significantly higher amounts of heavy metals compared to the sediment. Since heavy metals present in water and sediment are slowly absorbed by the aquatic plants and thereby concentrated in the root metabolism, the plants can be used as a bioindicator of heavy metal pollution in the lake.

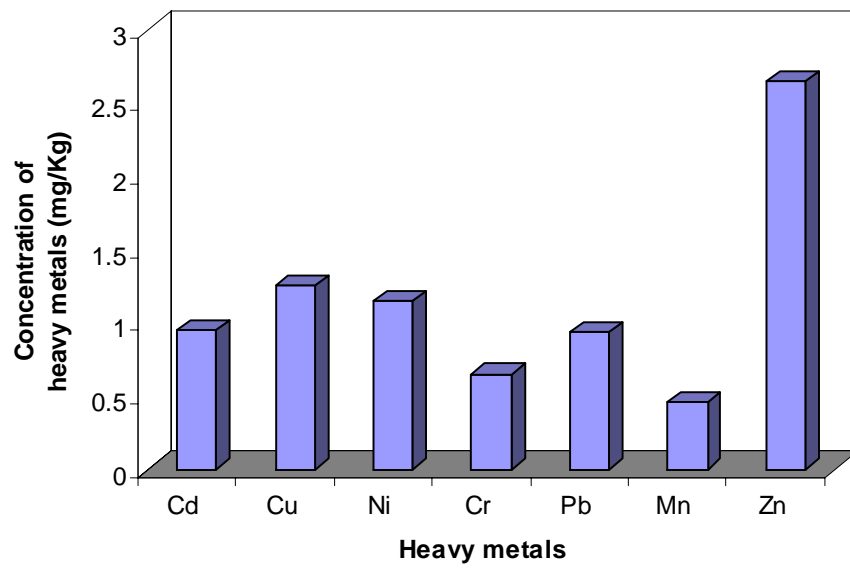


Figure 4. Levels of heavy metals in lake sediment

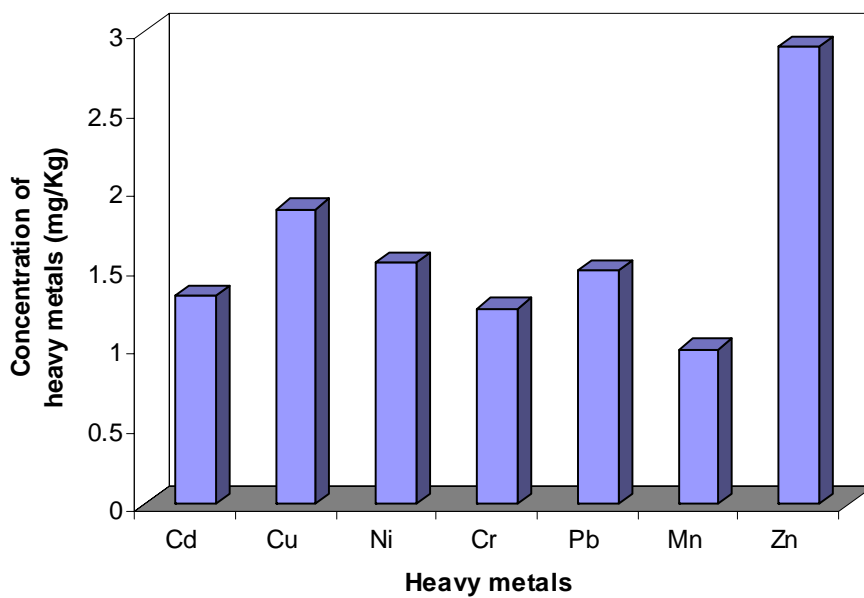


Figure 5. Levels of heavy metals in roots of *Typha latifolia*

Notably the three sampled items show distinct variation in metal contents. The concentration gradients (plant root > sediment > water) exist for all the heavy metals in the lake and it might be possible that the sedimental particles were transported towards the lower reach of the lake. Parallel gradients of organic matter contents and grain size distribution of the sediment are also likely to influence the heavy metal concentration in the lake [17-18]. The fine-grained sediment is reported to have a greater influence on the adsorption of heavy metals from the water [19].

It is also observed in many estuaries across the world that the concentration of heavy metals from known anthropogenic input generally increases [10,20]. In Wenchi Crater Lake area there are three inlets and two outlets. However, the outlet points are present only in the upper part of the lake and the volume of water discharge is comparatively small while the bulk of the lake water is lost through evaporation and absorption. Therefore the lake area becomes a large sink for heavy metals. The concentration factor is the main cause of sediment toxicity while this factor through bioaccumulation by plants (*Typha latifolia* in this case) is apparently more pronounced. Land erosion and natural weathering of bedrocks of the lake are probably the main factors responsible for the accumulation of heavy metals in the lake ecosystem.

### **Conclusions**

Most physico-physical properties of Wenchi Crater Lake conformed to the standards set out by WHO for drinking water, except for the level of magnesium, chloride, and sulphate ions, which just overstepped the borderlines. As for heavy metals, it was observed that only Cu, Mn, and Zn were well within the allowable concentrations while Cd, Ni, Cr, and Pb were significantly higher than the set limits allowable for potable water. Moreover, the lake sediment was found to be enriched with these heavy metals compared to the lake water. However, heavy metal enrichment through bioconcentration by plants in the lake was even more conspicuous.

The presence of increased amounts of heavy metals may have a direct impact on the health of humans as well as aquatic animals. Visibly the water looks very clean with no

contamination. The volume of water in the lake is very high and can potentially be used for various purposes by employing artificial recharging technologies and special purification methods. However, there is a dense population of macrophytes in the lake. Further research work is necessary to study them and their impact on the water quality of the lake.

### **Acknowledgement**

The authors wish to acknowledge the research and publication coordination office of the Ambo University College, Ambo Town, Ethiopia for the financial support.

### **References**

1. J. Mannio, M. Verta, and O. Jarvinen, "The trace metal concentrations in the water of small lakes, Finland", *Appl. Geochem. Suppl.*, **1993**, 2, 57-59.
2. B. L. Skjelkvale, T. Andersen, E. Fjeld, J. Mannio, A. Wilander, K. Johansson, J. P. Jensen, and T. Moiseeko, "Heavy metal survey in Nordic lakes: concentrations, geographic patterns and relation to critical limits", *Ambio*, **2001**, 30, 2-10.
3. T. Tulonen, M. Pihlstrom, L. Arvola, and M. Rask, "Concentration of heavy metals in food web components of small boreal lake", *Boreal Environ. Res.*, **2006**, 11, 185-194.
4. V. G. Caccia, F. J. Millero, and A. Palanques, "The distribution of trace metals in Florida Bay sediments", *Mar. Pollut. Bull.*, **2003**, 46, 1420-1433.
5. H. Feng, X. Han, W. Zhang, and L. Yu, "A Preliminary study of heavy metal concentration in Yangtze River intertidal zone due to urbanization", *Mar. Pollut. Bull.*, **2004**, 49, 910-915.
6. J. L. Gallasso, F. R. Siegel, and J. H. Kravitz, "Heavy metals in eight 1965 cores from the Novaya Zemlya Trough, Kara Sea, Russian Arctic", *Mar. Pollut. Bull.*, **2000**, 40, 839-852.
7. D. S. Manta, M. Angelone, and A. Bellanca, "Heavy metals in urban soils: a case study from the city of Palermo (Sicily), Italy", *Sci. Total Environ.*, **2002**, 300, 229-243.

8. H. Pekey, "The distribution and sources of heavy metals in Izmit Bay surface sediments affected by a polluted stream", *Mar. Pollut. Bull.*, **2006**, 52, 1197-1208.
9. C. P. Priju and A. C. Narayana, "Heavy and trace metals in Vembanad Lake sediments", *Int. J. Environ. Res.*, **2007**, 1, 280-289.
10. E. H. De Carlo and S. A. Anthony, "Spatial and temporal variability of trace element concentrations in an urban subtropical watershed, Honolulu, Hawaii", *Appl. Geochem.*, **2002**, 17, 475-492.
11. R. B. Owen and N. Sandhu, "Heavy metal accumulation and anthropogenic impacts on Tolo Harbour, Hong Kong", *Mar. Pollut. Bull.*, **2000**, 40, 174-180.
12. K. L. Spenser, "Spatial variability of metals in the inter-tidal sediments of the Medway Estuary, Kent, U.K", *Mar. Pollut. Bull.*, **2002**, 44, 933-944.
13. APHA, "Standard Methods for the Examination of Water and Wastewater." 20<sup>th</sup> Edn., American Public Health Association, Washington, DC, **1998**.
14. R. K. Trivedy and P. K. Goel, "Chemical and Biological Methods for Water Pollution Studies", Environmental Publications, Karad, India, **1984**, pp. 2-55.
15. W. Njenga, A. L. Ramanathan, and V. Subramanian, "Comparative studies of water chemistry of three tropical lakes in Kenya and India", Proceedings of the International Conference on Water and Environment (WE-2003), December 15-18, **2003**, Bhopal, India, pp. 51 – 61.
16. WHO, "Guidelines for Drinking Water Quality, Recommendations", World Health Organization, Geneva, **1984**, p. 130.
17. E. R. Daka, J. R. Allen, and S. J. Hawkins, "Heavy metal contamination in sediment biomonitors from sites around the Isle of Man", *Mar. Pollut. Bull.*, **2003**, 46, 784-794.
18. W. Halcrow, D. W. Mackay, and I. Thorton, "The distribution of trace metals and fauna in the firth of Clyde in relation to the disposal of sewage sludge", *J. Mar. Biol. Ass. U.K.*, **1973**, 53, 721-739.

19. J. C. Wasserman, F. B. L. Oliveira, and M. Bidarra, "Cu and Fe associated with humic acids in sediments of a tropical coastal lagoon, Organ", *Geochem.*, **1998**, 28, 813-822.
20. A. R. Karbassi, G. R. Nabi-Bidhendi, and I. Bayati, "Environmental geochemistry of heavy metals in a sediment core off Bushehr, Persian Gulf", *Iran J. Environ. Health. Sci. Eng.*, **2005**, 2, 255-260.

© 2007 by Maejo University, San Sai, Chiang Mai, 50290 Thailand. Reproduction is permitted for noncommercial purposes.

Full Paper

## **Design and fabrication of a micro-volume autotitrator with potentiometric end-point detection for the determination of acidity of some fruit juices**

Prinya Masawat <sup>1,\*</sup>, Saisunee Liawruangrath <sup>2</sup>, and Suphachock Upalee <sup>2</sup>

<sup>1</sup> Department of Chemistry, Faculty of Science, Naresuan University 65000, Thailand

<sup>2</sup> Department of Chemistry, Faculty of Science, Chiang Mai University 50200, Thailand

\* Corresponding author, e-mail : [prinyam@nu.ac.th](mailto:prinyam@nu.ac.th)

Received: 4 January 2008 / Accepted: 6 June 2008 / Published: 13 June 2008

---

**Abstract:** A miniaturised micro-volume autotitrator with potentiometric end-point detection was designed and fabricated for the determination of acidity of some Thai fruit juices. The method was based on on-line potentiometric titration of the organic acids with sodium hydroxide. The conditions such as volume of fruit juice sample, volume and concentration of potassium chloride used as supporting electrolyte, and flow rate of the titrant were optimised by using univariate optimisation. A sample throughput of 83 samples/hr at the titrant flow rate of 0.28 mL/min was achieved with satisfactory results. The results obtained by the proposed method agreed with those obtained by the classical titration method.

**Keywords:** micro-volume autotitrator, potentiometric end-point detection, acidity, fruit juice

---

### **Introduction**

Acidity serves numerous purposes in modern food processing in addition to its major role of rendering foods more palatable and stimulating. Various functions of acidity include flavouring agent, buffer, preservative, synergist, viscosity modifier, melting modifier and meat curing agent [1]. The acidity of a fruit juice is due to the presence of several organic acids such as citric, malic, fumaric, acetic, ascorbic, and galacturonic acids. Measuring organic acid levels in foods and beverages is important from the standpoint of monitoring of fermentation process, checking of product stability,

validating of authenticity of juices and concentrates, and studying of the organoleptic properties of fermented products such as wines [2]. The most common acid in soft drinks and citrus and other fruit juices is citric acid, which can be obtained either in anhydrous or monohydrate form [3]. Citric acid (2-hydroxy-1,2,3-propanetricarboxylic acid), unlike other hydroxy acids, is tribasic with a major advantage of high solubility in water. Several fresh fruits such as lemon and lime owe their tangy taste to the presence of citrate ions [1].

Acidity can be determined by a large number of methods such as ion chromatography [4], gas chromatography [5], high performance liquid chromatography [6], capillary electrophoresis [7], and flow injection analysis [8]. Although some methods can selectively determine different acids, the acidity is usually reported in terms of the citric acid content. Titration is used as the classical method for the determination of citric acid in fruit juices [9-10]. The disadvantage of titration is that it is time and reagent consuming. Potentiometry is also alternatively used to determine the total acid content in fruit juices in comparison with classical titration [11]. In this present work, we have designed and fabricated a micro-volume autotitrator with potentiometric end-point detection for the determination of acidity of the juices of eight Thai fruits collected in the northern area of Thailand. The method is based on an on-line potentiometric titration. Variables affecting the proposed method, viz. volume of fruit juice sample, volume and concentration of potassium chloride used as supporting electrolyte, and flow rate of titrant were evaluated and optimised.

## Materials and Methods

### *Materials*

Sodium hydroxide, potassium hydrogen phthalate (KHP), phenolphthalein, and potassium chloride were obtained from Merck (Germany). All chemicals were of analytical reagent grade.

Eight fruit samples, viz. lime, pomelo, tangerine, red and green grape, red and green apple, and pineapple were collected from the northern area of Thailand by random sampling.

### *Micro-volume autotitrator*

The schematic diagram of the designed autotitration system is shown in Figure 1. A peristaltic propeller was used as a device to aspirate accurately and continuously the amount of titrant in the range of 0.02 to 0.24 mL/min (depending on the tube resolution and rotor speed). The peristaltic pump was controlled by an AT89C4051 microcontroller which generated a pulse-width modulator (PWM) signal to drive the pump motor, which could be commanded by a software via a RS232 port. An aspiration volume calibration of the pump was carried out by water-weighting method.

A combined glass electrode (Horiba, USA) was used as a proton sensor. It was connected to an analog-to-digital converter device namely "UT60D" multimeter (Uni-Trend International Limited). The output of ASCII mV reading was sent to the PC via RS232C port with the baud rate of 2,400 bps no parity 7 data bit and 2 stop bits. A PC recorded the change and directly plotted the graph which could be saved for further calculation or exported in many formats.

A Microsoft Visual Basic 6.0 was used as a developed tool to control the peristaltic pump and receive the signal from the UT60D multimeter. It employed Microsoft Communication Control 6.0 ActiveX to communicate with the control board in ASCII mode.

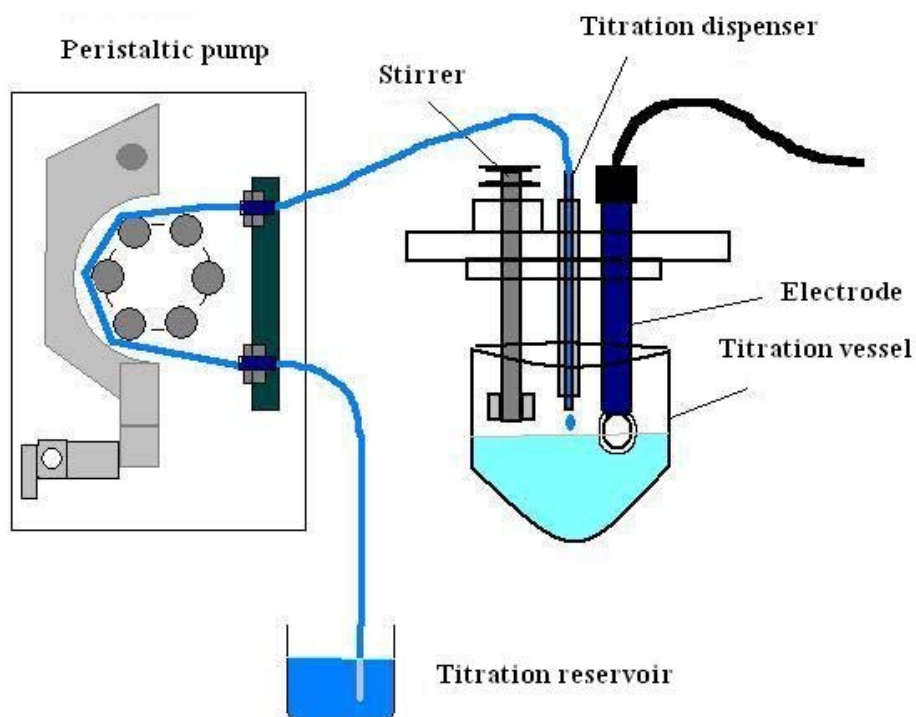


**Figure 1.** Schematic diagram of the designed autotitration system

### *Sample preparation*

Eight kinds of fresh fruits, viz. lime, pomelo, tangerine, red grape, green apple, green grape, pineapple, and red apple were separately squeezed with a juice extractor (Comfort HR I82I, Philips, Netherland). A 1.0 mL aliquot of each fresh juice was put in a 25 mL beaker containing 5.0 mL of 10 mM KCl as supporting electrolyte and 15.0 mL of deionised water. A micro-volume autotitrator as shown in Figure 1 was operated by propelling 0.1 M NaOH at the flow rate of 0.28 mL/min. A titration curve and the first derivative curve could be recorded as shown in Figure 2 for each titration batch.

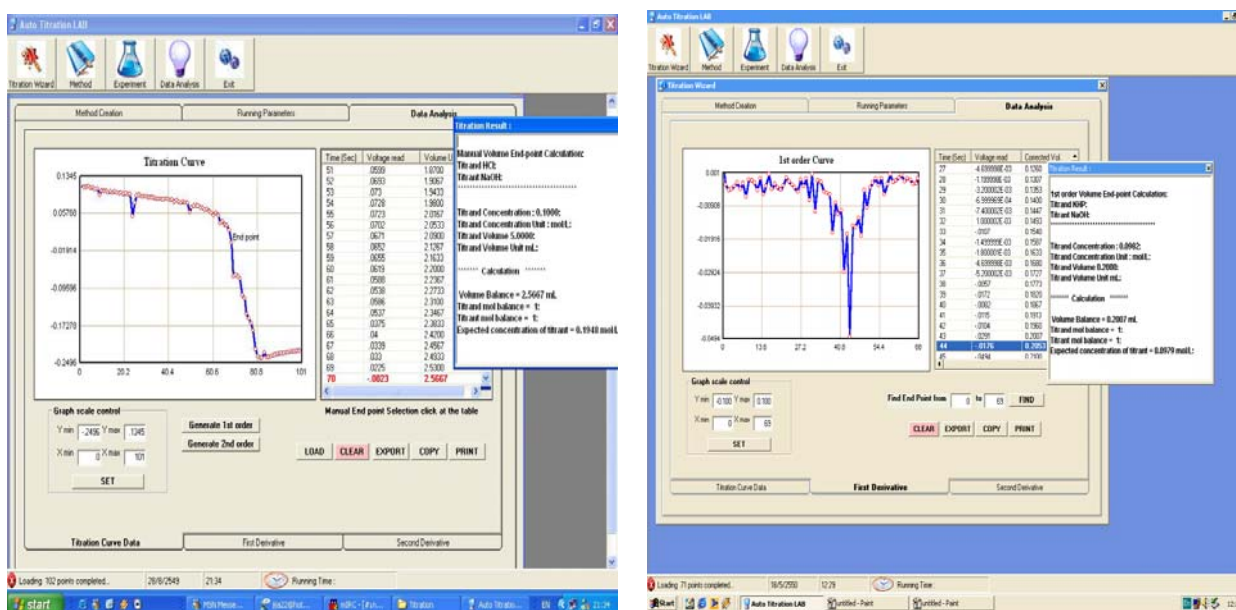


**Figure 2.** Titration curve and first derivative curve obtained from the designed autotitration

## Results and Discussion

### Optimisation for the determination of citric acid

In this experiment, the volume of KHP used as titrand, the volume and concentration of KCl used as supporting electrolyte, and the flow rate of titrant (NaOH) were optimised using the designed autotitration system as shown in Figure 1. The method for optimisation is the univariation, in which one parameter is varied while the others are kept constant. After optimisation of each parameter, the new optimised value is used for the optimisation of the next parameter. In the following optimisation, the reasonable %RSD and % Error were used for selecting the optimal value of each parameter. %RSD was calculated from 11 replicates ( $n = 11$ ) and %Error from comparing the result from the proposed technique with that from the standard classical acid-base titration method.

### Effect of KHP volume

The experiment was carried out by using 0.1000 M KHP (titrand) to titrate with 0.1000 M NaOH (titrant). Various volumes of KHP (50, 100, 150 and 200  $\mu$ L) were pipetted into a 25 mL beaker containing 15.0 mL of deionised water and 5.0 mL of 10 mM KCl (supporting electrolyte). Then the flow of titrant was generated at 0.20 mL/min. Titration curves and first derivative curves were obtained and the results were mathematically compared with those obtained with the classical acid-base titration. The influence of KHP volume on the percentage of relative standard deviation (%RSD) and error (%Error) is exhibited in Figure 3. The KHP volume of 200  $\mu$ L showed lowest %RSD and %Error, therefore it was chosen for the next experiment. (Although a little lower %RSD and %Error might be obtained when KHP volume was increased to more than 200  $\mu$ L, it was not used on the reason of waste reduction.)

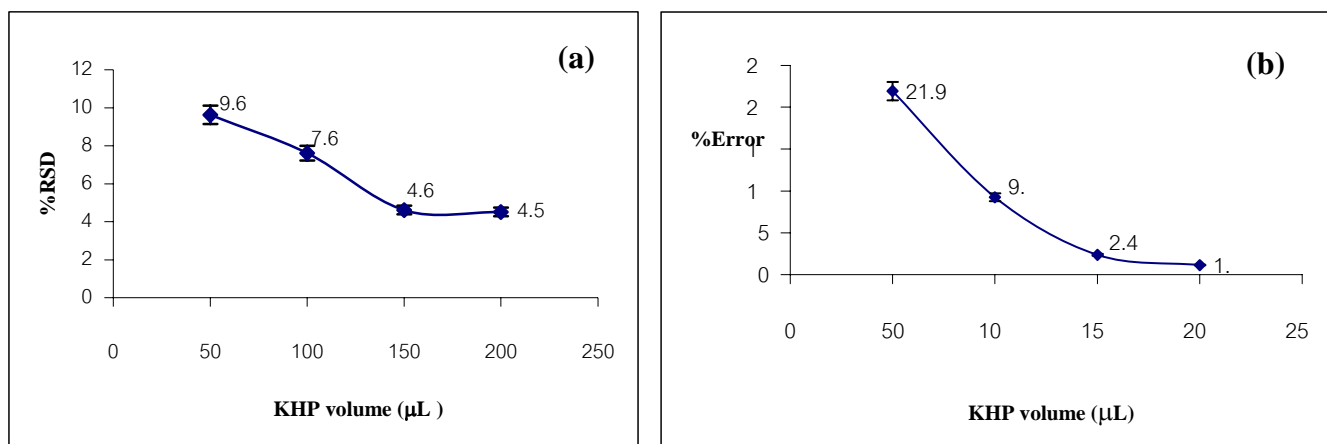


**Figure 3.** Influence of KHP volume on %RSD (a) and %Error (b) in acidity determination by the designed micro-volume autotitrator

#### *Effect of KCl volume*

Supporting electrolytes are required in controlled-potential experiments to decrease the resistance of the solution, to eliminate electromigration effects, and to maintain a constant ionic strength (i.e. to “swamping out” the effect of variable amounts of naturally occurring electrolytes) [12]. The inert supporting electrolyte may be an inorganic salt, a mineral acid, or a buffer. Potassium chloride or nitrate, ammonium chloride, sodium hydroxide, or hydrochloric acid are widely used as electrolyte in aqueous solution. The usual electrolyte concentration range is 0.1-1.0 M, i.e. in large excess of the concentration of all electroactive species.

A similar experiment to that for studying the effect of KHP volume was carried out but the volume of KHP and the flow rate of titrant were fixed at 200 μL and 0.20 mL/min respectively. Various volumes of 10 mM KCl used as supporting electrolyte (5, 10, 15 and 20 mL) were each pipetted into a 25 mL beaker containing 200 μL of KHP and 15.0 mL of deionised water. The results are shown in Figure 4. It was observed that at 5 mL of 10 mM KCl the results from 11 replicates showed no difference in each value of the results so %RSD was calculated to be zero. Comparing the results with those obtained from the standard acid-base titration, the %Error at 5 mL of 10 mM KCl was lowest. Therefore, it was selected for the next experiment.

#### *Effect of KCl concentration*

The experiment was carried out by varying KCl concentration between 0.1-10 mM at fixed KHP volume (200 μL), flow rate (0.20 mL/min), and KCl volume (5 mL). From Figure 5, it is found that 10 mM KCl gave lowest %RSD and %Error. Therefore, it was chosen for the next experiment.

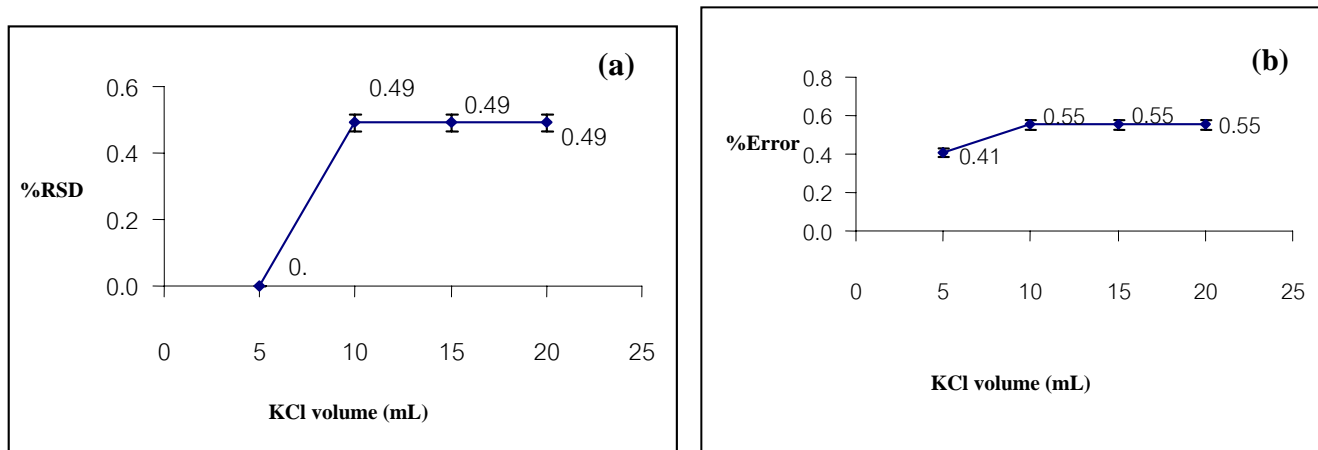


**Figure 4.** Influence of KCl volume on %RSD (a) and %Error (b) in acidity determination by the designed micro-volume autotitrator

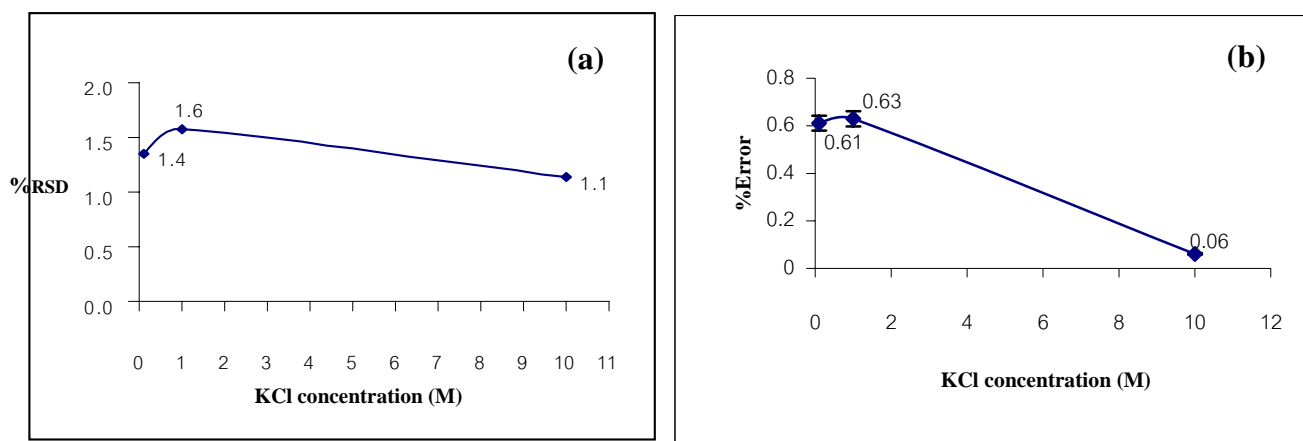


**Figure 5.** Influence of KCl concentration on %RSD (a) and %Error (b) in acidity determination by the designed micro-volume autotitrator

#### Effect of flow rate

By fixing the volumes of KHP and KCl at 200  $\mu$ L and 5 mL respectively, and the concentration of KCl at 10 mM, the flow rate of NaOH used as titrant was varied between 0.16-0.40 mL/min. From Figure 6, although the flow rate at 0.24 mL/min gave the lowest %RSD, it provided higher %Error than that at 0.28 mL/min. Moreover, the sample throughput was increased from 72 samples/hr to 83 samples/hr when the flow rate was changed from 0.24 to 0.28 mL/min. Therefore, the flow rate of 0.28 mL/min was chosen. The summary of the optimum conditions is shown in Table 1.

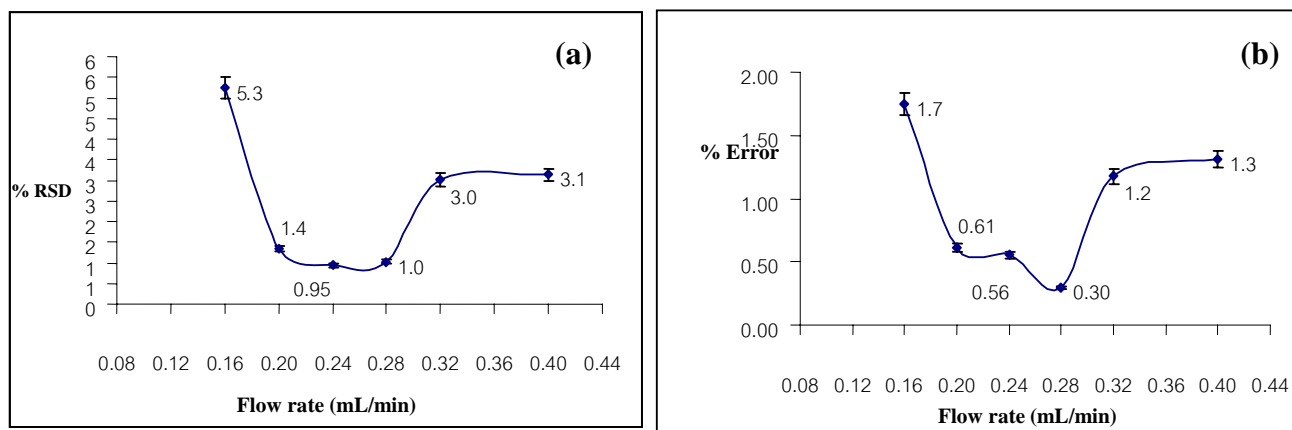


**Figure 6.** Influence of flow rate of NaOH (titrant) on %RSD (a) and %Error (b) in acidity determination by the designed micro-volume autotitrator

**Table 1.** Optimum values of variables for the on-line potentiometric titration using micro-volume autotitrator

Variable	Range studied	Optimum value
KHP volume ( $\mu\text{L}$ )	50-200	200
KCl volume (mL)	5-20	5
KCl concentration (mM)	0.1-10	10
Flow rate (mL/min)	0.16-0.40	0.28

#### *Application to real samples*

Though organic acids in Thai fruits are varied, a common component seems to be citric acid (which has three active protons). The organic acid content (calculated as citric acid) in the fruit juice from each kind of fruits determined by classical titration and on-line potentiometric titration is shown in Table 2. A paired t-test was used to compare the results obtained by both techniques. They were in excellent agreement at 95% confidential limit.

**Table 2.** Organic acid (calculated as citric acid) content in various Thai fruit juices

Fruit	Organic acid content obtained by classical titration (n=11) * ( $\times 10^{-3}$ M) (%RSD)	Organic acid content obtained by on-line potentiometric titration (n=11) * ( $\times 10^{-3}$ M) (%RSD)
Lime	5.26 (0.23)	5.42 (2.98)
Pomelo	3.76 (0.33)	3.77 (6.72)
Tangerine	3.24 (0.37)	3.29 (15.4)
Red grape	3.00 (0.40)	3.04 (7.33)
Green apple	2.89 (0.38)	2.88 (10.2)
Green grape	2.73 (1.05)	2.72 (6.92)
Pineapple	1.76 (0.63)	1.77 (9.30)
Red apple	1.49 (1.49)	1.51 (3.80)

\* 11 replicates

## Conclusions

Determination of organic acid content in fruit juices by the micro-volume autotitrator fabricated in our laboratory is fast and convenient with the sample throughput of 83 samples/hr at the titrant flow rate of 0.28 mL/min. It can be used in routine analysis of acid content. The titrant and titrand used are in the level of a few mL, much less than those used in the classical titration technique, thus contributing to the green and home-made technology.

## Acknowledgements

We gratefully acknowledge the Faculty of Science of Naresuan University for funding this research. Some of the devices and application softwares were developed in cooperation with Alpha Flow Research Group at Chiang Mai University.

## References

1. T. E. Furia, "CRC Handbook of Food Additives.", 2<sup>nd</sup> Edn., CRC Press, Boca Raton, **1983**, pp.225, 242.
2. S. M. Herschdoerfer, "Quality Control in the Food Industry.", 2<sup>nd</sup> Edn., Academic Press, London, **1987**, p.94.
3. FAO, "Compendium of Food Additive Specifications Addendum 5.", Food and Agriculture Organization of the United Nations, Rome, **1997**.
4. P. Masson, "Influence of organic solvents in the mobile phase on the determination of carboxylic acids and inorganic anions in grape juice by ion chromatography", *J. Chromatogr. A*, **2000**, 881, 387-394.

5. T. J. Barden, M. Y. Croft, E. J. Murby, and K. J. Wells, "Gas chromatographic determination of organic acids from fruit juices by combined resin mediated methylation and extraction in supercritical carbon dioxide", *J. Chromatogr. A*, **1997**, 785, 251-261.
6. E. Verette, F. Qian, and F. Mangani, "On-line dialysis with high-performance liquid chromatography for the automated preparation and analysis of sugars and organic acids in foods and beverages", *J. Chromatogr. A*, **1995**, 705, 195-203.
7. C. H. Wu, Y. S. Lo, Y. H. Lee, and T. I. Lin, "Capillary electrophoretic determination of organic acids with indirect detection", *J. Chromatogr. A*, **1995**, 716, 291-301.
8. K. Grudpan, P. Sritharathikhun, and J. Jakmunee, "Flow injection conductimetric or spectrophotometric analysis for acidity in fruit juice", *Anal. Chim. Acta*, **1998**, 363, 199-202.
9. P. Cunniff, "AOAC Official Methods of Analysis.", 16<sup>th</sup> Edn., AOAC, Arlington, **1995**.
10. I. M. Kolthoff and V.A. Stenger, "Volumetric Analysis II: Titration Method", 2<sup>nd</sup> Edn., Interscience Publisher, New York, **1947**, p. 129.
11. D. A. Skoog, D. M. West, F. J. Holler, and S. R. Crouch, "Fundamentals of Analytical Chemistry", 8<sup>th</sup> Edn., Thomson Learning, Inc., Canada, **2004**, pp. 623-625.
12. J. Wang, "Analytical Electrochemistry", VCH Publisher, New York, **1994**, pp. 71-72.

© 2007 by Maejo University, San Sai, Chiang Mai, 50290 Thailand. Reproduction is permitted for noncommercial purposes.

*Full Paper*

## **Design and fabrication of a micro-volume autotitrator with potentiometric end-point detection for the determination of acidity of some fruit juices**

**Prinya Masawat<sup>1,\*</sup>, Saisunee Liawruangrath<sup>2</sup>, and Suphachock Upalee<sup>2</sup>**

<sup>1</sup> Department of Chemistry, Faculty of Science, Naresuan University 65000, Thailand

<sup>2</sup> Department of Chemistry, Faculty of Science, Chiang Mai University 50200, Thailand

\* Corresponding author, e-mail : [prinyam@nu.ac.th](mailto:prinyam@nu.ac.th)

*Received: 4 January 2008 / Accepted: 6 June 2008 / Published: 13 June 2008*

---

**Abstract:** A miniaturised micro-volume autotitrator with potentiometric end-point detection was designed and fabricated for the determination of acidity of some Thai fruit juices. The method was based on on-line potentiometric titration of the organic acids with sodium hydroxide. The conditions such as volume of fruit juice sample, volume and concentration of potassium chloride used as supporting electrolyte, and flow rate of the titrant were optimised by using univariate optimisation. A sample throughput of 83 samples/hr at the titrant flow rate of 0.28 mL/min was achieved with satisfactory results. The results obtained by the proposed method agreed with those obtained by the classical titration method.

**Keywords:** micro-volume autotitrator, potentiometric end-point detection, acidity, fruit juice

---

### **Introduction**

Acidity serves numerous purposes in modern food processing in addition to its major role of rendering foods more palatable and stimulating. Various functions of acidity include flavouring agent, buffer, preservative, synergist, viscosity modifier, melting modifier and meat curing agent [1]. The acidity of a fruit juice is due to the presence of several organic acids such as citric, malic, fumaric, acetic, ascorbic, and galacturonic acids. Measuring organic acid levels in foods and beverages is important from the standpoint of monitoring of fermentation process, checking of product stability,

validating of authenticity of juices and concentrates, and studying of the organoleptic properties of fermented products such as wines [2]. The most common acid in soft drinks and citrus and other fruit juices is citric acid, which can be obtained either in anhydrous or monohydrate form [3]. Citric acid (2-hydroxy-1,2,3-propanetricarboxylic acid), unlike other hydroxy acids, is tribasic with a major advantage of high solubility in water. Several fresh fruits such as lemon and lime owe their tangy taste to the presence of citrate ions [1].

Acidity can be determined by a large number of methods such as ion chromatography [4], gas chromatography [5], high performance liquid chromatography [6], capillary electrophoresis [7], and flow injection analysis [8]. Although some methods can selectively determine different acids, the acidity is usually reported in terms of the citric acid content. Titration is used as the classical method for the determination of citric acid in fruit juices [9-10]. The disadvantage of titration is that it is time and reagent consuming. Potentiometry is also alternatively used to determine the total acid content in fruit juices in comparison with classical titration [11]. In this present work, we have designed and fabricated a micro-volume autotitrator with potentiometric end-point detection for the determination of acidity of the juices of eight Thai fruits collected in the northern area of Thailand. The method is based on an on-line potentiometric titration. Variables affecting the proposed method, viz. volume of fruit juice sample, volume and concentration of potassium chloride used as supporting electrolyte, and flow rate of titrant were evaluated and optimised.

## **Materials and Methods**

### *Materials*

Sodium hydroxide, potassium hydrogen phthalate (KHP), phenolphthalein, and potassium chloride were obtained from Merck (Germany). All chemicals were of analytical reagent grade.

Eight fruit samples, viz. lime, pomelo, tangerine, red and green grape, red and green apple, and pineapple were collected from the northern area of Thailand by random sampling.

### *Micro-volume autotitrator*

The schematic diagram of the designed autotitration system is shown in Figure 1. A peristaltic propeller was used as a device to aspirate accurately and continuously the amount of titrant in the range of 0.02 to 0.24 mL/min (depending on the tube resolution and rotor speed). The peristaltic pump was controlled by an AT89C4051 microcontroller which generated a pulse-width modulator (PWM) signal to drive the pump motor, which could be commanded by a software via a RS232 port. An aspiration volume calibration of the pump was carried out by water-weighting method.

A combined glass electrode (Horiba, USA) was used as a proton sensor. It was connected to an analog-to-digital converter device namely "UT60D" multimeter (Uni-Trend International Limited). The output of ASCII mV reading was sent to the PC via RS232C port with the baud rate of 2,400 bps no parity 7 data bit and 2 stop bits. A PC recorded the change and directly plotted the graph which could be saved for further calculation or exported in many formats.

A Microsoft Visual Basic 6.0 was used as a developed tool to control the peristaltic pump and receive the signal from the UT60D multimeter. It employed Microsoft Communication Control 6.0 ActiveX to communicate with the control board in ASCII mode.

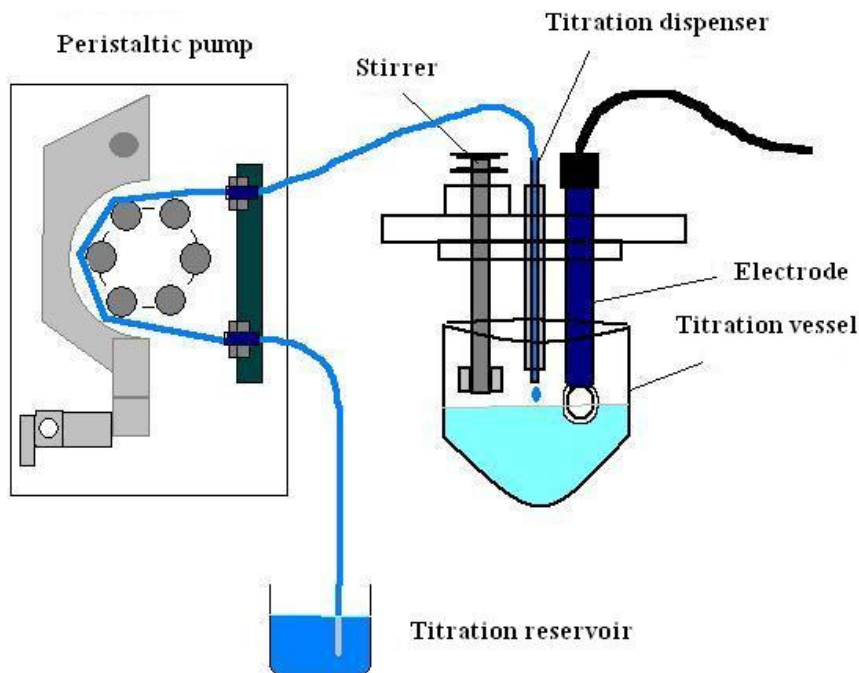


**Figure 1.** Schematic diagram of the designed autotitration system

### *Sample preparation*

Eight kinds of fresh fruits, viz. lime, pomelo, tangerine, red grape, green apple, green grape, pineapple, and red apple were separately squeezed with a juice extractor (Comfort HR 182I, Philips, Netherland). A 1.0 mL aliquot of each fresh juice was put in a 25 mL beaker containing 5.0 mL of 10 mM KCl as supporting electrolyte and 15.0 mL of deionised water. A micro-volume autotitrator as shown in Figure 1 was operated by propelling 0.1 M NaOH at the flow rate of 0.28 mL/min. A titration curve and the first derivative curve could be recorded as shown in Figure 2 for each titration batch.

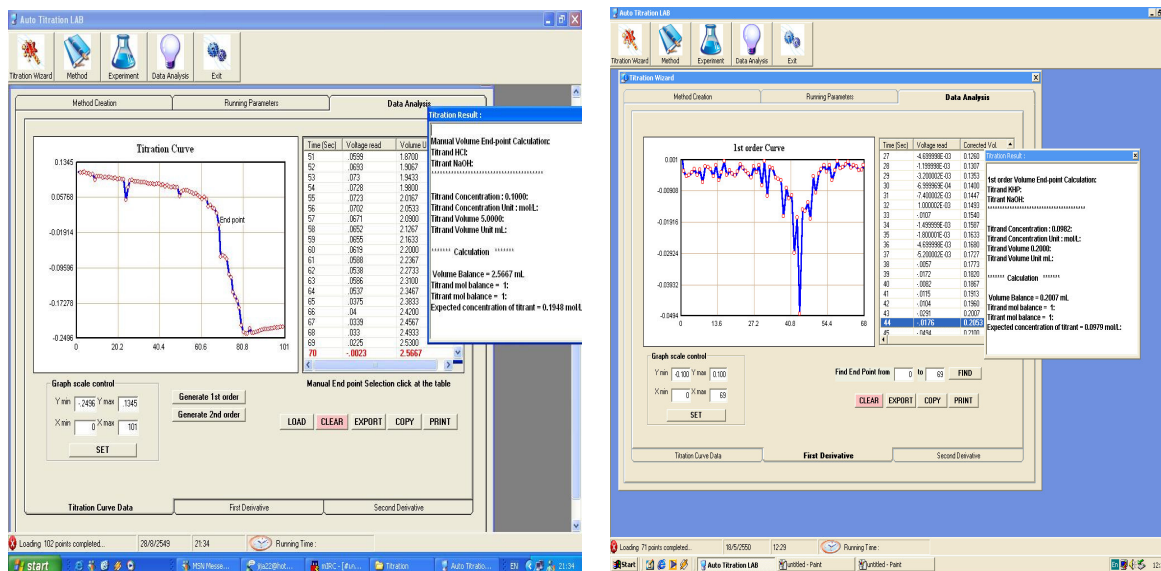


Figure 2. Titration curve and first derivative curve obtained from the designed autotitration

## Results and Discussion

### Optimisation for the determination of citric acid

In this experiment, the volume of KHP used as titrand, the volume and concentration of KCl used as supporting electrolyte, and the flow rate of titrant (NaOH) were optimised using the designed autotitration system as shown in Figure 1. The method for optimisation is the univariation, in which one parameter is varied while the others are kept constant. After optimisation of each parameter, the new optimised value is used for the optimisation of the next parameter. In the following optimisation, the reasonable %RSD and % Error were used for selecting the optimal value of each parameter. %RSD was calculated from 11 replicates ( $n = 11$ ) and %Error from comparing the result from the proposed technique with that from the standard classical acid-base titration method.

### Effect of KHP volume

The experiment was carried out by using 0.1000 M KHP (titrand) to titrate with 0.1000 M NaOH (titrant). Various volumes of KHP (50, 100, 150 and 200  $\mu\text{L}$ ) were pipetted into a 25 mL beaker containing 15.0 mL of deionised water and 5.0 mL of 10 mM KCl (supporting electrolyte). Then the flow of titrant was generated at 0.20 mL/min. Titration curves and first derivative curves were obtained and the results were mathematically compared with those obtained with the classical acid-base titration. The influence of KHP volume on the percentage of relative standard deviation (%RSD) and error (%Error) is exhibited in Figure 3. The KHP volume of 200  $\mu\text{L}$  showed lowest %RSD and %Error, therefore it was chosen for the next experiment. (Although a little lower %RSD and %Error might be obtained when KHP volume was increased to more than 200  $\mu\text{L}$ , it was not used on the reason of waste reduction.)

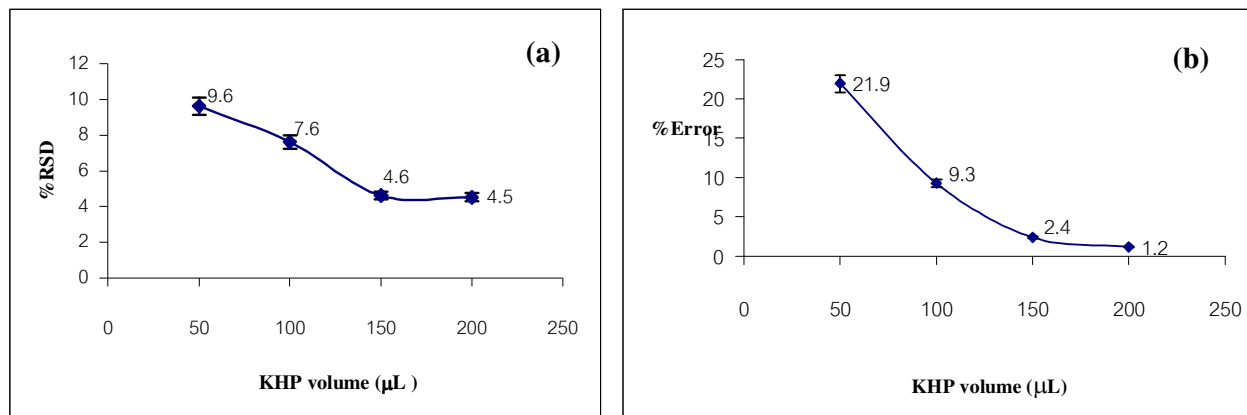


**Figure 3.** Influence of KHP volume on %RSD (a) and %Error (b) in acidity determination by the designed micro-volume autotitrator

#### *Effect of KCl volume*

Supporting electrolytes are required in controlled-potential experiments to decrease the resistance of the solution, to eliminate electromigration effects, and to maintain a constant ionic strength (i.e. to “swamping out” the effect of variable amounts of naturally occurring electrolytes) [12]. The inert supporting electrolyte may be an inorganic salt, a mineral acid, or a buffer. Potassium chloride or nitrate, ammonium chloride, sodium hydroxide, or hydrochloric acid are widely used as electrolyte in aqueous solution. The usual electrolyte concentration range is 0.1-1.0 M, i.e. in large excess of the concentration of all electroactive species.

A similar experiment to that for studying the effect of KHP volume was carried out but the volume of KHP and the flow rate of titrant were fixed at 200 μL and 0.20 mL/min respectively. Various volumes of 10 mM KCl used as supporting electrolyte (5, 10, 15 and 20 mL) were each pipetted into a 25 mL beaker containing 200 μL of KHP and 15.0 mL of deionised water. The results are shown in Figure 4. It was observed that at 5 mL of 10 mM KCl the results from 11 replicates showed no difference in each value of the results so %RSD was calculated to be zero. Comparing the results with those obtained from the standard acid-base titration, the %Error at 5 mL of 10 mM KCl was lowest. Therefore, it was selected for the next experiment.

#### *Effect of KCl concentration*

The experiment was carried out by varying KCl concentration between 0.1-10 mM at fixed KHP volume (200 μL), flow rate (0.20 mL/min), and KCl volume (5 mL). From Figure 5, it is found that 10 mM KCl gave lowest %RSD and %Error. Therefore, it was chosen for the next experiment.

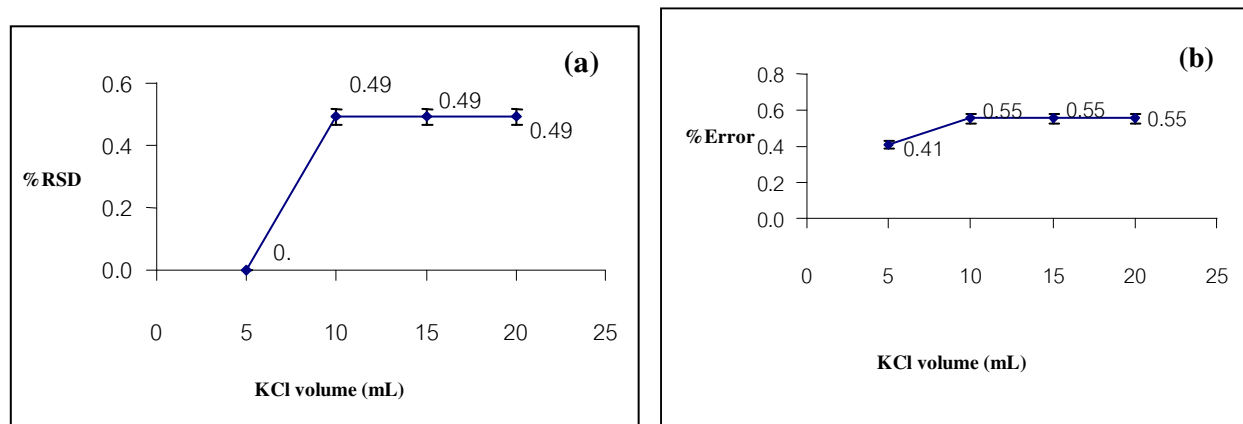


**Figure 4.** Influence of KCl volume on %RSD (a) and %Error (b) in acidity determination by the designed micro-volume autotitrator

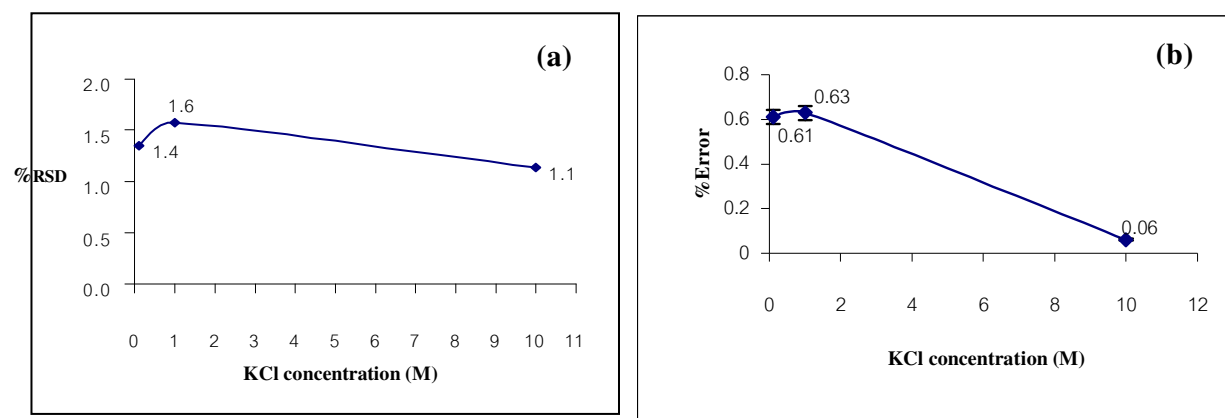


**Figure 5.** Influence of KCl concentration on %RSD (a) and %Error (b) in acidity determination by the designed micro-volume autotitrator

#### *Effect of flow rate*

By fixing the volumes of KHP and KCl at 200  $\mu\text{L}$  and 5 mL respectively, and the concentration of KCl at 10 mM, the flow rate of NaOH used as titrant was varied between 0.16-0.40 mL/min. From Figure 6, although the flow rate at 0.24 mL/min gave the lowest %RSD, it provided higher %Error than that at 0.28 mL/min. Moreover, the sample throughput was increased from 72 samples/hr to 83 samples/hr when the flow rate was changed from 0.24 to 0.28 mL/min. Therefore, the flow rate of 0.28 mL/min was chosen. The summary of the optimum conditions is shown in Table 1.

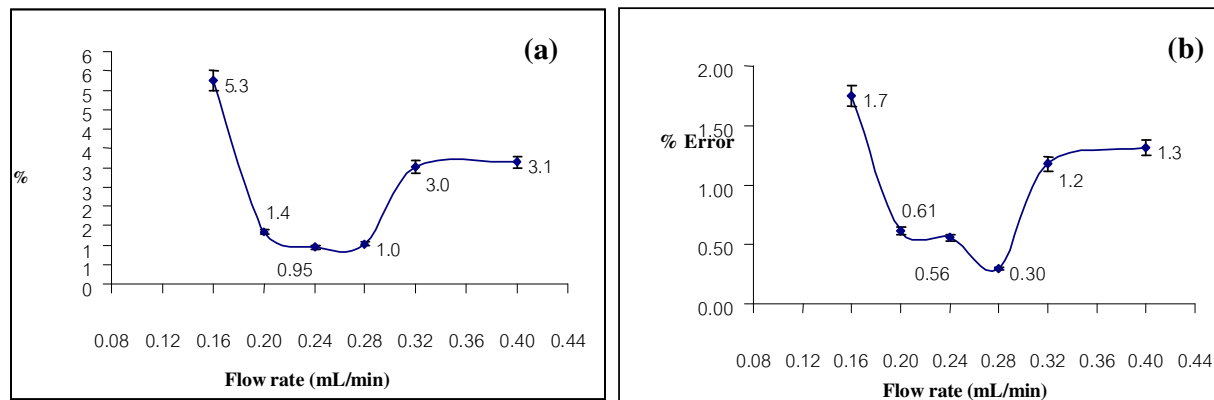


**Figure 6.** Influence of flow rate of NaOH (titrant) on %RSD (a) and %Error (b) in acidity determination by the designed micro-volume autotitrator

**Table 1.** Optimum values of variables for the on-line potentiometric titration using micro-volume autotitrator

Variable	Range studied	Optimum value
KHP volume ( $\mu\text{L}$ )	50-200	200
KCl volume (mL)	5-20	5
KCl concentration (mM)	0.1-10	10
Flow rate (mL/min)	0.16-0.40	0.28

#### *Application to real samples*

Though organic acids in Thai fruits are varied, a common component seems to be citric acid (which has three active protons). The organic acid content (calculated as citric acid) in the fruit juice from each kind of fruits determined by classical titration and on-line potentiometric titration is shown in Table 2. A paired t-test was used to compare the results obtained by both techniques. They were in excellent agreement at 95% confidential limit.

**Table 2.** Organic acid (calculated as citric acid) content in various Thai fruit juices

Fruit	Organic acid content obtained by classical titration (n=11) <sup>*</sup> (x10 <sup>-3</sup> M) (%RSD)	Organic acid content obtained by on-line potentiometric titration (n=11) <sup>*</sup> (x10 <sup>-3</sup> M) (%RSD)
Lime	5.26 (0.23)	5.42 (2.98)
Pomelo	3.76 (0.33)	3.77 (6.72)
Tangerine	3.24 (0.37)	3.29 (15.4)
Red grape	3.00 (0.40)	3.04 (7.33)
Green apple	2.89 (0.38)	2.88 (10.2)
Green grape	2.73 (1.05)	2.72 (6.92)
Pineapple	1.76 (0.63)	1.77 (9.30)
Red apple	1.49 (1.49)	1.51 (3.80)

<sup>\*</sup> 11 replicates

## Conclusions

Determination of organic acid content in fruit juices by the micro-volume autotitrator fabricated in our laboratory is fast and convenient with the sample throughput of 83 samples/hr at the titrant flow rate of 0.28 mL/min. It can be used in routine analysis of acid content. The titrant and titrand used are in the level of a few mL, much less than those used in the classical titration technique, thus contributing to the green and home-made technology.

## Acknowledgements

We gratefully acknowledge the Faculty of Science of Naresuan University for funding this research. Some of the devices and application softwares were developed in cooperation with Alpha Flow Research Group at Chiang Mai University.

## References

1. T. E. Furia, "CRC Handbook of Food Additives.", 2<sup>nd</sup> Edn., CRC Press, Boca Raton, 1983, pp.225, 242.
2. S. M. Herschdoerfer, "Quality Control in the Food Industry.", 2<sup>nd</sup> Edn., Academic Press, London, 1987, p.94.
3. FAO, "Compendium of Food Additive Specifications Addendum 5.", Food and Agriculture Organization of the United Nations, Rome, 1997.

4. P. Masson, "Influence of organic solvents in the mobile phase on the determination of carboxylic acids and inorganic anions in grape juice by ion chromatography", *J. Chromatogr. A*, **2000**, 881, 387-394.
5. T. J. Barden, M. Y. Croft, E. J. Murby, and K. J. Wells, "Gas chromatographic determination of organic acids from fruit juices by combined resin mediated methylation and extraction in supercritical carbon dioxide", *J. Chromatogr. A*, **1997**, 785, 251-261.
6. E. Verette, F. Qian, and F. Mangani, "On-line dialysis with high-performance liquid chromatography for the automated preparation and analysis of sugars and organic acids in foods and beverages", *J. Chromatogr. A*, **1995**, 705, 195-203.
7. C. H. Wu, Y. S. Lo, Y. H. Lee, and T. I. Lin, "Capillary electrophoretic determination of organic acids with indirect detection", *J. Chromatogr. A*, **1995**, 716, 291-301.
8. K. Grudpan, P. Sritharathikhun, and J. Jakmunee, "Flow injection conductimetric or spectrophotometric analysis for acidity in fruit juice", *Anal. Chim. Acta*, **1998**, 363, 199-202.
9. P. Cunniff, "AOAC Official Methods of Analysis.", 16<sup>th</sup> Edn., AOAC, Arlington, **1995**.
10. I. M. Kolthoff and V.A. Stenger, "Volumetric Analysis II: Titration Method", 2<sup>nd</sup> Edn., Interscience Publisher, New York, **1947**, p. 129.
11. D. A. Skoog, D. M. West, F. J. Holler, and S. R. Crouch, "Fundamentals of Analytical Chemistry", 8<sup>th</sup> Edn., Thomson Learning, Inc., Canada, **2004**, pp. 623-625.
12. J. Wang, "Analytical Electrochemistry", VCH Publisher, New York, **1994**, pp. 71-72.

Full Paper

## Stopped-flow injection spectrophotometric method for determination of chlorate in soil

Sarawut Somnam<sup>1</sup>, Kate Grudpan<sup>1,2</sup>, and Jaron Jakmunee<sup>1,2,\*</sup>

<sup>1</sup> Department of Chemistry, Faculty of Science, Chiang Mai University, Chiang Mai 50200, Thailand

<sup>2</sup> Institute for Science and Technology Research and Development, Chiang Mai University, Chiang Mai 50200, Thailand

\* Corresponding author, e-mail: [scijkmn@chiangmai.ac.th](mailto:scijkmn@chiangmai.ac.th)

Received: 17 March 2008 / Accepted: 18 June 2008 / Published: 19 June 2008

---

**Abstract:** A stopped-flow injection (FI) spectrophotometric procedure based on iodometric reaction for the determination of chlorate has been developed. Standard/sample was injected into a stream of potassium iodide solution and then merged with a stream of hydrochloric acid solution to produce triiodide. By stopping the flow while the sample zone is being in a mixing coil, a slow reaction of chlorate with iodide in acidic medium was promoted to proceed with minimal dispersion of the triiodide product zone. When the flow started again, a concentrated product zone was pushed into a flow cell and a signal profile due to light absorption of the product was recorded. Employing a lab-built semi-automatic stopped-FI analyser, the analysis can be performed with higher degree of automation and low chemical consumption. Linear calibration graph in the range of 5-50 mg  $\text{ClO}_3^- \text{L}^{-1}$  was obtained, with detection limit of 1.4 mg  $\text{ClO}_3^- \text{L}^{-1}$ . Relative standard deviation of 2.2% (30 mg  $\text{ClO}_3^- \text{L}^{-1}$ , n=10) and sample throughput of about 20  $\text{h}^{-1}$  were achieved. The system was applied to soil samples and validated by batch spectrophotometric and standard titrimetric methods.

**Keywords:** chlorate, stopped-flow injection, iodometry, soil

---

## Introduction

Chlorate is utilised in the bleaching process in the pulp and paper industry [1]. In addition, chlorate has been employed in agriculture as a herbicide and as a defoliant especially between the years 1930 and 1950. Recently, especially in Thailand, chlorate compounds, e.g. potassium chlorate, have been popularly used for promoting flowering and fruiting of longan. The plant can absorb chlorate through both leaf and root [2]. However, there have been some reports on the effect of chlorate causing damage to plants. The intake of chlorate in high amounts caused falling of leaves and death in plants [2]. Chlorate may compete with nitrate as a substrate for the enzyme nitrate reductase [3-5], which can reduce chlorate to chlorite which is toxic to plants [2,6].

From the above instance, information on chlorate content in soil is therefore useful for controlling the effect of chlorate on plants and the environment. Various methods for determination of chlorate have been reported such as ion chromatography [4], infrared spectrophotometry [7], batch spectrophotometry [8], and flow injection (FI) [9-10]. Ion chromatography and infrared spectrophotometry can quantitate chlorate at low concentration levels, but they require relatively high operating costs and complicated instruments. Batch and FI spectrophotometric methods have gained interest. They are based on different chemical reactions such as iodometric reactions [11], complexation of chlorate with rhenium- $\alpha$ -furildioxime [12], and decolourisation of indigo carmine by chlorate [8]. Although those procedures may provide simplicity and rapidness of analysis, they suffer from interferences and low sensitivities. Stopped-FI procedure can increase sensitivity by increasing the reaction time in a stopping period, thereby promoting more product. It also reduces the main interference due to oxygen in air by allowing the reaction to occur in a closed tube. The stopped-flow injection method with amperometric detection system has been developed for determination of chlorate in soil [13]. However, it involves a complicated system employing a water bath of 55 °C to accelerate the reaction.

In this work, we propose a stopped-FI spectrophotometric procedure for the determination of chlorate utilising iodometric reactions which were reported for batchwise analysis [14]. The sample is injected into a stream of potassium iodide and merged with a stream of acidic solution. Then, the sample-reagent mixture zone is stopped in a mixing coil to promote the slow reaction of chlorate with iodide in acidic medium to produce triiodide while no dispersion of the product zone occurs during the stopping period. When the flow starts again, the product zone is pushed into a flow cell giving rise to a highly sensitive signal to be recorded as a peak. Since the reaction proceeds in a closed system the interfering effect of oxygen in the air which is usually observed in a batch method is minimised. The peak height obtained is proportional to the chlorate concentration. A calibration graph in the range of 5-50 mg  $\text{ClO}_3^- \text{L}^{-1}$  is achieved with a detection limit of 1.4 mg  $\text{ClO}_3^- \text{L}^{-1}$ . Stopped FI also reduces the consumption of reagent and consequently minimises waste. The whole analysis cycle takes about 160 s, with a consumption of 2.3 mL of each reagent.

## Materials and Methods

### *Chemicals*

Deionised water (Milli RX, Millipore) was used throughout. All reagents were of analytical reagent grade unless otherwise stated. Potassium chlorate (99.5 %w/w, Merck) was used to prepare a stock standard solution of  $1000 \text{ mg L}^{-1} \text{ ClO}_3^-$ , by dissolving 0.1474 g of the chemical in water, making up to 100 mL in a volumetric flask. Potassium iodide (iodate free, Carlo Erba) (4.1711 g) was dissolved in 250 mL of water to obtain a 0.1 M iodide solution. Hydrochloric acid (7 M) was prepared by diluting 150 mL of conc. hydrochloric acid (Carlo Erba) with water to the final volume of 250 mL.

#### Sample preparation

Soil samples were collected from the longan plantation field in Chiang Mai, northern Thailand. A soil sample was taken from 15 points around the rim of the longan tree, at the depth of 15 cm. The sample was dried and ground before a portion of 100 g was taken for further treatment.

A portion (20 g) of each sample was extracted with water (20 mL) by shaking for 1 h. The mixture was then filtered through a filter paper (Whatman, No. 42), rinsed with water and the filtrate adjusted to a volume of 25.00 mL with water prior to analysis.

#### Stopped FI setup

The stopped FI system used is illustrated in Figure 1. A lab-built semi-automatic stopped-FI analyser as reported previously was employed. It consisted of a peristaltic pump (MP-3, Eyela, Japan), a 6-port injection valve (Upchurch, USA) and a microcontroller (Basic stamp II SX) for timing control of the pump and the valves. A detector was a simple spectrophotometer (Spectronic 21, Spectronic Instrument, USA), equipped with a 10 mm path-length flow-through cell (Hellma, Germany). All tubing used was of PTFE tubing of 0.5 mm inner diameter, except Tygon pump tubing (Saint-Gobain Performance Plastics, USA).

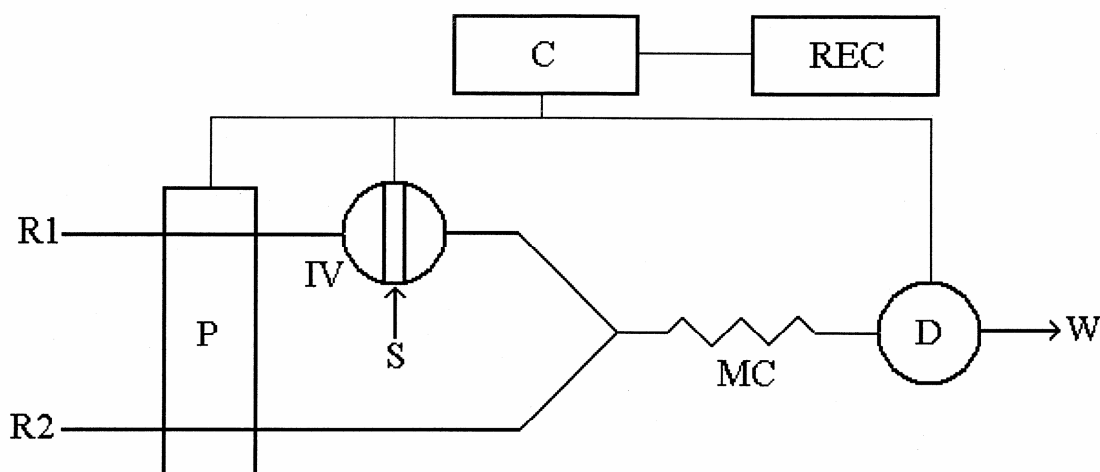


**Figure 1.** Stopped-FIA manifold for determination of chlorate: R1 = 0.1 M potassium iodide, R2 = 7 M hydrochloric acid, P = peristaltic pump, C = controller, IV = six-port injection valve, MC = mixing coil, D = detector, REC = recorder, S = standard/sample, W = waste

### Procedure

A standard or sample (55  $\mu\text{l}$ ) was injected into a stream of 0.1 M KI, before merging with a stream of 7 M HCl and flowing to a mixing coil (see Figure 1). This design prevents the contact of concentrated acid with the injection valve, which may cause corrosion of the valve. The flow rate of each stream was 2.0  $\text{mL min}^{-1}$ . The operation cycle and peak profiles are illustrated in Figure 2. After injection for 9.5 s, the sample zone was halted for 90 s in the mixing coil by stopping the pump via the control unit of the stopped flow analyser. Then the flow was restarted again to push the zone through the detecting flow cell where absorbance at 400 nm was continuously recorded. The last step would take 60 s. A calibration graph was a plot of peak height versus chlorate concentration. Concentration of chlorate in an unknown sample was then evaluated from the calibration graph.

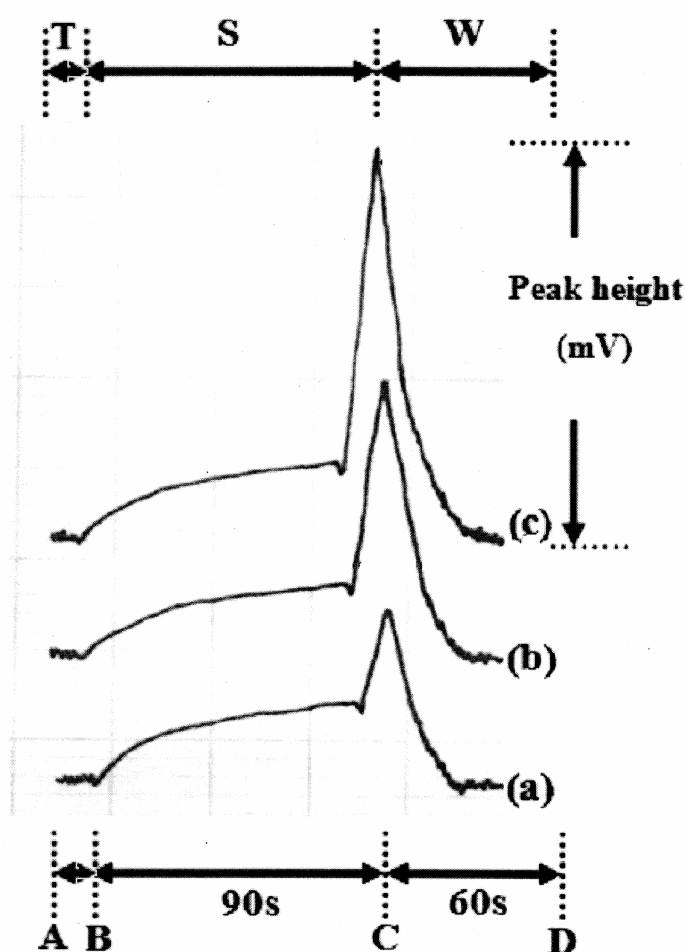


**Figure 2.** Stopped-FI signal profiles obtained for chlorate concentration of (a) 5 (b) 10 and (c) 20  $\text{mg ClO}_3^- \text{L}^{-1}$  (T = travelling time: a period from the injection to the stopping point, S = stopping period: a period during which the flow is halted, W = washing time: a period from the restarting of the flow to the end of the analysis, A = sample injecting point, B = point of stopping the flow, C = point of restarting the flow, D = end point of operation cycle)

## Results and Discussion

The stopped-FI method for determination of chlorate involves iodometric chemical reactions as follows [14]:



The triiodide from this reaction can be detected spectrophotometrically at 400 nm. Hydrochloric acid is appropriate for this reaction. An oxy acid such as nitric acid and sulphuric acid is to be avoided in this reaction because it can be oxidised by chlorate.

The first reaction is slow, depending on concentration of  $\text{ClO}_3^-$ ,  $\text{I}^-$  and  $\text{H}^+$ . By increasing the concentration of either  $\text{H}^+$  or  $\text{I}^-$  the reaction can be accelerated. Use of elevated temperature also helps [13,15]. However, at high temperature and/or high concentration of  $\text{H}^+$ , iodide is quantitatively oxidised by oxygen, so the determination cannot be easily carried out in a batch method. Employing a FI manifold, the reaction product can be enhanced during the stopping period designed to extend the reaction time in a closed system of the mixing coil before spectrophotometric measurement is taken [13,16]. This novel approach is different from the conventional stopped-FI in that the reaction zone is halted in the flow cell so that a change in absorbance can be monitored [17-18]. A calibration graph was plotted as peak height versus concentration of chlorate. Various parameters affecting the procedure were then studied.

### *Effect of stopping time*

With concentration of potassium iodide and hydrochloric acid being kept constant at 0.3 and 3 M respectively, stopping time was varied: 15, 30, 60 and 90 s. A series of standard chlorate solutions (100-500 mg  $\text{ClO}_3^- \text{L}^{-1}$ ) was injected. It was found that higher sensitivity was obtained the longer the stopping time. The stopping time of 90 s was chosen due to the limitation of the instrument for which a maximum stopping time of 99 s can be set and this period provided enough sensitivity for chlorate determination in soil sample.

### *Effect of iodide and hydrochloric acid concentration*

Effects of concentration of potassium iodide and hydrochloric acid solution were studied in the ranges of 0.1-0.6 M and 5-7 M respectively. With the stopping time of 90 s, a series of standard chlorate solutions (5-50 mg  $\text{ClO}_3^- \text{L}^{-1}$ ) were injected in order to construct a calibration graph for each condition. The slopes of the calibration graphs are shown in Figure 3. A higher slope of the calibration graph (higher sensitivity) was obtained with using of higher concentrations of either iodide or hydrochloric acid, except at 7 M hydrochloric acid wherein a higher concentration of potassium iodide led to a lower slope of the calibration graph. This may be due to the oxidation of the iodide ion by air or iodate impurity in potassium iodide chemical, which is more pronounced at high content of acid [13] causing high blank signal and low slope. However, the reaction was minimised at lower iodide

concentration (0.1 M) because of inadequate quantity of iodide and/or iodate ion for this reaction. Potassium iodide and hydrochloric acid at 0.1 M and 7 M respectively were selected for further study.

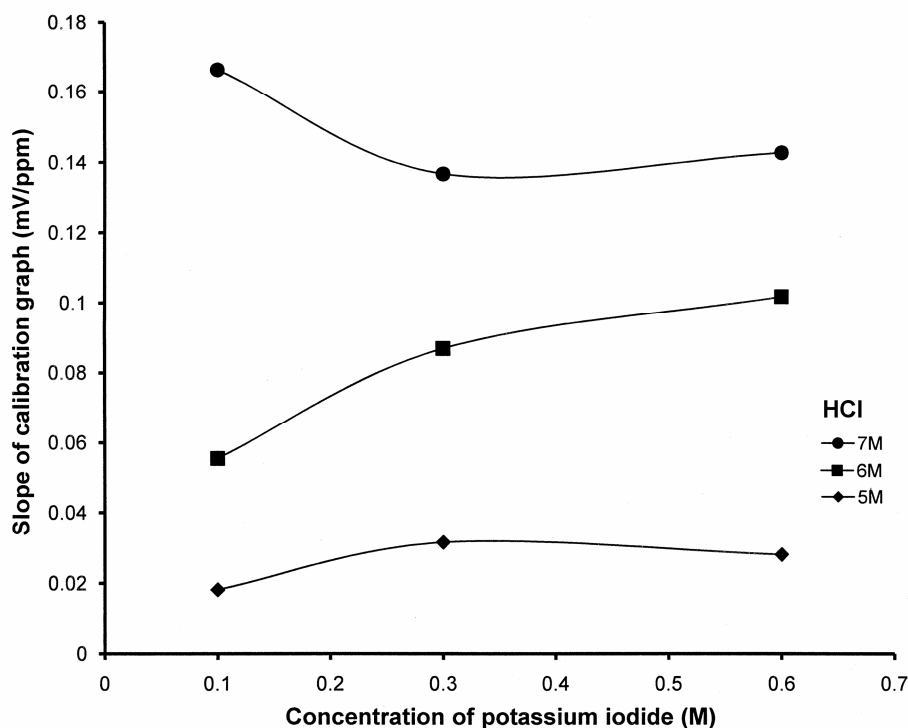


**Figure 3.** Effect of potassium iodide concentration on sensitivity (slope of the calibration graph of chlorate in concentration range of 5-50 mg  $\text{ClO}_3^- \text{L}^{-1}$ ) at different concentrations (5, 6 and 7 M) of hydrochloric acid

#### Analytical characteristics

A linear calibration graph in the range of 5-50 mg  $\text{ClO}_3^- \text{L}^{-1}$  ( $y=0.130x + 0.012$ ,  $R^2=0.996$ ) was obtained. The detection limit calculated from the calibration data was found to be 1.4 mg  $\text{ClO}_3^- \text{L}^{-1}$ . The relative standard deviation was 2.2% for 10 replicated injections of 30 mg  $\text{ClO}_3^- \text{L}^{-1}$ . With the stopped-FI, the consumption of reagent and consequently the production of waste could be reduced. Each analysis cycle consumed about 2.3 mL each of 0.1 M KI and 7 M HCl solutions.

#### Analysis of soil samples

Soil samples were analysed for chlorate content by the proposed method. They were also analysed by a batch spectrophotometric method [8] and the titrimetric standard method [14]. The results are summarised in Table 1. Chlorate content found by stopped-FI method (x) agrees well with that found by the standard titrimetric method (y), as indicated by the slope, intercept and  $R^2$  of the correlation graph of the two methods being closed to 1, 0 and 1 respectively ( $y=0.95x + 0.08$ ,  $R^2=0.997$ ). According to the t-test at 95% confidence level [19], there is no significant difference of the results from the three methods.

**Table 1.** Chlorate content in soil samples obtained by stopped-FI, standard titrimetric and batch spectrophotometric method

Sample number	Chlorate content found ( $\mu\text{g g}^{-1}$ ) by		
	Stopped-FI*	Titrimetry [14]*	Batch spectrophotometry[8]
1	194 $\pm$ 5	189 $\pm$ 1	196
2	258 $\pm$ 2	245 $\pm$ 1	226
3	107 $\pm$ 4	103 $\pm$ 7	101
4	36.5 $\pm$ 0.4	40 $\pm$ 2	33.7
5	49.5 $\pm$ 0.1	50 $\pm$ 1	47.8
6	69 $\pm$ 1	62 $\pm$ 2	75.7
7	167 $\pm$ 2	155 $\pm$ 2	142
8	57.8 $\pm$ 0.9	46 $\pm$ 2	28.9
9	37.8 $\pm$ 0.3	36 $\pm$ 2	32.3
10	101 $\pm$ 4	102 $\pm$ 1	91.2
11	127 $\pm$ 4	122 $\pm$ 1	91.7
12	9.8 $\pm$ 0.4	9 $\pm$ 1	10.8
13	50.4 $\pm$ 0.5	46 $\pm$ 1	43.1
14	106 $\pm$ 1	96 $\pm$ 1	119
15	214 $\pm$ 4	201 $\pm$ 2	163
16	30.0 $\pm$ 0.6	27 $\pm$ 1	22.7
17	10.6 $\pm$ 0.2	9 $\pm$ 1	6.4
18	12.6 $\pm$ 0.2	11 $\pm$ 0	6.2

\*mean of triplicate results

## Conclusions

A novel stopped-FI method is proposed, in which there is a stopping of the flow to hold an injected zone of standard/sample in a mixing coil for promoting the reaction to take place without dispersion of the resulting product. It is applied to a slow reaction of chlorate with acidic iodide for the determination of chlorate. The procedure provides a suitable sensitivity for analysis of soil from longan plantation fields where chlorate is used to promote fruiting of the longan trees. With a simple instrument set-up employing a lab-built semi-automatic stopped-FI analyser, the determination can be done with high degree of automation and low reagent consumption.

## Acknowledgements

We thank the Thailand Research Fund (TRF), the Centre for Innovation in Chemistry: Postgraduate Education and Research Program in Chemistry (PERCH-CIC), and the Commission on Higher Education (CHE) for support. Mr. Subhachai Jayavasti is gratefully acknowledged for the technical support on the semi-automatic stopped-FI analyser.

## References

1. M. Biesaga, M. Kwiatkowsha, and M. Trojanowicz, "Separation of chlorine-containing anions by ion chromatography and capillary electrophoresis", *J. Chromtogr. A.*, **1997**, 777, 375-381.
2. R. Borges, E. C. Miguel, M. R. D. Janice, M. Cunha, R. E. Bressan-Smith, J. G.. Oliveira, and G. A. Souza Filho, "Ultrastructural, physiological and biochemical analyses of chlorate toxicity on rice seedlings", *Plant Sci.*, **2004**, 166, 1057-1062.
3. H. S. Srivastava, "Multiple functions and forms of higher plant nitrate reductase", *Phytochem.*, **1992**, 31, 2941-2947.
4. B. Nowack and U. Guntan, "Determination of chlorate at low  $\mu\text{g/l}$  levels by ion-chromatography with postcolumn reaction", *J. Chromtogr. A.*, **1999**, 849, 209-215.
5. J. Xu, J. J. Trimble, L. Steinberg, and B. E. Logan, "Chlorate and nitrate reduction pathways are separately induced in the perchlorate-respiring bacterium *Dechlorosoma* sp. KJ and the chlorate-respiring bacterium *Pseudomonas* sp. PDA", *Water Res.*, **2004**, 38, 673-680.
6. K. R. Kosola and A. J. Bloom, "Chlorate as a transport analog for nitrate absorption by roots of tomato", *Plant Physiol.*, **1996**, 110, 1293-1299.
7. M. W. Miller, R. H. Philip, J. Underwood, and A. L. Underwood, "Infrared determination of chlorate in the presence of other oxyhalogen anions", *Talanta*, **1963**, 10, 763-768.
8. B. Chriswell and B. Keller-Lehmann, "Spectrophotometric method for the determination of chlorite and chlorate", *Analyst*, **1993**, 118, 1457-1460.
9. D. G. Themelis, D. W. Wood, and G. Gordon, "Determination of low concentrations of chlorite and chlorate ions by using a flow-injection system", *Anal. Chim. Acta*, **1989**, 225, 437-441.
10. K. Tian and P. K. Dasgupta, "Simultaneous flow-injection measurement of hydroxide, chloride, hypochlorite and chlorate in Chlor-alkali cell effluents", *Talanta*, **2000**, 52, 623-630.
11. D. P. Nikolelis, M. I. Karayannis, and T. P. Hadjhoannou, "Kinetic study of the iodate—iodide and chlorate—iodide reactions in acidic solutions, and a method for the microdetermination of bromide", *Anal. Chim. Acta*, **1977**, 94, 415-420.
12. N. L. Trautwein and J. C. Guyon, "Spectrophotometric determination of chlorate ion", *Anal. Chim. Acta*, **1968**, 41, 275-282.
13. O. Tue-ngeun, J. Jakmune, and K. Grudpan, "A novel stopped flow injection—amperometric procedure for the determination of chlorate", *Talanta*, **2005**, 68, 459-464.
14. G. H. Jeffery, J. Bassett, J. Mendham, and R. C. Denney, "Quantitative Inorganic Analysis", 5th Edn., Longmans, London, **1989**, p. 394.
15. G. Gordon, K. Yoshino, D. G. Themelis, D. Wood, and G. E. Pacey, "Utilisation of kinetic-based flow injection methods for the determination of chlorine and oxychlorine species", *Anal. Chim. Acta*, **1989**, 224, 383-391.
16. K. Grudpan, "Some recent developments on cost-effective flow-based analysis", *Talanta*, **2004**, 64, 1084-1090.
17. K. Grudpan, P. Ampan, Y. Udnan, S. Jayasvati, S. Lapanantnoppakhun, J. Jakmune, G. D. Christian, and J. Ruzicka, "Stopped-flow injection simultaneous determination of phosphate and silicate using molybdenum blue", *Talanta*, **2002**, 58, 1319-1326.
18. S. Somnam, K. Grudpan, and J. Jakmune, "Stopped-flow injection method for determination of phosphate in soils and fertilizers", *Mj. Int. J. Sci. Tech.*, **2008**, 2, 172-181.
19. G. D. Christian, "Analytical Chemistry", 6th Ed., John Wiley & Sons, New York, **1995**, p. 90.

*Full Paper*

## **Effect of heavy metals on the level of vitamin E, total lipid and glycogen reserves in the liver of common carp (*Cyprinus carpio* L.)**

**Vinodhini Rajamanickam\* and Narayanan Muthuswamy**

Aquatic Biodiversity Research Centre, Department of Advanced Zoology and Biotechnology,  
St.Xavier's College (Autonomous), Palayamkottai – 627 002, Tamilnadu, India

\*Corresponding author, e-mail: [swethasivani@yahoo.co.in](mailto:swethasivani@yahoo.co.in)

*Received: 31 December 2007 / Accepted: 17 June 2008 / Published: 27 June 2008*

---

**Abstract:** The aim of this study is to examine some changes in the biochemical profile of the liver tissue of common carp (*Cyprinus carpio* L.) exposed to a sublethal concentration of heavy metal mixture (cadmium, chromium, nickel and lead). The biochemical profile, specifically glycogen, total lipid and vitamin E content in the liver tissue was examined and compared to that of the control group. The exposed group showed a marked decline in glycogen and vitamin E reserves. Conversely an increase in total lipid in comparison to control was observed. The result reflects the sensitivity of these biochemical parameters to the effects of sublethal levels of combined heavy metals for this the widely consumed freshwater fish.

**Keywords:** heavy metals, *Cyprinus carpio* L., toxicity, liver damage, glycogen, total lipids, vitamin E

---

### **Introduction**

The toxicity of heavy metals to aquatic organisms has attracted considerable research attention, particularly as a result of the continuing anthropogenic mobilisation of the metals in the

environment. Like warm-blooded animals, changes due to heavy metals in fish occur because of injuries or infection which otherwise can be used to detect the dysfunction of the organs. These changes reflect the effect on fish survival, reproduction and growth [1]. Most of the heavy metal ions exhibit toxicity through the formation of coordination complexes and clusters in the animal cells [2]. Low concentration of heavy metals may induce a chronic stress which may not kill the individual fish but lower its size and body weight [3], thus reducing their ability to compete for food and habitat. Fish also have a tendency to bioaccumulate heavy metals and humans can therefore be at great risk through contamination of the food chain [4].

Cadmium causes poisoning in various tissues and animals [5-7]. It can react with polythiol groups of cellular macromolecules such as glycogen, lipids, amino acids. Cadmium bioaccumulated in tissues can replace the essential element zinc present in the enzymes carboxypeptidase [8] and metallothionein [9]. The metal causes oxidative damage by alteration of mitochondrial activity and genetic information [10-11]. In the environment, chromium exists primarily in the trivalent and hexavalent states, the latter being the predominant species in natural water [12]. Chromium in combination with nickel as trace metals function as potential health hazard that causes disturbances in gastrointestinal, hepatic and neurological activities. Hexavalent chromium generates reactive oxygen species (ROS) which increase risk for cellular and hepatic DNA fragmentation, enhance intracellular oxidised states, and decrease cell viability with necrosis and programmed cell death [13].

Nickel salts significantly increase the level of lipid peroxidation and simultaneously decrease glutathione level and glutathione peroxidase activity in the liver [14]. Lead exposure provokes adverse effect on the central nervous system as it is extremely toxic to most of the living things [15]. The assimilation of relatively small amounts of lead over a long period of time in the human body can lead to the malfunctioning of the organs [16].

Heavy metal contamination in aquatic environment exerts an extra stress on fish which tend to accumulate the heavy metals in metabolically active tissues and organs [17]. The liver is an important organ performing vital functions including biotransformation, migration of vitamins and lipids, glycogen storage, and release of glucose into the blood. Heavy metal chelation may disrupt the liver tissue by disintegrating the functional and structural properties of the cells.

Toxicity tests for xenobiotics serves as a sensitive index in predicting and preventing damage to aquatic life in receiving waters by regulating the toxic waste effluents [18]. Assessment of biochemical parameters in damaged fish organ can be used as a diagnostic tool to characterise such metal toxicity. There are considerable earlier information assessed by potential biomarkers indicating that heavy metals are responsible for many adverse effects in various types of fish and other animals [19-21]. In the majority of exotoxicological studies, effects of single metals on fish have been evaluated, while studies on the biochemical profile of fish subjected to the impact of combined heavy metals are limited. Therefore the aim of this study is to assess the biochemical changes in glycogen, lipid and vitamin E in common carp (*Cyprinus carpio* L.) in the case of liver injury by a model mixture of heavy metals, namely lead, cadmium, chromium and nickel.

## Materials and Methods

The freshwater common carp (10-13 cm in length and weighing  $35.70 \pm 0.60$ g) were collected from ponds of the southern districts of Tamilnadu, India and were acclimatised to laboratory conditions for a week. Twenty to twenty-five individuals were used for the experiments. All the fish were kept in batches under constant temperature ( $25 \pm 1^\circ\text{C}$ ) with a controlled photoperiod of 12:12 hour light and dark cycle and constant filtration. Analytical grade cadmium chloride, lead nitrate, potassium chromate and nickel sulphate (supplied by BDH, India) were used as metal toxicant throughout the experiment. The fish used for this experiment were maintained in 200 L recirculating tanks, filled with dechlorinated tap water. The physicochemical characteristics of the water during heavy metal induction period and the water used in control pond are presented in the Table 1. The water in the control and experimental tanks was changed every 3 days.

**Table 1.** Water quality parameters measured in the control and experimental ponds during heavy metal induction period

Water Quality Parameter	Mean $\pm$ SD		
	Control	Day	Night
Temperature ( $^\circ\text{C}$ )	$27 \pm 0.2$	$27 \pm 0.2$	$27 \pm 0.2$
pH	$7.20 \pm 0.2$	$7.2 \pm 0.1$	$7.1 \pm 0.1$
Electrical conductivity ( $\mu\text{S}/\text{cm}$ )	$1255.00 \pm 0.5$	$1650 \pm 5$	$1650 \pm 5$
Total dissolved solids(ppm)	$815.75 \pm 0.3$	$1072 \pm 5$	$1072 \pm 5$
Alkalinity (ppm)	$140.50 \pm 0.2$	$148 \pm 1.2$	$147 \pm 0.5$
Total hardness (ppm)	$280.45 \pm 0.5$	$355 \pm 5$	$355 \pm 5$
Dissolved oxygen (%)	$7.2 \pm 0.2$	$7.4 \pm 0.3$	$7.3 \pm 0.2$
Total ammonia (ppm)	$10.80 \pm 0.2$	$12.2 \pm 0.2$	$11.2 \pm 0.3$
Salinity (%)	$14.6 \pm 0.2$	$15 \pm 0.5$	$14.8 \pm 0.1$

Note: The values are statistically significant at  $p < 0.05$ .

The fish were divided into two groups, with the first group serving as control and the other as experimental group. The experimental group was exposed to a sublethal concentration of 5 ppm of a combined (Cd + Pb + Cr + Ni) metal solution containing 1.25 ppm of each metal ion (1/10th of LC50/48h) for a period of 32 days. The heavy metal concentration was selected based on preliminary results, which showed a sublethal effect after a 32-day period of exposure.

The fish was fed with commercially available fish feed at a daily rate of 3-4 % body weight throughout the experiment. The control and the experimental groups were starved for 24 hours before experimentation. Five specimens of the control group and 5 specimens of the metal-exposed group were then sacrificed during each exposure period of 1, 8, 16 and 32 days. The liver tissues of both experimental and control fish were dissected out, blotted free of blood and weighed, and processed for biochemical analysis. Glycogen (in mg/mL of liver homogenate) was assayed by the method of Seifter et al. [22]. Total lipid (in g/L of liver homogenate) was

determined using a method described by Bragdon [23]. Vitamin E content (in  $\mu\text{g/g}$  tissue) in liver homogenate was estimated by the method of Baker and Frank [24]. All the analyses were performed by adapting universally accepted standard protocols employing a Hitachi UV-Visible spectrophotometer. All experimental results are expressed as mean  $\pm$  SEM. Paired Student's t-test was employed, and  $p < 0.001$  was considered significant.

## Results and Discussion

The present study attempts to create awareness concerning the potential severe public health issues resulting from the toxic effects of heavy metals as pollutants from industrial, agricultural and urban wastes. The toxic effects of heavy metals on fish involve hepatotoxicity, neurotoxicity and nephrotoxicity [25]. Bioaccumulation of heavy metals and consequent alterations in gills, liver, kidney and flesh of common carp have been reported earlier [26].

The biochemical profile of the liver of the common carp exposed to a sublethal concentration of the combined heavy metal solution (5ppm) for the exposure period of 1, 8, 16 and 32 days is presented in Table 2. Glycogen reserves in liver tissue were depleted to a lower level compared to that of the control fish ( $p < 0.001$ ). The declined glycogen level explains the formation of glucose, a major source of energy by glycogenolysis mechanism. The content of glycogen seemed to increase initially, then showed a marked decline at the end of the 16<sup>th</sup> day onwards as shown in Figure 1. Total lipid in liver tissue exhibited a significant ( $p < 0.001$ ) increase after 32 days of exposure ( $9.17 \pm 0.05$  g/L) in comparison to the control value ( $5.66 \pm 0.06$  g/L) as reported in Table 2 and Figure 2. Vitamin E, a chain-breaking lipid-soluble antioxidant, showed significant progressively decreased activity ( $p < 0.001$ ) in the liver of the treated groups for the periods studied (Table 2, Figure 3). The result indicated the loss of vitamin E in the liver tissue, which served as an effective marker for assessing the degree of damage in the liver tissue by the action of heavy metals.

The decreased glycogen concentration in the liver of common carp could be due to its enhanced utilisation as an immediate source to meet the energy demand under metallic stress. Depleted glycogen level under chromium stress reported in *Labeo rohita* [21] also supports our research findings. The carbohydrate source is stored as a reserve fuel in the liver and muscle tissues of fish for the endogenous derivation of energy during acute and chronic stress [27]. The decreased glycogen content as a result of hypoxic or anoxic condition activates the glycolytic enzymes via catecholamines that initially enhance glycogen concentration. It was also found that cadmium could decrease glycogen reserves in the liver and muscle tissues of *Cyprinus carpio* [28].

**Table 2.** The biochemical profile of liver of common carp (*Cyprinus carpio* L.) exposed to sublethal concentration of combined heavy metal solution (5ppm)

Biochemical Profile	Duration of Exposure (Days)	Control Mean ± S.D	Experiment Mean ± S.D	% Change	Result
Glycogen (mg/mL)	1	0.63 ± 0.03	0.45 ± 0.02	28.57	p < 0.001**
	8	0.63 ± 0.03	0.58 ± 0.03	7.94	p < 0.01*
	16	0.63 ± 0.03	0.38 ± 0.02	39.68	p < 0.001**
	32	0.63 ± 0.03	0.32 ± 0.03	49.21	p < 0.001**
Total lipid (g/L)	1	5.66 ± 0.66	6.75 ± 0.06	-19.25	p < 0.001**
	8	5.66 ± 0.66	7.14 ± 0.14	-26.15	p < 0.001**
	16	5.66 ± 0.66	8.37 ± 0.14	-47.88	p < 0.001**
	32	5.66 ± 0.66	9.17 ± 0.05	-62.01	p < 0.001**
Vitamin-E (µg/g.tissue)	1	1800.85 ± 0.005	1640.67 ± 0.03	8.89	p < 0.001*
	8	1800.85 ± 0.005	1536.84 ± 0.04	14.66	p < 0.001*
	16	1800.85 ± 0.005	1290.25 ± 0.04	28.35	p < 0.001*
	32	1800.85 ± 0.005	1100.63 ± 0.03	38.88	p < 0.001*

Note: n = 5

\*\* Highly Significant

\* Significant

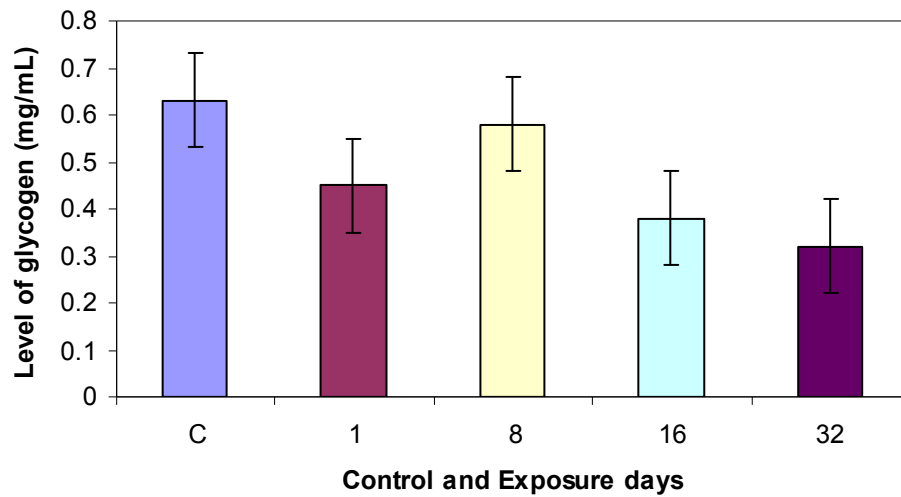


**Figure 1.** Level of glycogen in liver

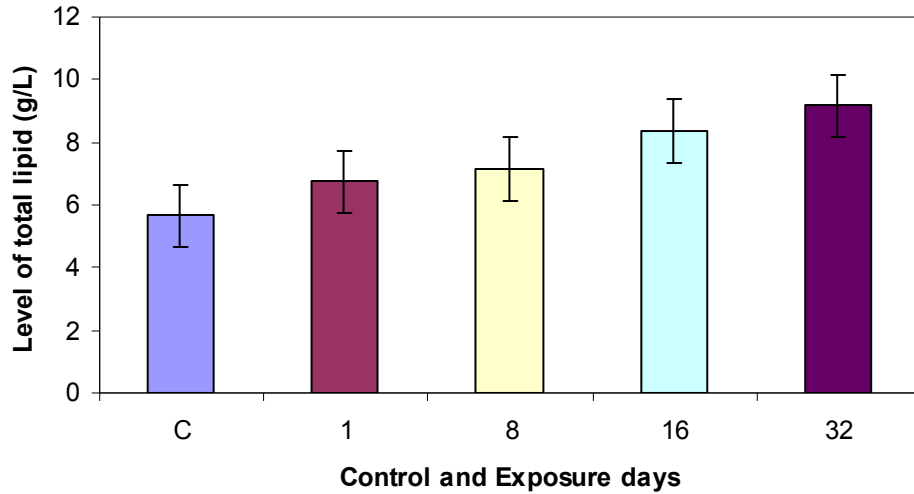


**Figure 2.** Level of total lipid in liver

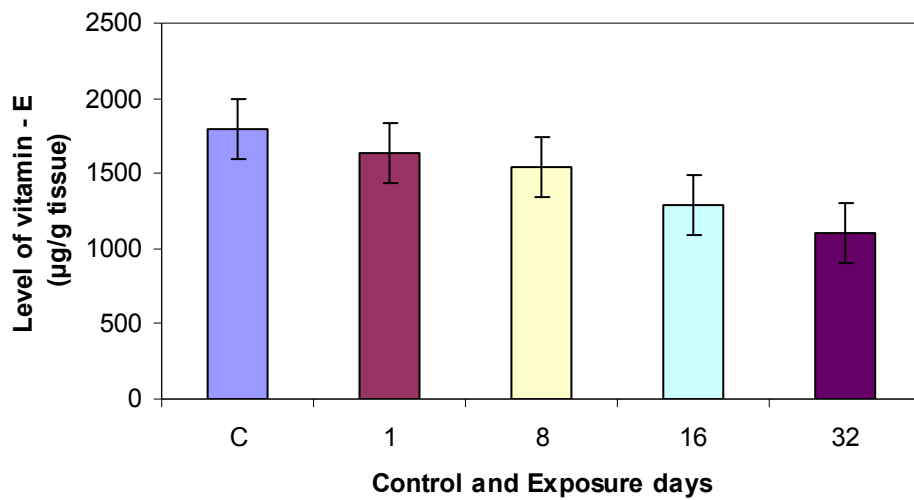


**Figure 3.** Level of vitamin E in liver

Indeed, prolonged stress after metal toxicity exerts weakness and hypoxic condition with the inability of hepatocytes to propagate the regular cellular metabolism [29]. The decreased glycogen content in fish, which was also observed during the present study, alters the enzymes of carbohydrate metabolism and might be utilised in the formation of glycoproteins and lipids [30].

In relation to the total lipid in this study, it was found that there was a significant increase of lipid in the heavy metal intoxicated groups as compared to control fish. Lipid blocks the metabolism of hepatic triglycerides due to the defective synthesis of very low density lipoproteins which are involved in the transport and mobilisation of triglycerides to extra hepatic tissues [31].

Results of this study show an abnormal increase in lipid, which may induce hyperlipidemia, premature atherosclerosis and excessive deposition of fat (obesity) loaded in carp tissues.

Vitamin E has a protective effect on the stabilisation of metabolic process in biological systems [32]. It performs a vital role in fish health by inactivating harmful oxy radicals stimulated by stress and environmental pollution. The reduced vitamin E could be attributed to the aggressive activation of heavy metals chelated in the liver. Numerous investigations documented vitamin E as exhibiting the greatest protection against heavy metal toxicity in humans and animals [e.g. 33-35]. In the present investigation the decreased vitamin E might be due to its utilisation as the first defense line in the protection of sub-cellular organelles and in the stabilisation of liver cell membranes against toxic reactive metabolites provoked by heavy metals.

## Conclusions

The present study has demonstrated that the effects of sublethal concentration of combined heavy metals for the exposure period of 1, 8, 16 and 32 days proved to be toxic to common carp (*Cyprinus carpio L.*). Glycogen in the liver tissue was depleted to lower levels compared to that in the control fish, while the level of total lipid was significantly increased during the 32 days of heavy metal exposure, but that of vitamin E, like glycogen, significantly decreased. The result could seriously alter the ability of cells to counteract with heavy metals. This observation further implies that there is dire need to focus on the harmful influences of heavy metals on the biochemical activities of aquatic organisms and on the environment at large.

## Acknowledgements

The authors wish to register their appreciation of the support provided by the College Principal Rev. Dr. Alphonse Manickam SJ and Prof. M. Thomas Punithan, Head of the Department of Advanced Zoology and Biotechnology, St. Xavier's College (Autonomous), Palayamkottai, Tamilnadu, India, which includes the provision of laboratory facilities at the College.

## References

1. M. Z. Vosyliene, "The effect of heavy metals on haematological indices of fish (survey)", *Acta Zoologica Lituanica, Hydrobiologia*, **1999**, 9, 76-82.
2. A. Lugauskas, L. Levinskaite, D. Peculyte, J. Repeckiene, A. Motuzas, R. Vaisvalavicius, and I. Prosycevas, "Effect of copper, zinc and lead acetates on microorganisms in soil", *Ekologija. Nr.*, **2005**, 1, 61-69.
3. M. Z. Vosyliene and A. Jankaite, "Effect of heavy metal model mixture on rainbow trout biological parameters", *Ekologija.*, **2006**, 4, 12-17.

4. J. Ui, "The Changing Chemistry of the Oceans", Almquist and Wiksells, Stockholm, **1972**.
5. L. Jarup, "Hazards of heavy metal contamination", *Br. Med. Bull.*, **2003**, 68,167-82.
6. N. Yadav and S. Khandelwal, "Effect of picroliv on cadmium – induced hepatic and renal damage in the rat", *Hum. Exp. Toxicol.*, **2005**, 25, 581-91.
7. G. Yapici, I. H. G. Timur, and A. Kaypmaz, "Lead and cadmium exposure in children living around a coal-mining area in Yatagan, Turkey", *Toxicol. Ind. Health.*, **2006**, 22, 357-62.
8. N. M. Price and F. M. M Morel, "Cadmium and cobalt substitution for zinc in a marine diatom", *Nature*, **1995**, 344, 658-660.
9. L. T. Jensen, W. R. Howare, J. J. Strain, D. R. Winge, and V. C. Culotta, "Enhanced effectiveness of copper ion buffering by Cup1 metallothionein compared with CRS5 metallothionein in *Saccharomyces cerevisiae*", *J. Biol. Chem.*, **1996**, 271, 18514-18519.
10. L. Patrick, "Toxic metals and antioxidants: Part II. The role of antioxidants in arsenic and cadmium toxicity", *Altern. Med. Rev.*, **2003**, 8, 106-126.
11. C. De Burbure, J. B. Buchet, A. Leroyer, C. Nisse, J. M. Haguenoer, A. Mutti, Z. Smerhovsky, M. Cikrt, M. Trzcinka-Ochacka, G. Razniewska, M. Jakubowski, and A. Bernard, "Renal and neurologic effects of cadmium, lead, mercury and arsenic in children: evidence of early effects and multiple interactions at environmental exposure levels", *Environ. Health Perspect.*, **2006**,114, 584-590.
12. S. Langard and T. Norseth, "Chromium", in "Handbook on the Toxicology of Metals" (Ed. L. Friberg, F. N. Gunnar, and B.V. Velimir), Biochemical Press, Amsterdam, **1979**, pp. 383-394.
13. D. Bagchi, S. J. Stons, B. W. Downs, M. Bagchi, and H. G. Preuss, "Cytotoxicity and oxidative mechanisms of different forms of chromium", *Toxicology*, **2002**,180, 5-22.
14. K. K. Das, S. N. Das, and S. Gupta, "The influence of nickel induced hepatic lipid peroxidation on rats", *J. Basic Clin. Physiol. Pharmacol.*, **2001**, 12, 187-195.
15. N. Abdus-Salam and F. A. Adekola, "The influence of pH and adsorbent concentration on adsorption of lead and zinc on a natural goethite", *AJST.*, **2005**, 6, 55-66.
16. M. A. O. Badmus, T. O. K. Audu, and B. U. Anyata, "Removal of lead ion from industrial waste waters by activated carbon prepared from periwinkle shells (*Typanotonus fuscatus*)", *Turkish. J. Eng. Environ. Sci.*, **2007**, 37, 251-263.
17. R. W. Langston, "Toxic effects of metals and incidence of marine ecosystem", in "Heavy Metals in the Marine Environment" (Ed. R. W. Furness and P. S. Rainbow), CRC Press, New York, **1989**, pp. 128-142.
18. APHA, AWWA, WPCP, "Standard Methods for the Examination of Water and Waste Water", 20<sup>th</sup> Edn., American Public Health Association, Washington DC, **1998**.
19. N. S. Hassan and S. M. Awad, "Reverse effect of vitamin-E on oxidative stress, derivatives and conductivity changes of hemoglobin induced by exposure to cadmium", *J. App. Sci. Res.*, **2007**, 3, 437-443.
20. B. Cिक and K. Engin, "The effect of cadmium on levels of glucose in serum and glycogen reserves in the liver and muscle tissues of *Cyprinus carpio* L. (1758)", *Turk. J. Vet. Anim. Sci.*, **2005**, 29, 113-117.

21. S. S. Vutkuru, "Acute effects of hexavalent chromium on survival, oxygen consumption, hematological parameters and some biochemical profiles of the Indian Major Carp, *Labeo rohita*", *Int. J. Environ. Res. Public Health*, **2005**, 2, 456-462
22. S. Seifter, S. Dayton, B. Novic, and E. Muntmyler, "Estimation of glycogen with the anthrone reagent", *Arch. Biochem.*, **1950**, 25, 291-295.
23. J. H. Bragdon, "Colorimetric determination of blood lipids", *J. Biol. Chem.*, **1951**, 190, 513-517.
24. H. Barker, O. Frank, and B. DeAngeles, "Plasma tocopherol in man at various times after ingestion free (or) acetylated tocopherol", *Nutr. Rep. Int.*, **1980**, 21, 531-536.
25. M. Valko, H. Morris, and M. J. D. Cronin, "Metal toxicity and oxidative stress", *Curr. Med. Chem.*, **2005**, 12, 1161-1208.
26. R. Vinodhini and M. Narayanan, "Bioaccumulation of heavy metals in organs of freshwater fish *Cyprinus carpio* (Common carp)", *Int. J. Environ. Sci. Tech.*, **2008**, 5, 179-182.
27. S. E. W. Bonga, "The stress response in fish", *Physiol. Rev.*, **1997**, 77, 591-625.
28. B. Cıck and K. Engin, "The effects of cadmium on levels of glucose in serum and glycogen reserves in the liver and muscle tissue of *Cyprinus carpio* L.", *Turk. J. Vet. Anim. Sci.*, **2005**, 29, 113-117.
29. A. Heath, "Water Pollution and Fish Physiology", CRC Press Inc., Boca Raton, Florida, **1995**.
30. H. M. Levesque, T. W. Moon, P. G. C. Campbell, and A. Hontela, "Seasonal variation in carbohydrate and lipid metabolism of Yellow perch (*Perca flavescens*) chronically exposed to metals in the field", *Aquat. Toxicol.*, **2002**, 60, 257-267.
31. T. Braunbeck, G. G. V. Storch, and R. Nagel, "Hepatic steatosis in zebra fish (*Brachydanio rerio*) induced by long term exposure to  $\gamma$ -Hexacyclohexane", *Ecotox. Environ. Safe.*, **1990**, 19, 355-374.
32. M. Valko, D. Leibfritz, J. Moncol, M. T. Cronin, M. Mazur, and J. Telser, "Free radicals and antioxidants in normal physiological functions and human disease", *Int. J. Biochem. Cell. Biol.*, **2007**, 3, 44-84.
33. B. Leibovitz, M. L. Hu, and A. L. Tappel, "Dietary Supplements of vitamin E, beta-carotene, coenzyme Q<sub>10</sub> and selenium protect tissues against lipid peroxidation in rat tissue slices", *J. Nutr.*, **1990**, 120, 97-104.
34. R. J. Sokol, "Antioxidant defense in metal induced liver damage", *Seminars in Liver Disease*, **1996**, 16, 39-46.
35. D. Appenroth, E. Karge, G. Kiessling, W. J. Wechter, K. Winnefield, and C. Heck, "LLU-alpha, an endogenous metabolite of gamma tocopherol, is more effective against metal nephrotoxicity in rats than gamma-tocopherol", *Toxicology*, **2001**, 112, 255-265.

Full Paper

## **Effects of *Terminalia bellerica* Roxb. methanolic extract on mouse immune response in vitro**

**Aurasorn Saraphanchotiwitthaya<sup>1,2,\*</sup>, Pattana Sripalakit<sup>2,3</sup>, and Kornkanok Ingkaninan<sup>3</sup>**

<sup>1</sup> Department of Pharmaceutical Technology, Faculty of Pharmaceutical Sciences, Naresuan University, Phitsanulok, Thailand, 65000

<sup>2</sup> Pharmaceutical Biotechnology Research Unit, Faculty of Pharmaceutical Sciences, Naresuan University, Phitsanulok, Thailand

<sup>3</sup> Department of Pharmaceutical Chemistry and Pharmacognosy, Faculty of Pharmaceutical Sciences, Naresuan University, Phitsanulok, Thailand

\*Author to whom correspondence should be addressed, e-mail: [aurasorns@nu.ac.th](mailto:aurasorns@nu.ac.th)

Received: 28 January 2008 / Accepted: 27 June 2008 / Published: 30 June 2008

---

**Abstract:** In this study, the effects of *Terminalia bellerica* methanolic extract (0.1, 1, 10, 100 and 500 µg/ml) on the mouse immune system were investigated in vitro. Phagocytic activity and lymphocyte proliferation were assayed. The results indicated the effect of the extract (500 µg/ml) on the stimulation of macrophage phagocytosis, through the production of superoxide anions and acid phosphatase, with a phagocytic index (PI) value of approximately 1.5 and 1.3, respectively. For the lymphocyte proliferation assay, the extract (500 µg/ml) with phytohemagglutinin exhibited maximal activation, with a stimulation index (SI) value of approximately 5.8. With concanavalin A, lipopolysaccharide, and pokeweed mitogen, similar activation (SI 4.5) of lymphocyte proliferation was observed. However, at low concentrations (0.1 µg/ml), *T. bellerica* extract with concanavalin A and pokeweed mitogen caused suppressant activity (SI 0.7). The results suggested that the effect of extract on T-lymphocyte proliferation occurred through the same mechanism as phytohemagglutinin, concanavalin A and B-lymphocyte proliferation through T-cell independent and T-cell dependent mechanisms, in manners similar to lipopolysaccharide and pokeweed mitogen respectively. It might be concluded that the methanolic extract of *T. bellerica* affected the mouse immune system, specifically both the cellular and humoral immune response in vitro, corresponding with its folklore applications. These results can be further applied to the treatment of human immune mediated diseases.

**Keywords:** *Terminalia bellerica* Roxb, in vitro immune response, lymphocytes, proliferation, macrophages, phagocytosis

---

## Introduction

*Terminalia bellerica* Roxb (Combretaceae) is a perennial herb mainly distributed in the tropical regions and commonly found in South-East Asia, including Thailand. It is one of the ingredients of “tripala”, an Ayurvedic formulation that is believed to promote health, immunity and longevity [1]. This formulation, rich in antioxidants, is frequently used in Ayurvedic medicine to treat many diseases such as anemia, jaundice, constipation, asthma, fever and chronic ulcers [2]. The fruit of *T. bellerica* has been used to treat various ailments in the folklore medicine [3]. Antibacterial [4], antidiabetic, and antioxidant [5] activities of crude extracts of *T. bellerica* have been reported. The fruit is also reported to have purgative [6], cardiac depressant, hypotensive and choleretic effects [7]. Chemically, the presence of  $\beta$ -sitosterol, gallic acid, ellagic acid, ethyl gallate, chebulagic acid, mannitol, glucose, galactose, rhamnose, and fructose have been reported in the fruit of *T. bellerica* [8-9]. To investigate the immunomodulatory effects of the *T. bellerica* extract in vitro, phagocytic activity of mouse peritoneal macrophages on nitroblue tetrazolium dye reduction and lysosomal enzyme activity and proliferation of murine splenic lymphocytes using the MTT assay were assayed.

## Materials and Methods

### Plant material

Dried fruits of *T. bellerica* were collected in February 2007 and were authenticated by the botanist at the Department of Pharmaceutical Chemistry and Pharmacognosy, Faculty of Pharmaceutical Sciences, Naresuan University, Phitsanulok, Thailand. A specimen was prepared and deposited at the herbarium of Faculty of Pharmaceutical Sciences, Naresuan University, Phitsanulok, Thailand.

### Chemicals

3-(4,5-Dimethylthiazol-2-yl)-2,5-diphenyltetrazolium bromide (MTT), nitroblue tetrazolium (NBT) dye, *p*-nitrophenyl phosphate (*p*-NPP), phytohemagglutinin (PHA), concanavalin A (Con A), lipopolysaccharide (LPS), pokeweed mitogen (PWM), dimethyl sulfoxide (DMSO), phorbol-12-myristate-13-acetate (PMA), zymosan A, and antibiotic-antimycotic solution (100 U penicillin, 100  $\mu$ g streptomycin, and 0.25  $\mu$ g/ml amphotericin B) were purchased from Sigma-Aldrich (Germany).  $\beta$  – Mercaptoethanol and Triton-X were purchased from Fisher Scientific (UK). Fetal bovine serum (FBS) and RPMI-1640 medium were purchased from GIBCO/BRL Invitrogen (Scotland).

### Animals

Female ICR mice (5-6 weeks old) were obtained from the National Laboratory Animal Center, Mahidol University, Bangkok, Thailand. The animals were housed under standard conditions at  $25\pm 2$  °C and fed standard pellets and tap water. The experiments were conducted under the surveillance of the Ethics Committee of Naresuan University, Thailand.

#### *Preparation of extracts*

The dried fruits of *T. bellerica* were extracted by maceration in methyl alcohol for 24 h and then filtered. The filtrate was evaporated under reduced pressure until dry, and a yield of 31% (w/w of dried material) of the extract was obtained. To prepare extract concentrations of 0.1, 1, 10, 100 and 500 µg/ml, the extract was dissolved in 0.1% DMSO in phosphate buffer saline (PBS) solution. Insoluble material was removed by centrifugation and the extract solution was sterilised by passage through a 0.2 µm filter. 0.1% DMSO in PBS was used as control in all experiments.

#### *Preparation of peritoneal mouse macrophages*

Peritoneal macrophages were isolated following intraperitoneal injection of FBS as a stimulant [10]. Three days later, the peritoneal exudate was collected by peritoneal lavage with RPMI 1640 medium supplemented with 10% heat-inactivated FBS, 50 µM 2-mercaptoethanol, 100 U penicillin, 100 µg streptomycin and 0.25 µg/ml amphotericin B (complete RPMI; CRPMI). The exudate was centrifuged at 2000 rpm at 25 °C for 10 min, and the cells were washed twice and re-suspended in CRPMI medium. The cell number was adjusted to  $1 \times 10^6$  cells/ml, and cell viability was tested by the trypan-blue dye exclusion technique.

#### *Preparation of mouse splenocytes*

Mice were sacrificed, and the spleens were removed aseptically. Single cells were prepared by mincing spleen fragments and pressing through a stainless 200-mesh screen in CRPMI medium. After centrifugation at 2000 rpm at 25 °C for 10 min, the cells were washed twice and re-suspended in CRPMI medium. The cell number was adjusted to  $1 \times 10^6$  cells/ml, and cell viability was tested by the trypan-blue dye exclusion technique.

#### *Nitroblue tetrazolium (NBT) dye reduction assay*

The NBT dye reduction assay was carried out as previously described [11]. Macrophages ( $1 \times 10^5$  cells/well) were treated with the extract for 24 h at 37 °C in a 5% CO<sub>2</sub> humidified incubator. Cells were incubated with zymosan A ( $5 \times 10^6$  particles/well) and 3 mg/ml NBT dye. After incubation for 60 min, the adherent cells were rinsed vigorously with RPMI medium and washed four times with methanol. After air drying, 2 M KOH and DMSO were added and the absorbance was measured at 570 nm using a microplate reader (Bio-Tek Instrument Inc., USA). The phagocytic index (PI) was determined by the ratio of optical density of the test sample to that of the control.

#### *Cellular lysosomal enzyme activity assay*

The cellular lysosomal enzyme activity was used to determine the acid phosphatase activity in the phagocytes as previously described [12]. Macrophages ( $1 \times 10^5$  cells/well) were treated with the extract for 24 h at 37 °C in a 5% CO<sub>2</sub> humidified atmosphere. The medium was removed by aspiration, and 0.1% Triton X-100, 10 mM *p*-NPP solution and 0.1 M citrate buffer (pH 5.0) were added to each well. The cells were further incubated for 30 min, and 0.2 M borate buffer (pH 9.8) was then added. The absorbance was measured at 405 nm using a microplate reader. The PI value was calculated as in the NBT dye reduction assay.

### *Mitogen-induced splenocyte proliferation assay*

The MTT technique was used to detect lymphocyte proliferation as previously described [13]. The optimum dose (5 µg/ml) of mitogen (PHA, Con A, LPS and PWM) was used as positive control. Briefly, splenocyte suspensions were treated with extract and mitogen for 48 h at 37 °C in a humidified 5% CO<sub>2</sub> atmosphere. Subsequently, 5 mg/ml MTT was added, and incubation continued for 4 h. The culture medium was removed by aspiration, and 0.04 M HCl in isopropyl alcohol and distilled water was added. The absorbance was measured at 570 nm using a microplate reader. The stimulation index (SI) was defined as the ratio of optical density of the test sample to that of mitogen.

### *Statistical analysis*

All experiments were performed in triplicate and the results were expressed as mean ± S.E. Statistical significance was analysed using the Student's *t*-test. P values less than 0.05 and 0.01 were considered significant.

## **Results and Discussion**

Immune activation is an effective and protective approach against emerging infectious diseases [14], and alternative medicine is becoming more popular for the treatment of these illnesses. *T. bellerica* has been used as a traditional remedy in Thailand [3] and various pharmacological activities, such as antioxidant [5], antibacterial [4], anti-HIV, antimalarial, and antifungal activities [15] have been reported. Among the array of medicinal properties attributed to it, a significant one is its therapeutic immunomodulating activity. Thus, this in vitro study was undertaken to determine whether an extract of *T. bellerica* fruit has any immunomodulatory activity.

It is well known that macrophages play a significant role in the defense mechanism against host infection and proliferation of tumour cells. The modulation of macrophage antitumour properties by various biological response modifiers is an area of interest for cancer chemotherapy [16].

As shown in Figure 1, macrophages treated with 500 µg/ml of *T. bellerica* extract stimulated NBT dye reduction, with the maximum PI value of about 1.5. After treatment, lysosomal activity was enhanced, with the PI value being approximately 1.3 compared to the control. The results indicated that the extract not only activated oxidative burst reduction, but also stimulated acid phosphatase production.

Although the phagocytic activity of the *T. bellerica* extract has never been reported, the superoxide anion production response of gallic acid, an active component isolated from *T. bellerica* extract, has been discussed. Previous reports of a slight increase of reactive oxygen species (ROS) production in macrophage RAW 264.7 cells in response to gallic acid [17] were consistent with our results. However, the suppressant effect on macrophage chemiluminescence [18] and the inhibition of superoxide scavenging of gallic acid [5] were also presented. Therefore, the compounds responsible for phagocytic activity may be either gallic acid or other phytochemicals present in *T. bellerica*.

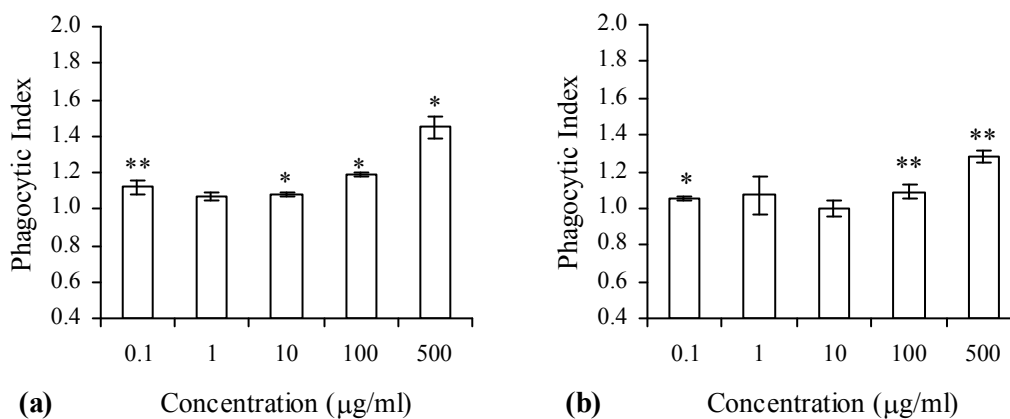


**Figure 1.** Effects of *T. bellerica* methanolic extract on in vitro phagocytosis response of mouse macrophages: (a) nitroblue tetrazolium (NBT) dye reduction, (b) lysosomal enzyme activity. Each value represents the mean  $\pm$  S.E. of triplicate experiments, compared to the control. (\* $P$ <0.01, \*\* $P$ <0.05)

The release of nitric oxide, superoxide anion, hydrogen peroxide and lysosomal enzyme from activated macrophages is an enzyme-controlled process. So it is possible that the extract may induce some alteration in the mechanism of activation of the related enzyme such as phosphotyrosine phosphatase, which could result in an increase of  $O_2^-$  [19]. Moreover, the effect of the extract at high concentrations on the stimulation of phagocytic activity may be due to a significant amount of active ingredients contained in *T. bellerica* extract. These observations suggest a possible application of *T. bellerica* to the treatment of microbial infections and cancer.

Lymphocyte transformation is an in vitro technique commonly used to assess cellular immunity in humans and other animals [20]. In this study, the proliferative response of lymphocytes, in terms of metabolic activity augmented by the *T. bellerica* extract, was assessed by a colorimetric MTT assay. Since the presence of mitogen in the system can affect the possible activation pathway of the extract [21], PHA and Con A were used for T cell activation whereas LPS and PWM were used to stimulate B cell proliferation through T cell-independent and T cell-dependent pathways respectively [10].

In the presence of PHA, the extract at 100 and 500  $\mu$ g/ml stimulated the lymphocyte proliferation with the maximum SI value of about 5.8 (500  $\mu$ g/ml), compared to treatment with PHA alone. Treatment with extract and Con A caused a dual response in a dose-dependent manner. The extract at low concentrations (0.1-10  $\mu$ g/ml) caused suppression of lymphocyte proliferation, with a minimal SI value of about 0.7 (0.1  $\mu$ g/ml), while the extract at high concentrations (100 and 500  $\mu$ g/ml) led to activation, with a maximal SI value of 4.5 (500  $\mu$ g/ml). With LPS, the extract at 100 and 500  $\mu$ g/ml increased lymphocyte proliferation with a maximal SI value of 4.5 (500  $\mu$ g/ml).

Moreover, a biphasic dose-dependent response was observed after treatment with the extract and PWM, similar to that observed after treatment with extract and Con A (Figure 2).

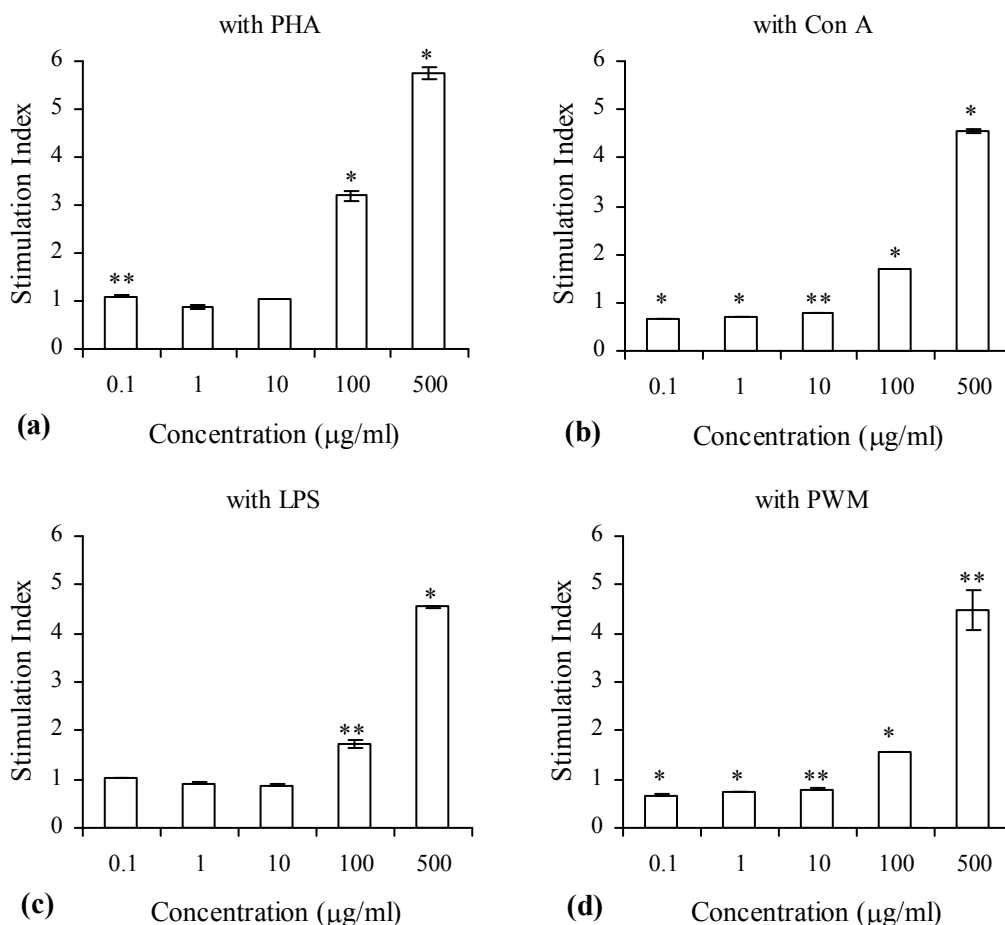


**Figure 2.** Effects of *T. bellerica* methanolic extract with 5 µg/ml mitogen on the in vitro proliferation response of mouse lymphocytes: (a) with PHA, (b) with Con A, (c) with LPS, (d) with PWM. Each value represents the mean ± S.E. of triplicates, compared to mitogen alone. (\* $P < 0.01$ , \*\* $P < 0.05$ )

Our investigation suggested that the *T. bellerica* extract affected T cell proliferation mainly through the same mechanism as PHA. The extract with LPS and PWM also affected B cell proliferation through T cell-independent and T cell-dependent mechanisms respectively. The results indicated that the extract affected cellular mediated immunity (CMI) rather than humoral mediated immunity (HMI). The extract inhibited PHA-induced human lymphocyte proliferation [22], but induced some enhancement of mouse splenic B-cells [23]. Since both inhibitory and stimulatory activities of gallic acid on lymphocyte proliferation have been previously reported, gallic acid might be responsible for this activity. Moreover, this circumstantiated the evidence that the same extract exerted a biphasic response, depending on the applied concentration. This was in agreement with the effects of other plants, which had either stimulatory or inhibitory activities on the immune response [24]. Besides gallic acid, there were other phytochemical compounds present in the fruit of *T. bellerica*, such as ellagic acid, ethyl gallate, chebulagic acid and  $\beta$ -sitosterol [8-9]. Three lignans and one flavan from the *T. bellerica* extract showed significant anti-HIV, antimalarial, and antifungal activity in vitro [15]

Therefore, it is possible that other compounds contained in *T. bellerica* extract might be responsible for the immunomodulatory activity as well.

## Conclusions

The present study has confirmed the traditional uses of *T. bellerica*, showing it has an immunomodulatory property that can differently alter both macrophage phagocytic activity and proliferation of splenic lymphocytes. Furthermore, the *T. bellerica* extract has immunosuppressant effects at low concentrations while stimulatory activity is observed at high concentrations. These results suggest a potential therapeutic application of this plant in the treatment of disease associated with the functions of phagocytes and lymphocytes. In vivo immunological assays and characterisation of the mechanism of action of the extract need to be further evaluated.

## Acknowledgement

This study was supported by the National Research Council of Thailand (Grant No. AR79/2550).

## References

1. G. C. Jagetia, M. S. Baliga, K. L. Malagi, and M. S. Kamath, "The evaluation of the radioprotective effect of Tripala (an ayurvedic rejuvenating drug) in the mice exposed to radiation", *Phytomedicine*, **2002**, 9, 99-108.
2. T. Sandhya and K. P. Mishra, "Cytotoxic of breast cancer cell line, MCF 7 and T 47 D to triphala and its modification by antioxidants", *Cancer Lett.*, **2006**, 238, 304-313.
3. N. Bunyaphatsara, "Medicine plants (4)", Prachachon Publishing Ltd., Bangkok, **2000**, pp. 477-482.
4. I. Ahmad, Z. Mehmood, and F. Mohammad, "Screening of some Indian medicinal plants for their antimicrobial properties", *J. Ethnopharmacol.*, **1998**, 62, 183-193.
5. M. C. Sabu and R. Kuttan, "Anti-diabetic activity of medicinal plants and its relationship with their antioxidant property", *J. Ethnopharmacol.*, **2002**, 81, 155-160.
6. M. D. Chakravarti and J. N. Tayal, "Preliminary examination of the fruits of *Terminalia bellerica* Roxb", *Sci. Culture*, **1947**, 13, 122.
7. H. N. Siddiqui, "Studies on *Terminalia bellerica* Roxb: effect on bile secretion and pharmacodynamic properties", *Indian J. Pharmacol.*, **1963**, 25, 297-302.
8. A. K. Nandy, G. Poddar, M. Sahu, P. Manto, and B. Shashi, "Triterpenoids and their glucosides from *Terminalia bellerica*", *Phytochemistry*, **1989**, 28, 2769-2772.
9. L. R. Row and P. S. Murty, "Chemical examination of *Terminalia bellerica* Roxb", *Indian J. Chem.*, **1970**, 8, 1047-1048.
10. A. Manosroi, A. Saraphanchotiwitthaya, and J. Manosroi, "Immunomodulatory activities of *Clausena excavata* Burm. f. wood extracts", *J. Ethnopharmacol.*, **2003**, 89, 155-160.
11. P. Rainard, "A colorimetric microassay for opsonins by reduction of NBT in phagocytosing bovine polymorphs", *J. Immunol. Methods*, **1986**, 90, 197-201.

12. I. Suzuki, H. Tanaka, Y. Adachi, and T. Yadomae, "Rapid measurement of phagocytosis by macrophages", *Chem. Pharm. Bull.*, **1998**, 36, 4871-4875.
13. T. Mosmann, "Rapid colorimetric assay for cellular growth and survival: application to proliferation and cytotoxicity assays", *J. Immunol. Methods*, **1983**, 65, 55-63.
14. C. J. Hackett, "Innate immune activation as a broad-spectrum biodefense strategy: prospects and research challenges", *J. Allergy. Clin. Immunol.*, **2003**, 112, 686-694.
15. R. Valsaraj, P. Pushpangadan, U. W. Smitt, A. Adersen, S. B. Christensen, A. Sittie, U. Nyman, C. Nielsen, and C. E. Olsen, "New anti-HIV-1, antimalarial, and antifungal compounds from *Terminalia bellerica*" *J. Nat. Prod.*, **1997**, 60, 739-742.
16. N-S. Kang, S-Y. Park, K-R. Lee, S-M. Lee, B-G. Lee, D-H. Shin, and S. Pyo, "Modulation of macrophage function activity by ethanolic extract of larvae of *Holotrichia diomphalia*" *J. Ethnopharmacol.*, **2002**, 79, 89-94.
17. V. Houde, D. Grenier, and F. Chandad, "Protective effects of grape seed proanthocyanidins against oxidative stress induced by lipopolysaccharides of periodontopathogens", *J. Periodontol.*, **2006**, 77, 1317-1319.
18. P. R. Tam and R. D. Hinsdill, "Screening for immunomodulators: effects of xenobiotics on macrophage chemiluminescence in vitro", *Fundam. Appl. Toxicol.*, **1990**, 14, 542-553.
19. M. C. Carreras, N. A. Riobo, G. A. Pargament, A. Boveris, and J. J. Poderoso, "Effects of respiratory burst inhibitors on nitric oxide production by human neutrophils", *Free Rad. Res.*, **1997**, 26, 325-334.
20. M. Horsmanheimo, "Correlation of tuberculin- induce lymphocyte transformation with skin test reactivity and with clinical sarcoidosis", *Cellular Immunol.*, **1974**, 10, 329-337.
21. A. Nakamura, K. Nagai, S. Suzuki, K. Ando, and G. Tamura, "A novel method of screening for immunomodulating substances, establishment of an assay system and its application to culture broths of microorganisms", *J. Antibiotic*, **1986**, 39, 1148-1154.
22. A. Serrano, C. Palacios, G. Roy, C. Cespon, M. L. Villar, M. Nocito, and P. Gonzalez-Porque, "Derivatives of gallic acid induce apoptosis in tumoral cell lines and inhibit lymphocyte proliferation", *Arch. Biochem. Biophys.*, **1998**, 350, 49-54.
23. Z. Q. Hu, M. Toda, S. Okubo, Y. Hara, and T. Shimamura, "Mitogenic activity of (-) epigallocatechin gallate on B-cells and investigation of its structure-function relationship", *Int. J. Immunopharmacol.*, **1992**, 14, 1399-1407.
24. N. Kovačević, M. Čolić, A. Backović, and Z. Došlov-Kokoruš, "Immunomodulatory effects of the methanolic extract of *Epimedium alpinum* in vitro", *Fitoterapia*, **2006**, 77, 561-567.

*Full Paper*

## **A flow injection system for the spectrophotometric determination of lead after preconcentration by solid phase extraction onto Amberlite XAD-4**

**Jintana Klamtet\*, Nungruthai Suphrom, and Chonthicha Wanwat**

Department of Chemistry, Faculty of Science, Naresuan University, Phitsanulok, 65000, Thailand

\* Corresponding author, e-mail: [jintanaki@nu.ac.th](mailto:jintanaki@nu.ac.th)

*Received: 6 February 2008 / Accepted: 7 July 2008 / Published: 9 July 2008*

---

**Abstract:** An on-line flow injection analysis (FIA) system for determination of lead (II) in water samples with a preconcentration step and spectrophotometric detection was investigated. The system is based on preconcentration of lead (II) on a column packed with Amberlite XAD-4 resin and detection by means of 4-(2-pyridylazo)resorcinol (PAR)-lead complex formation with maximum absorption at 523 nm. Chemical and FIA variables influencing performance of the system were optimised. Two linear calibration curves with a range of 0.01 - 0.40 and 0.40 – 0.80 mg L<sup>-1</sup> were obtained. The developed system allowed a throughput rate of 16 samples h<sup>-1</sup> with a 9-fold enrichment factor and a detection limit of 7 µg L<sup>-1</sup>. Relative standard deviation for 10 replicated injections of 0.25 mg L<sup>-1</sup> was 2.3%. Recoveries of the method were in the range of 80-94 %. The procedure was validated by analysis of lead (II) in real water samples, and the results were statistically compared with those obtained by flame atomic absorption spectrophotometry (FAAS). The results obtained both by the proposed method and by FAAS were in good agreement.

**Keywords:** flow injection analysis (FIA), determination of lead, 4-(2-pyridylazo)resorcinol, Amberlite XAD-4

---

## Introduction

Lead belongs to those trace heavy metals that are of major interest in environmental protection due to its high toxicity [1]. The determination of lead in environmental samples plays an important role in the monitoring of environmental pollution. Lead is used in storage batteries, cable sheaths, solders and radiation shields and it is widely distributed in the nature [2]. It is confirmed that most of the lead contamination in humans is from foods and drinks consumed. Lead in the water system has a serious influence on the quality of life especially in developing countries. Even small amounts of lead that enter the environment can result in elevated concentrations that can result in adverse effects. A regular absorption of small quantities of lead may cause serious injuries to health such as encephalopathy, kidney damage and several adverse effects in the body [3-4]. In natural water, its typical concentration lies between 2-10  $\mu\text{g L}^{-1}$ , whereas the upper limit recommended by WHO is less than 10  $\mu\text{g L}^{-1}$  [5]. Due to its toxicity and accumulative power, determination of lead has gained a wide interest. This metal is generally present in small concentrations in environmental samples, therefore sensitive and selective methods for determination of lead are needed. Electrothermal atomic absorption spectrometry (ETAAS) is a frequently used technique for determination of lead and other toxic trace elements. This technique is, however, very expensive and needs a separation and preconcentration procedure to avoid some shortcomings associated with matrix interferences [6]. Flame atomic absorption spectrometry (FAAS) is a more frequently used technique due to its simplicity and lower cost, although this method has a limited sensitivity for lead so a preconcentration step is often required to improve the detection limit [5, 7-9]. Other detection techniques are also used such as inductively coupled plasma mass spectrometry (ICP-MS) [10], hydride generation-inductively coupled plasma-atomic emission spectrometry (HG-ICP-AES) [11], and X-ray fluorescence spectrometry [12]. However, the spectrophotometric method is still one of the most important detection techniques in flow injection analysis for the determination of lead due to its ease of handling and comparatively low cost as well as its speed, precision and accuracy.

However, the lead content in natural water samples is incompatible with the detection limit of the spectrophotometric detection. To solve this problem a preconcentration procedure is required. Solid phase extraction is an attractive technique based on the use of a sorbent that retains the analyte, which is then eluted from the sorbent using a suitable solvent [13]. Various sorbents such as activated carbon [14], silica gel polymeric fibre [15-16] and Amberlite XAD resins [4-5, 13, 17-18] have been used to preconcentrate trace metal ions from various media. However, there is no report in the literature on the use of Amberlite XAD-4 packed in a minicolumn for preconcentration and determination of lead by flow injection analysis with spectrophotometric detection.

This present work reports on the procedure for the determination of lead in natural water samples by an on-line flow injection analysis system coupled with a minicolumn containing Amberlite XAD-4 resin (a non-ionic polystyrene-divinylbenzene polymer with a high surface area of 725  $\text{m}^2 \text{g}^{-1}$ ) which is usually used as solid adsorbent to adsorb hydrophobic molecules from a polar solvent. Amberlite XAD-4 has aromatic moieties in its structure which give the polymeric adsorbent excellent physical, chemical and thermal stability [19]. In addition, this resin has a high surface area and a suitable pore size for Pb(II) to be adsorbed before elution. However, the pH of the solution in this determination must be strictly controlled in order to enhance the selectivity. In this present study, the

optimisation of conditions for the on-line preconcentration and flow injection determination of lead has been carried out and applied successfully for natural waters.

## Materials and Methods

### *Materials*

All the reagents used were of analytical reagent grade, and the solutions were prepared in deionised water. A Pb (II) stock solution ( $100 \text{ mg L}^{-1}$ ), obtained by dissolving 0.1598 g of lead nitrate (Fluka, Switzerland) in deionised water and 2 mL of concentrated nitric acid then making up the solution to 1 L, was used to prepare working standard solutions of lead in the range 0.10-0.70  $\text{mg L}^{-1}$ . A  $0.20 \text{ mol L}^{-1}$  hydrochloric acid used as eluent solution was prepared from dilution of 4.27 mL concentrated hydrochloric acid (36%; J.T. Baker, U.S.A.) to 250 mL with deionised water.

A  $3 \times 10^{-4} \text{ mol L}^{-1}$  4-(2-pyridylazo)resorcinol monosodium hydrate (PAR) (Fluka) solution was obtained by dissolving 0.0178 g the chemical in 250 mL deionised water. Borate buffer solution (pH 9) was prepared by dissolving 19.08 g of sodium tetraborate (Ajax Finchem, New Zealand) in 1000 mL of deionised water.

### *Preconcentration column*

The acidic and basic impurities of Amberlite XAD-4 resin (Acros Organic, USA) were removed as described earlier [18] prior to its use. The preconcentration column was prepared by packing a small acrylic plastic tube (1.3 cm in length  $\times$  1 mm i.d.) with the Amberlite XAD-4 resin. The ends of the tube were fitted with a commercial absorbing cotton to keep the adsorbent material inside the tube.

### *Apparatus and method*

A flow injection manifold is depicted in Figure 1. It consists of two pumps (FIAS300 Perkin Elmer, Germany), a UV-Vis spectrometer (Lambda 2S, Perkin Elmer, Germany) as detector which has been described in previous papers [20-21]. The preconcentration column was incorporated with a six-way valve. The Amberlite XAD-4 was cleaned by passing deionised water into the column. The sample was loaded and passed through the column for 210 s with a flow rate  $2.2 \text{ mL min}^{-1}$ , after which time the valve was switched to allow HCl ( $0.20 \text{ mol L}^{-1}$ ) solution to pass through the column with a flow rate of  $2.9 \text{ mL min}^{-1}$  to elute the analyte. Then, the eluate was merged with the PAR solution and the buffer solution (pH 9) at the flow rate of 1.0 and  $1.8 \text{ mL min}^{-1}$  respectively, to form complex with the reagent in the reaction coil. The complex was detected at 523 nm [22] in a flow-through cell (8  $\mu\text{L}$  internal volume). PTFE tubing was used as flow lines and reaction coil in the system.

## Results and Discussion

### *Optimisation of chemical and FIA variables*

The operational conditions of the on-line FIA system and chemical variables were optimised in a univariant fashion in order to achieve a high signal and reproducibility. Both chemical and flow variables were studied using the flow system shown in Figure 1.

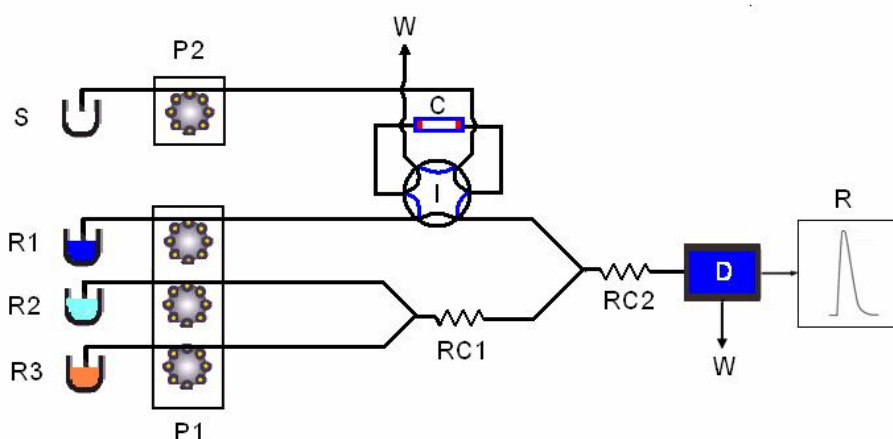


**Figure 1.** FIA system with on-line pre-concentration: R1 = eluent stream ( $0.20 \text{ mol L}^{-1}$  HCl), R2 = buffer solution, R3 =  $3.0 \times 10^{-4} \text{ mol L}^{-1}$  PAR solution, S = sample, P = peristaltic pump, I = injection valve, C = minicolumn, RC1 = reaction coil 1, RC2 = reaction coil 2, D = detector, W = waste, R = recorder or computer

### Preconcentration system

#### A. Sample loading time and flow rate

The sample loading time was investigated using  $0.10\text{--}0.70 \text{ mg L}^{-1}$  Pb(II) solutions at a sample flow rate of  $2.2 \text{ mL min}^{-1}$ . The result (Figure 2) clearly demonstrates that the sensitivity increases with an increase in preconcentration time and then gradually levels off, implying insufficient capacity of Amberlite XAD-4 resin and concentration of hydrochloric acid as eluent. Therefore, the loading time at 210 seconds was chosen as optimum time for subsequent experiments. The effect of sample loading flow rate was investigated by variation of the flow rate of sample at constant loading time. This means that the amount of Pb(II) passing through the column was changed as a function of flow rate. The result in Figure 3 shows that the best sensitivity and good reproducibility is obtained at a flow rate of  $2.2 \text{ mL min}^{-1}$ . (The sample flow rate higher than  $2.2 \text{ mL min}^{-1}$  gave distorted and double-peak signals due to high dispersion of sample zone in the FIA system and insufficient amount of resin for sorption.)

#### B. Elution

Dilute hydrochloric acid whose concentration was varied between  $0.10$  and  $0.30 \text{ mol L}^{-1}$  was selected for the elution of sorbed Pb(II) ions. The result indicated that  $0.20 \text{ mol L}^{-1}$  HCl was suitable for eluting Pb(II) without losing sensitivity. The optimum eluent flow rate was also determined to be  $2.9 \text{ mL min}^{-1}$ . All studied variables and their optimum values are listed in Table 1.

### FIA system

The influence of PAR concentration, used in pH 9 buffer solution, on complex formation was also studied within the range of  $1 \times 10^{-4}$ – $5 \times 10^{-4} \text{ mol L}^{-1}$ . As shown in Figure 4, further increase in PAR

concentration above  $3 \times 10^{-4} \text{ mol L}^{-1}$  does not give a significant increase in the sensitivity measured. The PAR concentration of  $3 \times 10^{-4} \text{ mol L}^{-1}$  was therefore chosen.

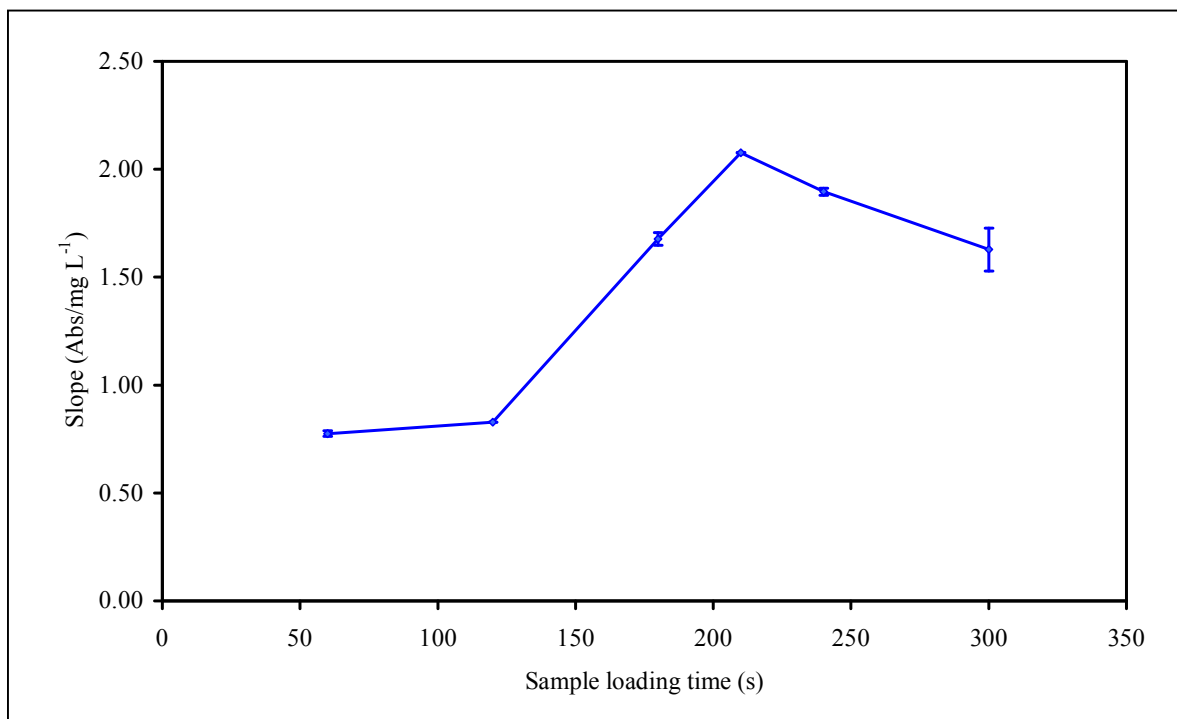


**Figure 2.** Effect of sample loading time on the sensitivity of Pb(II) determination using 1.3 cm × 1.0 mm column and sample flow rate of 2.2 mL min<sup>-1</sup>

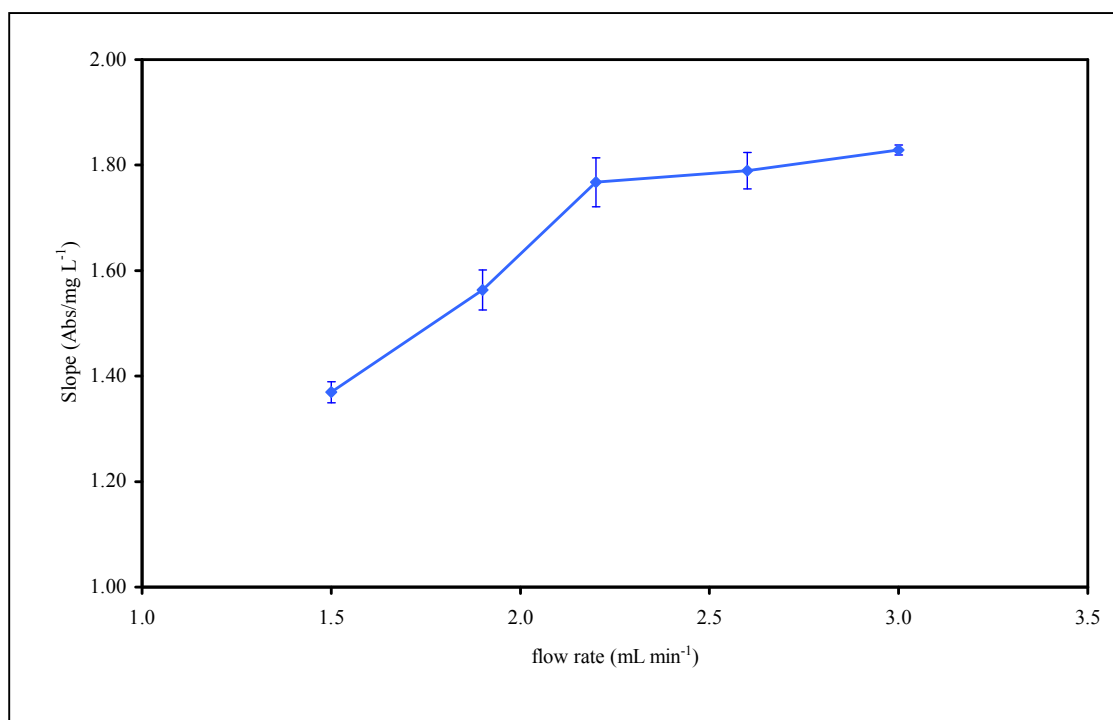


**Figure 3.** Effect of sample flow rate on the sensitivity of Pb(II) determination using 1.3 cm × 1.0 mm column and sample loading time of 210 s

Variation of the buffer solution and PAR solution flow rates was investigated between 0.8-2.2 mL min<sup>-1</sup>. The best responses were obtained at a flow rate of 1.0 and 1.8 mL min<sup>-1</sup> for buffer and PAR solution respectively. The flow rate of higher than 2.2 mL min<sup>-1</sup> was not used in order to avoid the dispersion and reduce consumption of the reagents.

In addition, the mixing coils were made from PTFE tubing with internal diameter and length of the two reaction coils (RC1 and RC2 in Figure 1) being 0.7 mm/400 mm and 0.7 mm/200 mm respectively. A longer coil and larger diameter gave broad and less intense signals due to excessive dispersion of the reactants into the sample stream. All studied variables and their optimum values are listed in Table 1.

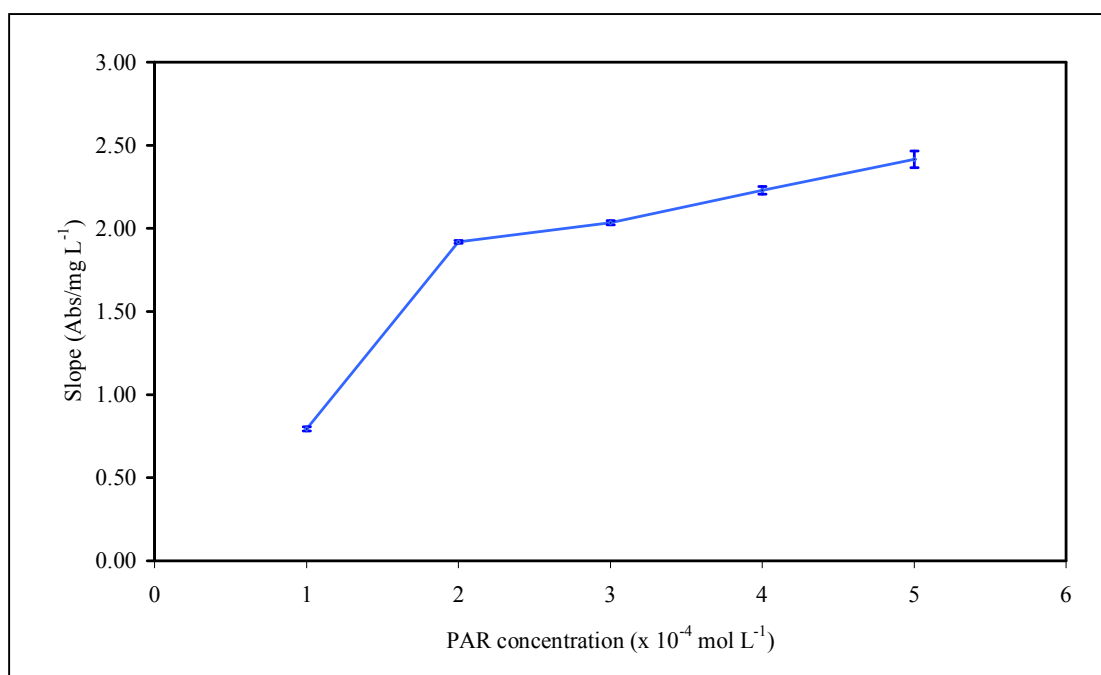


**Figure 4.** Effect of PAR concentration on the sensitivity of Pb(II) determination

#### *Interference study*

Potential interferences present in natural water, mainly Zn(II), Cd(II), Mn(II), Fe(II) and Ca(II), were evaluated. The levels of tolerated concentration of foreign ions were considered as maximum concentration found to cause less than 5 % change in signal compared with the signal for 0.25 mg L<sup>-1</sup> Pb(II) solution. Fe(II), Ca(II), Cd(II) or Zn(II) up to 10 µg L<sup>-1</sup> did not interfere with this determination. The maximum allowable values for Mn(II) and Cu(II) were 100 µg L<sup>-1</sup> and 50 µg L<sup>-1</sup> respectively. Thus, the pH for the determination of Pb(II) must be strictly controlled to enhance its specificity, coupled with using a solution containing phosphate and citrate to mask several interferences [23].

#### *Analytical performance*

The flow system using 210 s preconcentration time shows two linear ranges of concentration from 0.01 to 0.40 and 0.40 to 0.80 mg L<sup>-1</sup>. The calibration curve is represented by the regression

equation  $A = 2.403x + 0.0111$ ,  $r^2 = 0.9975$  and  $A = 1.278x + 0.530$ ,  $r^2 = 0.9970$  where  $A$  is the absorbance and  $x$  is the concentration of Pb(II) in  $\text{mg L}^{-1}$ . The detection limit estimated as three times

**Table 1.** Optimisation of FIA variables

Variable	Studied range	Optimum value
Sample loading time (s)	60-300	200
Elution time (s)	30-90	60
HCl concentration ( $\text{mol L}^{-1}$ )	0.10-0.30	0.20
PAR concentration ( $\text{mol L}^{-1}$ )	$1 \times 10^{-4}$ - $5 \times 10^{-4}$	$3 \times 10^{-4}$
pH of buffer solution	5-11	9
Flow rate ( $\text{mL min}^{-1}$ )		
- sample	1.5-3.0	2.2
- HCl	2.2-3.5	2.9
- PAR	0.8-2.2	1.8
- buffer	1.0-2.2	1.0
Reaction coil 1 (mm)		
- i.d.	0.5-1.0	0.7
- length	200-500	400
Reaction coil 2 (mm)		
- i.d.	0.5-1.0	0.7
- length	200-600	200

the standard deviation was  $7 \mu\text{g L}^{-1}$ . The repeatability of the method was calculated as the relative standard deviation (RSD) of the maximum absorbance from 10 replicates of injection of the standard solution containing  $0.25 \text{ mg L}^{-1}$  Pb(II), which was found to be 2.3%. The sample throughput of this method was 16 samples per hour. The recovery of lead from natural water samples was also studied. As can be seen in Table 2, the recovery of lead spiked to the water samples ranges from 80 to 94%. The result confirms the validity of the proposed method for the preconcentration of lead. Moreover, the preconcentration factor was calculated by comparing the slope of the analytical curve obtained before and after the preconcentration procedure [2], and was found to be *ca.* 9.

**Table 2.** The recovery results

Samples	Concentration of Pb(II) ( $\text{mg L}^{-1}$ )			
	Found	Added	Detected	% Recovery
3	0.02	0.15	0.14	80
		0.25	0.22	80
5	0.015	0.15	0.15	90
		0.25	0.25	94

*Determination of lead in natural water samples*

The on-line column preconcentration coupled with FIA method for lead determination was validated against FAAS method. The real water samples were collected from rivers and canals around Naresuan University in Phitsanulok province. To avoid effects of interference ions, the pH for the PAR-Pb(II) complex formation was carefully controlled and the determination carried out by using standard addition method to eliminate any matrix effect in the water samples. The results obtained (Table 3) have been calculated by assuming 100% recovery of lead ions. The statistical pair of *t*-test was used to compare the results from both methods. The results revealed no significant difference ( $t_{\text{cal}} = 2.56$  and  $t_{\text{critic } 95\%,4} = 2.77$ ) between them.

**Table 3.** Concentration of lead in real water samples (N=3)

Sample	Concentration of Pb(II) (mg L <sup>-1</sup> )	
	Proposed method	FAAS
1	0.057 ± 0.015	0.045 ± 0.003
2	0.057 ± 0.011	0.034 ± 0.007
3	0.053 ± 0.016	0.051 ± 0.002
4	0.060 ± 0.011	0.038 ± 0.005
5	0.038 ± 0.015	0.037 ± 0.002

### Conclusions

A simple, sensitive and low-cost FIA method with on-line preconcentration employing a column containing Amberlite XAD-4 resin has been proposed for the determination of lead in natural water. It gives good accuracy and reproducibility up to a maximum concentration of 0.25 mg L<sup>-1</sup> Pb(II) with a relative standard deviation of lower than 5%. The result can be obtained in 5 min after the sample introduction and the sample throughput is 16 h<sup>-1</sup>. The proposed system can achieve a detection limit of 7 µg L<sup>-1</sup> and a recovery of 80-94%. The preconcentration factor is 9-fold for the 7.7 mL sample loading. This method offers two linear detection ranges from 0.10-0.40 and 0.40-0.80 mg L<sup>-1</sup>. The method has been applied successfully to the analysis of real water samples and the results obtained are in good agreement with those obtained by FAAS method.

### Acknowledgement

The authors would like to thank the Faculty of Science, Naresuan University for the financial support during 2007 for this study.

**References**

1. United States Environmental Protection Agency, "Toxic Release Inventory", [http://www.epa.gov/tri/lawsandregs/lead/pb\\_fact.sheet.pdf](http://www.epa.gov/tri/lawsandregs/lead/pb_fact.sheet.pdf) (Retrieved, April **2001**).
2. A. S. di. Nezio, M. E. Palomeque, and B. S. Fernández band, "A sensitive spectrophotometric method for lead determination by flow injection analysis with on-line preconcentration", *Talanta*, **2004**, 63, 405-409.
3. T. W. Clarkson, I. Friberg , G. F. Nordberg, and P. R. Sager, "Biological monitoring of toxic metals", Kluwer Academic Publisher, New York, **1998**.
4. W. N. L. dos Santos, C. M. M dos Santos, J. L. O. Costa, H. M. C. Andrade, and S. L. C.Ferreira, "An on-line preconcentration system for determination of cadmium in drinking water using FAAS", *Microchem. J.*, **2004** , 77, 123-129.
5. P. K. Tewari and A. K. Singh, "Preconcentration of lead with Amberlite XAD-2 and Amberlite XAD-7 based chelating resins for its determination by flame atomic absorption spectrometry", *Talanta*, **2002**, 56, 735-744.
6. M. C. Yebra-Biurrun and A. Moreno-Cid Barinaga, "Literature survey of on-line spectroscopic methods for lead determination in environmental solid samples", *Chemosphere*, **2002**, 48, 511-518.
7. A. N. Araújo, R. C. C. Costa, and J. L. F. C. Lima, "Application of sequential injection analysis to the assay of lead retention characteristic by poly(vinylpyrrolidone):trace analysis of lead in waters", *Anal. Sci.*, **1999**, 15, 991-994.
8. I. Karadjova, G. Zachariadis, J. Boskou, and J. Stratis, "Electrothermal atomic absorption spectrometric determination of aluminium, cadmium, chromium, copper, iron, manganese, nickel and lead in olive oil", *J. Anal. Atom. Spectrom.*, **1998**, 13, 201-209.
9. P. Vinas, I. Lopaz-Garcia, M. Lanzon, and M. Hernandez-cordoba, "Direct determination of lead, cadmium, zinc and copper in honey by electrothermal atomic absorption spectrometry using hydrogen peroxide as a matrix modifier", *J. Agric. Food Chem.*, **1997**, 45, 3952-3956.
10. L. Hung-Wei, J. Shih-Jen, and L. Shin-Hung, "Determination of cadmium, mercury and lead in seawater by electrothermal vaporization isotope dilution inductively coupled plasma mass spectrometry", *Spectrochim acta B*, **1999**, 549, 1367-1375.
11. S. Chen, Z. Zhang, H. Yu, W. Liu, and M. Sun, "Determination of trace lead by hydride generation inductively coupled plasma-mass spectrometry, *Anal. Chim. Acta.*, **2002**, 463, 177-188.
12. A. Aragyraiki and M. H. Ramsey, "Evaluation of portable x-ray fluorescence instrumentation for in situ measurements of lead on contaminated land", *Analyst*, **1997**, 122, 743-749.
13. A. Uzun, M. Soylak, and L. Elçi, "Preconcentration and separation with Amberlite XAD-4 resin; determination of Cu, Fe, Pb, Cd, and Bi at trace levels in waste water samples by flame atomic absorption spectrometry" *Talanta*, **2001**, 54, 197-202.
14. Í. Narin, M. Soylak, L. Elçi, and D. Mehmet, "Determination of trace metal ions by AAS in natural water samples after preconcentration of pyrocatechol violet complexes on an activated carbon column", *Talanta*, **2000**, 52, 1041-1046.
15. A. Goswami, A. K. Singh, and B. Venkataramani, "8-Hydroxyquinoline anchored to silica gel via new moderate size linker: synthesis and applications as a metal ion collector for their flame atomic absorption spectrophotometric determination", *Talanta*, **2003**, 60, 1141-1154.

16. A. Goswami and A. K. Singh, "Enrichment of iron(II), Cobalt(II), Nickel(II), and Copper(II) by solid phase extraction with 1,8-dihydroxyanthraquinone anchored to silica gel before their determination by flame atomic absorption spectrometry", *Anal. Bioanal. Chem.*, **2002**, 374, 554-560.
17. W. Song, Z. Zhi, and L. Wang, "Amberlite XAD resin solid-phase extraction coupled on-line to a flow injection approach for the rapid enrichment and determination of phenols in water and waste waters" *Talanta*, **1997**, 44, 1423-1433.
18. P. K. Tewari and A. K. Singh, "Amberlite XAD-7 impregnated with Xylenol Orange: a chelating collector for preconcentration of Cd(II), Co(II), Cu(II), Ni(II), Zn(II) and Fe(III) ions prior to their determination by flame AAS", *Fresenius J. Anal. Chem.*, **2000**, 367, 562-567.
19. Rohm and Hass Company, "Amberlite XAD4", [http://www.ionexchanger.com/Pharmaceuticals/Bioprocessing\\_doc/us\\_english/xad4.pdf](http://www.ionexchanger.com/Pharmaceuticals/Bioprocessing_doc/us_english/xad4.pdf) (Retrieved, June **2008**).
20. J. Klamtet, "Development of flow injection analysis system for determination of iron(II) and total iron in ground water", *NU Science J.*, **2004**, 2, 4-8.
21. J. Klamtet, "Reverse flow injection analysis for determination of manganese (II) in natural water", *NU Science J.*, **2006**, 2, 165-173.
22. J. Klamtet, S. Sanguthai, and S. Sriprang, "Determination of lead in aqueous samples using a flow injection analysis system with on-line preconcentration and spectrophotometric detection", *NU Science J.*, **2007**, 4, 122-131.
23. F. R. P. Rocha, B. F. Reis, and J. J. R. Rohwedder, "Flow-injection spectrophotometric multidetermination of metallic ions with a single reagent exploiting multicommutation and multidetection", *Fresenius J. Anal. Chem.*, **2001**, 370, 22-27.

Full Paper

## **On-line preconcentration and determination of tetracycline residues in milk using solid-phase extraction in conjunction with flow injection spectrophotometry**

**Prinya Masawat<sup>1,\*</sup>, Sutthinee Mekprayoon<sup>1</sup>, Saisunee Liawruangrath<sup>2</sup>, Suphachock Upalee<sup>2</sup>, and Napaporn Youngvises<sup>3</sup>**

<sup>1</sup> Department of Chemistry, Faculty of Science, Naresuan University 65000, Thailand

<sup>2</sup> Department of Chemistry, Faculty of Science, Chiang Mai University 50200, Thailand

<sup>3</sup> Department of Chemistry, Faculty of Science and Technology, Thammasat University, 12121, Thailand

\* Corresponding author, e-mail : [prinyam@nu.ac.th](mailto:prinyam@nu.ac.th)

Received: 9 January 2008 / Accepted: 20 July 2008 / Published: 21 July 2008

---

**Abstract:** A simple, cheap and highly sensitive system with on-line preconcentration using solid-phase extraction in conjunction with flow injection spectrophotometry for the determination of tetracycline residues in milk samples is described. C<sub>18</sub> was used as packing material in a designed minicolumn used for preconcentration of tetracyclines. Tetracycline standard or sample solutions were dissolved in a mixed buffer solution of pH 4.0 containing boric acid, citric acid and sodium phosphate, then loaded to the minicolumn for 6 min followed by elution with a solution containing methanol : mixed buffer solution (40:60 by volume) of pH 6.5 The absorbance of the eluate was measured at 370 nm. The calibration graph was linear in the range of 0.20-1.00, 0.20-4.00, and 0.20-1.00 mg L<sup>-1</sup> for tetracycline (TC), oxytetracycline (OTC), and chlortetracycline (CTC) respectively. The limits of detection were 0.08, 0.10, and 0.09mg L<sup>-1</sup> for TC, OTC, and CTC respectively. Relative standard deviations for 20 replicated determinations of 0.20, 0.40, and 0.60 mg L<sup>-1</sup> of TC were 7.03, 7.23, and 6.55 % respectively. Per cent recoveries for four commercial types of milk: U.H.T., pasteurised, raw, and sterilised milk were in the range of 86–109 (TC), 90–109 (OTC), and 89–108 (CTC). The sample throughput was 6 h<sup>-1</sup>.

**Keywords:** tetracycline, oxytetracycline, chlortetracycline, tetracycline residues, solid-phase extraction flow injection spectrophotometry

---

## Introduction

The tetracyclines (Figure 1) have served for decades as an important class of antibiotics for the health of food-producing animals. They are antibiotics with a broad antibacterial spectrum and bacteriostatic activity, and have a good activity against acute diseases caused by Gram-positive and Gram-negative bacteria. They are licensed for use in a variety of food-producing animals including cattle, pigs, sheep, poultry and fish [1]. The use of these drugs has become a serious problem as regards their residues in milk or meat, which can be directly toxic to or else cause allergic reactions in some hypersensitive individuals. Even more important, low-level doses of the antibiotic in foodstuffs consumed for long periods can lead to problems regarding the spread of drug-resistant microorganisms. To ensure human food safety, maximum residue limits (MRLs) have been set for tetracycline, chlortetracycline and oxytetracycline in a number of tissue types, e.g. 0.3 mg kg<sup>-1</sup> in liver, 0.6 mg kg<sup>-1</sup> in kidney, 0.2 mg kg<sup>-1</sup> in eggs and 0.1 mg kg<sup>-1</sup> in milk and muscle tissues [2-3].

Generally, the presence of tetracyclines in milk arises from their use as part of therapy to treat animal diseases such as bovine mastitis and sometimes, in low concentrations, as constituents of animal feed to increase feed utility in accelerating animal growth. The availability of a simple and automatic method to control traces of these antibiotics in milk is of great analytical interest. High-performance liquid chromatography (HPLC) is one of the most popular and sensitive techniques for this purpose. Firstly, however, isolation of the tetracyclines from milk using some type of extraction and/or clean-up is required. One widely-used technique is solid-phase extraction (SPE). The tetracyclines are extracted then subjected to clean-up on a C<sub>8</sub> [4], a C<sub>18</sub> [5] and a copolymeric [6] SPE column followed by injection in the HPLC column. Because almost without exception these methods are time-consuming, the availability of alternative methods is always desirable.

Flow injection analysis (FIA) is a well-known technique that offers improvement in most batch methods, especially in the high sample throughput. For the tetracyclines, there are a few FIA methods available with several types of detection such as chemiluminescence [7], electrochemical method [8-9], and spectrophotometry [10-11]. The spectrophotometric FIA detection [10] for the tetracyclines is based on the formation of a coloured product by their reaction with 4-aminophenazone and hexacyanoferrate(III). However, this method has a limited concentration range. Under optimised conditions, the tetracyclines were determined in the range of 1-20 and 20-250 mg L<sup>-1</sup>. The lowest limit of detection is 0.2 mg L<sup>-1</sup> for doxycycline [10].

SPE off-line performance is both time consuming and complicated, and thus it is usually the slowest step of the analysis. One of the possibilities to facilitate and accelerate the analysis of samples is to integrate the mentioned preparation of samples with the use of SPE directly to FIA. There are some major trends in the on-line coupling of SPE to FI manifolds: (i) direct application of the real samples, without any pre-treatment, to the flow injection system ; (ii) integration of reaction (retention) and detection; and (iii) miniaturisation as a means of reducing sample and reagent consumption. In the present work, a simple system of on-line preconcentration using SPE in conjunction with flow injection spectrophotometry with low instrumental cost, high sensitivity and low detection limit has been developed for the determination of tetracycline residues in milk. The method is based on the retention of the tetracyclines onto C<sub>18</sub> and elution with mixed buffer solution and methanol adjusted to pH 6.5. The optimum conditions of this system were also studied such as wavelength, size and length of the minicolumn, type of eluent, preconcentration time, and flow rate of reagent. The performance of the developed system provided an enrichment factor [12] of about 30.

## Materials and Methods

### Chemicals and reagents

All chemicals were of analytical-reagent grade, except where otherwise stated. Deionised water was used.

Tetracycline (TC) standard solution (SIGMA, U.S.A) was dissolved in acetate buffer (pH 4.0). Working standard solutions ( $0.1-1.0 \text{ mg L}^{-1}$ ) were daily prepared by adequate dilution of  $50 \text{ mg L}^{-1}$  TC, the stock standard solution, in the acetate buffer.

Mixed buffer solutions of pH ranging from 2.0 to 7.5 were prepared by dissolving boric acid (Merck, Germany) (12.37 g), citric acid (Fisher Scientific, UK) (10.51 g) and trisodium phosphate dodecahydrate (Fisher Scientific, UK) (38.01 g) in de-ionised water, then diluting to 1 L.

A mixture of methanol (LAB-SCAN, Ireland) and mixed buffer solution (pH 6.5) at 40:60 volume ratio was used as eluent.

The reagents used for extraction of tetracycline antibiotics from milk were prepared from trichloroacetic acid (Fluka, Switzerland), citric acid monohydrate (Merck, Germany), disodium hydrogenphosphate dihydrate (Merck, Germany), and ethylenediaminetetraacetic acid (EDTA) disodium salt (Fisher Scientific, UK).

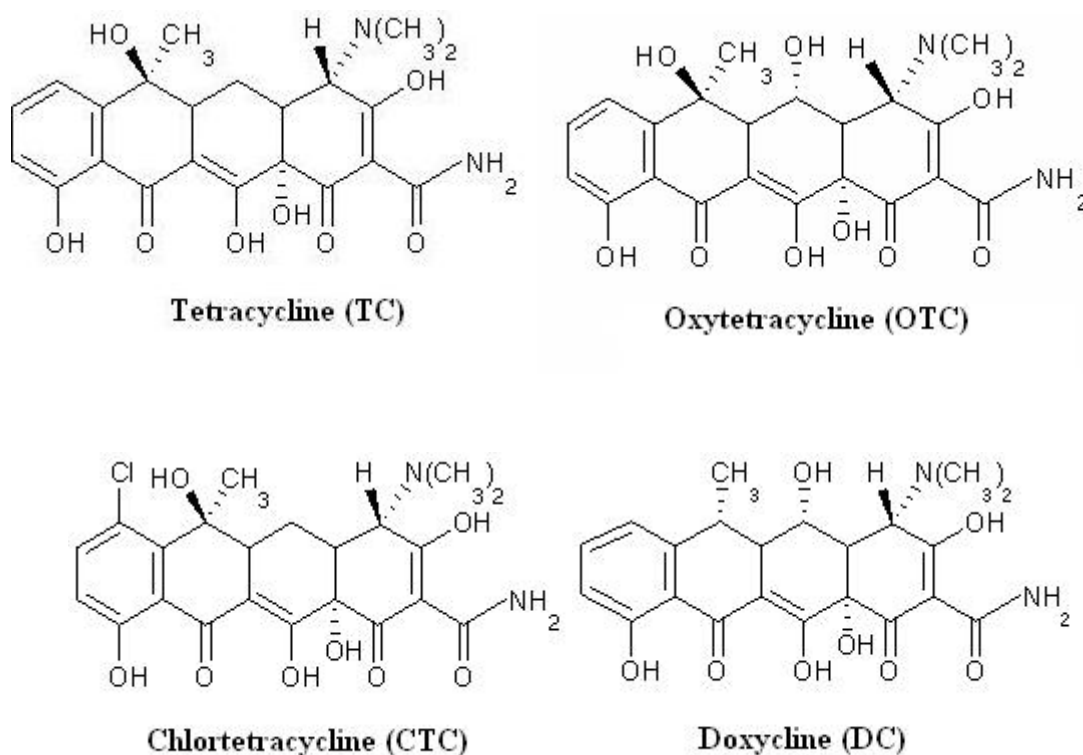


**Figure 1.** Structures of tetracycline antibiotics

### Sample preparation procedures

Tetracycline residues were determined in four commercial types of milk: U.H.T., pasteurised, sterilised, and raw milk obtained from a local market of Phitsanulok area in 2005. All samples were

collected in labeled dark plastic bags, transported to the laboratory and stored for a short time at 4°C prior to analysis.

An 5 mL aliquot of milk was placed in a glass centrifuge tube and 5 mL of 1.0 M trichloroacetic acid was added with shaking. Then 15 mL of McIlvain buffer (consisting of 10.5 g citric acid monohydrate, 14.2 g disodium hydrogenphosphate dihydrate, and 30.25 g EDTA disodium salt in 1 L of de-ionised water) was added and the mixture was centrifuged at 6000 rpm for 15 min. The supernatant was then passed through a filter with 0.45- $\mu\text{m}$  pore size followed by application to an online solid phase extraction-flow injection analysis (SPE-FIA) system.

#### *The on-line SPE-FIA*

The on-line SPE with flow injection spectrophotometric manifold is shown in Figure 2. A stream of solution (R1) containing a tetracycline (standard or sample) and eluent (R2) were controlled by a peristaltic pump (P, BIO RED, U.S.A). The tetracycline was loaded to a designed minicolumn (Figure 3) packed with  $\text{C}_{18}$  resin (Alltech, U.S.A). This minicolumn replaced the sample loop of the injection valve (Omnifit, England). The tetracycline adsorbed on the resin was desorbed by a stream of eluent (methanol : pH 6.5 buffer solution = 40:60) and carried past a flow-through cell (Hellma, Germany) located in the spectrophotometer (Ultrospec 4050, LKB BIOCHROM, UK) connected to a computer. All the tubing used was Teflon (0.8 mm id.), except the pump tubing which was Tygon. Connections were made with flexible T-piece sleeves. The absorbance of the tetracycline, which is proportional to its concentration, was recorded at 370 nm. Therefore, the amounts of the tetracycline in sample can be calculated from the calibration curve plotted between peak area and tetracycline concentration.

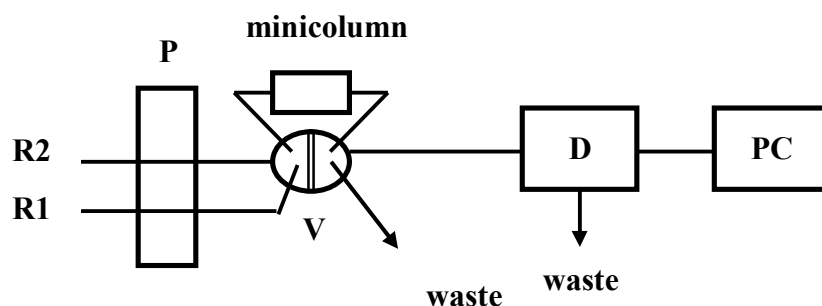


**Figure 2.** Flow injection manifold for the determination of tetracycline residues in milk: P = peristaltic pump, V = injection valve, D = detector (spectrophotometer), PC = personal computer,  $R_1$  = sample,  $R_2$  = eluent

#### *Recovery experiments, quantitative evaluation and detection limits*

Milk samples were fortified at 0.3, 0.5, 0.7, and 0.9  $\text{mg L}^{-1}$  by adding a solution of the tetracycline. The per cent recoveries of four commercial milk samples were in the range of 86-109% (for TC), 90-109% (for OTC), and 89-108% (for CTC). The detection limits calculated by using a

signal-to-noise (S/N) ratio of 3 [13] were 0.08, 0.10, and 0.09 mg L<sup>-1</sup> for TC, OTC, and CTC respectively. The quantity of each of the tetracyclines was calculated by applying the standard addition method.

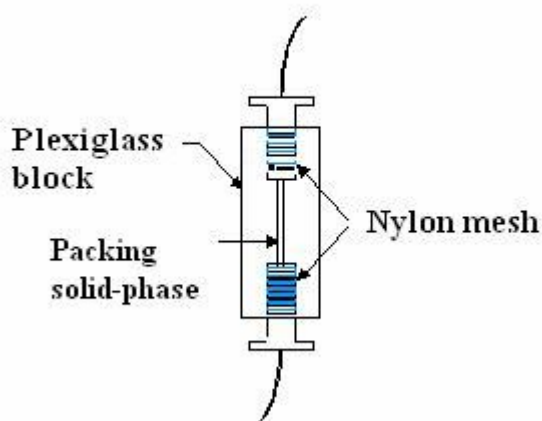


**Figure 3.** Minicolumn for the determination of tetracycline residues in milk (packing solid phase should be C<sub>18</sub> resin, 35-75 μm)

## Results and Discussion

In order to develop the method, various experiments were carried out. First, the absorption spectra were recorded to select the working wavelength. The influences of the following variables were then studied and the optimum values established: (a) preconcentration time; (b) pH of standard solutions; (c) type and pH of eluent; (d) flow rate; and (e) size and length of the designed minicolumn. Table 1 shows the initial conditions for optimisation of the on-line SPE-FIA using univariate method. After optimisation, the analytical figures of merit were studied. Finally, the developed procedure was applied to real milk samples.

**Table 1.** Initial conditions for optimisation of on-line SPE-FIA system for determination of tetracyclines

Condition	Initial value
wavelength	370 nm
TC concentration	0.1, 0.5 and 1.0 mg L <sup>-1</sup>
eluent (methanol: pH 7.0 mixed buffer solution)	50: 50 by volume
Flow rate	0.5 mL min <sup>-1</sup>
Size of minicolumn	1.0 cm in length, 0.3 cm i.d.
Solid-phase packing	C <sub>18</sub> , 35-75 μm

### *Absorption spectra*

The UV-VIS spectrum of TC ( $5 \text{ mg L}^{-1}$  in mixed buffer solution of pH 7.5) was obtained by batch method. The maximum absorption wavelength of TC was 370 nm as shown in Figure 4. This value was also obtained for OTC and CTC. Because of their polarity, the tetracyclines cannot be eluted from a polar normal-phase SPE cartridge (i.e. florisil, cyanopropyl, silica) and reverse-phase SPE cartridges are more commonly used [14]. The  $C_{18}$  clean-up method combined with McIlvaine buffer containing EDTA disodium salt for extraction was introduced in 1983 for the first time and appears to be the current standard method for the extraction and clean-up of tetracyclines in foods. Therefore,  $C_{18}$  was chosen as the packing material packed in the designed minicolumn, and the working wavelength was fixed at 370 nm.

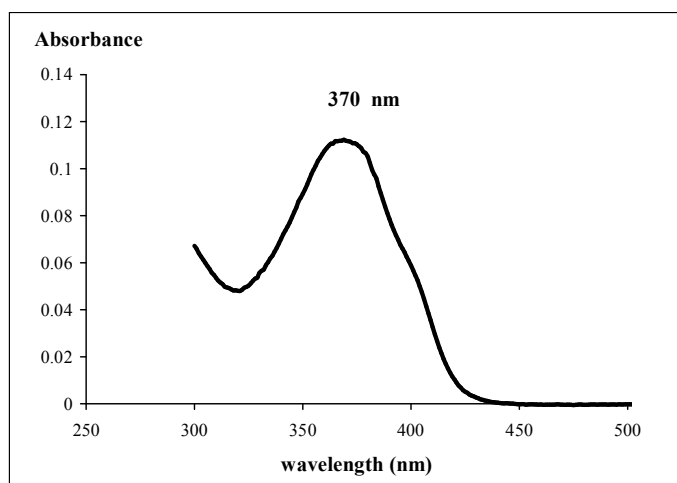


**Figure 4.** UV-VIS absorption spectrum of TC ( $5 \text{ mg L}^{-1}$  in pH 7.5 mixed buffer solution)

### *Preconcentration time*

The influence of preconcentration time on the analytical sensitivity was investigated between 2-8 min. As expected, the analytical sensitivity progressively increased with increasing preconcentration time (Figure 5). However, the peak shape of TC became distorted and broadened (not useable) when the preconcentration time was higher than 6 min. Thus, the preconcentration time of 6 min was chosen for the experiment.

### *pH of TC standard solution*

The influence of pH of the mixed buffer solution used for dissolving the TC standard was examined by varying the pH in the range of 2.0-7.5. As shown in Figure 6, the optimum pH that gave a high sensitivity for the analytes was in the acidic range (pH 3-4). At pH values higher than 4, the analytical sensitivity decreased significantly. A working pH value of 4.0 was chosen since the analytical sensitivity was highest.

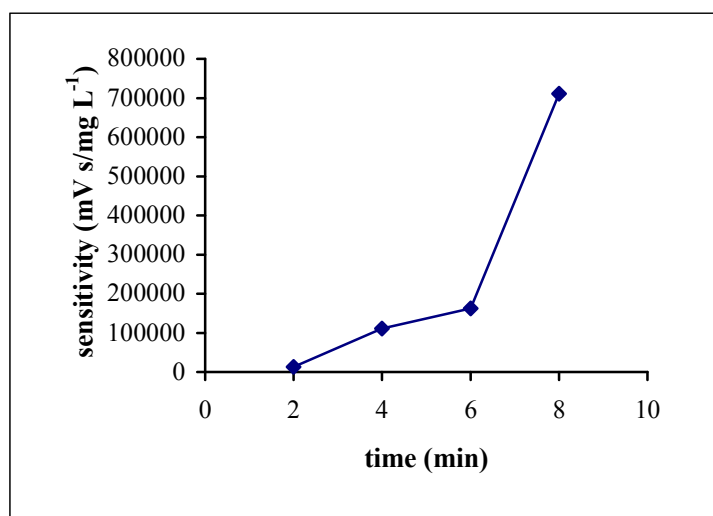


**Figure 5.** Effect of preconcentration time on analytical sensitivity for tetracycline standard solution

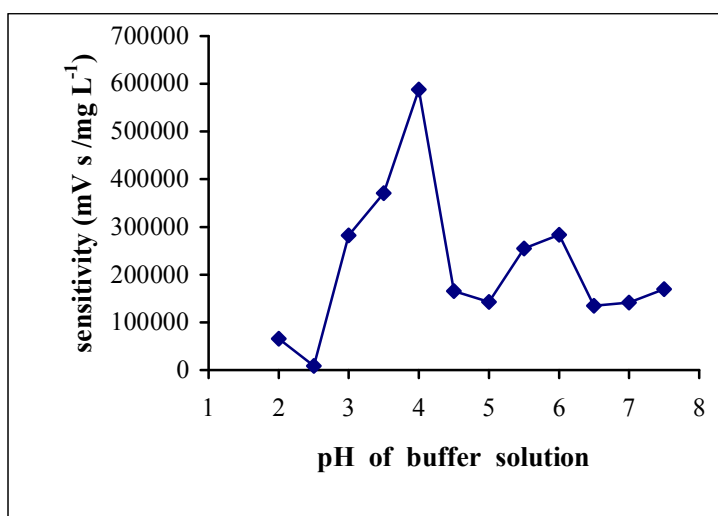


**Figure 6.** Effect of pH of buffer solution (for dissolving TC) on analytical sensitivity for tetracycline standard solution

#### *Type and pH of eluent*

The eluents containing methanol:mixed buffer solution at different ratios (10:90, 20:80, 30:70, 40:60, 50:50, and 60:40) were tested. It was found that bubbles were formed when more than 50% of methanol was used and the peak shapes became broadened when more than 60% of the buffer solution was used. The ratio of 40:60 for methanol to buffer solution was therefore chosen as eluent for TC. The influence of pH of the buffer solution used as eluent was investigated by varying the pH in the range of 2.0-7.5. As shown in Figure 7, a working pH value of 6.5 was chosen since the sensitivity was highest at this pH.

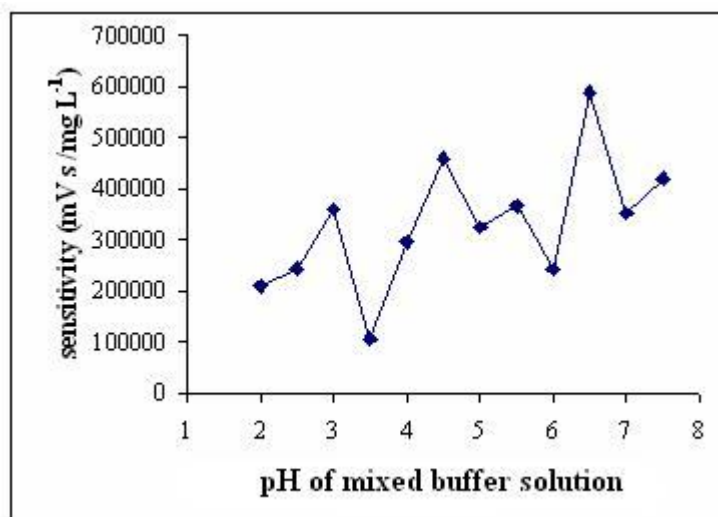


**Figure 7.** Effect of pH of mixed buffer solution (eluent) on analytical sensitivity for tetracycline standard solution

#### Flow rate

The effect of flow rate was investigated between 0.3-0.8 mL min<sup>-1</sup>. When the flow rate increased the analytical sensitivity (Figure 8) and the elution time progressively decreased and, consequently, the sampling frequency increased (3 h<sup>-1</sup> at 0.3 mL min<sup>-1</sup> to 7 h<sup>-1</sup> at 0.6 mL min<sup>-1</sup>). At lower flow rate, the peaks of TC were broader than those obtained at higher flow rate. However, no peak of TC at low concentration was detected when using flow rate higher than 0.6 mL min<sup>-1</sup>. This is apparently due to low sorption of TC on the C<sub>18</sub> resin. As a compromise, a 0.5 mL min<sup>-1</sup> flow rate was chosen.

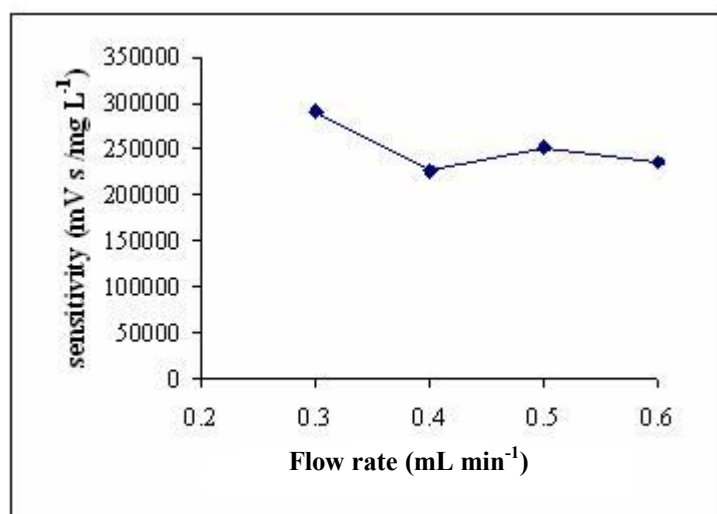


**Figure 8.** Effect of flow rate on analytical sensitivity for tetracycline standard solution

*Size and length of designed minicolumn*

In order to determine tetracycline residues in milk, preconcentration on the C<sub>18</sub> resin packed in a minicolumn is the crucial step. The influence of size and length of the designed minicolumn was then tested as exhibited in Table 2. It was found that the analytical sensitivity was strongly dependent on the length of the minicolumn. However, as the length increased the total analysis time also increased. Thus, the minicolumn type 1 (1.0 cm length and 0.3 cm i.d.) was chosen for the preconcentration purpose.

**Table 2.** Effect of minicolumn dimension on analytical sensitivity for tetracycline standard solution

Type	Size of minicolumn		Cell volume (cm <sup>3</sup> )	Analytical sensitivity* (mV s /mg L <sup>-1</sup> )
	Length (cm)	i.d. of minicolumn (cm)		
1	1.0	0.3	0.071	374162
2	3.0	0.3	0.210	661810

\* in triplicate

*Figures of merit*

Using the optimum conditions obtained (Table 3), figures of merit of the method proposed for the determination of tetracyclines are provided in Table 4. The linear range of the tetracyclines was 0.08-1.00 mg L<sup>-1</sup> for TC, 0.20-4.00 mg L<sup>-1</sup> for OTC and 0.20-1.00 mg L<sup>-1</sup> for CTC, with regression coefficients higher than 0.99 in all cases. It can be seen from Table 4 that the detection limits of TC, OTC, and CTC are lower than the MRL of each tetracycline [2-3]. Thus, the proposed on-line SPE-FIA is suitable for the determination of the tetracyclines in food samples.

**Table 3.** Optimum values of the variables of on-line SPE with flow injection spectrophotometric system for the determination of tetracyclines

Variable	Range studied		Optimum value	
1. Wavelength of tetracycline standard solution (nm)	300-700		370	
2. Preconcentration time (min)	2-8		6	
3. pH of tetracycline standard solution	2.0-7.5		4.0	
4. pH of eluent	2.0-7.5		6.5	
5. Ratio of eluent (methanol:buffer solution)	10:90, 20:80, 30:70, 40:60, 50:50, 60:40		40:60	
6. Size of minicolumn	length (cm)	i.d.(cm)	length (cm)	i.d. (cm)
	1.0	0.3	1.0	0.3
	3.0	0.3		
7. Flow rate (mL min <sup>-1</sup> )	0.3-0.8		0.5	

**Table 4.** Figures of merit of the proposed method for determination of tetracyclines

Standard solutions	Linear range (mg L <sup>-1</sup> )	Detection limit (mg L <sup>-1</sup> ) [13]	Calibration curve	
			Sensitivity (mV s /mg L <sup>-1</sup> )	r <sup>2</sup>
TC	0.08-1.00	0.08	321198	0.9947
OTC	0.20-4.00	0.10	171091	0.9909
CTC	0.20-1.00	0.09	162191	0.9916

#### Analysis of milk samples

The proposed method was applied to the determination of TC, OTC and CTC in four commercial types of milk: U.H.T., pasteurised, raw, and sterilised. For this purpose, different amounts of the tetracyclines were added to each sample in order to carry out the recovery study. It was found that, fortunately, tetracyclines were not detected in any of the original samples. From Table 5, the per cent recoveries obtained were in the range of 86–109 for TC, 90–109 for OTC, and 89–108 for CTC.

Unlike HPLC, the proposed method obviously cannot discriminate between TC, OTC and CTC in a sample. Nevertheless, it is quite convenient to operate, uses less reagent and produces less waste. Moreover, since the tetracyclines can be preconcentrated on the minicolumn by an enrichment factor of 30 [12], the method is good enough for analysis of milk samples.

**Table 5.** Percent recovery obtained from the proposed method for determination of tetracyclines in four types of milk

Milk sample	Standard	Added (mg L <sup>-1</sup> )	Found (mg L <sup>-1</sup> )	% Recovery (n = 3)
U.H.T.	TC	0.30	0.26	86
		0.50	0.54	109
		0.70	0.73	105
		0.90	0.86	96
	OTC	0.30	0.32	107
		0.70	0.64	92
		0.90	0.94	104
	CTC	0.30	0.32	106
		0.50	0.47	95
		0.90	0.91	101

Milk sample	Standard	Added (mg L <sup>-1</sup> )	Found (mg L <sup>-1</sup> )	% Recovery (n = 3)
Pasteurised	TC	0.30	0.26	88
		0.50	0.54	108
		0.70	0.73	104
		0.90	0.88	97
	OTC	0.30	0.27	90
		0.50	0.54	109
		0.70	0.70	101
		0.90	0.88	98
	CTC	0.30	0.27	89
		0.50	0.53	107
		0.70	0.73	105
		0.90	0.87	96
Raw	TC	0.30	0.28	94
		0.50	0.51	101
		0.70	0.74	105
		0.90	0.87	97
	OTC	0.30	0.27	90
		0.50	0.54	109
		0.90	0.88	98
	CTC	0.30	0.32	108
		0.50	0.48	97
		0.70	0.66	95
		0.90	0.93	103
	Sterilised	TC	0.30	0.31
0.50			0.51	103
0.70			0.65	94
0.90			0.93	103
OTC		0.30	0.30	101
		0.50	0.49	100
		0.70	0.69	100
		0.90	0.90	100
CTC		0.30	0.30	102
		0.50	0.49	99
		0.90	0.90	100

## Conclusions

The first use of on-line SPE-FIA for the determination of tetracycline antibiotics in real milk samples was described. It is highly sensitive as a result of the preconcentration of the tetracyclines onto the C<sub>18</sub> resin. Only small amounts of sample, sorbent and reagent are required. A high enrichment factor can be attained by employing large sample volumes, making it possible to work at different concentration levels. Tetracycline residues, however, were not detected in the studied milk samples collected.

## Acknowledgements

We gratefully acknowledge the Faculty of Science, Naresuan University for funding this research. Some of the devices and Windows applications were developed in cooperation with Alpha Flow Research, Chiang Mai University.

## References

1. Y. Debuf (Ed.), "The Veterinary Formulary", Pharmaceutical Press, London, **1988**, p.97.
2. EC Regulation 2377/90, incorporating amending regulation 281/96.
3. Commission Regulation No. 508/99, *Off. J. Eur. Commun.*, No. L609, March **1999**.
4. N. Furusawa, "Isolation of tetracyclines in milk using a solid-phase extracting column and water eluent", *Talanta*, **2003**, 59, 155-159.
5. A. L. Cinquina, F. Longo, G. Anastasi, L. Giannetti, and R. Cozzani, "Validation of a high-performance liquid chromatography method for the determination of oxytetracycline, tetracycline, chlortetracycline and doxycycline in bovine milk and muscle", *J. Chromatogr. A*, **2003**, 987, 227-233.
6. W. C. Andersen, J. E. Roybal, S. A. Gonzales, S. B. Turnipseed, A. P. Pfenning, and L. R. Kuck, "Determination of tetracycline residues in shrimp and whole milk using liquid chromatography with ultraviolet detection and residue confirmation by mass spectrometry", *Anal. Chim. Acta*, **2005**, 529, 145-150.
7. A. Townshen, W. Ruengsitagoon, C. Thongpoon, and S. Liawruangrath, "Flow injection chemiluminescence determination of tetracycline", *Anal. Chim. Acta*, **2005**, 541, 103-109.
8. C. M. C. M. Couto, J. L. F. C. Lima, M. Conceição, B. S. M. Montenegro, and S. Reis, "Tetracycline, oxytetracycline and chlortetracycline determination by flow injection potentiometry", *J. Pharm. Biomed. Anal.*, **1998**, 18, 527-533.
9. P. Masawat and J. M. Slater, "The determination of tetracycline residues in food using a disposable screen-printed gold electrode (SPGE)", *Sens. Actuators B*, **2007**, 24, 127-132.
10. R. Karlíček and P. Solich, "Flow-injection spectrophotometric determination of tetracycline antibiotics", *Anal. Chim. Acta*, **1994**, 285, 9-12.
11. P. Masawat, "Design and fabrication of low-cost home-made all-in-set colorimetric detector with PC-interface embed for the determination of tetracycline antibiotics", *NU Sci. J.*, **2007**, 3, 215-230.
12. Z. Fang, "Flow Injection Separation and Preconcentration", VCH Publisher, Weinheim, **1993**.
13. D. A. Skoog, D. M. West, and H. Muller, "Fundamentals of Analytical Chemistry", 6<sup>th</sup> Edn., Harcourt Brace & Company, Florida, **1992**.

*Mj. Int. J. Sci. Tech.* **2008**, 2(02), 418-430

14. H. Oka, Y. Ito, and H. Matsumoto, "Chromatographic analysis of tetracycline antibiotics in foods"  
*J. Chromatogr. A*, **2000**, 882, 109-133.

© 2008 by Maejo University, San Sai, Chiang Mai, 50290 Thailand. Reproduction is permitted for noncommercial purposes.

Full Paper

## **Variability in growth, nutrition and phytochemical constituents of *Plectranthus amboinicus* (Lour) Spreng. as influenced by indigenous arbuscular mycorrhizal fungi**

Sevanan Rajeshkumar<sup>1,\*</sup>, Mathan C. Nisha<sup>2</sup>, and Thangavel Selvaraj<sup>3</sup>

<sup>1</sup> Botanical Sciences Unit, Department of Applied Biology, Faculty of Natural and Computer Sciences, Ambo University College, Post Box No. 19, Ambo, Western Shoa, Ethiopia, East Africa

<sup>2</sup> Department of Botany, Kongunadu Arts and Science College (Autonomous), Coimbatore, Tamilnadu, India

<sup>3</sup> Department of Plant Sciences, Faculty of Agricultural Sciences, Ambo University College, Post Box No. 19, Ambo, Western Shoa, Ethiopia, East Africa

\* Corresponding author, e-mail: [dhiksha\\_rajesh@yahoo.co.in](mailto:dhiksha_rajesh@yahoo.co.in)

Received: 28 February 2008 / Accepted: 14 July 2008 / Published: 22 July 2008

---

**Abstract:** A study was conducted under greenhouse nursery condition on the efficacy of seven indigenous arbuscular mycorrhizal (AM) fungi in the improvement of growth, biomass, nutrition and phytochemical constituents, namely total phenols, ortho dihydroxy phenols, flavonoids, alkaloids, tannins and saponins, in the roots and leaves of *Plectranthus amboinicus* (Lour) Spreng. Seedlings were raised in polythene bags containing soil inoculated with isolates of seven different indigenous AM fungi, viz. *Acaulospora bireticulata*, *A. scrobiculata*, *Gigaspora margarita*, *Glomus aggregatum*, *G. mosseae*, *G. geosporum*, and *Scutellospora heterogama*. *P. amboinicus* seedlings raised in the presence of AM fungi generally showed an increase in plant growth, nutritional status and phytochemical constituents over those grown in the absence of AM fungi. The extent of growth, biomass, nutritional status and phytochemical constituents enhanced by AM fungi varied with the species of AM fungi inhabiting the roots and leaves of *P. amboinicus* seedlings. Considering the various plant growth parameters, nutritional status of the plant, total phenols, ortho dihydroxy phenols, alkaloids, flavonoids, tannins, and saponins in the roots and leaves, it was observed that *Gigaspora margarita* is the best AM symbiont for *P. amboinicus* used in this experiment.

**Keywords:** *Plectranthus amboinicus*, AM fungi, biomass, nutrition, phytochemicals

---

## Introduction

The introduction of beneficial organisms into soil is a present crux of applied mycorrhizal research. Utilisation of mycorrhizal biofertilisers in the cultivation of medicinal and aromatic plants is of recent interest. Arbuscular mycorrhizal (AM) fungi have been used to enhance the plant growth and yield of medicinal crops and to help maintain good soil health and fertility that contributes to a greater extent to a sustainable yield and good quality of the products [1]. The activity has gained momentum in recent years due to the higher cost and hazardous effects of heavy doses of chemical fertilisers. These fungi are a ubiquitous group of soil fungi colonising the roots of plants belonging to more than 90% of the plant families [2]. These zygomycetous fungi represent an important component in the soil microbial biomass due to their ubiquity and their direct involvement in essential processes at the plant-soil interface [3]. Interest in this association is mainly because of the manifold benefits conferred on the host by the fungi. They are known to improve the nutritional status of plants as well as their growth and development, and to protect plants against root pathogens and confer resistance to drought and soil saline condition [4]. With over 130 species of AM fungi recognised and classified [5] and the wide host range they inhabit, there exists a wide variation in the ways they benefit the host, which in turn are related to the extent of the colonisation of host roots by the fungus. The extent of the root colonisation varies with several soil and climatic factors apart from the host involved. However, these fungi show a preferential colonisation to hosts and thus the extent to which the host benefits depends of the fungal species involved in the symbiosis [6]. The existence of inter- and intra-specific variations among the plant species involved in relation to their phosphorus requirement and the ability of the host to translocate the native soil phosphorus further determine the efficacy of these fungi [7]. Thus it is essential to screen for an efficient AM fungus for a particular host in order to harness the maximum benefit from the fungus. Furthermore, since AM fungi cannot be grown on laboratory media, production of a large quantity of the inoculum for inoculation of the soil under field conditions is difficult. Nevertheless, since most of the commercially important medicinal crops are raised under nursery conditions before being transplanted to the main field, the inoculation of soil in the nursery would not only result in the saving of the inoculum needed but also help in better establishment of the transplanted seedlings.

There are few published reports on the influence of AM fungi on the growth, nutrition and phytochemical constituents of medicinal plants [1,8,9,]. Indian borage (*Plectranthus amboinicus* Lour. Spreng.) is an important medicinal plant largely used in Indian siddha medicine and the leaves are used for the treatment of urinary diseases, epilepsy, chronic asthma, cough, bronchitis, and malarial fever, in addition to acting as a powerful aromatic carminative. Hence the present investigation was done to screen for an efficient AM fungus for *P. amboinicus* and also to study the effects of the association on the growth, biomass, nutritional status and phytochemicals, viz. total phenols, ortho di-hydroxy phenols, alkaloids, flavonoids, tannins and saponins in the leaves and roots of *P. amboinicus*.

## Materials and Methods

This investigation was carried out under nursery condition in a glass house. The soil used in this study was collected from an uncultivated field at a depth of 0-30 cm and was classified as fine, entisol, isohyperthermic kanhaplustalfs. The soil pH was 7.2 (1:10 soil to water extract ratio), and it contained 2.7 ppm available phosphorus (extractable with  $\text{NH}_4\text{F} + \text{HCl}$ ) and an indigenous AM fungal population of 60 spores/50 g of soil. Nursery was raised by sterilising the seeds of *P. amboinicus* with 5% chloramine T solution for 30 min, then washing and sowing in poly bags (10 x 15 cm) containing sterilised soil: vermiculite mix (1:1v/v). Ruakura nutrient solution at 50ml per poly bag was applied once in 10 days. After 30 days seedlings were transplanted to polythene bags of size 25 x 15 cm containing 2 kg of unsterilised soil:sand:compost in the ratio of 2:1:0.5 (v/v/v).

The AM fungal species used in this study (Table 1) were isolated from the rhizosphere soil of Indian borage cultivated at the herbal garden of Tamil University, Tamilnadu, India. These AM fungal species were isolated by using wet sieving and decanting technique [10]. The species level identification of different AM fungal species was done following the keys provided by Trappe [11] and Schenck and Perez [12]. These fungi were multiplied using sterilised sand:soil mix (1:1 v/v) as the substrate and onion as the host. After 90 days of growth, shoots of onion was severed and the substrate containing hyphae, spores and root bits was air dried and used as inoculum. The inoculum potential (IP) of each culture was estimated adopting the Most Probable Number (MPN) method as outlined by Porter [13]. The soil in each polythene bag was mixed with this inoculum at different rates so as to maintain an initial IP of 12,500 per polythene bag. Each bag containing the potting mixture, with or without AM inoculum as the treatment may be, was planted with one seedling of *P. amboinicus*. One set of plants without inoculation was the control. Each treatment with 5 replications was maintained in a glass house and watered regularly so as to maintain the field capacity of the soil. Ruakura plant nutrient solution [3] without phosphate was added to the polythenebags at the rate of 50 ml per polythene bags once in 15 days.

Ninety days after transplanting, the plants were harvested for determination of the mycorrhizal status, growth response, nutritional status and phytochemical constituents. Plant height was measured from soil surface to the growing tip of the plant. Dry biomass was determined after drying the plant sample at 60°C to a constant weight in a hot air oven. Soil sample (50 g) was collected from each polythene bag and subjected to wet sieving and decantation method as outlined by Gerdemann and Nicolson [10] to estimate the population of spores. The root system was removed and assessed for AM fungal infection by the grid-line intersect method [14] after clearing the roots with 10% KOH and staining with trypan blue (0.02%) as described by Phyllips and Hayman [15]. Estimation of soil aggregates (<50µm size), which indirectly denote the extent of external hyphae in soil, was done as described by Van Bavel [16].

Phosphorus and potassium content of the plant tissue were determined by employing the vanadomolybdate phosphoric yellow colour and flame photometric method [17] respectively. Atomic absorption spectrophotometry was employed to estimate zinc, copper and iron content of the plant

samples, using respective hollow cathode lamps. Sturdiness quotient, biovolume index (a measure of the total volume of a seedling), and quality index, which reflects the quality of a seedling, were determined using the formulae given by Hatchell [18]. The content of secondary metabolites, viz. total phenols [19], ortho dihydroxy phenols [20], flavonoids, tannins, saponins, and alkaloids in the leaves of the tested plants, were assayed according to the methods described by Sadasivam and Manickam [21] and Zakaria [22]. The data thus generated were subjected to statistical analysis of completely randomised block design and the means were separated by Duncan's Multiple Range Test (DMRT) [23].

## Results and Discussion

In the field survey, Indian borage plants growing in uncultivated P-deficient sandy loam soils were almost the same as those growing in cultivated soils. Microscopic examination of their roots revealed extensive colonisation by AM fungi with 94.5% level of infection. A large number of inter and intra-matrical vesicles were noticed between 120µm and 140µm in size. The vesicles were globose to subglobose and the subtending hyphae were simple. Based on the morphological characters, the AM fungal isolate was identified as *Glomus* species. Altogether seven AM fungi were isolated from root-zone soils and identified (Table 1). Among them *Glomus aggregatum* and *Gigaspora margarita* were predominant. However, *Acaulospora* and *Scutellospora* rarely occurred. Soil-borne auxiliary cells of *Gigaspora* and *Scutellospora* were also isolated and identified.

**Table 1.** Different native AM fungi and their influence on growth of *P.amboinicus*

Treatment	Plant height (cm)		Plant dry weight (g/plant)	
	Shoot	Root	Shoot	Root
Control (without AM fungi)	62.0a	23.5a	16.5a	12.5a
<i>Acaulospora bireticulata</i>	68.6b	28.6b	19.8b	18.2b
<i>Acaulospora scrobiculata</i>	66.4b	28.2b	18.8b	17.5c
<i>Gigaspora margarita</i>	90.6d	52.4d	24.5d	23.2d
<i>Glomus aggregatum</i>	84.5cd	42.0cd	23.8c	19.9b
<i>Glomus geosporum</i>	72.4c	34.5c	20.2bc	19.8b
<i>Glomus mosseae</i>	86.5d	46.2cd	24.0c	20.4cd
<i>Scutellospora heterogama</i>	68.5b	29.2b	19.2b	17.6c

Note: Means (n = 5) in each column followed by the same letter are not significantly different (p < 0.05) from each other according to DMR test.

The growth response, nutritional status and mycorrhizal development of plants raised in sandy loam soils were assessed for the impact of inoculation with different native AM fungi. The responses of the Indian borage plants to inoculation with different AM fungi were found to be varied. Mycorrhizal inoculation resulted in a significant increase in height, biomass, nutrient content and phytochemical constituents of *P. amboinicus* seedlings. However, there was no positive correlation between plant growth parameters and mycorrhizal colonisation. Earlier studies also showed the same trend for medicinal plants subjected to AM inoculation [1,9, 24-25] and these studies also indicated the host preference to the AM fungi. Bagyaraj and Varma [4] and Jeffries [26] stressed the need for selecting efficient native AM fungi for plant species. The present study conducted with an objective of screening for an efficient indigenous AM fungi for *P. amboinicus* seedlings has also resulted in varied plant growth responses to different AM fungi.

Mycorrhizal treatments resulted in an increase in the number of spores in the rhizosphere soils and this was maximum with *Gigaspora margarita* followed by *Glomus mosseae*. It is well known that enhanced nutritional status of a plant is manifested in its improved growth [26]. *P. amboinicus* plants grown in the presence of AM fungi showed a general increase in such growth parameters as plant height and total dry weight as against those grown in soils uninoculated with AM fungi (Table 1). The nutritional status of *P. amboinicus* seedlings, viz. phosphorus, potassium, zinc, copper and iron content, was also significantly higher in plants raised in soil inoculated with AM fungi (Table 2). Seedlings raised in the presence of *Gigaspora margarita* showed an increase of 108%, 81%, 82%, 80.5% and 82.5% in the tissue P, K, Zn, Cu and Fe content respectively as compared to seedlings raised as uninoculated control. The extent of increase in plant P, K, Zn, Cu and Fe content varied among the fungi studied with seedlings grown in the presence of *Gigaspora margarita* containing significantly highest content of these nutrients, followed by those grown in the presence of *Glomus aggregatum* and *G. mosseae*. Such a variation in the plant nutrient status in relation to the fungal species for other medicinal plant species is well documented [1,24]. The enhancement in growth and nutritional status is also related to the per cent root colonisation apart from several soil and environmental factors.

The phytochemical constituents total phenols (ortho di-hydroxy phenols, flavonoids, alkaloids, tannins and saponins) of *P. amboinicus* seedlings were found to be significantly higher in plants raised in soil inoculated with AM fungi (Table 3), with seedlings raised in the presence of *Gigaspora margarita* showing the most increase of all phytochemical constituents in the plant tissues. Such a variation in the phytochemical constituents in relation to the fungal species for other medicinal plant species is also well documented [1,27].

**Table 2.** Influence of native AM fungi on P, K, Zn, Cu, and Fe content in shoot and root of *P. amboinicus*

Treatment	Phosphorus content (mg/plant)	Potassium content (mg/plant)	Zinc content (µg/plant)	Copper content (µg/plant)	Iron content (µg/plant)
Control (without AM fungi)	3.29 <sup>a</sup>	3.2 <sup>a</sup>	162.8 <sup>a</sup>	61.7 <sup>a</sup>	59.5 <sup>a</sup>
<i>Acaulospora bireticulata</i>	5.50 <sup>b</sup>	4.1 <sup>b</sup>	195.0 <sup>bc</sup>	74.9 <sup>b</sup>	64.2 <sup>b</sup>
<i>Acaulospora scrobiculata</i>	5.38 <sup>ab</sup>	4.2 <sup>c</sup>	198.5 <sup>b</sup>	105.8 <sup>c</sup>	72.8 <sup>c</sup>
<i>Gigaspora margarita</i>	6.56 <sup>d</sup>	5.4 <sup>d</sup>	296.9 <sup>d</sup>	112.3 <sup>d</sup>	95.6 <sup>d</sup>
<i>Glomus aggregatum</i>	6.23 <sup>d</sup>	4.2 <sup>c</sup>	280.9 <sup>c</sup>	108.9 <sup>d</sup>	92.2 <sup>d</sup>
<i>Glomus geosporum</i>	5.95 <sup>c</sup>	4.4 <sup>c</sup>	241.3 <sup>bc</sup>	98.5 <sup>c</sup>	88.5 <sup>c</sup>
<i>Glomus mosseae</i>	6.35 <sup>d</sup>	4.6 <sup>c</sup>	286.2 <sup>d</sup>	109.2 <sup>d</sup>	94.2 <sup>d</sup>
<i>Scutellospora heterogama</i>	5.45 <sup>b</sup>	3.4 <sup>a</sup>	223.2 <sup>bc</sup>	104.4 <sup>c</sup>	88.2 <sup>c</sup>

Note: Means (n = 5) in each column followed by the same letter are not significantly different (p < 0.05) from each other according to DMR test.

**Table 3.** Influence of different native AM fungi on phytochemical constituents in the leaves of *P. amboinicus*

Treatment	Total phenols (µg/g fresh wt.)	o-Dihydroxy-phenols (µg/g fresh wt.)	Flavonoids (µg/g dry wt)	Alkaloids (µg/g dry wt.)	Tannins (µg/g dry wt)	Saponins (µg/g dry wt.)
Control (without AM fungi)	95.0 <sup>a</sup>	65.2 <sup>a</sup>	3.12 <sup>a</sup>	4.32 <sup>a</sup>	0.280 <sup>a</sup>	0.160 <sup>a</sup>
<i>Acaulospora bireticulata</i>	120.5 <sup>c</sup>	75.2 <sup>d</sup>	3.25 <sup>b</sup>	4.38 <sup>b</sup>	0.290 <sup>b</sup>	0.172 <sup>b</sup>
<i>Acaulospora scrobiculata</i>	114.2 <sup>b</sup>	70.2 <sup>b</sup>	3.16 <sup>b</sup>	4.36 <sup>b</sup>	0.298 <sup>b</sup>	0.176 <sup>b</sup>
<i>Gigaspora margarita</i>	130.5 <sup>d</sup>	85.4 <sup>d</sup>	3.76 <sup>d</sup>	5.12 <sup>d</sup>	0.435 <sup>d</sup>	0.210 <sup>d</sup>
<i>Glomus aggregatum</i>	128.2 <sup>d</sup>	82.3 <sup>d</sup>	3.62 <sup>c</sup>	4.86 <sup>c</sup>	0.382 <sup>c</sup>	0.195 <sup>c</sup>
<i>Glomus geosporum</i>	118.5 <sup>b</sup>	80.5 <sup>c</sup>	3.58 <sup>c</sup>	4.82 <sup>c</sup>	0.365 <sup>c</sup>	0.192 <sup>b</sup>
<i>Glomus mosseae</i>	129.2 <sup>d</sup>	83.4 <sup>d</sup>	3.64 <sup>cd</sup>	5.01 <sup>d</sup>	0.395 <sup>d</sup>	0.199 <sup>c</sup>
<i>Scutellospora heterogama</i>	115.5 <sup>b</sup>	72.72 <sup>b</sup>	3.18 <sup>c</sup>	4.38 <sup>b</sup>	0.340 <sup>ab</sup>	0.185 <sup>b</sup>

Note: Means (n = 5) in each column followed by the same letter are not significantly different (p < 0.05) from each other according to DMR test.

Other items studied in relation to effects of soil inoculation with AM fungi are shown in Table 4. *Gigaspora margarita* and *Glomus mosseae* inhabited a significantly higher percentage of roots compared to other AM fungi. Similarly, spore number was also highest in the soil samples inoculated with *Gigaspora margarita* followed by soil inoculated with *Glomus mosseae*, indicating a better proliferating ability of these fungi with *P. amboinicus* as the host.

**Table 4.** Effects of soil inoculation with AM fungi on per cent root colonisation, spore numbers in root zone soil, percent aggregation of rhizosphere soil, sturdiness quotient, biovolume and quality index of *P. amboinicus*

Treatment	AM fungi colonisation in root (%)	Number of AM fungi spores / 100 g of soil	Aggregation of soil	Sturdiness quotient	Biovolume index	Quality index
Control (without AM fungi)	0 <sup>a</sup>	0 <sup>a</sup>	18 <sup>a</sup>	16.4 <sup>a</sup>	2442.2 <sup>a</sup>	0.45 <sup>a</sup>
<i>Acaulospora bireticulata</i>	53.5 <sup>b</sup>	320 <sup>b</sup>	36 <sup>b</sup>	16.8 <sup>b</sup>	2526.4 <sup>b</sup>	0.46 <sup>b</sup>
<i>Acaulospora scrobiculata</i>	45.5 <sup>b</sup>	310 <sup>b</sup>	39 <sup>b</sup>	16.9 <sup>b</sup>	2527.2 <sup>b</sup>	0.47 <sup>b</sup>
<i>Gigaspora margarita</i>	92.5 <sup>d</sup>	760 <sup>d</sup>	52 <sup>d</sup>	17.4 <sup>d</sup>	3245.4 <sup>d</sup>	0.58 <sup>d</sup>
<i>Glomus aggregatum</i>	85.5 <sup>cd</sup>	680 <sup>cd</sup>	48 <sup>c</sup>	17.1 <sup>c</sup>	3162.8 <sup>c</sup>	0.55 <sup>c</sup>
<i>Glomus geosporum</i>	82.0 <sup>cd</sup>	620 <sup>cd</sup>	42 <sup>c</sup>	16.9 <sup>c</sup>	2526.4 <sup>b</sup>	0.47 <sup>b</sup>
<i>Glomus mosseae</i>	88.5 <sup>cd</sup>	690 <sup>cd</sup>	45 <sup>c</sup>	17.2 <sup>d</sup>	2975.9 <sup>b</sup>	0.56 <sup>c</sup>
<i>Scutellospora heterogama</i>	63.0 <sup>c</sup>	460 <sup>c</sup>	32 <sup>b</sup>	16.6 <sup>b</sup>	2469.4 <sup>b</sup>	0.46 <sup>b</sup>

Note: Means (n = 5) in each column followed by the same letter are not significantly different (p < 0.05) from each other according to DMR test.

Mycorrhizal fungi are also implicated in soil structure improvement by increasing soil aggregation by their hyphae [28]. Soil aggregation is a measure of the amount of extramatrical hyphae, which is in turn related to the efficiency of the fungus [24]. This observation is further strengthened by the present study as mycorrhizal fungi used in this study significantly improved the aggregation of soil compared to that of the control (Table 4). Soil aggregation was highest in soil inoculated with *Gigaspora margarita* and *Glomus aggregatum* in that order. Other seedling parameters (sturdiness quotient, biovolume index and quality index) were also found to be all higher than those of the control, the increase being to the extent of 6.08%, 33.20% and 29.4% respectively (Table 4). Such values indicate a sturdier stem and a greater dry weight of the plant, qualities which are desirable among nursery seedlings [1,18].

AM fungi differ greatly in their symbiotic effectiveness which depends on their preference for particular soils or host plant specificity [29], direct ability to stimulate plant growth, rate of infection, competitive ability, and tolerance to applied chemicals. Giving weighting to quality index, but not neglecting the other parameters, *Gigaspora margarita* and *Glomus mosseae* were found to be the best and the next best fungus respectively for inoculating *P. amboinicus* in the nursery in order to obtain healthy, vigorously growing seedlings that could establish and perform better when planted in sandy loam soils.

## Conclusions

*P. amboinicus* seedlings show varied responses to different AM fungi, with *Gigaspora margarita* conferring greater benefits compared to all other fungi used in this study. Further consideration of the ability for higher root colonisation, plant biomass, biovolume index, and mineral and phytochemical constituents suggested that a clear and specific relationship exists between a particular species of fungus and the plant.

## References

1. S. K. Rajan, D. J. Bagyaraj, and J. Arpana, "Selection of efficient arbuscular mycorrhizal fungi for inoculating *Acacia holosericea*", *J. Soil Biol. Ecol.*, **2004**, *24*, 119-126.
2. M. Brundett, "Mycorrhizas in natural ecosystem", *Adv. Ecol. Res.*, **1991**, *21*, 171-313.
3. J. L. Harley and S. E. Smith, "Mycorrhizal Symbiosis", Academic Press, London, **1983**, p. 245.
4. D. J. Bagyaraj and A. Varma, "Interactions between arbuscular mycorrhizal fungi and plants: their importance in sustainable agriculture in arid and semi arid tropics", *Adv. Microb. Ecol.*, **1995**, *14*, 119-142.
5. M. Giovannetti and V. Gianinnazzi-Pearson, "Biodiversity in arbuscular mycorrhizal fungi", *Mycol. Res.*, **1994**, *98*, 705-715.
6. R. M. Miller, A. G. Jarstfer, and J. K. Pillai, "Biomass allocation in an *Agropyron smithi* - *Glomus* symbiosis", *Am. J. Bot.*, **1987**, *74*, 114-122.
7. R. T. Koide, "Nutrient supply, nutrient demand and plant response to mycorrhizal infection", *New Phytol.*, **1991**, *117*, 365-386.
8. M. Gupta and K. K. Janardhanan, "Mycorrhizal association of *Glomus aggregatum* with palmarosa enhances growth and biomass", *Plant and Soil*, **1991**, *131*, 261-263.
9. N. Earanna, A. A. Farooqi, D. J. Bagyaraj, and C. K. Suresh, "Influence of *Glomus fasciculatum* and plant growth promoting rhizo-microorganism on growth and biomass of periwinkle", *J. Soil Biol. Ecol.*, **2002**, *22*, 22-26.
10. J. W. Gerdemann and T. H. Nicolson, "Spores of mycorrhizal *Endogone* species extracted from soil by wet sieving and decanting", *Trans. Br. Mycol. Soc.*, **1963**, *46*, 235-244.
11. J. M. Trappe, "Synoptic key to the genera and species of zygomycetous mycorrhizal fungi", *Phytopathology*, **1982**, *72*, 1102-1108.
12. N. C. Schenck and Y. Perez, "Manual for the Identification of VA Mycorrhizal Fungi", 3rd Edn., INVAM Publications, University of Florida, Gainesville, **1990**, p. 245.
13. W. M. Porter, "The most probable number method for enumerating propagules of VAM fungi in soil", *Aust. J. Soil Res.*, **1979**, *17*, 515-519.
14. M. Giovannetti and B. Mosse, "An evaluation of techniques to measure vesicular-arbuscular infection in roots", *New Phytol.*, **1980**, *84*, 489-500.
15. J. H. Phillips and D. S. Hayman, "Improved procedures for clearing roots and staining parasitic and vesicular arbuscular mycorrhizal fungi for rapid assessment of infection", *Trans. Br. Mycol. Soc.*, **1970**, *55*, 158-161.
16. C. H. M. Van Bavel, "Mean weight diameter of soil aggregates as a statistical index of aggregation", *Soil Sci. Soc. Am. Proc.*, **1980**, *14*, 20-23.
17. M. L. Jackson, "Soil Chemical Analysis", Printice Hall of India, New Delhi, **1973**, p 239.
18. G. E. Hatchell, "Production of bare root seedlings", *Proc. 3<sup>rd</sup> Bio. South S. I. Res. Conf.*, **1985**,

*Mj. Int. J. Sci. Tech.* **2008**, 2(02), 431-439

pp. 395-357.

19. G. L. Farkas and Z. Kiraly, "Role of phenolic compounds in the physiology of plant disease and disease resistance", *Phytopathol.*, **1962**, 2, 105-150.
20. A. Mahadevan and S. Sridhar, "Methods in Physiological Plant Pathology", Sivakami Publications, Madras, **1996**.
21. S. Sadasivam and A. Manickam, "Biochemical Methods", 2nd Edn., New Age International, New Delhi, **1996**.
22. M. Zakaria, "Isolation and characterization of active compounds from medicinal plants", *Asia Pacif. J. Pharmacol.*, **1991**, 6, 15-20.
23. D. M. Duncan, "Multiple range and multiple tests", *Biometrics*, **1955**, 42, 1-42.
24. J. Reena and D. J. Bagyaraj, "Responses of *Acacia nilotica* and *Calliandra calothyrsus* to different VA mycorrhizal fungi", *Arid Soil Res. Rehabil.*, **1990**, 4, 261-268.
25. K. Chandrika, R. Lakshmiathy, Blakrishna Gowda, A. N. Balakrishna, M. D. Rajanna, and D. J. Bagyaraj, "Response of *Centella asiatica* (L.) urban. to VA mycorrhizal inoculation", *J. Soil Biol. Ecol.*, **2002**, 22, 35-39.
26. P. Jeffries, "Use of mycorrhizae in agriculture", *Crit. Rev. Biotechnol.*, **1987**, 5, 319-357.
27. D. S. Rao, D. Indira, A. J. Raj, and R. Jayaraj, "Influence of vermicompost on the growth and the content of secondary metabolites in *Adhathoda vasica* Nees", *J. Soil Biol. Ecol.*, **2004**, 24, 163-166.
28. R. M. Miller and J. D. Jastrow, "The role of mycorrhizal fungi in soil conservation", in "Mycorrhizae in Sustainable Agriculture" (Ed., G. J. Bethlenfalvay and R. C. Linderman), ASA Special Publication, Wisconsin, **1992**, pp. 29-44.
29. S. S. Dhillon, "Evidence for host-mycorrhizal preference in native grassland species", *Mycological Res.*, **1992**, 94, 359-362.

© 2008 by Maejo University, San Sai, Chiang Mai, 50290 Thailand. Reproduction is permitted for noncommercial purposes.

*Communication*

## **Preparation of aluminium lakes by electrocoagulation**

**Prapai Pradabkham\* and Neeranuch Chairungsi**

Department of Chemistry, Faculty of Science, Chiang Mai University, Chiang Mai 50200, Thailand

\*Corresponding author, e-mail: [p\\_pradabkham@hotmail.com](mailto:p_pradabkham@hotmail.com)

*Received: 17 March 2008 / Accepted: 25 July 2008 / Published: 28 July 2008*

---

**Abstract:** Aluminium lakes have been prepared by electrocoagulation employing aluminium as electrodes. The electrocoagulation is conducted in an aqueous alcoholic solution and is completed within one hour. The dye content in the lake ranges approximately between 4-32%.

**Keywords:** lake, lake pigment, aluminium lake, electrocoagulation

---

### **Introduction**

Lake pigments or lakes [1] are a class of pigments composed of organic dyes that have been rendered insoluble by interaction with a compound of a metal, e.g. barium sulphate, calcium sulphate, and aluminium hydroxide. The interaction may involve the precipitation of a salt in which the proportions of dye to metal are fixed, or it may be a less well defined attraction between the dye and the surfaces of particles of the inorganic compound. Some lakes are prepared by a combination of both processes. Lakes considerably extend the range of colours available in the production of paints, cosmetics, and inks for printing and lithography. Moreover, they can also be used as food colours [e.g. 2].

Basically, a lake pigment is prepared by interaction of a freshly formed metal compound with a dye. As an example, madder (alizarin) lake can be produced by reacting the dye alizarin (in the form of an emulsifiable paste) with aluminium hydroxide formed by reaction between aluminium sulphate and sodium carbonate [3]. A little phosphate and calcium salt are also added. The method suffers, however, from a relatively high reaction temperature (100°C or boiling temperature) and a long reaction time (6 hours in this case).

## Discussion

We have attempted successfully to prepare a number of lake pigments by a simple method which requires a lower temperature and a much shorter preparation time. The method makes use of electrocoagulation, an electrochemical process long known in waste water treatment researches [4]. In this process, a set-up for electrolysis is employed. In its simplest form, a pair of metal plates, usually aluminium or iron, is used as electrodes. They are dipped into an aqueous solution or suspension containing a supporting electrolyte (usually sodium chloride of about 0.2 % concentration). Direct current is then passed through the aqueous medium in a container via the two electrodes.

The reactions that occur as the result of the above operation have been elucidated and established [e.g. 5,6]. In the case of using aluminium as electrodes, the aluminium will be oxidised at the anode to aluminium ions, while water molecules are dissociated into hydrogen molecules and hydroxide ions at the cathode. Aluminium hydroxide (and other hydrated forms of aluminium) molecules are thus formed as a result. As well known, these molecules are efficient adsorbents for many types of molecules or particles, including those of most dyes.

However, if the dye molecules happen to be phenolic in nature, e.g. most natural anthraquinones and flavonoids, another type of interaction is most likely to occur in which a complex in the form of a metal phenolate salt is formed from the metal ions (e.g.  $\text{Al}^{3+}$ ) and the phenolic dye molecules [6]. If the dye molecules are acidic in nature due to the presence of a carboxyl group or sulphonic acid group, similar salt formation will also occur. All these metal salts or complexes as well as the adsorbate containing  $\text{Al}(\text{OH})_3$  above are insoluble and will precipitate or coagulate from the aqueous solution. Thus, in effect, a lake has been formed. If the electrodes used are aluminium, this will then become an aluminium lake.

Preparation of a lake by electrocoagulation has two important advantages over conventional methods of preparation. Firstly, the preparation time is much shorter since coagulation of a dye electrolytically can be completed in an hour or less. Completion of coagulation can be observed visually when the electrolysed solution becomes colourless or very pale in colour. Secondly, no external heating is required since the electrolytic process can be and is normally carried out at ambient temperature, although the electrolysed solution will gradually warm up slowly by itself.

Factors that determine the percentage of dye in the resulting lake include the relative solubility of the dye in water and alcohol, and the coagulation time, although these are not always mutually exclusive. Normally, the water-soluble dye will be electrocoagulated most readily. The percentage of the dye in the coagulum will then be large. If the dye is less water soluble, alcohol has to be added to make it more soluble. Electrocoagulation in an aqueous alcoholic solution [7-9] usually takes place less readily, i.e. requires more time and even then may not be complete. In this case the percentage of the dye in the coagulum will be smaller due to more formation of the metal compound (e.g. aluminium hydroxide). In our case, we can achieve a percentage range of approximately 4-32 depending on the individual dye.

### Preparation Details

Lakes from 5 dyes, viz. alizarin, purpurin, erythrosine, chlorophyllin, and amaranth, were prepared. A representative procedure is as follows.

Two aluminium plates (dimension 14 x 5 cm) were used as electrodes. These were spaced 3 cm apart and dipped 5.5 cm into a magnetically-stirred ethanolic (up to 85%) dye solution (250 ml) contained in a 400-ml beaker. Sodium chloride was added to the solution as supporting electrolyte at a concentration of 0.2%. Direct current (about 0.6 A) was passed through the solution via the two aluminium electrodes until the dye solution was colourless or very pale in colour. The resulting precipitate was filtered and dried to afford the lake pigment. The IR spectra of all the lakes prepared were very similar to that of aluminium hydroxide, which confirms the presence of this compound as the main matrix in the lakes obtained. Typical results are shown in Table 1 and Figure 1.

**Table 1.** Results of preparation of 5 lake pigments by electrocoagulation

Dye used	Starting weight of dye (g)	Dye concentration in electrolysed solution (%w/v)	Time for complete coagulation (minutes)	Weight of lake obtained (g)	% Dye in lake
Alizarin	0.05	0.02	30	0.87	5.7
Purpurin	0.10	0.04	30	0.97	10.3
Erythrosine	0.10	0.04	30	0.90	11.1
Chlorophyllin	0.10	0.04	5	0.31	32.2
Amaranth	0.10	0.04	60	2.78	3.6

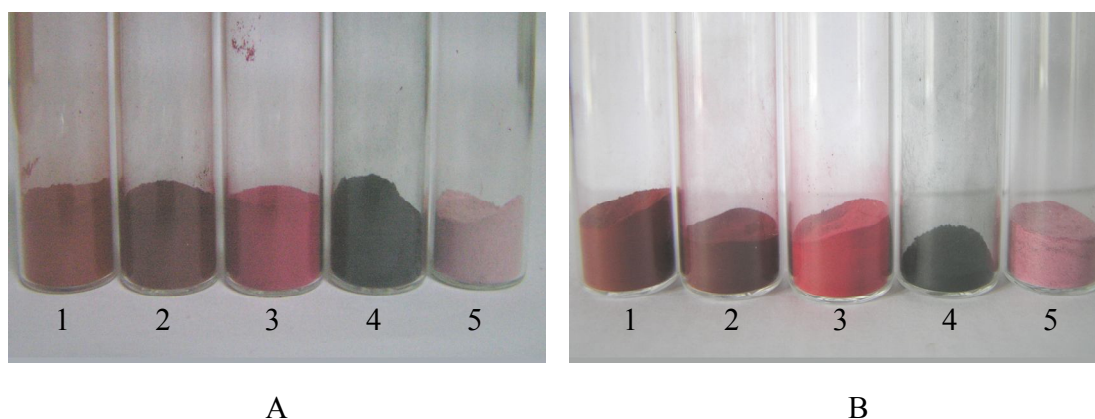


**Figure 1.** Aluminium lakes prepared by: (A) conventional method [3] and (B) electrocoagulation method (1 = lake alizarin, 2 = lake purpurin, 3 = lake erythrosine, 4 = lake chlorophyllin, and 5 = lake amaranth)

## Conclusions

Electrocoagulation can be used to prepare lake pigments from dyes. In this short report, aluminium lakes from a number of dyes have been prepared successfully by this simple technique, in which a much shorter time as well as a lower temperature is required.

## Acknowledgements

The Graduate School of Chiang Mai University is gratefully acknowledged for its partial support financially for this project. We would also like to thank our supervisor, Dr. Duang Buddhasukh, for his guidance throughout the course of the work.

## References

1. Encyclopaedia Britannica, 15th Edn., Micropaedia Vol. 5, Encyclopaedia Britannica Inc., Chicago, **1981**, p. 996.
2. A. Downham and P. Collins, "Colouring our foods in the last and next millennium", *Int. J. Food Sci. Tech.*, **2000**, 35, 5-22.
3. "Pigments through the ages", <http://www.webexhibits.org/pigments/indiv/recipe/alizarin.html> (retrieved on 23 July **2008**).
4. W. Phutdhawong and D. Buddhasukh, "Applications of Electrocoagulation", Chotana Print Co. Ltd., Chiangmai, 2007.
5. M. Y. A. Mollah, R. Schennach, J. R. Parga, and D. L. Cocke, "Electrocoagulation (EC)--science and applications", *J. Hazardous Mat.* B84, **2001**, 29-41.
6. W. Phutdhawong, S. Chowwanapoonpohn, and D. Buddhasukh, "Electrocoagulation and subsequent recovery of phenolic compounds", *Anal. Sci.*, **2000**, 16, 1083-1084.
7. K. Jumpatong, W. Phutdhawong, S. Chowwanapoonpohn, M. J. Garson, S. G. Pyne, and D. Buddhasukh, "Electrocoagulation in aqueous alcoholic solutions", in "Trends in Electrochemistry Research" (Ed. M. Nunez), Nova Publishers, New York, **2007**, Ch. 5.
8. N. Chairungsi, K. Jumpatong, W. Phutdhawong, and D. Buddhasukh, "Solvent effects in electrocoagulation of selected plant pigments and tannin", *Molecules*, **2006**, 11, 309-317.
9. N. Chairungsi, K. Jumpatong, P. Suebsakwong, W. Sengpracha, W. Phutdhawong, and D. Buddhasukh, "Electrocoagulation of quinone pigments", *Molecules*, **2006**, 11, 514-522.